Faculty of Resource Science and Technology

Geochemical and Ecological Risk Assessment of Heavy Metals and Hydrocarbons in Sediments of the Coastal and Four Rivers Estuary of Kuching Division of Sarawak, Malaysia

Ebenezer Aquisman Asare

Doctor of Philosophy
2023

Geochemical and Ecological Risk Assessment of Heavy Metals and Hydrocarbons in Sediments of the Coastal and Four Rivers Estuary of Kuching Division of Sarawak, Malaysia

Ebenezer Aquisman Asare

A thesis submitted

In fulfillment of the requirements for the degree of Doctor of Philosophy

(Chemistry)

Faculty of Resource Science and Technology
UNIVERSITI MALAYSIA SARAWAK
2023

DECLARATION

I declare that the work in this thesis was carried out in accordance with the regulations of Universiti Malaysia Sarawak. Except where due acknowledgements have been made, the work is that of the author alone. The thesis has not been accepted for any degree and is not concurrently submitted in candidature of any other degree.

Signature

Name: Ebenezer Aquisman Asare

Matric No.: 18010066

Faculty of Resource Science and Technology

Universiti Malaysia Sarawak

Date : 15/03/2023

ACKNOWLEDGEMENT

I owe my gratitude to God, the Most Gracious and the Most Merciful whose guidance and protection sustained me throughout my entire life and makes my educational career a reality.

My sincere gratitude goes to Professor Dr. Zaini Assim for his proper supervision, fatherly advice, supports, and encouragement throughout the entire study period at Universiti Malaysia Sarawak. His knowledge and expertise in Chemistry research will always remain with me as guidance to follow. Without your guidance, the research would have been impossible.

I would also like to thank my co-supervisor, Assoc. Prof. Dr. Rafeah Wahi for her sincere advice. I also appreciate Mr. Benedict Samling (GC-MS) and Mr. Tomy Bakeh (ICP-OES) for their supports regarding sample analysis. I would also like to thank Univeristi Malaysia Sarawak (UNIMAS) for financial support for this study under postgraduate Student Research Grant (F07/PGRG/1896/2019).

My special and profound gratitude goes to my mother Grace Baidoo and my entire family members for their supports and prayers.

Finally, I would like to appreciate the efforts of friends and colleagues towards the successful completion of the program. The contributions of authors whose works have been duly cited in this research are hereby acknowledged. I am grateful to all.

ABSTRACT

Contamination of heavy metals and hydrocarbons in the coastal and estuarine sediment could harm water quality and aquatic organisms, leading to potential long-term health risks on the environment and humans. Thus, this study was carried out to determine the concentration of heavy metals, aliphatic hydrocarbons (AHs), and polycyclic aromatic hydrocarbons (PAHs) distribution in surface sediments and to establish baseline concentrations of heavy metals using core sediments from the coastal and four rivers estuary of the Kuching Division of Sarawak, Malaysia. Validated inductively coupled-optical emission spectroscopy (ICP-OES) was used to determine heavy metals and their distribution in surface sediments was evaluated for eco-toxicological impacts. Source appointment of the heavy metals within the catchment area was determined using geochemical indices. The ICP-OES technique validated was appropriate and less laborious for determining the 12 metals of interest (i.e., Al, Mn, Ca, Cd, Cu, Fe, Cr, Ni, Co, Zn, and Pb) in the sediments. Heavy metals concentrations were recorded based on dry weight (d.w). The concentrations of heavy metals in core sediments varied in the range: Pb (8.9 – 188.9 mg/kg), Zn(19.4 – 431.8 mg/kg), Cd(0.014 – 0.061 mg/kg), Ni(6.6 – 33.4 mg/kg), Mn(2.4 – 16.8 mg/kg), Cu(9.4 – 133.3 mg/kg), Ba(1.3 – 9.9 mg/kg), As(0.4 – 7.9 mg/kg), Co(0.9 – 5.1 mg/kg), Cr(1.4 – 7.8 mg/kg), Mg(68.8 – 499.3 mg/kg), Ca(11.3 – 64.9 mg/kg), Al(24.7 – 141.7 mg/kg), Na(8.8 – 29.4 mg/kg), and Fe (12011 – 35124.6 mg/kg). The enrichment factor assessment suggested enrichment of Pb, Zn, Cu, As, Co, and Mg occurred at the top layer of the core sediments. Continuous accumulation of Pb and Cu metals over time can be detrimental to living organisms and the ecology. The pollution load index values indicated that the study area is unpolluted. Sediment quality guidelines (SQGs) compared to the detected heavy metals suggested no likely deleterious impact on

bottom-dwelling living things. The risk index estimation in each study site showed a low ecological risk impact on the environment. The statistical analysis suggested that the deposition of As, Cd, Pb, Cu, Mn, and Zn in the study sites is due to anthropogenic inputs from the adjacent land-based sources while Fe, Al, Mg, Na, Ni, and Ba are from lithogenic origin. This study further explains the monitoring, sources, and risk assessment of hydrocarbons in surface sediments. Validation on the performance of gas chromatography-flame ionization detector (GC-FID) and gas chromatography-mass spectrometry (GC-MS) showed that these techniques are in excellent position to quantify aliphatic and polycyclic aromatic hydrocarbons, respectively. Total *n*-alkanes (C_{10} – C_{33}) concentrations varied from 96.63 – 367.28 ng/g. The lowest and highest *n*-alkane content was observed at Santubong estuary (CZ10) and the offshore of Batang Rambungan opposite small Satang Island (CZ2), respectively. The contents of ∑PAHs varied from 12.54 – 21.20 ng/g. The highest ∑PAHs content was detected in the sediments of coastal site CZ8 (21.20 ng/g), whereas; the lowest content was recorded in the sediments of coastal site CZ3 (12.54 ng/g). The aliphatic diagnostic indices values showed hydrocarbons input from biogenic and petrogenic sources. The isomeric ratios values also indicated that PAHs in sediments are from a mixture of petrogenic and pyrogenic origins. The carcinogenic PAHs risk assessment suggested no risk impacts of carcinogenic PAHs in the study area. The findings from this study can be used to understand the sources and possible risks of hydrocarbons and provide information for safeguarding human health and aquatic bodies in coastal and estuary settings.

Keywords: Metalloids, petroleum, pollution indices, carcinogenic risks

Penilaian Risiko Geokimia dan Ekologi Logam Berat dan Hidrokarbon dalam Sedimen Pantai dan Empat Sungai Muara Bahagian Kuching Sarawak, Malaysia

ABSTRAK

Pencemaran logam berat dan hidrokaron dalam sedimen pantai dan muara boleh membahayakan kualiti air dan organisma akuatik, yang membawa kepada potensi risiko kesihatan jangka panjang terhadap alam sekitar dan manusia. Oleh itu, kajian ini dijalankan untuk menentukan kepekatan logam berat, hidrokarbon alifatik (AHs), dan taburan hidrokarbon aromatik polisiklik (PAH) dalam sedimen permukaan dan untuk menentukan kepekatan asas logam berat menggunakan sedimen teras dari muara pantai dan empat sungai. Bahagian Kuching Sarawak, Malaysia. Spektroskopi pelepasan optik gandingan induktif (ICP-OES) yang disahkan telah digunakan untuk menentukan logam berat dan pengedarannya dalam sedimen permukaan dinilai untuk kesan eko-toksikologi. Pelantikan sumber logam berat dalam kawasan tadahan ditentukan menggunakan indeks geokimia. Teknik ICP-OES yang disahkan adalah sesuai dan kurang susah payah untuk menentukan 12 logam yang diminati (iaitu, Al, Mn, Ca, Cd, Cu, Fe, Cr, Ni, Co, Zn, dan Pb) dalam sedimen. Kepekatan logam berat direkodkan berdasarkan berat kering (d.w). Kepekatan logam berat dalam sedimen teras berbeza dalam julat: Pb (8.9 – 188.9 mg/kg), Zn(19.4 – 431.8 mg/kg), Cd(0.014 – 0.061 mg/kg), Ni(6.6 – 33.4 mg/ kg), Mn(2.4 – 16.8 mg/kg), Cu(9.4 – 133.3 mg/kg), Ba(1.3 – 9.9 mg/kg), As(0.4 – 7.9 mg/kg), Co(0.9 – 5.1 mg/ kg), Cr(1.4 – 7.8 mg/kg), Mg(68.8 – 499.3 mg/kg), Ca(11.3 – 64.9 mg/kg), Al(24.7 – 141.7 mg/kg), Na(8.8 – 29.4 mg/ kg), dan Fe (12011 – 35124.6 mg/kg). Nilai indeks beban pencemaran menunjukkan bahawa kawasan kajian tidak tercemar. Garis panduan kualiti sedimen (SQGs) berbanding dengan logam berat yang dikesan mencadangkan tiada kesan yang memudaratkan kepada hidupan bawah.

Anggaran indeks risiko di setiap tapak kajian menunjukkan kesan risiko ekologi yang rendah terhadap alam sekitar. Analisis statistik mencadangkan bahawa pemendapan As, Cd, Pb, Cu, Mn, dan Zn di tapak kajian adalah disebabkan oleh input antropogenik daripada sumber berasaskan tanah bersebelahan manakala Fe, Al, Mg, Na, Ni, dan Ba adalah daripada asal litogenik. Kajian ini selanjutnya menerangkan pemantauan, sumber, dan penilaian risiko hidrokarbon dalam sedimen permukaan. Pengesahan prestasi kromatografi gas-pengionan nyalaan pengesan (GC-FID) dan kromatografi gas-spektrometri jisim (GC-MS) menunjukkan bahawa teknik ini berada dalam kedudukan yang sangat baik untuk mengukur hidrokarbon aromatik alifatik dan polisiklik. Jumlah kepekatan n-alkana (C10 – C33) berbeza daripada 96.63 – 367.28 ng/g. Kandungan n-alkana yang paling rendah dan tertinggi didapati di muara Santubong (CZ10) dan di luar pesisir Batang Rambungan yang bertentangan dengan Pulau Satang kecil (CZ2). Kandungan ∑PAH berbeza dari 12.54 – 21.20 ng/g. Kandungan ∑PAHs tertinggi dikesan dalam sedimen tapak pantai CZ8 (21.20 ng/g), manakala; kandungan terendah dicatatkan dalam sedimen tapak pantai CZ3 (12.54 ng/g). Nilai indeks diagnostik alifatik menunjukkan input hidrokarbon daripada sumber biogenik dan petrogenik. Nilai nisbah isomer juga menunjukkan bahawa PAH dalam sedimen adalah daripada campuran asal-usul petrogenik dan pirogenik. Penilaian risiko PAH karsinogenik mencadangkan tiada kesan risiko PAH karsinogenik di kawasan kajian. Penemuan daripada kajian ini boleh digunakan untuk memahami sumber dan kemungkinan risiko hidrokarbon dan menyediakan maklumat untuk melindungi kesihatan manusia dan badan akuatik di kawasan pantai dan muara.

Kata kunci: *Metaloid, petroleum, indeks pencemaran, risiko karsinogenik*

TABLE OF CONTENTS

		Page
DECLARATION		i
ACKNOWLEDGEMENT		ii
ABSTRACT		iii
ABSTRAK		v
TABLE OF CONTENTS		vii
LIST OF TABLES		xiii
LIST OF FIGURES		xvi
LIST OF ABBREVIATION		xviii
CHAPTER 1: INTRODUCTION		1
1.1	Study Background	1
1.2	Problem Statement	5
1.3	Reseach Hypothesis	8
1.4	Objectives	9
1.5	Chapter Summary	10
CHAPTER 2: LITERATURE REVIEW		11
2.1	Geology and Hydrogeology of the Kuching Zone	11
2.2	Importance of Estuarine Environment	13

2.3 Coastal Area of Kuching 14

2.4 Geochemical Behaviour of Heavy Metals in the Estuarine Environment 14

2.4.1 Sources of Heavy Metals 15

2.4.2 Heavy Metals Contamination in Sediments 17

2.4.3 Distribution of Heavy Metals in Marine Sediments in Malaysia 20

2.5.1 Composition of Petroleum Hydrocarbons 20

2.5.2 Aliphatic Hydrocarbons (AHs) 21

2.5.2.1 Natural/Biogenic Sources of Aliphatic Hydrocarbons 21

2.5.2.2 Anthropogenic Sources of Aliphatic Hydrocarbons 21

2.5.2.3 Distribution and Fate of Aliphatic Hydrocarbons in Marine Sediments 22

2.5.2.4 Distribution of Aliphatic Hydrocarbons in Marine Sediments in Malaysia 23

2.5.3 Polycyclic Aromatic Hydrocarbons (PAHs) 26

2.5.3.1 Natural Sources of Polycyclic Aromatic Hydrocarbons 28

2.5.3.2 Anthropogenic Sources of Polycyclic Aromatic Hydrocarbons (PAHs) 29

2.5.3.3 Distribution and Fate of Polycyclic Aromatic Hydrocarbons in Marine Sediments 29

2.5.3.4 Distribution of Polycyclic Aromatic Hydrocarbons in Marine Sediments in Malaysia 30

2.6 Chapter Summary 33

CHAPTER 3: DISTRIBUTION OF HEAVY METALS IN COASTAL AND FOUR RIVERS ESTUARY SEDIMENTS IN THE KUCHING DIVISION OF SARAWAK 34

3.1 Introduction 34

3.2 Materials and Methods 36

3.2.1 Description of Study Area 36

3.2.2 Sediment Sampling and Treatment 38

3.2.3 Proximate Analyses 39

3.2.3.1 Moisture Content 39

3.2.3.2 Ash Content 40

3.2.3.3 Total Organic Matter 41

3.2.3.4 Particle Size Analysis 41

3.2.3.5 Other Physicochemical Parameters 42

3.2.4 Heavy Metal Analysis 42

3.2.4.1 Sediment Extraction and Analysis 42

3.2.4.2 Quality Assurance and Control (QA/QC) 43

3.2.4.3 Inductively Coupled Plasma-Optical Emission Spectrophotometry 43

3.2.5 Environmental Assessment of Heavy Metals Contamination 48

3.2.5.1 Enrichment Factor (EF) 48

3.2.5.2 Contamination Factor (CF) 48

3.2.5.3 Geo-accumulation Index (Igeo) 49

3.2.5.4 Pollution Load Index 49

3.2.6 Ecological Risk Assessment 51

3.2.6.1 Sediment Quality Guidelines 51

3.2.6.1.1 Threshold Effect Concentration (TEC) 51

3.2.6.1.2 Probable Effect Concentration (PEC) 52

3.2.6.1.3 Median Effect Concentration (MEC) 52

3.2.6.2 Potential Ecological Risk Index 53

3.2.7 Statistical Analysis 54

3.2.7.1 Pearson Correlation 54

3.2.7.2 Cluster Analysis (CA) 55

3.2.7.3 Principal Component Analysis (PCA) 55

3.3 Results and Discussion 55

3.3.1 Moisture Content, Ash Content and Total Organic Matter 55

3.3.2 Heavy Metals and Sediment Size Fractions Relationships 57

3.3.3 Distribution of Heavy Metals in Surface Sediments 63

3.3.4 Assessment of Heavy Metals Contamination in Surface Sediment 73

3.3.5 Eco-toxicological Risk Assessment 78

3.3.6 Vertical Distribution Analysis of Heavy Metals in Core Sediments 81

3.3.7 Trend Analysis of Anthropogenic Activities Affecting Heavy Metals Deposition in Core Sediments of each Sampling Site 83

3.3.8 Trend of Heavy Metal Enrichments in Core Sediments 90

3.3.9 Possible Sources of Heavy Metals Contamination 93

3.3.9.1 Pearson's Correlation Analysis 93

3.3.9.2 Cluster Analysis 95

3.3.9.3 Principal Component Analysis (PCA) 96

3.4 Chapter Summary 98

CHAPTER 4: DISTRIBUTION OF HYDROCARBONS IN COASTAL AND FOUR RIVERS ESTUARY SEDIMENTS IN THE KUCHING DIVISION OF SARAWAK 100

4.1 Introduction 100

4.2 Materials and Methods 102

4.2.1 Spiking and Extraction of AHs and PAHs 102

4.2.2 Column Chromatography 103

4.2.3 Gas Chromatographic Analysis 104

4.2.4 Quality Assurance and Quality Control (QA/QC) 105

4.2.5 AHs Diagnostic Indices 105

4.2.5.1 Carbon Preference Index (CPI) 105

4.2.5.2 Low Molecular Weight AHs/High Molecular Weight AHs 105

4.2.5.3 Long Chain Hydrocarbons/Short Chain Hydrocarbons 106

4.2.5.4 Average Carbon Length of LCH 107

4.2.5.5 Natural *n*-alkane ratio 107

4.2.5.6 *n*-alkane proxy (P_{aq}) 107

4.2.6 Isomeric Ratios for Sources Identification of PAHs 108

4.3 Results and Discussion 109

4.3.1 Validation of GC-FID and GC-MS Methods for AHs and PAHs Analysis 109

4.3.2 Evaluation of AHs in Sediment Samples 120

4.3.2.1 Nature of AHs Chromatogram Detected in Sediment Samples by GC-FID 120

4.3.2.2 Assessment of AHs Contamination and Potential Sources 122

4.3.3 Evaluation of PAHs in Sediment Samples 129

4.3.3.1 Characteristic PAHs Chromatogram Detected from Sediment Samples by GC-MS 129

4.3.3.2 Assessment of PAHs Contamination, Sources and Carcinogenic PAHs Risk 130

4.4 Chapter Summary 143

CHAPTER 5: CONCLUSION AND RECOMMENDATIONS 145

5.1 Conclusion 145

5.2 Recommendations 146

REFERENCES 148

APPENDICES 198

LIST OF TABLES

		Page
Table 2.1	Concentration of AHs in sediments from several locations off the Malaysian coast	25
Table 2.2	Concentration of PAHs contents in marine sediments off the Malaysian coast	32
Table 3.1	Coordinates of sampling locations	38
Table 3.2	Sediment texture and particle size range	41
Table 3.3	Detected heavy metals in CRM (i.e., sewage sludge amended soil) standardized by BCR	47
Table 3.4	Enriched factor (EF), contamination factor (CF), geo-accumulation index (Igeo) and pollution load index (PLI) range values and their environmental risk grades	50
Table 3.5	Metal contamination factor (Fi) of the selected trace metals, classification and environmental risk intensity	54
Table 3.6	Results of % moisture, % ash, and total organic matter in each of the sample locations	56
Table 3.7	Textural classification of core sediment at sampling sites	57
Table 3.8	Pearson's correlation matrix between analyzed heavy metals and sediment granulometric fraction expressed in percentage of the surface sediment samples	59
Table 3.9	Sediment pH, EC, and other chemical features of the investigated	

surface sediment samples at each sampling site 62

Table 3.10 Heavy metals concentrations (mg/kg) in surface sediments from the coastal and in four rivers estuary of Sarawak. 65

Table 3.11 Detected heavy metals concentrations in surface sediments in the study sites and in some selected world Rivers 70

Table 3.12 Enrichment of detected trace metals in surface sediments of the selected sampling sites 74

Table 3.13 Contamination levels of detected heavy metals in surface sediments of the selected study sites 76

Table 3.14 Geo-accumulation indices (I*geo*) and pollution load indices (PLI) values of detected heavy metals in surface sediments of the selected study sites 77

Table 3.15 Comparisons of consensus-based sediment-quality guidelines (SQGs) with detected heavy metals levels in the surface sediments of the selected study sites 79

Table 3.16 The potential ecological risk index values (RI) of detected heavy metals in surface sediments of the selected study sites 81

Table 3.17 Detected average concentration of Fe (mg/kg d.w) in core sediment sample 86

Table 4.1 The results of GC-FID linear ranges and limits of detection from analysis of standard solutions 111

Table 4.2 The results of GC-MS linear ranges and limits of detection from analysis of standard solutions 113

Table 4.3 Limits of detection, limits of quantification, and relative standard

deviation for *n*-alkanes analysis 117

Table 4.4 Limits of detection, limits of quantification, and relative standard deviation for PAHs analysis 118

Table 4.5 Content of *n*-alkanes determined in representative coastal and four rivers estuary sediment samples 123

Table 4.6 Concentrations of *n*-alkanes (ng/g) detected and calculated distribution indices in surface sediments of coastal and in four rivers estuary of Sarawak 125

Table 4.7 Concentration of PAHs (ng/g dw) assessed in representative coastal and four rivers estuary sediment samples of Sarawak 132

Table 4.8 Comparison of PAHs contents in sediments recorded from the coastal and four rivers estuary of Sarawak with those from different coastal and estuaries of the world 134

Table 4.9 Sum of individual PAH compounds analyzed in all stations with its abbreviation and number of aromatic rings 136

Table 4.10 Percentage distribution of PAHs in various stations based on the number of carbon rings 137

Table 4.11 PAHs isomeric ratio in sediment from the coastal and four rivers estuary of Sarawak 139

Table 4.12 Guidelines values (i.e., ERL and ERM) of PAHs in surface sediments 142

LIST OF FIGURES

		Page
Figure 2.1	The sedimentary basins of the Kuching Zone	13
Figure 2.2	Potential sources of heavy metal pollution on groundwater and drinking water supplies due to rural and urban activities	16
Figure 3.1	Map of study area showing sampling sites	37
Figure 3.2	Graph of average concentrations of selected heavy metals (mg/kg d.w.) against sediment depth/cm	82
Figure 3.3	Detected average concentrations of heavy metals (mg/kg d.w.) in core sediment samples in respective sample sites	84
Figure 3.4	Significant strong negative and positive correlations between Pb and Ni, Ba and Al, As and Fe, and Mg and Na in the surface layer of the core sediments.	93
Figure 3.5	Cluster analysis of detected average concentrations of heavy metals in the core sediments of selected study sites	96
Figure 3.6	Plot of loading of three principal components in PCA results	97
Figure 4.1	GC-FID chromatogram of AHs standard solutions	110
Figure 4.2	GC-MS chromatogram of PAHs standard solutions	110
Figure 4.3	*n*-alkanes recoveries from fortified coastal sediment	115
Figure 4.4	PAHs recoveries from fortified coastal sediment	115
Figure 4.5	The link between combined uncertainty (U_c) and spiked concentrations for (a) C_{20} and (b) C_{30}, respectively.	119

Figure 4.6 The link between combined uncertainty (U_c) and spiked concentrations for (a) naphthalene and (b) chrysene, respectively. 120

Figure 4.7 Characteristic gas chromatogram of AHs (*n*-alkanes) fractions extracted from coastal sediments in location (a) CZ5 and (b) CZ8, respectively. 121

Figure 4.8 Sum of *n*-alkanes of the two ranges (∑LHC and ∑SHC) at all sampling stations 126

Figure 4.9 Characteristic gas chromatogram of PAHs fractions extracted from coastal sediments in location (a) CZ5 and (b) CZ8, respectively. 129

Figure 4.10 PAHs source characterization in sediment 137

LIST OF ABBREVIATIONS

ACL	Average Carbon Length
AH	Aliphatic Hydrocarbons
ANN	Artificial Neural Network
ANZECC	Australian and New Zealand Enviornment and Conservation Council
ARMCANZ	Agriculture and Resource Management Council of Australia and New Zealand
ATSDR	Agency for Toxic Substances and Disease Registry
CA	Cluster Analysis
CF	Contamination Factor
CPI	Carbon Preference Index
CNN	Central Nervous System
DO	Dissolved Oxygen
EF	Enrichment Factor
EFr	Exposure Frequency
EC	Electrical Conductivity
ERM	Effect Range Medium
ERL	Effect Range Low
FC	Faecal Coliform
FS	Float Solids
GC-FID	Gas Chromatography-Flame Ionization Detector
GC-MS	Gas Chromatography-Mass Spectrometry
GPS	Global Positioning System

HDPE	High Density Polyethylene
HMW	High Molecular Weight
ICP-OES	Inductively Coupled Plasma – Optical Emission Spectroscopy
Igeo	Geoaccumulation Index
LOD	Limit of Detection
LOQ	Limit of Quantification
LOL	Limit of Linearity
LMW	Low Molecular Weight
LHC	Long Hydrocarbon Chain
MEC	Median Effect Concentration
MMT	Methylcyclo – Pentadienyl Manganese Tricarbonyl
MMWQI	Malaysian Marine Water Quality Index
NAR	Natural n-alkanes Ratio
OMC	Organic Matter Content
PAH	Polycyclic Aromatic Hydrocarbons
PC	Pearson Correlation
PCA	Principal Component Analysis
PEC	Probable Effect Concentration
PHC	Petroleum Hydrocarbons
PLI	Pollution Load Index
RSD	Relative Standard Deviation
RI	Risk Index
SHC	Short Hydrocarbon Length
SSP	Sediment Sampling Plan

SQGs	Sediment Quality Guidelines
TEC	Threshold Effect Concentration
THQ	Target Hazard Quotient
TEL	Tetraethyl Lead
TSS	Total Suspended Solids
US-EPA	United State – Environmental Protection Agent
WHO	World Health Organisation

CHAPTER 1

INTRODUCTION

1.1 Study Background

Coastal and estuarine territories are essential for human inhabitants (Likuku et al., 2013; Weissmannova et al., 2015). Nevertheless, with rapid urbanization and heavy industrialization, contaminants such as heavy metals and petroleum hydrocarbons are frequently conveyed to the coastal and estuarine sediments upstream of the bay (Kara et al., 2015; Weissmannova & Pavlovsky, 2017). Mining activities often cause pollution by heavy metals due to weathering (Wei et al., 2008; Sim et al., 2016). Sediment is part of the natural compositions of the earth's crust and thus, its biochemical equivalence and geochemical periods can be altered prominently by human activities (Di Baccio et al., 2003). Contamination of sediment by heavy metal is mainly attributed to human's actions such as smelting, mining, and various industrial activities (Kachenko & Singh, 2006). Urbanization and industrialization have tainted soils progressively with heavy metals caused threats to ecosystems, food safety, human and animal health (Wang et al., 2005; Weissmannova & Pavlovsky, 2017). Heavy metals are elements with a specific gravity greater than 4, and atomic weight ranged between 63.54 and 200.59 g/mol with a density greater than 6 g/mL (Kennish, 1992; Tariq et al., 2016). Heavy metals are called trace metals or toxic metals from an industrial point of view. Heavy metals can exist as essential elements, including Co, Cu, Fe, Mn, and Zn, which their deficiencies can affect the productivity of crops and livestock. They can also exist as non-essential, contaminate the soil and water and affect human and animal health through the food chain. They also act as micronutrients, macronutrients as well toxic agents. Several heavy metals are required by a

living organism in an amount that is not harmful (Berti & Jacobs, 1996; Tariq et al., 2016). Some essential and non-essential heavy metals are contaminants and can affect the environment even at low concentrations. Rodriguez et al. (2012) reported that the primary sources of heavy metals include coal combustion, pesticides, mining and smelting, medical waste, fertilizers, batteries, and burning of leaded petrol. Other sources of contamination include the unsafe application and excess usage of pesticides, fungicides, or fertilizers (Shen et al., 2002). Industrial effluent and sewage can contaminate the irrigation water supply with heavy metals, which leads to soil and vegetation contamination (Bridge, 2004). Rock explosion and rock seepage are natural sources of heavy metal pollution. In contrast, human activities contributing to heavy metal contamination are smelting operations, mining, thermal power plants, and battery industries (Cheng et al., 2018).

The environmental pollution by heavy metals primarily originates from natural and anthropogenic sources. The most crucial natural sources of heavy metals include erosion, weathering of minerals, and the activities of a volcano (Sabiha-Javied et al., 2009). Anthropogenic sources of heavy metals are sludge dumping, mining, smelting, biosolids in agriculture, fertilizer applications, electroplating, use of pesticides, industrial discharge, atmospheric deposition. Arsenic, for example, is usually used in wood preservatives and artificial pesticides (Cheng et al., 2018). In comparison, Cd can be found in pigments, incineration of cadmium-containing plastics, paints, plastic electroplating, plastic stabilizers, phosphate fertilizers, and others (Pulford & Watson, 2003). Cr can be found in fly ash, steel industries, and the discharge of tanneries, while Cu has been detected in pesticides and fertilizers (Ali & Khan et al., 2017). Surgical instruments, industrial effluents, automobile batteries, steel alloys, and kitchen appliances contained Ni (Tariq et

al., 2016). Pb can be found in battery manufacture, herbicides, aerial emission from combustion of leaded petrol, and insecticides (Wuana & Okieimen, 2011).

Heavy metal pollution is regarded as one of the primary threats to water resources, soil, sediments, plants, and human health (Yoon et al., 2006). As and Co compounds have been listed among the likely carcinogenic agents to humans according to International Agency for Research on Cancer (IARC) (Nwaichi & Dhankher, 2016). Cd, Cu, Zn, and As in soil and sediment have increased due to phosphate fertilizers (Zarcinas et al., 2004). A total of 53 elements have been classified as heavy metals, and they are known as ubiquitous contaminants found in industrial settings (Sarma, 2011). The concentration of metals in the soil/sediment ranged from trace levels to higher levels, up to 100,000 mg/kg depending on the type of element and its location (Blaylock & Huang, 2000). Humans contact heavy metals through several activities carried out within their environment. Industrial activities such as manufacturing processes, refining, mining, and smelting are the primary sources of heavy metals exposure by human (Nriagu, 1992; Tsang et al., 2011; Cheng et al., 2018).

Aliphatic and polycyclic aromatic hydrocarbons (AHs and PAHs) have been named among persistent organic pollutants (POPs) (Christensen & Arora, 2007; Chung et al., 2007; Tsang et al., 2011; Hu et al., 2016). AHs and PAHs can cause negative impacts on the ecosystem and human health, although their sources are far away (Lehnik-Habrink et al., 2010). Petroleum hydrocarbons produced from industrial processes and human activities are extensive and exert significant environmental problems because of their nature, such as toxic, highly persistent, bioaccumulative, mutagenic, and carcinogenic characteristics (Sakari et al., 2008; Omorinoye et al., 2019b). AHs and PAHs enter the

environment via spills or accidents, leaks, emissions from industries, and by-products from domestic or commercial uses (Ou et al., 2004; Aly Salem et al., 2014). AHs comprise carbon atoms connected by single, double, or triple bonds to create non-aromatic structures. The profile pattern of odd or even number carbons raised from C6 – C40 exhibiting natural and anthropogenic origins can be predicted (EL Nemr & El-Said, 2012; EL Nemr et al., 2013; Aly Salem et al., 2014). PAH is an organic class of compounds consisting of two or three aromatic rings with a linear, cluster, and angular configuration (Aly Salem et al., 2014). These compounds have been classified into two groups depending on their molecular weight. Low-molecular-weight (LMW), comprising two or three joined benzene rings such as naphthalene, anthracene, and fluorene. Whereas high-molecular-weight (HMW) compounds consist of four to six combined rings such as indeno (1, 2, 3-c, d) pyrene, and others (Abdollahi et al., 2013; Tehrani et al., 2016).

Heavy metals and petroleum hydrocarbons contaminate the soil surface, groundwater, and other aquatic bodies such as rivers, estuaries, lakes, lagoons, coastal areas, and others, causing major environmental problems worldwide, which indirectly affect the entire economy. Sediments serve as a major sink for trace elements activities generated by man and discharged into the environment because of the actions by man (Nawrot et al., 2018). Environmental variation caused by anthropogenic activities can be evaluated by determining enhanced pollutants in sediments (Alexakis & Gamvroula, 2014; Guo et al., 2019). Wang et al. (2015) opined that the variations in environmental conditions in and around rivers and other water storage media are recorded in sediment profiles. According to Wen et al. (2016), the accumulation of heavy metals in sediments in various forms is mobilized and becomes a threat to the ecology. About 1% of heavy metals emitted from sediments containing exchangeable or carbonate-bond fractions are regarded safe to

the environment. More than 50% of heavy metals can enter the food chain in the aquatic ecosystem and become inaccessible for accumulation in biota (Nayak, 2015).

1.2 Problem Statement

Some of the most important places for human settlements are coastal and estuarine areas (Likuku et al., 2013; Weissmannova´ et al., 2015; Ali & Khan, 2017); nevertheless, with heavy industrialization and speedy urbanization, trace metals and hdrocarbons are constantly transported to the estuarine and coastal sediments from up-stream of the creek (Kara et al., 2015; Weissmannova´ & Pavlovsky´, 2017). The contamination of heavy metals and hdrocarbons in surface and core sediment could harm water quality (Ali & Khan, 2017; Ali et al., 2019). Bioaccumulation of heavy metals and hydrocarbons in aquatic organisms could result in long-term adverse health effects on humans (Sekabira et al., 2010; Nawrot et al., 2020; Omorinoye et al., 2020). The presence of heavy metals and hydrocarbons in water, soils, and sediments cannot be regarded as non-aligned to the ecosystem or humans because of their mutagenicity and accumulation via the food chain (Ergonul & Altindag, 2014; Maanan et al., 2015; Guo et al., 2019).

The differences in ecological conditions in and around storage reservoirs and streams are documented in the sediment profiles (Wang et al., 2016). Sediments contamination increases because they are an important indicator of environmental variation caused by anthropogenic activities (Alexakis & Gamvroula, 2014; Guo et al., 2019). Heavy metals and hydrocarbons gather in sediments in different forms; are probable to be mobilized and become toxic in the environment in the path of utilization (Wen et al., 2016). Heavy metals within the exchangeable or carbonate-bond portions emitted from sediments, approximately 1% is regarded safe to the ecosystem, and more than 50% of the

total quantity may constitute an immense risk and perhaps through the food chain (Nayak, 2015).

Quantification of environmental contamination with heavy metals generally includes the various geochemical indices such as enrichment factor (EF), pollution load index (PLI), contamination factor (CF), and geoaccumulation index (Igeo) (Hakanson, 1980; Likuku et al., 2013; Weissmannova´ & Pavlovsky´, 2017). For AHs, diagnostic indices such as carbon preference index (CPI), terrigenous/aquatic ratio (TAR), natural *n*-alkanes ratio, etc., are used for AHs identification in the environment. In regards to PAHs, isomeric ratios are used for source identification to predict environmental contamination. This include ratio of anthracene/(anthracene+phenalthrene), ratio of fluoranthene /(fluoranthene+pyrene), etc. The determination of heavy metals and hydrocarons distribution in surface and core sediments and the levels of its enrichment provide the foundation for the understanding of sediments improvement techniques and assessment of the possible emission of metals into water and conveying downstream (Pan & Wang, 2012; Yan et al., 2018; Nawrot et al., 2020).

The Kuching Division of Sarawak, Malaysia underlines the South China Sea which forms part of the Pacific Ocean, surrounding an area from Kalimantan and Malacca Straits to the Taiwan Straits with about 3,500, 000 km^2 (Chen et al., 2015). The nature of the estuarine and coastal sediments in Kuching is dependent on the complex interaction of several factors that control sediment composition, transportation, deposition, and postdeposition of sediment (Morni et al., 2017). Furthermore, it is all based on the origin of material such as biological or geological sources or both to ascertain the constituents (Bale & Kenny, 2008). Generally, the continental shelf content of sediments in Sarawak particularly the Kuching Division is biogenic, volcanic, and terrigenous substance (Liu et

al., 2013) which is comprised of kaolinite, illite, smectite, chlorite, and a mixture of clay minerals (Chen et al., 2015). If interaction remains stable, the sedimentary environment will continue unchanged unless any of the factors change in the period to cause alteration of sediment (Gray, 1981; Holme & Mclntyre, 1984). Approximately 80% of the organic matter (hydrocarons) buried on the continental shelf was obtained from the rigorous sedimentary accumulation and high biological production (Kao et al., 2007).

The Kuching Division of Sarawak has experienced population growth and increased in development in the past 20 years, which is probably contributing to environmental contamination (Sim, 2007). Sarawak's urbanization rate stood at 53.80% in 2010, compared with 36.00% in 1991 and 15.50% in 1970 as reported by the Department of Statistics Malaysia. In 2020 population and housing census conducted by the Department of Statistics Malaysia showed an increase in the human population in Kuching from the year 2010 with 617,877 inhabitants to 711,500 residents in the year 2020. The effect of urbanization on water quality and the macrobenthos community structure in the Fenhe River, Shanxi Provine, China reported by Wang et al. (2020) indicate that intensification of urbanization has strongly affected the water, sediment, and macrobenthos in the Fenhe River watershed. In addition, Sarawakians depend on gas fuels for heating and burning which produces numerous air contaminants such as PAHs, heavy metals, carbon (II) oxide, sulfide, particulate matter, etc. into the environment. Floods gathered sediments within the nearby communities could be relocated inside the estuarine and finally transport to the coast of the South China Sea. The last major flood incident that occurred on 17th January 2015 has a massive influence on the quality of underneath sediments and transport contaminants such as heavy metals and hydrocarbons downstream. These contaminants trapped in the sediments can create environmental or human health risks which can be a

problem of the greatest consequence in partially crowded areas like nearby towns of the study sites. However, pollutants deposition prevents their movement further downstream and accumulation in the ocean (Nawrot et al., 2020).

Most of the studies on heavy metals distribution in sediments within the estuarine and coastal sites of Sarawak region were mostly concentrated on quantitative data only without dealing with the anthropogenic activities affecting heavy metals and hydrocarbons availability and their implications on the environment (Sim, 2007; Sim et al., 2016; Omorinoye et al., 2019). Furthermore, information regarding sediment fractions on heavy metals and hydrocarbons availability in the sediment of the estuarine and coastal sites of study region is lacking. Even if they exist they have not been well documented for easy retrieval. Hence, this study is an investigation of geochemical and ecological Risk assessment of heavy metals and hydrocarbons in sediments of the coastal and in four rivers estuary of Kuching Division of Sarawak, Malaysia. This study is important because the results of the investigation would be of great importance to policymakers to identify the vulnerability site and take appropriate remedial effort to protect the studied coastal ecosystem.

1.3 Research Hypothesis

Based on the problem statement, it can be deduced that there has been heavy metals and hydrocarons deposition in the surface and core sediments of the coastal and four rivers estuary of the study area due to both natural and anthropogenic activities. Hence, this research is driven by the hypotheses that:

i. There are significant strong relationships between heavy metals concentrations and particle size fractions in sediments collected from the coastal region and four rivers estuary of Sarawak,

ii. There is a significant difference in heavy metals/hydrocarbons concentrations in surface and bottom bed sediments between the coastal sites and the selected estuaries,

iii. There is an enrichment of heavy metals from the top layers to the bottom layers of the core sediments from the study area, and

iv. The sources of heavy metals/hydrocarons deposition in the sediment are greatly influenced by anthropogenic inputs.

1.4 Objectives

To test these hypotheses, surface and core sediments were collected from the coastal and four rivers estuary in the Kuching Division of Sarawak, Malaysia to evaluate heavy metals/hydrocarons concentrations and predict the sources influencing their availability. Thus, the objectives of this study are:

i. To assess heavy metal concentrations in sediments and their eco-toxicological impacts

ii. To investigate the anthropogenic activities influencing the deposition of heavy metals in surface and core sediments

iii. To apply bivariate and multivariate analyses to predict the likely sources of heavy metals contamination using the surface layer of the core sediments.

iv. To assess the concentration and distribution of hydrocarbons in sediments

v. To examine the sources of hydrocarbons in sediment using AHs diagnostic ratios and PAHs isomeric ratios

vi. To investigate the carcinogenic PAHs in sediments of the study area.

1.5 Chapter Summary

This section explains the research background of the study. The following key concepts were introduced in the research background: heavy metals, AHs, PAHs, sediments, estuarine, coastal sites, etc. The section discussed the problem statement of the study area, which called for this research to be undertaken, and the relevant of this study to the policy makers. Questions raised before carrying out the study were also highlighted in this section in the form of hypothesis. The objective of the study to help solve the problem statement has been outlined including the specific objectives to address the hypotheses stated.

CHAPTER 2

LITERATURE REVIEW

2.1 Geology and Hydrogeology of the Kuching Zone

East of Sarawak, the Ketungau and Kayan basins are the two sedimentary basins found in the Kuching Zone. The successions of the terrestrial sedimentary in the basins form part of the Kuching Super group that stretches into Kalimantan (Breitfeld et al., 2018). The uppermost Cretaceous and Lower Eocene Kayan group result in the formation of sedimentary rock. The sedimentary rock settles directly above the Pedawan Unconformity, which identifies the ending of subduction-related magnetism beneath the Schwaner Mountains and Sarawak due to the cessation of the Paleo-Pacific subduction (Breitfeld et al., 2018). The Penrissen and Kayan sandstones form the successions and are influenced by alluvial fans, floodplain, and fluvial channels deposits associated with deltaic to tidally-dominated sections in the Kayan Sandstone (Tan, 1981; Morley, 1998; Breitfeld et al., 2018). In the late early or early mid-Eocene, there was a cessation of sedimentation in the basin and formed a new basin at the east called the Ketungau Basin. The Kayan Unconformity exhibits this variation. Sedimentation continued to occur in the Mid-Eocene with the marginal marine, tidal to Silantek and deltaic Ngili Sandstone formation (Pieters et al., 1987; van Hattum et al., 2013; Hennig et al., 2017). The upper sequence of Silantek formation was influenced by floodplain and subsidiary fluvial accumulations (Breitfeld et al., 2014; Breitfeld, 2015; Breitfeld et al., 2018). The uppermost part of the Ketungau Group at the west of Sarawak formed the fluvially-controlled Tutoop Sandstone (Doutch, 1992). The Ketungau Basin stretches from West Sarawak to Kalimantan and is segregated by the Ridge of Semitau from the Melawi Basin

(Doutch, 1992) and is considered the largest of the Cenozoic sedimentary basins of the Kuching Zone (Breitfeld et al., 2018). Figure 2.1 shows the sedimentary basins of the Kuching as depicted by the brown kite shape.

The geological features or paleocurrent indicators for the Kuching Zone ascertain the direction of water flowing (river systems) in the geologic past are complex but can be considered the primary water source from the southern zone (Breitfeld et al., 2018). This indicates that the uplift of the south Borneo started in the region of the current Schwaner Mountains from the new Cretaceous onwards (Haile, 1974; Breitfeld et al., 2018). Furthermore, other water sources of river systems are local sources in the West Borneo province, Mesozoic malanges to the east, and likely the Malay Peninsula (Breitfeld et al., 2018). The Kuching Supergroup sediments are mainly horizontal or dip associated with low angles and constitutes large open synclines (Wilford & Kho, 1965; Breitfeld et al., 2018).

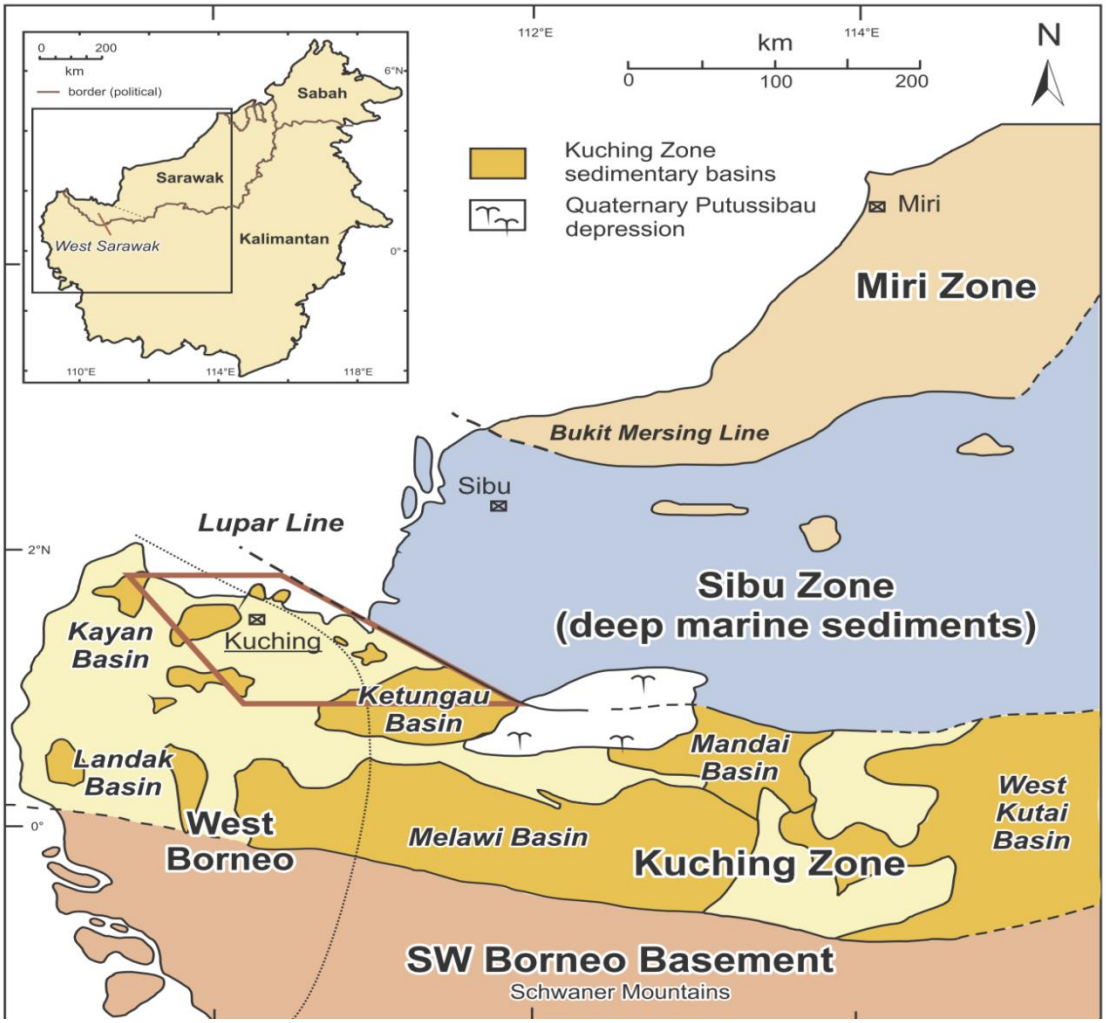

Figure 2.1: The sedimentary basins of the Kuching Zone (adapted from Breitfeld et al., 2018). The study area is depicted in a brown kite shape

2.2 Importance of Estuarine Environment

Estuaries are unique and vital natural environments. They constitute an extensive range of habitats and ecosystems such as unconsolidated sediments, large areas of open water, intertidal sand, rock reefs, mudflats, saltmarshes, mangroves, and seagrass beds. Estuarine provides significant habitat for species that are esteemed recreationally, commercially, and culturally. Insects, amphibians, fish, birds, and other wildlife rely on estuaries to reproduce, nest, feed, and live. Other organisms including oysters make estuaries their everlasting residence. For example, crabs use the estuary's environment to

complete only part of their life cycle. Migratory bird species such as canvasback ducks, mallards, and others use estuaries as stopovers. Estuaries also filter contaminants out of the water flowing through them, such as heavy metals, hydrocarbons, herbicides, pesticides, etc.

2.3 Coastal Area of Kuching

The coastal area of Kuching is a tropical climate and is one of the dynamic ecosystems on earth. Regarding Kuching, the preponderance of the inhabitants resides in coastal areas. Approximately 80% of the Sarawak population live along the 800 km coastline; there is a notice of constant change of the size and shape. Kuching coastal zone is unique. Mangrove forests, daily tides, tidal flats, storm waves can only be observed on the coast. The coastal area of Kuching is considered as a sensitive ecological system with great value in the aesthetic, recreational, social, economic, and environmental conservation sites. Man's activities may interrupt the ecosystem of the coastal area. These include industry, agriculture, and coastal settlements, which contaminate the coastal area. Sand mining activities disrupt the coastal dynamic and contribute to erosion.

2.4 Geochemical Behaviour of Heavy Metals in the Estuarine Environment

Heavy metals originated from the natural source are transferred by rivers and transported to the coastal environment via estuaries. Heavy metals are dispensed between the dissolved and particulate phases (Adriano, 2001; Sparks, 2005). The fate and bioavailability of heavy metals rely on the particle chemistry and contention between surface and dissolved forms concerning the processes of complexation (Adriano, 2001; Adriano et al., 2004). Thus, estuaries serve as a natural reactor whereby heterogeneous processes occur at the interface between suspended particulate matter and dissolved phase

and compose an essential contribution of the heavy metals geochemical cycles (Sparks, 2005). Heavy metals' distributions and reactivity rates vary extensively between estuaries, depending on environmental factors such as transport processes, mixing patterns, and hydrodynamic residence times. Thus, there are no particular patterns of heavy metals behavior in the estuaries (Sparks, 2005).

2.4.1 Sources of Heavy Metals

Ali et al. (2019) reported that heavy metals are obtained from geogenic or lithogenic and anthropogenic sources. Numerous extensive studies have confirmed that these metals are originated from multiple lithogenic and geogenic sources (Cheloni & Slaveykova, 2018). Hazardous metals emit natural radiations under a variety of physiological and climatological factors in the biosphere. The radiations emerge from sea-salt sprays, rock weathering, volcanoes, and others. Heavy metals may occur as sulfides, sulfates, phosphates, and organic ligands. Common examples of these metals are Pb, Ni, Cr, Cu, As, Hg, Cd, and others. The metals exist as microelements and can damage health predicaments to live organisms (Pourkhabbaz et al., 2014). The pollution of hazardous metals within soils from diverse anthropological origins, including waste from industries, agriculture, emissions from automobiles and mining, has merited several research works (Davies & Ginnever, 1979; Garcia-Miragaya, 1981; Parry et al., 1981; Culbard et al., 1983; Cheloni & Slaveykova, 2018). Heavy metals from these origins can cause numerous environmental and health-related challenges such as ecosystem perturbation, bioaccumulation, plant and animal toxicity because of their topsoil accretion potential.

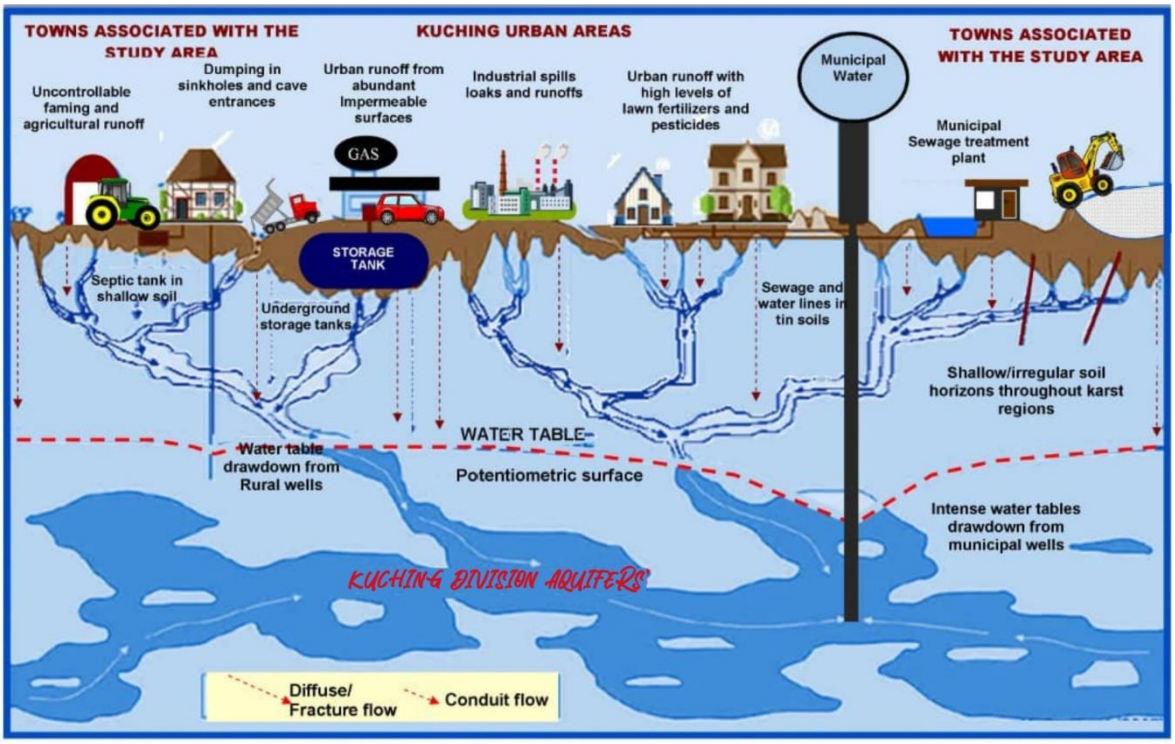

Figure 2.2: Potential sources of heavy metal pollution on groundwater and drinking water supplies due to rural and urban activities (adapted from Abbas and Abdelhafez, 2013)

Pourkhabbaz et al. (2014) stated that the sector that contributes heavily to heavy metal contamination within the biosphere in Malaysia is manufacturing. The primary sources of wastes with high Cr, Cu, Zn, Ni, Cd, Fe, Sn, Mn, and Al concentrations are companies engaged in electroplating, etching, and metal component preparation (Rahman & Surif, 1993). In 1992 over 69,000 m^3 per annum of hazardous metal-filled sludge was generated by companies that use metalloids and electronic components for their operations within numerous states in the Malaysian Peninsula (Hamid & Sidhu, 1993). Moreover, agriculture has equally generated its fair share of wastes that contain heavy metals. For instance, waste products from piggeries have been linked with mollusks and sediment pollution due to high copper concentrations (Ismail & Rosniza, 1997). Figure 2.2 denotes the potential sources of heavy metal pollution on groundwater and drinking water supplies due to rural and urban activities.

2.4.2 Heavy Metals Contamination in Sediments

Due to the continuous deleterious actions of humankind within the environment, contamination caused by heavy metals has become a recent global albatross (Pourkhabbaz et al., 2014). In an attempt to satisfy the demands of the worldwide populace, there is an upsurge in the processing and utilization of heavy metals in several human endeavors, and this has grossly aggravated pollution caused by heavy metals into a ubiquitous problem. Mining, farming activities, runoff due to urbanization, emissions from automobiles, and industrialization account for the release of hazardous metals into the environment. Heavy metals pose a critical threat to aquatic and terrestrial ecosystems (Cheloni & Slaveykova, 2018). The main targets of heavy metal contaminants in the environment are water, air, soils, and sediments. According to Pourkhabbaz et al. (2014), sediments are generally aggregates of various constituents, comprising organic materials and a variety of minerals. These constituents are vital in the exchanges involving sediment and water and contaminant remobilization within aquatic ecosystems. Sediments from the origin receive heavy metals in aquatic ecosystems (Ali et al., 2019). The contamination of sediments by heavy metals is caused by anthropogenic factors such as waste disposal, pesticide and fertilizer application, mining, automobile, industrial operations, combustion of coal, and petrochemical spillage. Heavy metals are non-biodegradable and thus cannot be decomposed by microbes and chemicals. Toxic elements stay in the sediment for a period of time after being released (Ali et al., 2019). Heavy metals can damage an entire biome because they can be incorporated into food chains. The presence of heavy metals in the biosphere impedes the decomposition of organic contaminants, and the phenomenon doubles the contamination rate. The effects of these hazardous metals on the entire ecosystem, humans, animals, and plants are enormous. The results are evident in soil

quality, food chains, oral ingestion, plant absorption, sediment, and water pollution (Pourkhabbaz et al., 2014).

2.4.3 Distribution of Heavy Metals in Marine Sediments in Malaysia

Coast and estuarine areas are the essential storage tanks for countless persistent contaminants, and they are deposited and accumulated in sediments and organisms (Szefer et al., 1995). The geochemical behavior of marine sediments can serve as an indicator to comprehend the trends and the origins of pollution. Fine-grained particles have been observed as the principal repository of heavy metals because of considerable adsorption potential and temporal contamination variations. Therefore, marine sediment can be used as the historical trend to study pollution variability. Over the last several decades, both surface and core sediments have been used to evaluate the impacts of natural processes and anthropogenic activities on depositional environments. Considerable studies have used sediment profiles to explain the pollution history. Saraee et al. (2011) have investigated the heavy metals distribution in sediments from the South China Sea of Malaysia region. The metals at the east coast of Peninsular Malaysia constituted a redistribution of territorial substances in the ecology. The levels of metals within the studied region could be considered natural background concentrations in sediment. Heavy metal concentrations of Zn, Cr, Pb, Cu, and Cd were examined in surface sediments and seawater collected from the coastal of Tuaran, Sabah, Malaysia by Tan et al. (2016). This study concluded that the level of metals in seawater and sediments were different at each station in the following order: Cr < Cu < Cd < Zn < Pb and Cd < Pb < Cr < Cu < Zn, respectively due to anthropogenic activities in the study area. This study also revealed that urbanization and

anthropogenic effluent, including naturally occurring processes, were the primary sources of trace elements.

Spatial distribution of trace elements in core sediments off Tanjung Pelepas harbor of Malaysia has been reported by Yusoff et al. (2015). The trace elements source and the date of the deposition of sediment that took place at Tanjung Pelepas harbor have been evaluated using the vertical profile of ^{210}Pb. Thus, the study revealed that historical differences of Cu and Zn exhibited the highest enrichment factor values in the late 1990s when the harbor was being established. Khodami et al. (2017) appraised the spatial and temporal trace elements distribution (Cr, V, Ni, Cu, Pb, Co, Zn, and Fe) in the sediments of Bayan Lepas Free Industrial Zone (FIZ) of Penang, Malaysia. The level of heavy metals varied from lower concentration to higher concentration at various study sites dependent on the interim sediment quality guidelines (ISQG). This study also revealed that heavy metals enrichment in the sediments ranged from no enrichment to extremely high enrichment due to the difference of anthropogenic activities and lithogenic in origin at various sampling sites. The likely ecological risk values obtained suggested that sediments collected from Bayan Lepas FIZ have low risks. The establishment of trace element pollution baseline in sediments collected from the Bernam River, Malaysia, has been conducted by Kadhum & Zulkifli (2016). The contents of the trace elements increased in the order of Cd < Fe < Ni < Cr < Sn. The results also indicated that the sediment samples collected from the middle and lower stream of the river had higher metal contents as a result of high anthropogenic activities and lithogenic in origin. In contrast, sediments from the upper stream of the river had lower contents of metals owing to low anthropogenic activities. Omorinoye et al. (2019a) have reported the vertical profile of metals levels in sediments from Sadong River, Sarawak, Malaysia. Fe was the most copious metal, whereas

Cd had the lowest concentration. Enrichment factors exhibited moderate to significant enrichment of metals along with the sediment profile.

2.5 Petroleum Hydrocarbons (PHCs)

Numerous amounts of sewage, spilled oil, dredged spoils, rainwater, industrial and waste from the municipal are released into the coastal water bodies via their rivers with inadequate or no treatment, particularly under developed and semi-industrialized economy (Wu et al., 2003; Muthukumar et al., 2013; Adeniji et al., 2017). Such emissions occurred mainly in the urban regions, even though at a low level, might not cause any instantaneous menace but could activate considerable problems in the long term (Quevenco, 2011). Some of these waste matters are discharged into the environment containing crude petroleum.

2.5.1 Composition of Petroleum Hydrocarbons

Crude petroleum is a tremendously multiplex combination of fossil material, fundamentally of plant and animal source (Laflamme & Hites, 1978; Bacosa & Inoue, 2015). It consists of thousands of organic, with a few inorganic compounds (Hu et al., 2016). Unrefined oils differ incredibly in chemical makeup, relative levels of various chemicals, and physical characteristics with no two indistinguishable. Crude oils are purified to produce several refined and leftover products, primarily fuels consisting of a bit of the number of chemicals traditionally within an established range of boiling points. A specific crude oil may consist of organic compounds varying in molecular weight from sixteen (methane), a gas at room temperature and pressure, to composite polymeric structures. For instance, asphaltenes have molecular weights of more than one hundred

thousand (Watkinson & Morgan, 1990; Xu et al., 2014; Dong et al., 2015). Hydrocarbons are, without a doubt, the most profuse chemicals found in crude and purified oils. Varying quantities of organic chemicals accommodating oxygen, sulfur, or nitrogen exist in all crude and part of purified oils. Petroleum hydrocarbons include aliphatic, aromatic, and amalgamation of both.

2.5.2 Aliphatic Hydrocarbons

Aliphatic Hydrocarbons (AHs), known as alkanes or paraffin, consist of carbon atom chains joined by single covalent bonds. Hydrogen atoms are occupied when carbon-carbon bonds do not occupy chemical bonds. AHs in petroleum are perhaps a linear chain, branched, or cyclic. Purified oil, specifically light fuels, such as kerosene and gasoline, contained olefins produced during the process.

2.5.2.1 Natural /Biogenic Sources of Aliphatic Hydrocarbons

AHs in the marine ecosystem come from biogenic/natural sources including bacteria and marine phytoplankton, terrestrial plant waxes, biomass combustion, and digenetic transformation of biogenic precursors. Petroleum, coal, and natural gas are the natural sources of AHs. These sources are commonly known as fossil fuels because they are the remains of plants and animals that died millions of years ago. Owing to great heat and pressure in the earth's crust, the remains of plants and animals are deposited and transformed into sediment. AHs are sources of fuels, burnt to release heat and other forms of energy. Petroleum is a dark and viscous liquid fuel, sometimes called crude oil while coal is a solid fuel. Gaseous fuel is natural gas. Alkanes are often used to distinguish organic matter in several environments. Long-chain alkanes containing the odd number of

carbon atoms (C27 - C35) are the major constituents of higher plants waxes. However, alkanes that are dominated with aquatic algae are the shorter chains with an odd number of carbon atoms (mostly C15, C17, and C19) (Meyer, 2014).

2.5.2.2 Anthropogenic Sources of Aliphatic Hydrocarbons

Anthropogenic AHs inputs are usually common in areas connected with industrial discharges (i.e., refinery and petroleum distributor), sewage outfalls (sewage) and shipping activities. Additionally, the release of unburned oil products, combustion/pyrolysis of fossil fuel, and domestic waste outfalls are the primary sources of anthropogenic AHs (Medeiros et al., 2005). Other anthropogenic sources of AHs are vehicular emission products and discarded plastics (Rushdi et al., 2013). AHs are many constituents of crude oils and petroleum products (Mouton et al., 2009). Gasoline and kerosene from petroleum products possibly contain some olefins. Olefins are commonly produced through refining, which constitutes double bonds and sometimes triple bonds. Still, these have a tiny percentage in hydrocarbons fuel (MADEP, 2004). ATSDR (1996) reported that AHs are found in diesel fuel, with about 60 – 90% of normal, branched, and cyclic alkanes by volume and 0 – 10% by volume of alkenes. When purified and by-products of petroleum are discharged into the environment, they may assemble in the soil and sediments and undergo weathering processes such as evaporation, dissolution, dispersion, and degradation (Neff et al., 1979). AHs with low molecular weight are insoluble in water due to the high Kow values. However, they are highly dissolvable, which can generate toxicity in soil and sediment. On the contrary, high molecular weight AH has higher Kow values and does not influence the chemical toxicity of oil-polluted soil and sediment (Neff et al., 1979).

2.5.2.3 Distribution and Fate of Aliphatic Hydrocarbons in Marine Sediments

AHs are global environmental contaminants (Guo et al., 2016). The primary origin of AHs in the aquatic environment are geological processes (diagenetic), biological processes, pyrolytic and petroleum processes (Hu et al., 2016). Hydrocarbons are associated with specific organic materials in the aquatic environment because of their hydrophobic features. They are settled in the bottom sediment (Tolosa et al., 2004; Qiu et al., 2009). They are regarded as necessary submerge for such contaminants. Volkman et al. (1997) stated that alkanes derived from petroleum prove little or no preponderance of either odd or even chain lengths. The existence of AHs in the environment does not pose a detrimental impact on humans.

Moreover, the toxicity of a particular AH relies on several features such as the path of exposure through inhalation dermal contact, or oral contact, exposure duration, the quantity taken, and the number of chronic exposure (Guo et al., 2016; Sammarco et al., 2016). Agnello et al. (2016) opined that an inhabitant could be endangered by some chemicals, fumes of gasoline at the pump, pesticides, and spilled crankcase oil on concrete slabs. Other paths that may give rise to AHs exposure are inhaling these compounds from a spill or leakage of the petroleum product, polluted drinking water containing petroleum, and exposure by children to contaminated soil (Smargiassi et al., 2014). The individual who works for the extraction and refining of crude oil, production of AHs, and petroleum products companies are more likely to be exposed to petroleum hydrocarbons effects (Rushton et al., 2014; Sammarco et al., 2016). The harmful impacts of AHs differed depending on the types of compounds available in the hydrocarbons fractions. For instance, n-hexane can bring about a nerve disorder known as peripheral neuropathy. Gonullu et al. (2013) reported that consuming many petroleum products such as gasoline

and kerosene can result in throat irritation, stomach pain, central nervous system depression, pneumonia, and dyspnea (difficulty breathing). Other petroleum materials can lead to eyes and skin irritation, whereas some can have adverse effects on kidneys, immune system, liver, blood, spleen, lungs, and fetus development (Bahadar et al., 2014).

2.5.2.4 Distribution of Aliphatic Hydrocarbons in Marine Sediments in Malaysia

Extensive studies have been conducted to determine AHs in marine sediments in Malaysia to ascertain the contamination levels and their sources. Most of these studies have been focused on regions associated with shipping activities in the Straits of Malacca exploration and exploitation of oil and gas reserves in the South China Sea. Yusoff et al. (2012) have reported the distribution of AHs from 18 surface sediments collected from the South China Sea off Kuching Division. It was found that sediments from Kuching bay ranged between 35.6 μg/g to 1466.1 μg/g d.w. The values of carbon preference index (CPI) showed anthropogenic input influence the environmental status of the study area. Forensic examination of AHs in sediments collected from mangrove environments on the west coast of Peninsular Malaysia was conducted by Vaezzadeh et al. (2015). This study revealed that total concentrations of n-alkanes (C10 – C36) varied from 27,945 – 254,463 ng/g dw. Petrogenic and biogenic were the sources controlling n-alkanes contents. Petrogenic influences on n-alkanes were more significant at the downstream part of the rivers than biogenic sources, which were predominantly heavy and degraded oil. Biogenic sources of n-alkanes were more predominant upstream of the rivers. Table 2.1 summarizes the distribution of AHs in sediments off the Malaysian coast.

Table 2.1: Concentration of AHs in sediments from several locations off the Malaysian coast

Location	AHs concentration in sediment (mg/kg dw)	Number of stations	Reference
South China Sea, Terengganu, >130 km from shore	6.4 -1,332.1	21	Law & Yusof (1986)
South China Sea, Pahang, 35 – 155 km from shore	10.7 – 85.3	14	Law & Zulkifli (1987)
South China Sea, Sarawak, >180 km from shore	2.9 -1,153.5	13	Law & Libi (1988)
South China Sea, Sabah, >70 km from shore	19.8 – 226.4	11	Law (1990)
Straits of Malacca, near-shore, Pulau Langkawi	164.2 – 847.4	2	Abdullah (1995)
Straits of Malacca, West coast Peninsular Malaysia (near-shore)	52.8 – 733.7	21	Abdullah et al. (1994)
East Coast, Peninsular Malaysia	0.244 – 5.77 5.48 – 139	12	Abdullah & Samah (1996)
West Coast, Peninsular Malaysia	0.053 – 9.51 5.61 – 704	37	Abdullah & Samah (1996)
Straits of Malacca, near-shore, Port Dickson	2.1 – 70.4	-	Law & Veelu (1989)
Straits of Malacca, near-shore, Port Dickson	21.7 – 74.5	23	Law et al. (1991)
Penang Island	0.47 – 2.01 18.4 – 179	18	Abdullah & Samah (1996)
Sarawak and Labuan	0.573 – 9.03	13	Abdullah & Samah (1996)

2.5.3 Polycyclic Aromatic Hydrocarbons

Aromatic hydrocarbons constituted one or more benzene rings (i.e., organic chemical containing six-carbon rings and nine equally shared carbon-carbon bonds). All carbon atoms in benzene are bonded to a single H atom but can be exchanged with an alkyl group(s) such as methyl, ethyl, or longer-chain aliphatic group(s). Benzene and alkylbenzenes containing one or two methylene or ethylene groups such as ethylbenzene, m-, p-, and o-xylene, and toluene are the profuse aromatic hydrocarbons in almost all crude and purified oils. Benzene is possibly fused to other benzene molecules by single covalent bonds to create compounds, for example, in biphenyl and terphenyl (Ou et al., 2004). Two or more benzenes can be linked by sharing two carbons to produce well-known PAHs (Neff, 1979). The principal constituent of petroleum hydrocarbons is PAHs. PAHs and their derivatives can be detected in the biome, including soil, sediments, water, air, and living organisms. PAHs are organic chemicals containing more than ten thousand compounds comprising two or more linked benzene rings in different configurations (Blumer, 1976; Qiao et al., 2008). Neff (1979) stated that a handful of PAHs compounds can be mutagen, a carcinogen, and trouble the endocrine systems of humans.

Consequently, PAHs have been grouped as environmental top precedence pollutants (Dong et al., 2012). PAHs are organic compounds composed of two to seven benzene rings where the two to four (2 – 4) rings are grouped as lower molecular weight (LMW) PAHs, while five to seven rings as higher molecular weight (HMW) (Wang et al., 2014). Neff (1979) suggested that the LMW PAHs are more dissolvable in water and highly toxic to human and living organisms, while HMW is highly dissolvable in lipid and more mutagenic, carcinogenic with prolonged impacts. The lipophilic and hydrophobic characteristics of some HMW make them not dissolvable in water, consequently resulting

in assemble in non-polar matrices or on surfaces (Zheng et al., 2015). Baker et al. (1989) suggested that the sorptive features of PAHs are influenced mainly by the organic particulate portion of suspended and settled sediments. Entity-bound PAHs have a short-lived time in the water path before their deposition at the deepest layer sediments at where they will re-suspend, degenerate, or be subjected to perpetual retention. Wong et al. (1995) suggested that the degree of any discharge back to the water path relies on the extent of physical re-suspension, bioturbation, and the physico-chemical characteristics of the contaminants. Worries over PAHs in the ecology emerged because they have been tenacious in the ecosystem for a very long time. PAHs can be induced from anthropogenic and natural origins. Natural products of PAHs are limited to several compounds, for instance, retene, phenanthrene, and perylene, which do not posed a health impact on humans and the ecosystem (Neff, 1979).

On the contrary, PAHs from anthropogenic sources are extensive contaminants generated from the burning of biomass and partial combustion of fossil fuel (Curtosi et al., 2007). There are two significant sources of which anthropogenic PAHs enter the marine ecosystem: pyrogenic and petrogenic. Pyrogenic PAHs originated from the pyrolytic process, including natural fire and biomass burning, urban and industrial activities, and combustion of fossil fuels that enhanced HMW with fewer non-alkylated PAHs (Sakari et al., 2011). After production, the combusted PAHs released as soot particles travel far distances and finally settle on terrestrial plants, soil, surface layers of sediments at the river, lagoon, and sea bottom. Several pyrogenic PAHs can be found in fine particles from charcoals, and they are carried away from the site of manufacture through precipitations and sewage plants to the aquatic ecosystem (Sakari et al., 2008). The sources of petrogenic PAHs are mainly from the discharge of crude oil and petroleum products including diesel

fuel, kerosene, lubricating oil, and asphalt (Wilcke et al., 2003; Omorinoye et al., 2020). PAHs can also enter the environment through tanker accidents, oil spills, and routine tanker activities such as discharge from vehicle workshops and ballast water discharge (NRC, 2003; Sakari, 2012).

2.5.3.1 Natural Sources of Polycyclic Aromatic Hydrocarbons

PAHs can be formed naturally, and most of them are carcinogen and possess toxic characteristics (Wang et al., 2015). PAHs' natural sources include grass and brush fires, chlorophyllous and non-chlorophyllous (bacteria and fungi) plants, weathering rocks, volcanoes, oil seeps, and decomposition of dead plants. There is no well-documented generation of PAHs biologically. Although PAHs can be synthesized by some bacteria and plants or derived in the course of vegetative matter degradation. The main contributors of PAHs in the environment include petroleum refining and transport activities (Caruso et al., 2015; Mulder et al., 2015). Loadings of PAHs into the environment may occur via discharges of industrial effluents and emission of raw and refined PAHs products (Moorthy et al., 2015). Other sources by which PAHs are released into the environment include fuel combustion, and tobacco smoke, diesel, and gasoline (Zhang & Balasubramanian, 2016). PAHs can be found in sediment, groundwater, soil, air, surface water, groundwater, and road runoff (Adam et al., 2015). The dispersion of PAHs are from the atmosphere to vegetation, contaminated food, and medicinal herbs (Duedahl-Olesen et al., 2015). Pongpiachan et al. (2013) opined that PAHs contents in soil and sediment collected from polluted and unpolluted sites varies from 1 mg/kg to over 300 g/kg.

2.5.3.2 Anthropogenic Sources of Polycyclic Aromatic Hydrocarbons

Discharge from the routine oil spill, oil transportation, biomass burning, power plants that uses fossil fuel, pyrolysis of internal combustion in engines and wood are the anthropogenic sources of PAHs. Several probable sources of PAHs contamination in the aquatic environments include city runoff, industrial and municipal wastes, atmospheric input, and riverine discharge have a higher amount of PAHs (Villanueva et al., 2015). The combination of natural and anthropogenic PAHs sources is due to global transport occurrence contributed to their worldwide distribution (Vignet et al., 2015). The formation of PAHs is usually due to the burning of fossil fuels in the course of heating processes from automobile exhausts and waste incinerators (Tang et al., 2015). PAHs are extensively distributed ecological contaminants with harmful biological effects, mutagenicity, carcinogenicity, and toxicity (Suman et al., 2016). The contents of PAHs in the ecosystem vary extensively, due to the proximity of the polluted site to the source of production, the mode(s) of transport, and the level of industrial development (Shih et al., 2016). According to Cui et al. (2014), PAHs may be available as pollutants in wastewater sewage sludge.

2.5.3.3 Distribution and the Fate of Polycyclic Aromatic Hydrocarbons in Marine Sediments

PAHs are discharged into the ecosystem through anthropogenic and natural sources. There are four groups of PAHs released to the marine ecosystem, a). biogenic are PAHs that are produced by the organism, b). petrogenic PAHs that are obtained from fossil fuels, c). pyrogenic PAHs that are derived from the processes of combustion, and finally d). diagenic PAHs obtained from changes undergone on the organic matter during deposition and burial in sediment before catagenesis (Neff, 1979; Peters & Moldowan,

1993; Harris, 2010). PAHs obtained from petrogenic and pyrogenic sources usually exhibit indistinguishable characteristics and fates after infiltrating into the ecosystem. Pyrogenic PAHs generated through combustion possessed high and strong affinity to organic particles that might travel long distances by an agent of wind and other atmospheric factors. PAHs carried by airborne particles stretch out to the upper layer of the water path in the marine ecosystem, enter the water path and then deep layer of the sea and finally deposited in the sediment. Petroleum and its products can enter into the marine ecosystem and expose to chemical transformation, dispersion, dispersion, evaporations, and weathering, settlement in the deepest layer on the sediments, microbial degradation (bacteria, fungi, and yeast), and sunlight effects (photo-oxidation) in short and long term duration (Neff, 1979). PAHs in sediment derived from Petrogenic sources may attach to particles and therefore, PAHs are subjected to various biological and chemical changes. Most PAHs found in the environment are ultimately degraded or metabolized by indigenous bacteria because of their energetic and carbon needs for growth and reproduction, as well as the requirement to relieve physiological stress caused by the presence of PAHs in the microbial community (Li & Duan, 2015). Despite the source of PAHs in the aquatic ecosystem, they attach to the microbes, debris, organisms, silt, and clay particles. They are deposited in the sediments, where different microbes (indigenous bacteria, fungi, etc.) degrade them into simple and low molecular weight.

2.5.3.4 Distribution of Polycyclic Aromatic Hydrocarbons in Marine Sediments in Malaysia

Several studies on PAHs have been conducted in marine sediments in Malaysia. Tavakoly Sany et al. (2014) investigated the PAHs in sediment collected from the coastal Strait of Klang, Malaysia. Their study were concentrated on the PAHs

distribution, risk assessment, and their sources in 22 sampling sites which is believed to be contaminated due to anthropogenic activities in the Klang Strait (Malaysia). The total PAH content was 994.02 ± 18.1 μg/kg d.w, with sites of the Klang River mouth and near the coastline exhibiting the highest concentrations. The study revealed that petrogenic and pyrogenic emissions are the primary inputs from vehicular and coal combustion, with great petroleum sources. However, ecological risk assessment showed that only site 13 was moderately contaminated; the remaining sites suffered rare or slight unfavorable biological impacts with PAHs exposure at the surface sediment, indicating that PAHs are not regarded as pollutants of threat in the Klang Strait.

Li and Duan (2015) assessed the PAHs pollution level in the China Sea by evaluating PAHs' contents, origins, and fates in China Sea sediment. The contents of PAHs in sediments of the China Sea increased from South to North due to the lower emissions in South China. The primary transporter of PAHs at the north was presumably the atmosphere because of higher amounts of fine atmospheric entities and higher wind speeds. Nevertheless, inputs from the riverine were the significant primary origins of PAHs in the South China coastal sediments because of higher rainfall.

PAHs distribution in sediments of the Straits of Malacca revealed that the total PAH contents in the surface sediments varied from 8.07 to 390.03 ng/g with the mean value of 133.5 ng/g (Razak et al., 2016). It was observed that all sampling sites were dominated by the low molecular weight PAH (3-ring) with 44% and 28% from high molecular weight PAHs (4-ring). The study also exhibited a mixture of pyrogenic and petrogenic PAHs sources with a dominance of pyrogenic inputs. Other studies related to PAH level in coastal sediments from Malaysia are summarized in Table 2.2

Table 2.2: Concentration of PAHs contents in marine sediments off the Malaysian coast

Location	PAH concentration in sediment (ng/g dw)	Number of stations	Reference
Langkawi Island, northwest of Peninsular Malaysia	228.13 – 990.25	32	Chiu et al. (2018)
Terengganu coast, covering an area from Dungan to Kemaman coast	6.01 – 20.2 4.89 – 34.7	16	Sanip et al. (2019)
Pulau Merambong and Muar river, Peninsular Malaysia	15.5 – 165.7 38.6 – 122.8	2	Vaezzadeh et al. (2013)
Strait of Johor, near the southern tip of Peninsular Malaysia	650.5 – 1441.2	5	Keshavarzifard et al. (2019)
Contaminated sediments in Malacca Strait, Malaysia	347.05 – 6207.5 179.32 – 1657.5	2	Keshavarzifard et al. (2017)
Mangrove estuary in the western part of Peninsular Malaysia	20 – 112	10	Raza et al. (2013)
Malacca Coastal Waters: 130 years of evidence for their land-based sources		3	Sakari et al. (2011)
Near Shore station core	177 (year 1949 – 1955) – 4447 (year 1963 – 1969)		Sakari et al. (2011)
	452 (year 1991 – 1997)		
In the Near Shore sample			Sakari et al. (2011)
Off Shore core	1.71 – (year 1914 – 1920) – 714.37 (1963 – 1969)		Sakari et al. (2011)

2.6 Chapter Summary

This chapter reviewed and summarized the concepts of heavy metals, AHs, and PAHs in the marine environment. The geological and hydrogeological aspects of the Kuching Division, Sarawak, have been highlighted together with the importance of the estuarine environment. Heavy metals classifications, characteristics, sources, and behavior in marine sediment distribution of heavy metals in Malaysian marine settings have been reported. Heavy metals in the environment can be categorized as either essential or non-essential, depending on their roles in biological ecosystems. Hazardous heavy metals contact air, soil, sediments, plants, and water through adsorption, precipitation, complexation, exchange of ions, and others. These metals originated from geogenic and anthropogenic sources. Heavy metals can pose a threat to both aquatic and terrestrial ecosystems. Exposure to heavy metals such as Hg, As, Pb, and Cd in either the short or the long term can cause cancers and other severe diseases in humans. Heavy metals such as Au, Fe, Cu, and others are essential constituents of the material utilized in the real estate, automobile, electronic and electrical industries. Cd serves as an anti-friction agent and many essential applications from most heavy metals. Hydrocarbons are everywhere, and their impacts on the environment and humans have raised many concerns. AHs and PAHs have been discussed in this chapter. Their fate and distribution in the environments have been discussed accordingly in this section. Several studies carried by various researchers within the Malaysian zone to predict and ascertain AHs and PAHs have been pointed out.

CHAPTER 3

DISTRIBUTION OF HEAVY METALS IN COASTAL AND FOUR RIVERS ESTUARY SEDIMENTS IN THE KUCHING DIVISION OF SARAWAK

3.1 Introduction

Heavy metals are a pressing concern regarding pollution in aquatic ecosystems because of their persistence, bioaccumulation, and environmental toxicity (Bryan & Langston, 1992; Redwan & Elhaddad, 2017; Zhang et al., 2017). Aquatic bodies, for example, reservoirs (Nguyen et al., 2019), rivers (Li et al., 2019), estuaries and coastal (Asare et al., 2021a, b), wetlands (Jia et al., 2019), and lakes (Chen et al., 2019), receive heavy metals in inadequately treated or untreated wastewater from agricultural, domestic, and industrial sources. As an essential constituent in riverine and estuarine environments, sediments are a source and a sink of trace metals (Pejaman et al., 2015; Huang et al., 2019). Trace elements entering rivers and estuaries rapidly deposit into the sediment and are much more concentrated than in the water body of riverine, estuarine, or coastal systems (Shyleshchandran et al., 2018). When there is an alteration of the hydrological or the physicochemical conditions, trace metals in the sediment may resuspend or desorb to result in secondary pollution in the water body (Kouidri et al., 2016; Asare et al., 2021b). Heavy metals accumulation in the sediment directly influences benthic organisms. Heavy metals in sediment also affect many other organisms via the food chain and threaten the comfort of the aquatic environment. Hence, it is important to evaluate and understand the accumulation and distribution of trace metals in sediment.

Rambungan, Sibu, Salak, and Santubong Rivers are key rivers in the Sarawak state of Malaysia. They flow through the Kuching city and support many less densely

populated towns, offering services to both agriculture and industry. Over the past few decades, there have been trace metals pollution in riverine, estuarine, and coastal sediment of the Sarawak state of Malaysia because of the wastewater discharge from agricultural, metallurgical, and mining industries carrying trace metals. Even though many researchers have studied trace metals pollution in the Rambungan, Sibu, Salak, and Santubong Rivers and their associate estuary (Omorinoye et al., 2019a); a systematic study is still lacking to correlate the sediment with trace metals distribution, characteristics, risk assessment, likely sources, and their effect on the aquatic environment.

Geochemical indices used for ecological risk assessment of heavy metals in surface sediments comprised of computation of enrichment factor (EF), contamination factor (CF), geo-accumulation index (Igeo), pollution load index (PLI) (Yi et al., 2011; Yang et al., 2012), potential ecological risk indices (Wu, 2014), and excess regression analysis (Hilton & Ochsenbein, 1985; Yi et al., 2011). Heavy metals analyses in river sediments have been used considerably for the essence of pollution monitoring (Pekey et al., 2004; Liu et al., 2007; Yang et al., 2012). A handful of these studies focused on the paths of imparting heavy metals content in sediments without evaluating their ecotoxicological risks (Omorinoye et al., 2019a). Therefore, this study aimed to determine ten trace metals (i.e., Zn, As, Fe, Mg, Mn, Ni, Cr, Cu, Co, and Cd) in sediments of the coastal and in four rivers estuary of the Kuching Division of Sarawak. Also, using the geochemical indices to evaluate the contribution of anthropogenic activities carrying trace metals into estuary and coastal sediment, determining the likely risks linked with trace metal toxicity using sediment quality guidelines and ecotoxicological risk index, and finally, ascertaining the source distribution of trace elements using statistical tools such as Pearson's coefficient correlation and principal component analysis.

3.2 Materials and Methods

3.2.1 Description of Study Area

The field studies and sampling were carried out in the coastal and in four rivers (i.e., Santubong, Salak, Sibu, and Rambungan) estuary in the Kuching Division of Sarawak in the North-Western portion of Borneo Island, Malaysia. The study area has a tropical rainforest climate, moderately hot yet very humid once in a while, and receives considerable rainfall. The mean annual precipitation is about 4,200 mm. The study area receives an average of 247 rainy days per year with an average of 6 hours of sunshine and a mean of 3.7 hours per day during January. North-East Monsoon months of November to February is the wettest time whiles June to August is considered the driest months. The temperature of the study area range between 19 °C to 36 °C with a mean temperature of roughly 23 °C in the early hours of the morning and rises to approximately 33 °C in the course of mid-afternoon and can reach 42 °C in the dry season. Figure 3.1 shows the sampling locations of the coastal and four rivers estuary.

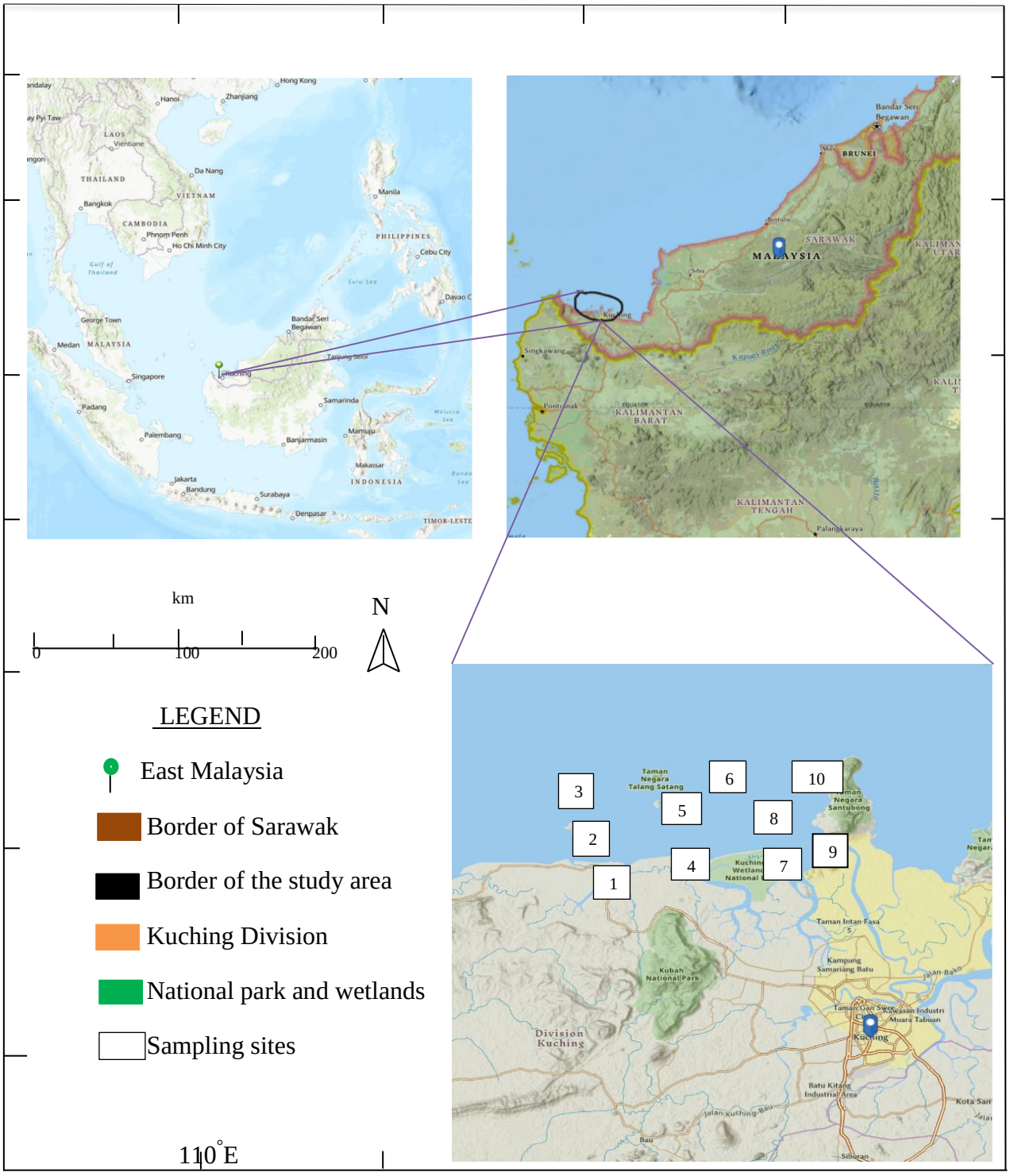

Figure 3.1: Map of study area showing sampling sites

Note: On the map, the sampling site codes were labelled numerically for easy identification of sampling position but the actual naming of each sampling site is attached with CZ for example sample site 1 denotes CZ1.

Table 3.1: Coordinates of sampling locations

Sample site code	Locality	Coordinates
CZ1(1),(2)	Rambungan River Estuary	N01°41'37.7" E110°08'24.5"
CZ2(1),(2)	Offshore of Batang Rambungan opposite small Satang Island	N01°44'46.8" E110°08'45.4"
CZ3(1),(2)	Offshore of Batang Rambungan adjacent big Satang Island	N01°46'22.6" E110°08'37.8"
CZ4(1),(2)	Sibu River Estuary	N01°44'46.8" E110°08'45.4"
CZ5	Offshore of Telaga Air opposite to small Satang Island	N01°45'50.4" E110°11'30.2"
CZ6	Offshore of Telaga Air adjacent big Satang Island	N01°47'23.5" E110°10'39.7"
CZ7(1),(2)	Salak River Estuary	N01°40'41.1" E110°16'59.2"
CZ8	Santubong Bay	N01°42'45.7" E110°27'63.1"
CZ9(1),(2)	Offshore of Santubong Resort	N01°44'49.6" E110°29'72.3"
CZ10	Santubong River Estuary	N01°42'32.6" E110°19'02.3"

3.2.2 Sediment Sampling and Treatment

The field studies and sample collection were conducted according to the procedure outlined by Gao (2019) from September to October 2020. The coordinates for each sampling site were determined using a handheld portable GPS, Garmin etrex. Table 3.1 shows the coordinates of sampling locations. Ten surface sediments were collected from sampling sites and four replications from each station. Sample site code designated as (1), (2) for example CZ7(1),(2) indicate that at station CZ7, two separate location each four replications with the same coordinates were sampled and thus they were treated differently. Samples were collected to a 5.0 cm depth using a Wildco grab sampler. To minimize contamination, the grab sampler was disinfected using biodegradable detergent and rinsed

with deionized water before and after each use. Sediments were placed in cleaned polyethylene containers and kept in the cooler box at a temperature of 5 °C during transportation. In the laboratory, samples were air-dried in a well-ventilated area for a week. The bulky materials such as stones and unwanted materials were removed from the sediments using stainless-steel forceps and homogenized. The dried sediment samples were pulverized into fine particles using a mortar and a pestle. Pulverized sediments were then sieved using a 55 μm mesh size sieve to obtain powdered sediments which were then placed in cleaned polyethylene containers. The samples were kept in a refrigerator for further analysis (US EPA, 2009).

The gravity corer equipped plastic tube with 50 cm length and 5 cm diameter. About 30 cm long core sediments were collected from the bottom of each sample site. Core sediments were segmented at an interval of 5 cm and then placed in cleaned plastic bags, kept in the cooler box during transportation.

3.2.3 Proximate Analyses

Proximate analyses were performed based on the procedure defined by ASTM D3976-92 (2015). The proximate analyses include the determination of moisture content, ash content, and total organic matter (TOM).

3.2.3.1 Moisture Content

Moisture content is the water available in the sediment samples. It was determined by measuring the mass loss after the sample was heated under controlled conditions. Empty crucibles were weighed before placing 2.5 g of a sediment sample into it. Next, the crucibles were placed into the oven at 107 ± 1 °C for about an hour to remove

the water content of sediments (Zhu, 2014). Then the samples are cooled to room temperature before they were weighed. The differences between the weights represent the moisture of each of the sediment samples. The moisture content was expressed in percentage. Percentage moisture content was calculated using equation 3.1 below:

$$\% \text{ Moisture} = \frac{W_2 - W_3}{W_1} \times 100 \qquad \text{Equation 3.1}$$

Where W_1 = weight of the sample, W_2 = weight of dried sample and crucible at 107 °C, W_3 = weight of the empty crucible.

3.2.3.2 Ash Content

Ash content was evaluated by weighing the remaining after the combustion of sediment samples in the air. The dried sample in each of the crucibles is heated in the air over Bunsen burner until no fumes are produced. After that, they were placed into a furnace at 500 ℃ for 60 minutes. After completion, the samples were cooled in the desiccator and then weighed (W_4). The percentage of ash content was calculated using equation 3.2 below:

$$\% \text{ Ash} = \frac{W_4 - W_3}{W_1} \times 100 \qquad \text{Equation 3.2}$$

Where W_1 = weight of the sample, W_4 = weight of ash sample and crucible, W_3 = weight of empty crucible.

3.2.3.3 Total Organic Matter (TOM)

Organic carbon content was evaluated by loss on ignition (LOI) which has been extensively recognized as a proxy for organic carbon concentration (Kadhum et al., 2015). The TOM of each of the samples was calculated by using equation 3.3:

$$\text{Total organic matter} = W_4 - W_5 \quad \text{Equation 3.3}$$

Where W_4 = weight of ash content and W_5 = weight of moisture

3.2.3.4 Particle Size Analysis

Granulometric analysis was performed to determine particle size fractions in sediment and was carried according to the procedure established by US EPA (2007). Briefly, six sieves with different diameters i.e., < 0.0625 mm, 0.125 mm, 0.50 mm, 1.0 mm, and 2.0 mm were used. 300 g of dried sediment samples were sieved for 15 minutes using a mechanical shaker. The leftover of each sieve was quantified (0.01 g accuracy). Particle fractions of individual sediment texture for each study site were determined and expressed in percentage (Table 3.2).

Table 3.2: Sediment texture and particle size range (US EPA, 2007)

Sediment texture	**Particle size range (mm)**
Clay	< 0.0625
Silt	0.125 – 0.0625
Sand	0.5 – 2.0
Gravel	> 2.0

3.2.3.5 Other physicochemical parameters

The protocol for determining the particle size distribution was the hydrometer method adapted by Gee & Bauder (2002). An electrical conductivity meter was used to evaluate the electrical conductivity of the sediment samples. A glass electrode in water suspension in a ratio of 1:4 (sediment/water) was the protocol used to determine sediment's pH. The method formulated by Gupta (2007) was used to determine the proportions of carbonate ion (CO_3^{-2}) and hydro carbonate ion (HCO_3^{-1}). This was achieved by titrating with 0.05 $moldm^{-3}$ sulfuric acid. The calcium carbonate ($CaCO_3$) contents in sediment samples were evaluated using a calcimeter (Loeppert & Suarez, 1996). The turbid metric method determined the sulfate ion (SO_4^{-2}) presence in sediment samples, while spectroscopy evaluated turbidity (Gupta, 2007). The sodium acetate ($C_2H_3NaO_2$) method was used to quantify cation exchange capacity (CEC) (Loeppert & Suarez, 1996).

3.2.4 Heavy Metals Analysis

3.2.4.1 Sediment Extraction and Analysis

The procedure used to analyze sediment total heavy metal contents is acid digestion adapted by Hossner (1996). A powdered sediment sample of 0.5 g was placed in a crucible. About 3 mL of H_2SO_4 (95%) and 4 mL of HCl (96%) were added to the crucible contents. The contents of the crucibles were subjected to heating in an oven (Memmert model 30 – 70, UN 30) for 22 hours at a temperature of 125 °C to break down all organic materials. After heating, each crucible was weighed and recorded. Reheating of sediment samples was carried out in a muffle furnace (Model Ney Vulcan D – 550 series) for 4 hours at 450 °C. This was done to help remove water, moisture, and other solvents

from the sediment samples. The weights were recorded after the samples were allowed to cool. The samples were heated to dryness on a hot plate (Model Favorit HS070V2 Serial 5434) after added 1.5 mL of distilled water and 1.5 mL of concentrated HNO_3. Crucible contents were stirred for uniformity for 5 minutes after 8 mLof distilled water and 2.0 mL of concentrated HCl were added. The mixture was then filtered via filter paper (Whatman No. 42), and the content (filtrate) was top up with distilled water to 100 mL. The following dilutions were prepared; × 1.0, × 10.0, and × 100.0, and the extracts were analyzed for heavy metals of interest using Inductively Coupled Plasma-Optical Emission Spectroscopy (ICP-OES).

3.2.4.2 Quality Assurance and Control (QA/QC)

To ensure the quality and efficiency of the instrumental outcomes, QA and QC techniques were established. It includes cleaning laboratory materials and apparatus using 15% H_2SO_4, applying standard operating methods, analyzing blanks, and standard calibration and recovery of actual additions.

3.2.4.3 Inductively Coupled Plasma-Optical Emission Spectrophotometer (ICP-OES)

Analyses of the heavy metals in the samples were performed on brand PerkinElmer© ICP-OES model Avio 560 Max (Saleem et al., 2016). 1300W RF power, 2.0 L min^{-1} auxiliary flow, 0.8 L min^{-1} nebulizer flow, 15 L min^{-1} plasma flow, and 1.5 mL min^{-1} sample uptake rate were the operating conditions used for ICP-OES determination. Metals were determined using the axial view. The analytical signal was measured using 2-

point background correction and 3 replicates. Nitric acid 0.5% (v/v) was used to dilute the stock multi-elemental standard solution (1000 mg L^{-1}) to prepare the calibration standards.

The correlation coefficient between the laboratory and certified values was around 0.999984, indicating excellent agreement between the certified and measure values. The percentage recoveries obtained varied from 98 – 101%. The acceptable recovery range of CRM is 90.0 – 110% (Misa et al., 2014). Hence, the obtained values in this current study were found to be within the acceptable recovery range. Hence, the analytical instrument is suitable to for analysis of selected trace metals. Concerning precision, the relative standard deviation varied from 0.19 – 2.77%. The limit of detection (LOD) was calculated for the ten trace metals after establishing the calibration curves and equation of ICP-OES. The LOD values were computed as $3.3 \times (S.d_{blank}/y)$, where; S.d refers to mean standard deviation of blanks, and y represents the sensitivity of the calibration curve. The limit of detection (LOD) was as follows: Ni = 0.038 mg/kg, Pb = 0.009 mg/kg, Cr = 0.026 mg/kg, Mn = 0.013 mg/kg, Ba = 0.007 mg/kg, Mg = 0.015 mg/kg, Cd = 0.044 mg/kg, As = 0.003 mg/kg, Zn = 0.020 mg/kg, Al = 0.099 mg/kg, Co = 0.035 mg/kg, Na = 0.042 mg/kg, Cu = 0.031 mg/kg, and Ca = 0.068 mg/kg.

The test of accuracy shows how close a measured value or the result of the laboratory value emerges to the reference value. The accuracy performance was evaluated using sewage sludge amended soil, standardized by the Community Bureau of Reference (BCR) reference material. The motive is that the outcome of the measured values obtained from the certified reference material (CRM) analysis is often convenient for the evaluation of the accuracy of any analytical instrumentation owing to the fact that it is easy to make a comparison between the certified values and measure values and make a deduction. SPSS statistics was applied to construct the regression lines to detect the regression values. The

measure values were plotted as the horizontal axis and the certified values as the vertical axis. It was found that the certified values at which the laboratory values were obtained are assembled around the perfect correlation line, suggesting that the laboratory values were in excellent connection with the certified values.

Furthermore, accuracy was ascertained from the *Z*-score value (Misa et al., 2014). The standard score commonly called the *Z*-score is a score that produce a notion of how far a measure value from an average a data point is. In a realistic form, it is a measure of how many standard deviations above or below the mean variable a raw score is. Equation 3.4 was used to compute the *Z*-score of individual metal.

$$Z = \frac{R_{lab} - R_y}{U} \qquad \text{Equation 3.4}$$

Where U is the uncertainty of the certified value, R_v is certified value accepted as the true one, and R_{lab} is laboratory or measured value. Equation 3.5 was used for the evaluation of uncertainty of the certified values quantified at the 95% confidence level (Eurachem, Middlesex, 1998),

$$U = k \times RSD \qquad \text{Equation 3.5}$$

Where k is the coverage factor (k = 1.740, for 95% and 18 points) and U is the uncertainty of the reference value. Laboratory performance is reported as satisfactory and acceptable if *Z*-score < 2 but the performance is questionable if *Z*-score > 2 but < 3. If the *Z*-score > 3 then laboratory performance becomes unsatisfactory (Funk et al., 2007; Misa et al., 2014). The calculated *Z*-score values, the measured values, and the ratio of difference relative to the certified values expressed in percentage have been detailed in Table 3.3. The Z-score

values for all the trace elements of interest were less than 2, suggesting that laboratory performance is satisfactory and acceptable.

Table 3.3: The recovery of detected heavy metals in CRM (i.e., sewage sludge amended soil) standardized by BCR

Heavy metal	Pb	Zn	Cd	Ni	Mn	Cu	Ba	As	Co	Cr	Mg	Ca	Al	Na	Fe
CV (ppm)	171.00 ± 6.00	1059.00 ± 22.00	76.00 ± 1.20	40.60 ± 3.50	873.00 ± 12.00	137.00 ± 9.00	53.40 ± 4.10	42.00 ± 1.30	23.50 ± 2.80	415.00 ± 9.60	307.00 ± 7.10	924.00 ± 11.00	219.00 ± 6.40	89.90 ± 5.20	1072.00 ± 14.00
[a]MV (ppm)	171.88 ± 0.83	1061.79 ± 3.08	77.08 ± 0.42	41.86*	873.90 ± 0.91	138.01*	55.07*	42.69 ± 0.41	24.03 ± 0.31	416.51 ± 0.40	309.11 ± 0.68	926.1 ± 0.73	221.03 ± 0.84	92.03 ± 0.76	1078.35 ± 0.96
R_{Lab} - R_y	1.01	2.79	1.08	1.26	0.90	1.01	1.67	0.69	0.53	1.51	2.11	2.10	2.03	2.13	6.35
U	10.44	38.28	2.09	6.09	20.88	15.66	7.13	2.26	4.87	16.70	12.35	19.14	11.14	9.05	24.36
|*Z*-score|	0.10	0.07	0.52	0.21	0.04	0.07	0.23	0.31	0.11	0.09	0.17	0.11	0.18	0.24	0.26
[b]Diff (%)	0.21	0.26	1.42	3.10	0.10	0.74	3.13	1.64	2.26	0.36	0.69	0.23	0.93	2.37	0.59

CV denotes the certified value
MV represents the measured value
[a] Mean measured values of three determinations
[b] Diff. - Percentage of difference to true values (*Z*-scores) calculated based using equation 3.4
* Values without uncertainty due to insufficient CRM sample measurement repetitions

3.2.5 Environmental Assessment of Heavy Metals Contamination

3.2.5.1 Enrichment Factor

EF deals with estimating the anthropogenic impact on the media, such as soil, sediments, and others. Fe is used as a normalization metal because the sediments collected from the study area are abundant in Fe. The EF can be calculated by equation 3.6 proposed by Muller (1979).

$$EF = \left(\frac{Xn}{Fe}\right)_{sample} \div \left(\frac{Xn}{Fe}\right)_{crust} \quad \text{Equation 3.6}$$

Where $(Xn/Fe)_{sample}$ represents ratios of arithmetic average concentrations (mg/kg, dry wt) of the target heavy metals; $(Xn/Fe)_{crust}$ denotes Fe in the investigated sediments and continental earth crust according to Muller (1979). The classifications of heavy metals enrichment and their environmental risk grades in soil/sediment are shown in Table 3.4.

3.2.5.2 Contamination Factor (CF)

CF is applied to assess pollution in an aquatic ecosystem by a given toxic substance. Thus, it serves as a vital indicator of sediment contamination (Kadhum et al., 2015). The CF was computed using equation 3.7 formulated by Hakanson (1980) as:

$$CF = (Cm)_{sample}/(Cm)_{background} \quad \text{Equation 3.7}$$

Cm_{sample} denotes the concentration of a given trace metal in sediment, and $(Cm)_{background}$ is the values of reference metal, which are the average shale values of each study metal for

sedimentary rock (Turekian & Wedepohl, 1961). The CF values are grouped into four categories as listed in Table 3.4.

3.2.5.3 Geo-accumulation index (Igeo)

I*geo* makes it possible to determine pollution by comparing the present and pre-industrial concentrations of heavy metals in the earth's crust (Muller, 1979). The geo-accumulation index (I*geo*) can be calculated using equation 3.8 (Muller, 1979):

$$I_{geo} = \text{Log}_2 (C_n/1.5*B_n) \quad \text{Equation 3.8}$$

Where C_n refers to the measured concentration of the heavy metals in the sediment samples and B_n represents the geochemical background value in the earth's crust. The factor of 1.5 is introduced to reduce the impact of possible variations in the background values due to lithogenic variations (Saleem et al., 2016). The interpretation of the I*geo* values is summarised in Table 3.4.

3.2.5.4 Pollution Load Index (PLI)

PLI for each sampling site is derived as the n^{th} root of n number multiplied together by the values of the CF suggested by Tomilson et al. (1980) as shown by equation 3.9 below.

$$PLI = (CF_1 * CF_2 * CF_3 * \ldots CF_n)^{1/n} \quad \text{Equation 3.9}$$

Where n represents the number of heavy metals. PLI index is ranked into several classes, as shown in Table 3.4.

Table 3.4: Enriched factor (EF), contamination factor (CF), geo-accumulation index (Igeo) and pollution load index (PLI) range values and their environmental risk grades

Index type Single Indices	Value	Environmental risk grade	Reference
EF			Muller (1979)
	0 – 1	Background concentration or no enrichment	
	1 – 3	Minor enrichment	
	3 – 5	Moderate enrichment	
	5 – 10	Moderately severe enrichment	
	10 – 25	Severe enrichment	
	25 – 50	Very severe enrichment	
	> 50	Extremely serve enrichment	
CF			Hakanson (1980)
	< 1	Minimum contamination	
	1 to 3	Moderate contamination	
	3 to 6	Considerable contamination	
	> 6	Very high contamination	
I*geo*			Muller (1979)
	0	Uncontaminated or background concentration	
	0-1	Uncontaminated	
	1-2	moderately contaminated to uncontaminated	
	2-3	moderately contaminated	

Table 3.4 continued

	3-4	moderately to highly contaminated
	4-5	Highly contaminated
	> 5	Very highly contaminated
Integrated Index		
PLI		Tomilson et al. (1980)
	0	Perfection
	1	Baseline
	> 5	Increasing contamination

3.2.6 Ecological Risk Assessment

3.2.6.1 Sediment Quality Guidelines

Sediment-quality guidelines (SQGs) were developed in Australia and New Zealand in 2000 to predict the adverse biological impacts caused by contaminated sediments (ANZECC/ARMCANZ, 2001). The technique has been employed to determine the potential risk to aquatic organisms due to trace metal pollution in aquatic bodies (Wang et al., 2016). The assessment is established by comparing the measured trace metal contents in sediment samples with the consensus-based threshold effect concentration (TEC), probable effect concentration (PEC) values, and midway values between the TEC and PEC (i.e., MEC) (Decena et al., 2018).

3.2.6.1.1 Threshold Effect Concentration (TEC)

TEC is a sediment contamination concentration at which a toxic response has begun to be observed in benthic organisms. The state of Florida developed equation 3.10 to determine TEC based on the concentrations at which benthic organisms from aquatic

ecosystems exhibited toxic responses in the laboratory (Florida Department of Environmental Protection, 2008).

$$TEC = \sqrt{(EDS - L * NEDS - M)} \quad \text{Equation 3.10}$$

EDS-L represents the concentration at which 15% of benthos showed effects, and NEDS-L denotes concentration at which 50% of benthos showed no impact. There is no established data for EDS-L and NEDS-L for benthic organisms for this region/tropical region thus, TEC calculations may be loosely useful in temperate regions. For this reason, there is a need for the establishment of EDS-L and NEDS-L for EDS-L and NEDS-L for benthic organisms for tropical region in order for TEC to be more relevant to this region.

3.2.6.1.2 Probable Effect Concentration (PEC)

PEC is the concentration at which a large percentage of the benthic population shows a toxic response. PEC can be calculated using equation 3.11 as proposed by the Florida Department of Environmental Protection (2008).

$$PEC = \sqrt{(EDS - M * NEDS - H)} \quad \text{Equation 3.11}$$

EDS-M denotes concentration at which 50% of benthos showed effects, and NEDS-H indicates concentration at which 85% of benthos showed no impact.

3.2.6.1.3 Median Effect Concentration (MEC)

It is assumed that sediment contamination concentrations below TEC are acceptable and concentrations above the PEC are unacceptable. The region in between the

TEC and PEC is called median effect concentration (MEC). The MEC values require further study and judgment to ascertain the likelihood of environmental consequences.

3.2.6.2 Potential Ecological Risk Index (RI)

RI can be calculated using equations 12 – 14 developed by Hakanson (1980). RI is widely used in evaluating the ecological risk of heavy metals contamination in sediments (Jernelov et al., 1975). Thus, RI is calculated using the formula:

$$RI = \Sigma E_i \qquad \text{Equation 3.12}$$

$$Ei = TiFi \qquad \text{Equation 3.13}$$

$$Fi = Ci/Cb \qquad \text{Equation 3.14}$$

Where RI is the sum of all risk factors in the sediment samples; Ei is the monomial potential ecological risk factor for individual factors; Ti is the metal toxic response factor and Fi is the metal contamination factor, Ci is the calculated concentration of trace metal in the sediment sample, and Cb refers to the value of the reference element (Turekian & Wedepohl, 1961). Metal contamination factor (Fi), risk index classification, and their environmental risk intensity are highlighted in Table 3.5. The metal contamination factor data of eight out of the ten detected heavy metals in the samples were available in literature (Hakanson, 1980). Therefore, the potential ecological risk assessment of eight heavy metals was evaluated in this work.

Table 3.5: Metal contamination factor (Fi) of the selected heavy metals, classification and environmental risk intensity

Heavy metal	Co	Cu	Ni	Cr	Zn	Mn	Cd	As
Metal contamination factor	5.0	5.0	5.0	2.0	1.0	1.0	30.0	10.0
	Risk Index Value				Environmental Risk Categories			
1	< 150				Low ecological risk			
2	≥ 150 < 300				Moderate ecological risk			
3	≥ 300 < 600				Considerable ecological risk			
4	≥ 600				Very high ecological risk			

3.2.7 Statistical Analyses

SPSS 24.0 software (IBM Corp., Armonk, NY, USA) was used for basic descriptive statistical analysis of the sample data (StatSoft, 1999). This provided the mean and standard deviation for the sampled heavy metal concentrations. Bivariate analysis such as Pearson's correlation method was used to assess the correlations between trace metals and multivariate analysis such as cluster analysis and principal component analysis (PCA) were applied to study the source distribution of the selected heavy metals.

3.2.7.1 Pearson’s Correlation

The correlation coefficient of the various heavy metal pair was calculated with the aid of the Pearson’s product-moment coefficients to show the association of the heavy metals pairs in sediments. Considering heavy metals in surface sediments, Pearson's coefficient correlation analysis was carried out to assess the interrelationships between the heavy metals studied.

3.2.7.2 Cluster Analysis

Cluster analysis (CA) is an exploratory method of problems. CA aims to sort cases, data, or objects into groups or clusters. Hierarchical agglomerative cluster analysis was carried out using the Ward linkage method and the results were reported in the form of a dendrogram (Silveira et al., 2016; Decena et al., 2018).

3.2.7.3 Principal Component Analysis (PCA)

PCA is a technique that allows the examination of the correlation between variables and the identification and elimination of those that contribute little to overall variation. Principal component analysis (PCA) was carried out to assess the sources of the trace metals. PCA usually minimizes the dimensionality of the variables and amalgamates most of the variables (heavy metals) with lesser factors that describe the major variations within the data (Silveira et al., 2016).

3.3 Results and Discussion

The coastal and four rivers estuary (i.e., Santubong, Salak, Sibu, and Rambungan) are vital agricultural and transportation water resources for the Kuching Division of Sarawak. Therefore, it is necessary to evaluate their pollution status, eco-toxicological risks, and likely sources of heavy metals in the surface and core sediments to predict the contamination levels.

3.3.1 Moisture Content, Ash Content, and Total Organic Matter

Table 3.6 shows the results of percentage moisture, ash content, and TOM content in each of the samples collected from ten locations.

Table 3.6: Results of % moisture, % ash, and total organic matter in each of the sampling from different locations

Sample site code	% Moisture	% Ash	Total Organic Matter (mg)
CZ1	11.11 ± 0.07	85.52 ± 0.17	5.47 ± 0.08
CZ2	10.64 ± 0.12	89.03 ± 0.09	3.51 ± 0.11
CZ3	9.21 ± 0.09	83.93 ± 0.14	2.85 ± 0.05
CZ4	10.89 ± 0.33	91.07 ± 0.16	6.03 ± 0.14
CZ5	10.21 ± 0.10	87.22 ± 0.11	2.01 ± 0.07
CZ6	10.24 ± 0.16	85.91 ± 0.14	4.69 ± 0.11
CZ7	12.74 ± 0.11	94.11 ± 0.19	5.98 ± 0.15
CZ8	11.03 ± 0.21	88.18 ± 0.10	6.05 ± 0.10
CZ9	9.66 ± 0.18	84.79 ± 0.08	3.25 ± 0.09
CZ10	11.25 ± 0.14	89.25 ± 0.09	4.16 ± 0.15

Details of sample site codes are mentioned in the materials and methods section.

Heavy metals contents in the sediment depend not only on the chemical characteristics of the sediment but also the physical properties which usually affect the availability, mobility and ecotoxicological impact of heavy metals (El-Amier et al., 2017). The percentage moisture content in all study sites were in the range of 9.21 – 12.74% (Table 3.6). It was observed that sediments from the estuaries have high moisture content compared to coastal sediments. This maybe attributed to the texture and organic content of the sediment. Soil texture type with considerable amount of organic matter have high retaining moisture capacity. The obtained percentage ash content in all sediment samples varied from 83.93 – 94.11% (Table 3.6). Low ash content was detected in sediment from the offshore of Batang Rambungan adjacent big Satang Island, while high ash content was found in sediment collected from Salak River estuary.

The TOM obtained for the set of sediment samples analysed varied from 2.01 – 6.05 mg. Organic matter is one of the characteristics that are important in improving

sediment qualities such as the sediment structure, sediment fertility, and microbial activity. There is a variation in the functions of organic matter in the sediment, which mainly depends on the different fractions viz. particulate organic carbon, humus organic carbon, resistant organic carbon, and dissolved organic carbon (Rasheed et al., 2015).

3.3.2 Heavy metals and Sediment Size Fractions Relationships

Sediment samples collected from four rivers estuary and in the coastal of Kuching comprised of 11 – 33% of clay minerals, 53 – 71% of sand particles, and the silt fraction was 9 – 21%. The textural classifications of the various fractions of core sediment at sampling sites are summarized in Table 3.7.

Table 3.7: Textural classification of core sediment at sampling sites

Sample site code	Locality	% Sand	% Silt	% Clay	Textural Classification
CZ1	Rambungan River Estuary	68	21	11	Sandy loam
CZ2	Offshore of Rambungan River opposite to small Satang Island	53	18	29	Sandy clay loam
CZ4	Sibu River Estuary	64	25	11	Sandy loam
CZ5	Offshore of Telaga Air opposite to small Satang Island	56	13	31	Sandy clay loam
CZ7	Salak River Estuary	71	09	20	Sandy
CZ8	Santubong Bay	58	16	26	Sandy clay loam
CZ10	Santubong River Estuary	61	28	10	Sandy loam
CZ11	Offshore of Santubong Resort	54	13	33	Sandy clay loam

Sediment from the estuary of Salak River (i.e, CZ7) recorded the highest content of sand particles (71%), about 23% of the sand fraction from the Salak River estuary was coarse sand, fine sand content was 41% and 7% was very coarse sand. The textural properties exhibited that Salak River estuary sediment (CZ7) is sandy. Rambungan River estuary sediment (CZ1) recorded the second-highest amount of sand fraction (68%), 11% silt fraction, and 21% clay minerals. It was noticed that the percentage of coarse sand (i.e., 39%) is higher than the percentage of fine sand (i.e., 25%). The other 4% constitutes very coarse sand. The nature of the sediment texture from the estuary of Rambungan River (CZ1) is sandy loam. The behaviour of sediments texture from the other remaining estuaries (i.e., estuary of Sibu River (CZ4) and estuary of Santubong River (CZ10)} were similar to that of the estuary of Rambungan River (CZ1). Hence, they were detected to be sandy loam. Concerning the respective percentages of sediment textural compositions, it was noticed that all sediments sampled from the coastal stations were sandy clay loam. The order of very coarse sand recorded in all sediment samples is as follows: CZ2 < CZ11 < CZ5 < CZ8 < CZ10 < CZ4 < CZ1 < CZ7. It was observed that smaller and lighter material were assembled in the sediments from the coastal sites whereas larger and heavier fractions of suspended materials were seen deposited in the sediments from the selected river estuaries during the separation of sediment into various fractions. Farkas et al. (2007) opined that with the decrease in flow velocity in the reservoirs, smaller and lighter materials assembled towards the outlet of the reservoir while larger and heavier materials are gathered close to the inlet. With regards to the visual examination of the materials deposited in the sediment samples, confirmation from the granulometry analysis, and Farkas et al. (2007) study, it can be deduced that there is a likelihood of a decrease in flow velocity within the vicinity of the estuaries as water is flowing from the rivers to join the ocean. That may be the reason why

there are depositions of smaller and lighter materials in sediments collected from the coastal sites and depositions of larger and heavier materials in sediments from the selected estuaries.

To evaluate the correlations between sediment particle fractions (Table 3.7) and detected heavy metals (Table 3.9), Pearson's correlation matrix between sediment particle fractions and detected heavy metals concentrations was carried out (Table 3.8). Significant strong negative relationships were noticed between Cd and 0.0625 – 2.0 mm fraction ($r = -0.71$, $p < 0.01$) and Zn and 0.0625 – 2.0 mm fraction ($r = -0.69$, $p < 0.01$). There was an observation of significant strong positive relationships between Zn and < 0.0625 – 2.0 mm fraction ($r = 0.98$, $p < 0.05$), Pb and < 0.0625 mm fraction ($r = 0.74$; $p < 0.05$), Ba and < 0.0625 mm fraction ($r = 0.71$; $p < 0.01$), and Cu and < 0.0625 mm fraction ($r = 0.88$; $p < 0.05$). Additionally, strong positive correlations were observed between Ca and < 0.0625 mm fraction ($r = 0.68$) and As and < 0.0625 mm fraction ($r = 0.61$). Notification of positive medium correlations were recorded between Co and < 0.0625 mm fraction ($r = 0.51$) and Al and < 0.0625 mm fraction ($r = 0.51$). Wang et al. (2016) and Nawrot et al. (2020) studies confirmed this correlations connected with fraction > 0.0625 mm, the absolute content of trace elements in sediments decreases. No correlations happened between the granulometric fractions and the other trace metals (i.e., As, Mn, Al, Ca, Fe, Co, Ni, Na, and Mg). Silveira et al. (2016) and Ji et al. (2018) have reported that trace elements are predominantly connected with finer portion of sediments. Their studies confirm the significant strong positive relationships between some trace elements (i.e., Zn, Ba, Pb, and Cu) and clay minerals and strong positive correlations between As or Ca and clay fractions including positive medium relationship between clay fractions and Al, unlike gravel or sand portions.

Table 3.8: Pearson's correlation matrix between analyzed heavy metals and sediment granulometric fraction expressed in percentage of the surface sediment samples

Particle fraction	< 0.0625 mm	0.0625–2.0 mm
Pb	0.74*	-0.39
Zn	0.98*	-0.69*
Cd	0.36	-0.71*
Ni	0.16	-0.21
Mn	0.29	0.26
Cu	0.88*	-0.17
Ba	0.71**	-0.21
As	0.61	-0.44
Co	0.51	-0.51
Cr	0.41	0.52
Mg	0.41	-0.41
Ca	0.68	-0.24
Al	0.51	0.25
Na	0.24	-0.56
Fe	0.28	0.06

*Correlation is significant at the 0.5 level (2 – tailed)
**Correlation is significant at the 0.1 level (2 – tailed)

Sediment pH, EC, and other chemical properties of sediments influence heavy metals availability, movement (mobility), and eco-toxicological effects (Aslam et al., 2021). The average pH values obtained from the sediment samples were in the range of 7.29 ± 0.10 to 8.30 ± 0.05, suggesting alkaline conditions (Table 3.9). A pH value between 6.5 and 7.0 is viewed as a compost indicator where decomposition of organic matter occurs (Alsaleh et al., 2018). The surrounding vegetation (mangrove) of the study area is the major contribution of high compost desposition in the sediment and the last major flood incident that occurred on 17th January 2015 may have a huge influence on the compost deposit in the sediments. The

major indicator for assessing salinity in sediment is electrical conductivity (EC). The obtained results for the EC varied from 0.62 ± 0.01 to 2.13 ± 0.02 µS/m (Table 3.9). Dissolved salt and other inorganic chemicals conduct electrical current, conductivity increases as salinity increases. Organic compounds like oil do not conduct electrical current very well and therefore have low sediment conductivity. Sediment samples collected from ten different sampling locations at the study sites showed low CEC values (i.e., 6.21 ± 0.04 – 8.13 ± 0.02 $cmol_{(+)}/kg$). For $CaCO_3$, samples collected at sampling sites with high $CaCO_3$ content is in the order of CZ1 < CZ6 < CZ5 < CZ7 < CZ10 < CZ2 < CZ4 < CZ9 < CZ8 < CZ3 (Table 3.9). Carbonate sediment deposition is due to the combination of light penetration and siliciclastic. Increasing sediment pressure may account of increases the slubility of calcium carbonate in sediment. Sediment that has an elevated pH, those above 7, is usually dominated by carbonate and most commonly calcium carbonate. Also, carbonate sediments are commonly formed in shallow, warm oceans either by direct precipitation out of seawater or by biological extraction of calcium carbonate from seawater to form skeletal material.

Table 3.9: Sediment pH, EC, and other chemical features of the investigated surface sediment samples at each sampling site (n = 4).

Parameters/Location	CZ1	CZ2	CZ3	CZ4	CZ5	CZ6	CZ7	CZ8	CZ9	CZ10
Sediment pH and EC										
pH	7.94 ± 0.03	8.30 ± 0.05	7.68 ± 0.05	7.59 ± 0.08	7.99 ± 0.03	7.88 ± 0.24	7.99 ± 0.21	7.73 ± 0.05	7.29 ± 0.10	7.61 ± 0.12
EC µs/m	0.64 ± 0.01	2.13 ± 0.02	2.29 ± 0.01	1.83 ± 0.02	2.04 ± 0.01	2.13 ± 0.22	2.04 ± 0.11	0.62 ± 0.01	1.85 ± 0.02	0.88 ± 0.06
Soluble Anions (mmol/L)										
CO_3^{2-}	-	-	0.01	0.05	-	0.01	0.05	-	0.07	0.09
HCO_3^-	0.37 ± 0.01	0.53 ± 0.02	0.89 ± 0.01	0.64 ± 0.01	1.21 ± 0.01	0.44 ± 0.01	0.62 ± 0.04	0.94 ± 0.06	0.88 ± 0.03	1.55 ± 0.14
Cl^-	0.15 ± 0.01	0.31 ± 0.07	0.28 ± 0.03	0.25 ± 0.06	3.51 ± 0.02	0.13 ± 0.01	0.42 ± 0.06	0.31 ± 0.03	0.51 ± 0.07	4.02 ± 0.16
SO_4^{2-}	4.11 ± 0.02	5.21 ± 0.01	1.94 ± 0.02	9.66 ± 0.03	2.97 ± 0.01	3.99 ± 0.13	4.78 ± 0.11	1.69 ± 0.11	7.05 ± 0.33	3.46 ± 0.09
Other soluble Cations (mmol/L)										
CEC ($cmol_{(+)}$/kg)	8.13 ± 0.02	8.02 ± 0.21	6.41 ± 0.04	7.81 ± 0.02	6.69 ± 0.02	6.22 ± 0.15	8.61 ± 0.17	5.61 ± 0.11	5.81 ± 0.19	7.71 ± 0.25
Gypsum %	0.31 ± 0.07	0.18 ± 0.03	0.15 ± 0.03	0.26 ± 0.02	0.51 ± 0.04	0.49 ± 0.03	0.23 ± 0.05	0.48 ± 0.09	0.57 ± 0.05	1.21 ± 0.05
$CaCO_3$ %	0.81 ± 0.01	8.51 ± 0.04	15.24±0.06	9.33 ± 0.01	6.16 ± 0.03	0.93 ± 0.07	7.33 ± 0.08	11.04±0.89	10.13 ± 0.16	8.22 ± 0.21

3.3.3 Distribution of Heavy Metals in Surface Sediments

Heavy metal concentrations in surface sediments sampled from the coastal and in four rivers estuary are shown in Table 3.10. Ten heavy metals were detected in all sediment samples, and their average concentration followed the order: Cd < As < Co < Cu < Ni < Cr < Zn < Mn < Mg < Fe. The obtained evaluation showed moderate As, Mg, Cr, and Ni pollution. The concentration of detected zinc (Zn) in the surface sediments varied from 57.02 to 155.05 mg/kg with an average concentration of 133.45 mg/kg. Anthropogenic activities including municipal wastewater discharges, manufacturing processes involving metals; and atmospheric fallout are the major source of Zn pollution in the sediments. The high mobility nature of Zn and it ability to adsorb and scavenged by hydroxides and oxides are the reasons of its biological availability in sediments of the study area. Because, it has been reported that Zn has high mobility, and dissolved Zn can potentially increase its biological availability in an aquatic ecosystem (Morillo et al., 2004; Mito et al., 2004; Yang et al., 2012). O'sullivan et al. (2012) suggested that Zn can readily adsorb and be scavenged by the hydroxides and oxides. The high level of Zn concentration in the surface sediments could also be attributed to the fuel station, vehicle emissions, and commercial discharges nearby the study area (Sekabira et al., 2010; Yang et al., 2012).

The detected arsenic (As) concentration in the samples detected ranged from 3.02 to 6.88 mg/kg with a mean value of 5.13 mg/kg (Table 3.10). The dominant factors that influence the concentration of As in the sediments of the study area are the parent rocks and human activities. The factors such as climate, the organic and inorganic components of the sediments and redox potential status also affect the level of As in the sediments. As primarily exists in the ecosystem because of natural processes (i.e., volcanic processes and weathering of rocks, etc.) and anthropogenic activities such as mining,

industrial pollution, fertilizer, pesticides, and insecticides (Giesy et al., 1999; US EPA, 2009). The elevated concentration of As in the study area could also be attributed to the excessive use of inorganic fertilizer and domestic sewage discharges (Barak & Mason, 1989). This study confirmed Barak and Mason (1989) study.

The iron (Fe) concentrations in the analysed samples ranged from 10142 to 18483 mg/kg, with a mean value of 16415 mg/kg (Table 3.10). In the current study, it was observed that Fe concentrations detected in all samples were higher compared to other trace metals. Two sources of Fe, dust and flash floods transported material, were found to possess distinct geochemical signatures: dust was found to be enriched in total and highly reactive Fe relative to the sediments in creek beds. Combination of these two sources leads to an increase of highly reactive Fe in sediments with water depth. This increase, in turn, results in formation of a lateral redox gradient with sulfidic pore-waters near the shore, and ferruginous-manganous pore-waters and cryptic sulfur cycling at the deeper water sites. It has been reported that, apart from erosion, weathering, and some natural sources; the dominance of Fe in sediments is caused by large-scale anthropogenic processes including agricultural activities, solid waste, and urban-industrial discharges (Pandey & Singh, 2015). Nearby agricultural activities at the study sites is a factor of Fe element dominance in the sediment.

Table 3.10: Heavy metals concentrations (mg/kg) in surface sediments from the coastal and in four rivers estuary of Sarawak (n=4)

Sample site code	Zn	As	Fe	Mg	Mn	Ni	Cr	Cu	Co	Cd
CZ1(1)	57.02±0.09	3.02±0.08	13572±5.21	7261±2.02	102.61±0.94	18.63±0.71	21.64±1.13	11.02±1.05	5.08±0.31	0.01±0.003
CZ1(2)	101.34±0.21	3.73±0.11	14356±8.61	7183±5.06	116.43±1.52	11.30±1.01	34.56±1.10	10.82±0.84	3.98±0.16	0.01±0.001
CZ2(1)	104.09±0.17	2.98±0.04	14895±9.87	7929±2.71	99.42±0.83	16.42±0.81	33.81±2.21	10.13±0.95	4.33±0.41	0.02±0.003
CZ2(2)	107.14±0.26	5.41±0.10	10142±6.41	8018±1.81	98.93±0.74	19.95±1.21	33.53±1.41	10.01±0.46	2.99±0.11	0.03±0.001
CZ3(1)	134.03±0.11	4.19±0.07	15524±9.01	8099±2.68	108.67±2.11	20.06±0.09	34.66±0.89	9.69±0.89	4.73±0.31	0.01±0.001
CZ3(2)	137.11±0.42	4.88±0.13	15872±5.81	8131±1.41	117.59±2.48	24.01±0.16	36.61±2.22	9.89±0.41	5.93±0.24	n.d
CZ4(1)	141.26±0.39	5.43±0.09	16324±6.91	9562±0.96	142.07±1.79	24.98±0.71	38.11±1.51	10.98±1.21	5.98±0.31	0.06±0.001
CZ4(2)	144.09±0.41	6.29±0.10	18483±10.73	8938±2.31	149.62±1.69	22.00±0.11	40.21±2.61	12.06±1.13	6.07±0.43	0.02±0.002
CZ5	147.03±0.72	6.67±0.09	17327±9.19	9183±4.86	152.88±2.51	25.57±0.94	41.85±1.31	12.77±0.91	7.01±0.68	n.d
CZ6	148.17±0.18	5.99±0.13	17114±12.61	9173±3.14	183.36±3.10	26.11±0.69	41.28±1.88	13.61±1.01	6.99±0.77	0.01±0.003
CZ7(1)	150.06±0.21	6.88±0.23	17210±6.43	9317±2.51	183.94±1.42	26.91±0.76	44.69±2.10	14.93±1.66	7.61±0.39	0.03±0.005
CZ7(2)	154.19±0.66	5.96±0.11	18222±12.11	8990±5.19	194.90±3.51	27.28±0.82	43.74±1.21	14.96±1.44	7.92±0.94	n.d
CZ8	151.14±0.28	4.85±0.27	17982±7.17	9077±2.38	164.27±2.62	20.32±0.91	47.99±0.99	15.05±0.89	6.28±0.61	0.03±0.002
CZ9(1)	155.05±0.53	5.12±0.11	14943±6.46	9141±4.92	154.99±1.11	17.32±0.94	38.28±1.03	14.91±0.64	6.81±0.95	0.04±0.001
CZ9(2)	150.18±0.81	5.11±0.15	15337±8.04	8553±3.41	158.26±2.75	10.54±0.61	36.18±1.71	10.64±0.48	5.01±0.91	n.d

Table 3.10 Continued

CZ10	153.22±0.95	5.59±0.21	15194±8.71	9003±3.21	158.84±1.46	11.45±0.94	33.60±2.04	10.71±0.71	5.13±0.17	n.d
Mean	133.45±0.01	5.13±0.021	16415±6.36	8597±2.49	142.92±1.25	20.18±0.72	37.55±0.61	12.01±0.89	5.74±0.01	0.02±0.001
Average shale	95.00	13.00	47200	15000	850.00	68.00	90.00	45.00	19.00	0.300

n.d: Not detected

The occurrence of magnesium (Mg) in sediments is either a solute in pore-fluids or an essential constituent in the formation of late-stage diagenetic chlorite and dolomite (US EPA, 1989). Mg concentration ranged from 7183 to 9562 mg/kg with an average value of 8597 mg/kg (Table 3.10). Mg is the second highest concentration following Fe in the collected surface sediments from the study area. High Mg concentration in sediments of the study area is largely controlled by continental weathering and coastal authigenic formation. In addition, the relatively high content of Mg is attributed to $CaCO_3$ leaching out from the sedimentary column or human activities such as industrial pollution, waste discharges, excessive pesticides, and fertilizer application (Cardwell et al., 1999). Seawater is also a dominance source of Mg in the study area because of decomposition of pre-existing rocks by weathering, transportation, and deposition of the weathering products as sediments.

Manganese (Mn) concentration varied from 98.93 to 194.90 mg/kg with an average of 142.92 mg/kg (Table 3.10). Mn occurs naturally in sediment due to weathering of parent rocks, yet anthropogenic sources such as industrial wastewater and mining around the study area increases Mn concentration. Also, the avaialability of Mn in the sediments can also be influenced by the existence of MnO_2 in oxic surface sediments (Pradit et al., 2010; Yang et al., 2012). Loska & Wienchula (2003) suggested that Mn pollution results from deposition in the atmosphere and organic material emissions. The nickel (Ni) concentration in the surface sediments ranged from 10.54 to 27.28 mg/kg with an average value of 20.18 mg/kg (Table 3.10). Direct leaching from rocks is the major factor of high concentrations of Ni in sediment water of the study site. Wind-blown dust, derived from weathering of rocks and soils, and forest fires is another source of Ni content in sediment samples. Loska & Wienchula (2003) suggested that Ni is primarily available in

the organically bound form in the soil, which under certain pH (acidic or neutral) conditions accelerate its movement and biological availability. According to Anderson et al. (1978) the primary anthropogenic sources of Ni pollution are fuel combustion and agricultural wastes. Thus, agricultural activities and activities which require fuel burning closed to the study site are the man-made sources of Ni pollution in the sediments.

The concentration of chromium (Cr) varied from 21.64 to 47.99 mg/kg with an average concentration of 37.55 mg/kg (Table 3.10). Cr in sediment is as result of abundant industrial and transport-related sources at the study area. Although, Cr is regarded as low mobility trace metal usually under moderately oxidizing and reducing conditions and nearly neutral pH but can find themselves in sediment due to solid-phase chemical speciation of Cr and its environmental mobility. Zarei et al. (2014) reported that Cr and its associate compounds are used in synthesizing steel and some alloys, pigment production, and chrome plating. Thus, it can also be deduced that the steel and iron industry and chrome plating are the primary sources of Cr in the study area. Copper (Cu) concentration levels detected in all sampling sites varied from 9.69 to 15.05 mg/kg with a mean concentration of 12.01 mg/kg (Table 3.10). The concentrations of Cu in the sediments come from many sources, e.g. building material and in electronic products.Cu as a mineral is of great importance for the proper growth and development of plants due to its constituent of different enzymes and proteins (Loska & Wiechula, 2003; Decena et al., 2018). Cu is extensively applied in roofing, electrical wiring, and manufacturing pigments, piping, alloys, and cooking utensils (Giesy et al., 1999). Therefore, manufacturing industries of electrical appliances, alloys, roofing materials, etc., near the study area are the primary source of Cu. It has also been reported that the pollution of the aquatic system with Cu is linked with agrochemicals (Adekola & Eletta, 2007; Yang et al., 2012).

Therefore, agricultural activities that deal with agrochemicals around the study area are also a contributor of Cu content in sediment. Increasing concnetrations of Cu in the sediments of the study is due to boat stations and boats lanes close to the study sites.

Cobalt (Co) concentration levels in the surface sediment varied from 2.99 to 7.92 mg/kg with an average concentration of 5.74 mg/kg (Table 3.10). The concentration levels of the detected cadmium (Cd) in the samples ranged from below detection level to 0.06 mg/kg with a mean concentration of 0.02 mg/kg (Table 3.10). The low concentration of Cd in sediments is due to differences in natural factors (these are usually related to geological structure) but primarily relate to human pressure, particularly land use in the catchment and air pollution. It was noticed that the estuarine sediments exhibited the highest concentration of Zn, Fe, Mg, and Mn compared to the coastal sediments. This may be due to the new deposition of sediments in the estuarine sediments. Average concentrations of ten trace metals were compared to the average shale value for sedimentary rock (Turekian & Wedepohl, 1961). It was observed that only Zn contents in all sampled sites exceeded the average shale concentration for sedimentary rock. The other heavy metals concentrations in all sampled sites were below the average shale values for sedimentary rock. Thus, it can be concluded that the fundamental source of heavy metals at the studied sites is due to natural activities and little influence of anthropogenic activities which include industrial production (foundries, smelters, petrochemical plants, pesticide production and usage, chemical industry), untreated sewage sludge, and diffuse sources such as metal piping, traffic etc.

Table 3.11: Detected heavy metals concentrations in surface sediments in the study sites and in selected rivers

Location	Unit	Zn	As	Fe	Mg	Mn	Ni	Cr	Cu	Co	Cd	Reference
Coastal and selected estuaries, Malaysia	mg/kg	133.45	5.13	16415	8598	142.92	20.18	37.55	12.01	5.74	0.02	This study
Langat River, Malaysia	µg/g	-	-	28300	-	-	7.84	21.03	-	-	-	Kadhum et al. (2015)
River Subin, Ghana	mg/kg	49.70	4.82	-	-	-	-	55.80	6.66	-	1.16	Adomako et al. (2008)
River Ganga, India	µg/g	67.76	-	31989	-	372.04	26.70	69.94	29.75	-	-	Pandey & Singh (2015)
River Tigris, Turkey	mg/kg	509.84	-	-	-	-	284.00	135.81	1257.76	-	-	Chien et al. (2002)
River Jialu, China	mg/kg	107.58	-	-	-	-	42.44	60.80	39.22	-	-	Fu et al. (2014)
Mangonbangon River, Philippines	mg/kg	213.45	-	22006	-	261.97	61.14	89.45	116.36	15.31	-	Decena et al. (2018)
Shur River, Iran	Ppm	522.00	-	-	-	-	-	-	9174.00	-	-	Karbassi et al. (2008)

Table 3.11 Continued

Korotoa River, Bangladesh	mg/kg	-	-	-	-	-	95.00	109.00	76.00	-	-	Islam et al. (2015)
River Gomti, India	mg/kg	76.34	-	-	-	-	23.92	16.19	23.23	-	-	Gupta et al. (2014)
River Huaihe, China	mg/kg	-	-	28300	-	-	7.84	21.03	-	-	-	Wang et al. (2016)

The average concentrations of heavy metals in surface sediment were compared with other studies of heavy metals in rivers in the world (Table 3.11). The Zn concentrations detected in all sampled sites were lower than Zn content in Tigris River sediment, Mangobangon River sediment (Decena et al., 2018), and shur River sediment (Karbassi et al., 2008). The high detected Zn concentration in the sediments of the study sites is due to discharges of smelter slags and wastes and the use of commercial products such as fertilizers and wood preservatives that contain Zn. Furthermore, the average concentrations of Cu in the studied area were below Cu contents reported values from surface sediments from Tigris River (Chien et al., 2002), Mangonbangon River sediment (Decena et al., 2018), Jialu River sediment (Fu et al., 2001), Krotoa River sediment (Islam et al., 2015), and Gomti River sediment (Gupta et al., 2014) (Table 3.11). Low level of Cu in sediments of the studied sites is due to low anthropogenic sources of diffuse Cu contamination which include fungicidal treatments, sewage sludge, atmospheric deposition, local industrial contamination, and particles from car brakes. The mean concentrations of Ni in all sediment samples were lower than values reported in surface sediments from Tigris River (Chien et al., 2002), Jialu River (Fu et al., 2014), Mangonbangon River (Decena et al., 2018), Korotoa River (Islam et al., 2015), and Gomti River (Gupta et al., 2014). Low Ni in sediments from the studied sites is due to low Ni emitted anthropogenic sources, including sulphides, oxides, silicates, soluble compounds, and metallic Ni. The average concentration of Cr in this current study was below the detected level of Cr in surface sediment's from the Subin River (Adomako et al., 2008), Tigris River (Chien et al., 2002), Mangonbangon River (Decena et al., 2018), and Korotoa River (Islam et al., 2015). Low activities of electroplating, leather tanning, and textile industries around the study sites is the reason of low Cr concentration in sediments as

compared to the selected studied rivers. The content of Mn in the sediments of Mangonbangon River (Decena et al., 2018) exceeded the values of Mn concentration in this study due to low anthropogenic sources of environmental Mn which include municipal wastewater, discharges, sewage sludge, emissions from alloy, steel, and iron production, and emissions from the combustion of fuel additives occurring at this study sites unlike Mangonbangon River. Furthermore, the detected level of Cd was higher than Cd levels detected in surface sediments from the Subin River (Adomako et al., 2008). High Cd concentrations in sediments of the study site unlike Subin River are due excessive application of phosphate fertilizers and waste incineration and disposal near the study sites. In contrast, the average concentrations of detected Fe in this study were below the concentrations of detected Fe in surface sediments from Mangonbangon River (Decena et al., 2018) and Huaihe River (Wang et al., 2016) due to the difference in continental shelf sediments.

3.3.4 Assessment of Heavy Metals Contamination in Surface Sediment

Although, the single factor pollution index (i.e., EF, CF, and *Igeo*) method has been extensively used; it is only useful to a single pollutant and does not necessarily consider the mixture of heavy metals usually available in the contamination conditions but it has helped to determine how much the presence of a metal in sampling sites has increased relative to average natural abundance due to human activity (Chien et al., 2002). The average shale concentrations for sedimentary rock were used as background concentrations for heavy metals for calculating the geochemical indices because there were no geochemical background concentrations for the selected heavy metals for the study area (Turekian & Wdepohl, 1961). Based on EF results, the trend of heavy metal enrichments in

all sample sites followed the order: Cd < Cu < Mn < Ni < Co < As < Mg < Cr < Zn (Table 3.12). Zn is more enriched in sample sites CZ2 (i.e., offshore of Rambungan River opposite to small Satang Island), CZ9 (i.e., offshore of Santubong resort), and CZ10 (i.e., Santubong River estuary). The other sample sites showed moderate enrichments of Zn (Table 3.12).

Table 3.12: Enrichment of detected trace metals in surface sediments of the selected sampling sites

Sample site code	Zn	As	Mg	Mn	Ni	Cr	Cu	Co	Cd
CZ1(1)	2.09	0.81	0.17	0.42	0.95	0.84	0.85	0.93	0.12
CZ1(2)	3.51	0.94	1.58	0.45	0.55	1.26	0.79	0.67	0.11
CZ2(1)	3.47	0.73	2.49	0.37	0.77	1.19	0.71	0.72	0.21
CZ2(2)	5.25	1.94	1.64	0.39	1.37	1.73	1.04	0.73	0.47
CZ3(1)	4.29	0.98	1.61	0.75	0.90	1.17	0.66	0.76	0.10
CZ3(2)	4.29	1.12	1.61	0.80	1.05	1.21	0.65	0.93	n.d
CZ4(1)	4.30	1.21	1.84	0.83	1.06	1.22	0.71	0.91	0.58
CZ4(2)	3.87	1.24	1.52	0.93	0.83	1.14	0.68	0.82	0.17
CZ5	4.22	1.40	1.67	0.92	1.02	1.27	0.77	1.00	n.d
CZ6	4.30	1.27	1.69	1.11	1.06	1.27	0.83	1.02	0.09
CZ7(1)	4.33	1.45	1.70	1.10	1.09	1.36	0.91	1.10	0.27
CZ7(2)	4.20	1.19	1.55	1.20	1.04	1.26	0.86	1.08	n.d
CZ8	4.18	1.00	1.59	1.00	0.78	1.40	0.88	0.87	0.26
CZ9(1)	5.15	1.24	1.93	0.94	0.80	1.34	1.05	1.13	0.42
CZ9(2)	4.88	1.21	1.76	1.03	0.48	1.24	0.73	0.81	n.d
CZ10	5.01	1.34	1.86	0.98	0.52	1.16	0.74	0.84	n.d
Mean	4.21	1.19	1.64	0.83	0.89	1.25	0.80	0.90	0.18

Details of sample site codes are mentioned in the materials and methods section.
n.d: not detected

High enrichment of Zn was detected in a sample collected from the offshore of Batang Rambungan opposite small Satang Island i.e., CZ2(2), which could be attributed to industrial discharges and domestic sewage. The EF values for As in collected samples at sampled sites CZ1 (i.e., Rambungan River estuary), CZ2 (i.e., Batang Rambungan opposite small Satang Island), and CZ3(1) (i.e., offshore of Batang Rambungan adjacent big Satang

Island) were below 1, indicating no enrichment. The EF values for As for other sampled sites were between 1 and 3, showing minor enrichments. The highest EF value for Mg is observed in a sample collected from Rambungan River estuary, CZ2(1), with a value of 2.49, indicating minor enrichment (Table 3.12). Except for CZ1(1), the other sampled sites have EF values for Mg between 1 and 3, suggesting minor enrichment. Most of the EF values for Ni and Cr in the samples were between 1 and 3, indicating minor enrichment while, most of the estimated EFs for Co and Cd were below 1, suggesting background concentration. The high EF values obtained for some heavy metals in some sampled stations may be ascribed to anthropogenic sources such as urbanization, industrial wastes deposition, etc. Heavy metals bioavailability and toxicity in sediments are determined by their concentrations and chemical form (Kwon et al., 2001; Yang et al., 2012). Thus, heavy metals in sediments with high EF values associated with labile fractions have the potential for mobility and bioavailability in aquatic environments (Islam et al., 2015).

The list of CFs of ten detected heavy metals concentrations in surface sediments are highlighted in Table 3.13. The trend of obtained CFs values for heavy metals in all samples were similar and followed the order: Cd < Mn < Cu < Ni < Co < As < Fe < Cr < Mg < Zn. Almost all the CFs values of detected heavy metals were below 1 in all sample sites, suggesting minimum contamination conditions except for Zn, which showed moderate contamination in some sample sites (Table 3.13). The highest CF value for Zn (i.e., CF = 1.63) was recorded in a sample collected from the offshore of Santubong Resort i.e., CZ9(1), suggesting moderately contamination. This may be attributed to commercial activities and vehicular effluence. Also, the obtained CFs values for As, Fe, Mg, Mn, Ni, Cr, Cu, Co, and Cd were below 1, which could be ascribed to lithogenic influences.

Anthropogenic activities such as residential discharges, chemical control of surrounding weeds, etc., may also play a minor role.

Table 3.13: Contamination levels of detected heavy metals in surface sediments of the selected study sites

Sample site code	Zn	As	Fe	Mg	Mn	Ni	Cr	Cu	Co	Cd
CZ1(1)	0.60	0.23	0.29	0.48	0.12	0.27	0.24	0.25	0.27	0.03
CZ1(2)	1.07	0.29	0.30	0.48	0.14	0.17	0.38	0.24	0.21	0.03
CZ2(1)	1.10	0.23	0.32	0.53	0.12	0.24	0.38	0.22	0.23	0.07
CZ2(2)	1.13	0.42	0.22	0.54	0.12	0.29	0.37	0.22	0.25	0.10
CZ3(1)	1.41	0.32	0.33	0.54	0.13	0.30	0.39	0.22	0.31	0.03
CZ3(2)	1.44	0.38	0.34	0.54	0.14	0.35	0.41	0.22	0.32	n.d
CZ4(1)	1.47	0.42	0.35	0.64	0.17	0.37	0.42	0.24	0.32	0.07
CZ4(2)	1.52	0.48	0.39	0.60	0.18	0.32	0.45	0.27	0.37	0.07
CZ5	1.55	0.51	0.37	0.61	0.18	0.38	0.47	0.28	0.37	n.d
CZ6	1.56	0.46	0.36	0.61	0.22	0.38	0.46	0.30	0.40	0.03
CZ7(1)	1.58	0.53	0.37	0.62	0.22	0.38	0.50	0.33	0.42	0.10
CZ7(2)	1.62	0.46	0.37	0.60	0.23	0.40	0.47	0.33	0.33	n.d
CZ8(1)	1.59	0.37	0.38	0.61	0.19	0.30	0.53	0.33	0.36	0.10
CZ9(1)	1.63	0.39	0.32	0.61	0.18	0.25	0.43	0.33	0.26	0.13
CZ9(2)	1.58	0.39	0.33	0.57	0.19	0.16	0.40	0.24	0.26	n.d
CZ10	1.61	0.43	0.32	0.60	0.19	0.17	0.37	0.24	0.26	n.d
Mean	1.40	0.33	0.34	0.57	0.17	0.30	0.42	0.27	0.31	0.05

Details of sample site codes are mentioned in the materials and methods section.
n.d: not detected

The I*geo* values for heavy metals in surface sediments from the coastal area and in four rivers estuary of Kuching Division were shown in Table 3.14. The I*geo* values for each heavy metals are as follows: -0.49 to 0.11 for Zn, -2.74 to -1.50 for As, -2.81 to -1.94 for Fe, -1.62 to -1.22 for Mg, -3.69 to -2.71 for Mn, -3.28 to -1.91 for Ni, -2.64 to -1.49 for Cr, -2.80 to -2.18 for Cu, -3.25 to -1.85 for Cd, and -5.49 to -2.91 for Co. The I*geo* values for As, Fe, Mg, Mn, Ni, Cr, Cu, Cd, and Co in the sediments from the study area were below class 0, indicating unpolluted site. The high I*geo* value for Zn was recorded in

surface sediment collected from the offshore of Santubong resort i.e., CZ9(1), suggesting unpolluted to moderately polluted. The positive I*geo* values for Zn at the sampled sites from CZ4(2) to CZ10 may be attributed to sewages discharges and/or effluents.

Table 3.14: Geo-accumulation indices (I*geo*) and pollution load indices (PLI) values of detected heavy metals in surface sediments of the selected study sites

Sample site code	Zn	As	Fe	Mg	Mn	Ni	Cr	Cu	Co	Cd	PLI
CZ1(1)	-1.32	-2.69	-2.38	-1.62	-3.64	-2.45	-2.64	-2.62	-2.49	-5.49	0.22
CZ1(2)	-0.49	-2.38	-2.30	-1.58	-3.46	-3.17	-1.97	-2.64	-2.84	-5.49	0.24
CZ2(1)	-0.45	-2.74	-2.25	-1.49	-3.68	-2.64	-2.00	-2.74	-2.72	-4.49	0.22
CZ2(2)	-0.41	-1.85	-2.81	-1.47	-3.69	-2.35	-2.01	-2.76	-3.25	-3.91	0.29
CZ3(1)	-0.09	-2.22	-2.19	-1.46	-3.56	-2.35	-1.96	-2.80	-2.59	-5.91	0.28
CZ3(2)	-0.06	-2.00	-2.16	-1.45	-3.44	-2.09	-1.88	-2.77	-2.27	-	0.34
CZ4(1)	-0.01	-1.84	-2.12	-1.22	-3.17	-2.03	-1.82	-2.62	-2.25	-2.91	0.34
CZ4(2)	0.02	-1.63	-1.94	-1.32	-3.10	-2.21	-1.75	-2.48	-2.23	-4.49	0.35
CZ5	0.05	-1.55	-2.03	-1.28	-3.06	-2.00	-1.69	-2.40	-2.02	-	0.52
CZ6	0.06	-1.70	-2.05	-1.28	-2.80	-1.97	-1.71	-2.31	-1.91	-5.49	0.34
CZ7(1)	0.08	-1.50	-2.04	-1.26	-2.79	-1.92	-1.60	-2.18	-1.85	-3.91	0.40
CZ7(2)	0.11	-1.71	-1.96	-1.31	-2.71	-1.91	-1.63	-2.18	-1.85	-	0.49
CZ8	0.08	-2.01	-1.98	-1.29	-2.96	-2.33	-1.49	-2.19	-2.18	-3.91	0.37
CZ9(1)	0.12	-1.93	-2.45	-1.28	-3.04	-2.56	-1.82	-2.18	-2.06	-3.49	0.35
CZ9(2)	0.08	-1.93	-2.21	-1.38	-3.01	-3.28	-1.90	-2.65	-2.45	-	0.35
CZ10	0.11	-1.80	-2.22	-1.31	-3.69	-3.16	-1.79	-2.64	-2.47	-	0.36
Mean	-0.11	-1.97	-1.62	-1.38	-3.24	-2.40	-1.85	-2.07	-2.34	-3.09	0.31

Details of sample site codes are mentioned in the materials and methods section.

An integrated pollution index (i.e., PLI) was employed to help consider the mixture of heavy metals present in the contamination conditions. The PLI values for heavy metals of the studied area were summarized in Table 3.14. The PLI values varied from 0.22 to 0.52 and with a mean value of 0.31. This indicates that there has been no occurrence of contamination in the studied area. High PLI value was found in sediment from the offshore of Telaga Air opposite to small Satang Island. In contrast, low PLI value was observed in sediment from the Rambungan River estuary and the offshore of Batang

Rambungan opposite small Satang Island. Based on the PLI values, no significant disturbances of the aquatic environment due to heavy metals pollution were observed. The PLI values can be used as baseline contamination levels in the future for pollution monitoring in the studied area.

3.3.5 Eco-toxicological Risk Assessment

The ecological risk index has been demonstrated as a highly productive tool to evaluate the total pollution of sediments of an aquatic ecosystem (Pradit et al., 2010). Protano et al. (2014) narrated that the inadequacy of updated reference metal values for a specified ecological site or geographical zone can lead to underestimating or overestimating the actual pollution load in sediments and the environmental risk index. Decena et al. (2018) reported that to get an accurate estimation of the ecological risk of metals, regular updates of reference concentrations after a certain period are required, especially in geological zones with sensitive ecological environments. To determine the risks associated with trace metals toxicity on organisms living at or near the bottom of the aquatic bodies (i.e., bodies of water forming a physiological feature for example a river, sea, etc.,); heavy metals concentrations were compared with consensus-based threshold effect concentration (TEC), probable effect concentration (PEC), and the midway concentration between TEC and PEC (i.e., MEC) values fetched from the sediments quality guidelines developed by ANZECC/ARMCANZ, 2000.

Table 3.15 presents the comparisons of consensus-based sediment-quality guidelines (SQGs) with detected heavy metals levels in the surface sediments of the selected study sites. The TEC, MEC, and PEC data of eight out of the ten detected trace metals in the samples were available in the sediments quality guidelines developed by

ANZECC/ARMCANZ, 2000. Thus, risks associated with 8 trace metals toxicity on bottom-dwelling organisms in the study area were appraised. Twenty-five percent of the samples contained Zn concentrations less than the TEC value for Zn, while 62.50% of the sampled sites contained Ni concentrations lower than the TEC value for Ni (Table 3.15). In addition, 81.25% of the samples had Cr concentrations below the TEC value for Cr. All the sampled sites contained As, Fe, Mn, Cu, and Cd concentrations below TEC values for As, Fe, Mn, Cu, and Cd, respectively. None of the samples contained heavy metals exceeding the PEC values. Heavy metals concentrations in surface sediments below TEC values were unlikely to negatively impact bottom-dwelling organisms (Chien et al., 2002). Seventy-five percent of the sampled sites contained Zn concentrations exceeding TEC but equal or less than MEC, whereas 37.50% of the samples had Ni concentrations surpassing TEC but equal or less than MEC. Furthermore, 18.75% of the sampled sites contained Cr concentrations above TEC but equal or less than MEC.

Table 3.15: Comparisons of consensus-based sediment-quality guidelines (SQGs) with detected heavy metals levels in the surface sediments of the selected study sites

		Zn	As	Fe	Mn	Ni	Cr	Cu	Cd
SQGs	TEC	120	9.8	20000	460	23	43	32	0.99
	MEC	290	21.4	30000	780	36	76.5	91	3.00
	PEC	460	33	40000	1100	49	110	150	5.00
% sample sites of detected trace metal less than TEC		25.00	100.00	100.00	100.00	62.50	81.25	100.00	100.00
% sample sites of detected trace metal greater than TEC but equal or less than MEC		75.00	0	0	0	37.50	18.75	0	0
% sample sites of detected trace metal greater than PEC		0	0	0	0	0	0	0	0

The monomial potential ecological risks (Ei) for each heavy metal and possible environmental risk index (RI) in all collected samples from the coastal and in four rivers estuary were detailed in Table 3.16. The RI index was computed based on the eight heavy metals (i.e., Zn, As, Ni, Cr, Cu, Co, and Cd). The mean potential ecological risk for studied heavy metals follow the order of Mn < Cr < Ni < Cu < Zn < Cd < Co < As. Among the analyzed heavy metals; Mn, Cr, and Ni had relatively lower RI values due to their low toxicity response factors. Futhermore, RI results in the surface sediment varied from 8.05 (CZ1) to 16.75 (CZ7). The obtained RI values for all sampled sites were lower than 150, indicating that the sediments in the studied area posed a minimum risk. The most significant Ei values were recorded for As, because, based on Hakanson's approach, the toxic response of this metal is the highest. Besides, it does not show a high ecological risk in the coastal and in four rivers estuary sediment, owing to the reason that the quantified As values are positioned below the acceptable limit. The other metals that made an important contribution to the final result of the RI index include Cu, Ni and Co.

Table 3.16: The potential ecological risk index values (RI) of detected heavy metals in surface sediments of the selected study sites

Sample site code	Ei								RI
	Zn	As	Mn	Ni	Cr	Cu	Co	Cd	
CZ1(1)	0.60	2.30	0.12	1.35	0.48	1.25	1.35	0.90	8.05
CZ1(2)	1.07	2.90	0.14	0.85	0.76	1.20	1.05	0.90	8.87
CZ2(1)	1.10	2.30	0.12	1.20	0.76	1.10	1.15	2.10	9.83
CZ2(2)	1.13	4.20	0.12	1.45	0.74	1.10	1.25	3.00	12.99
CZ3(1)	1.41	3.20	0.13	1.50	0.78	1.10	1.55	0.90	10.57
CZ3(2)	1.44	3.80	0.14	1.75	0.82	1.10	1.60	-	10.65
CZ4(1)	1.47	4.20	0.17	1.85	0.84	1.20	1.60	2.10	13.43
CZ4(2)	1.52	4.80	0.18	1.60	0.90	1.35	1.85	2.10	14.30
CZ5	1.55	5.10	0.18	1.90	0.94	1.40	1.85	-	12.92
CZ6	1.56	4.60	0.22	1.90	0.92	1.50	2.00	0.90	13.60
CZ7(1)	1.58	5.30	0.22	1.90	1.00	1.65	2.10	3.00	16.75
CZ7(2)	1.62	4.60	0.23	2.00	0.94	1.65	1.65	-	12.69
CZ8	1.59	3.70	0.19	1.50	1.06	1.65	1.80	3.00	14.49
CZ9(1)	1.63	3.90	0.18	1.25	0.86	1.65	1.30	3.90	14.67
CZ9(2)	1.58	3.90	0.19	0.80	0.80	1.20	1.30	-	9.77
CZ10	1.61	4.30	0.19	0.85	0.74	1.20	1.30	-	10.19
Mean	1.40	3.30	0.17	0.85	0.84	1.35	1.55	1.50	10.96

Details of sample site codes are mentioned in the materials and methods section.

3.3.6 Vertical Distribution Profile of Heavy Metals in Core Sediments

Figure 3.2 illustrates the vertical profile of Pb, Zn, Cd, Ni, Mn, Cu, Ba, As, Co, Cr, Mg, Ca, Al, and Na concentrations in sample sites CZ1, CZ2, CZ4, CZ7, and CZ10. These sample sites where selected for the vertical profiling because the other sample sites

look similar to that of CZ1 and CZ7, thus the chosen sample sites give true representation of the study sites. In general, all the heavy metals exhibited the consistent trend from surface toward the bottom of sediment with an exception for Cd at station CZ2 (i.e., offshore of Batang Rambungan opposite small Satang Island), Al at sampled site CZ1 (i.e., Rambungan River estuary) and CZ2, and Mg at site CZ4 (i.e., Sibu River estuary). The level of Pb, Zn, Ni, Cu, Ba, As, Na, and Co showed consistent at the upper layer (0 – 15 cm) and decreased at the bottom layer (15 – 30 cm) in almost all sampled sites. This indicates that same quantum of contamination is affecting the section of the sediments. Similar trend has been noticed for Ca and Mn, where their concentrations showed decreasing trend from 10 cm toward the bottom sediment in all sampled sites. It suggests that sediments collected from the various stations has received additional input of Pb, Zn, Ni, Cu, Ba, As, Na, Co, Ca, and Mn from other sources. Cu and Cr content showed consistent trend from surface toward the bottom sediment in almost all sampling station.

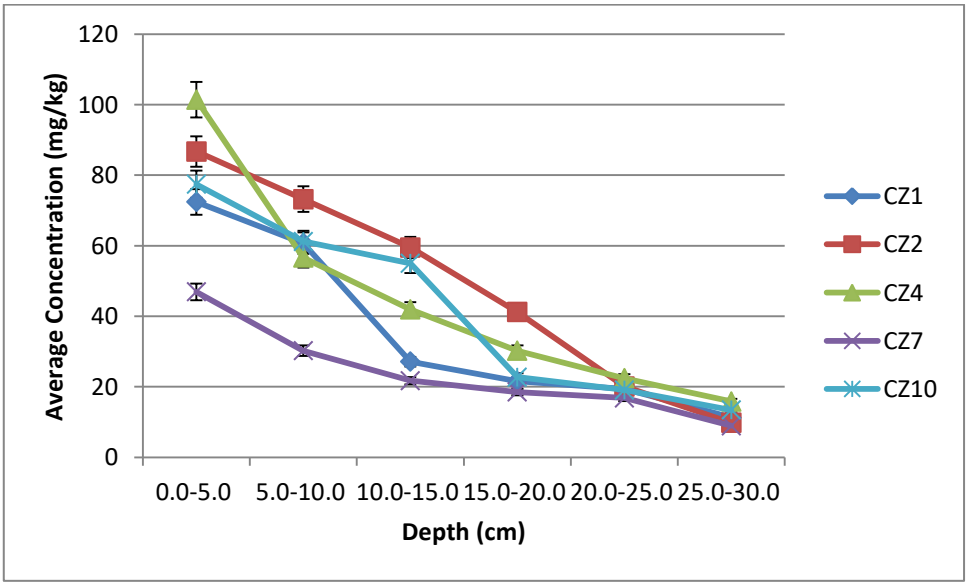

(a) Mean concentrations of Pb (mg/kg d.w)

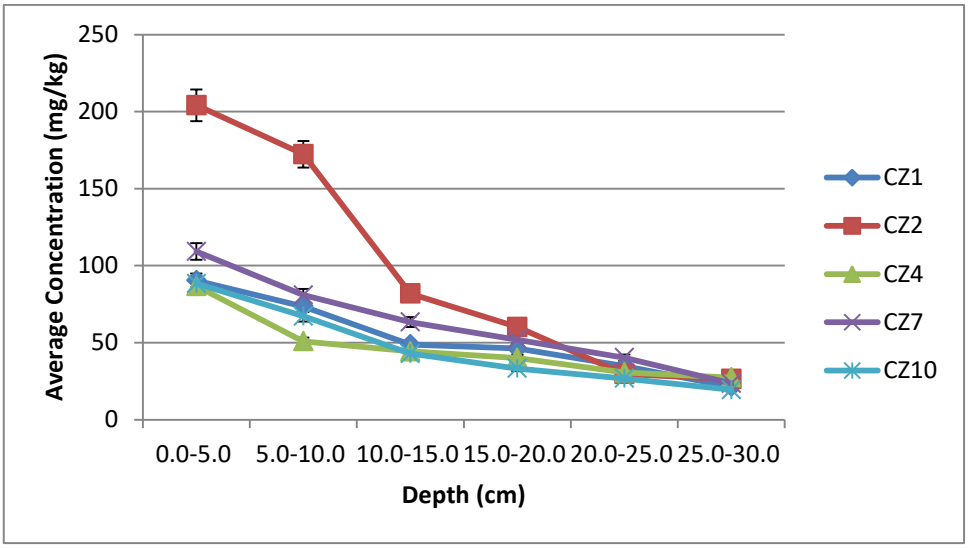

(b) Mean concentrations of Zn (mg/kg d.w)

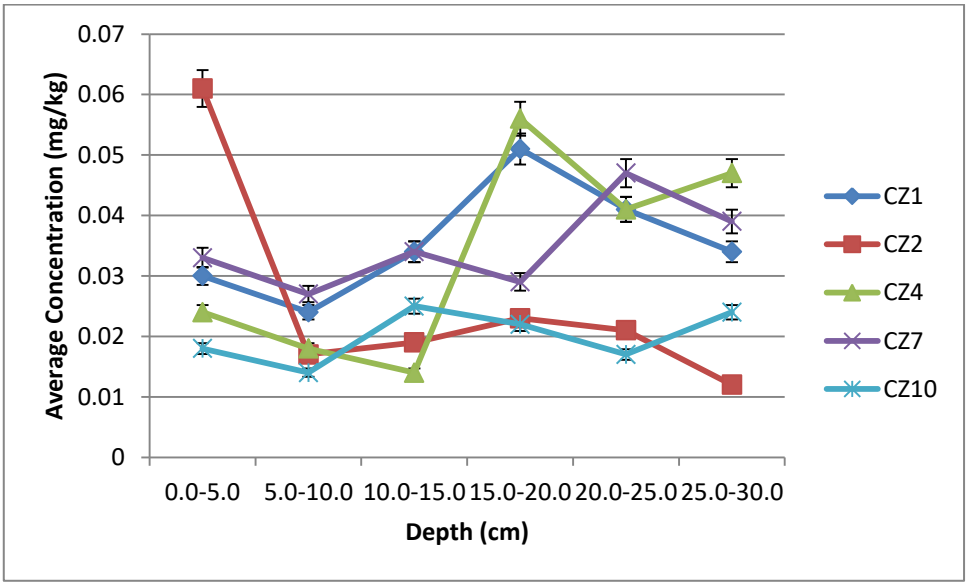

(c) Mean concentrations of Cd (mg/kg d.w)

Figure 3.2: Graph of average concentrations of selected heavy metals (mg/kg d.w.) against sediment depth/cm

3.3.7 Trend Analysis of Anthropogenic Activities Affecting Heavy Metals Deposition in Core Sediments of each Sampling Site

Figure 3.3 presents the average concentrations of heavy metals detected in core sediments from the individual sampling sites. The average concentration of Fe element

detected in each sediment samples was not included in the plots because the detected Fe concentrations were too high. Thus, Table 3.16 outlined the mean concentrations and standard deviations of Fe element detected in each sediment samples depth/cm of each sampling site of four determinations (n = 4). Surprisingly, the charts of the average heavy metal concentrations at each study site were alike and therefore, the levels of each element in each sample followed the order: Fe > Mg > Al > Cu > Zn > Pb > Ca > Na > > Ni > Mn > Cr > Ba > As > Co > Cd.

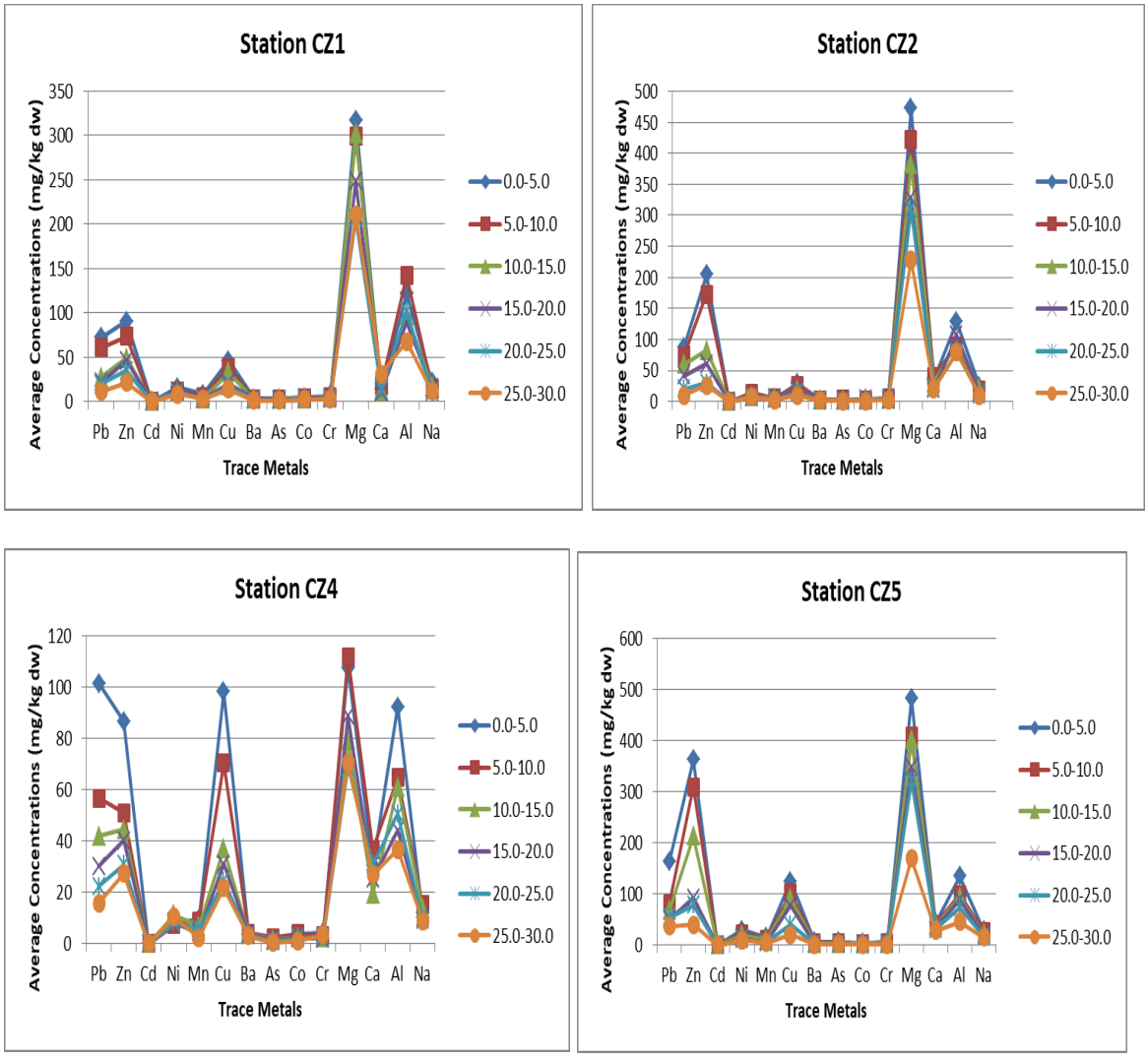

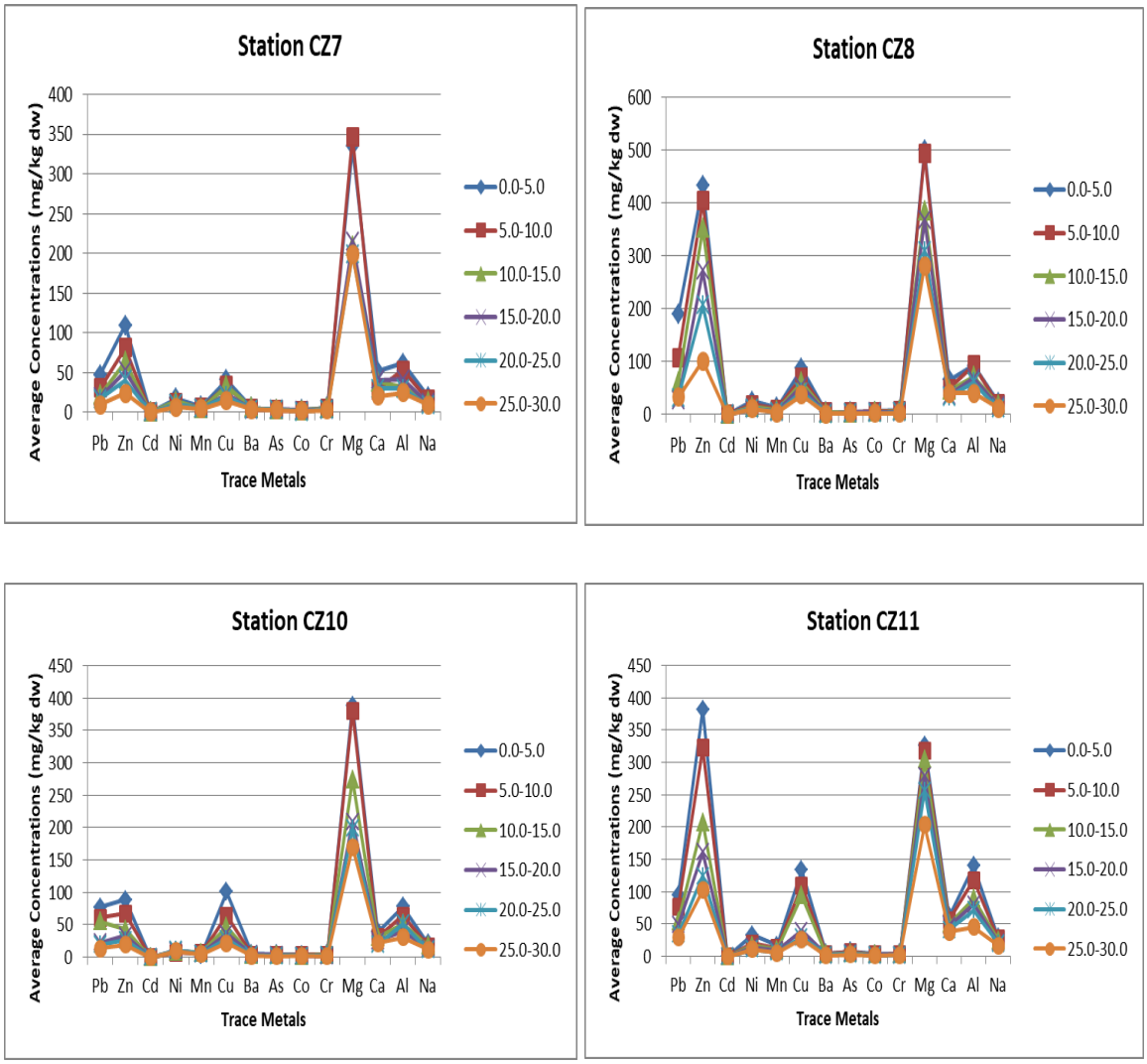

Figure 3.3: Detected average concentrations of heavy metals (mg/kg d.w.) in core sediment samples in respective sample site

Table 3.17: Detected average concentration of Fe (mg/kg d.w) in core sediment samples

Depth (cm)	CZ1	CZ2	CZ4	CZ5	CZ7	CZ8	CZ10	CZ11
0 – 5	19142 ± 6.7	20186 ± 6.4	16322 ± 5.4	33381 ± 6.3	19244 ± 5.2	29131 ± 6.2	24170 ± 5.5	35125 ± 8.9
5 –10	16033 ± 4.2	18464 ± 4.1	14276 ± 3.7	31685 ± 5.9	17169 ± 4.4	27427 ± 3.8	23673 ± 6.1	33644 ± 3.6
10 – 15	15189 ± 5.8	16336 ± 10.3	14381 ± 9.8	30926 ± 9.7	16301 ± 5.1	25872 ± 5.1	23088 ± 8.9	30911 ± 7.9
15 – 20	13946 ± 4.6	14898 ± 9.5	13914 ± 5.6	29118 ± 9.6	15398 ± 2.9	24812 ± 3.7	22814 ± 6.8	29350 ± 4.3
20 – 25	13529 ± 7.7	14146 ± 8.8	12636 ± 3.9	26763 ± 9.1	15004 ± 6.4	23090 ± 8.9	22077 ± 6.1	27081 ± 5.1
25 – 30	12086 ± 8.5	13862 ± 7.9	12012 ± 2.9	20431 ± 5.8	14118 ± 6.6	19339 ± 4.1	21463 ± 7.4	24654 ± 6.8

Details of sample site codes are mentioned in the materials and methods section

The mean concentrations of heavy metals in the core sediment from the selected estuaries were lower than the average concentrations of heavy metals in sediments collected from the coastal sites. This observation could be the confirmation of the results obtained from the granulometry investigation in this work and studies carried out by Silveira et al. (2016) and Ji et al. (2018). The low mean concentrations of heavy metals in the selected estuaries and also the higher mean concentrations of heavy metals in sediments from the coastal site may further substantiate the study carried out by Farkas et al. (2007). There was an observation of low contents of heavy metals detected in the bottom and in the middle layers sediments in almost all study sites while, high levels of heavy metals were detected in the surface layers. Significant differences existed between

heavy metal contents detected in the bottom layers sediment and the surface layers sediment. This is because the p-value (< 0.00001) for heavy metal contents detected in the bottom layers sediment and the surface layers sediment was less than the α-value of 0.05. This concern could be attributed to new heavy metals deposition due to anthropogenic influence occurring in the study sites and natural sources such as variations in geochemical features or flood incident which occurred on 17th January 2015 in Kuching.

The average contents of Pb detected in sediment samples varied from 8.9 mg/kg d.w to 188.9 mg/kg d.w. in the bottom layer of the estuary of Salak River (CZ7) to the top layer of the coastal site CZ8. Average Pb concentration in sediment from the estuary of Sibu River is three times higher compared to the Pb concentrations reported by Omorinoye et al. (2019). The contents of Pb detected in all sampling sites were lower than the mean continental shale value of Pb for sedimentary rock. The higher average concentrations of Pb in the study sites may be due to natural processes such as erosion and bush fires. In addition, influence from the anthropogenic activities such as metallic ores mining can results in high Pb concentration and Pb dispersion (Kao et al., 2007).

The surface layer sediment collected from coastal site CZ8 (i.e., Santubong Bay) recorded the highest concentration of Zn whereas the bottom layer of the estuary of Santubong River recorded the lowest concentration of Zn. The surface layer of the Salak River estuary and the surface to the middle layer sediments of the coastal sites recorded concentrations higher than the natural background level (100 mg/kg d.w.). Zn concentrations detected along the sediment depth/cm of each study sites were lower as compared to the natural background level. This shows that there is some degree of influence of anthropogenic taken place around the study sites which contributed in higher concentrations of Zn. Phosphate fertilizers, motor oil and grease, undercoating and

concrete, sewage sludge, and transmission fluid are the likely sources of Zn in the study sites (Monaci & Bargagli, 1997; Shaari et al., 2015).

Iron (Fe) concentrations detected ranged from 12011 mg/kg d.w to 35124.6 mg/kg d.w in the bottom layer of the Salak River estuary (CZ4) to the top layer of the coastal site (CZ11) (Table 3.17). It was noticed that all the surface layer sediments recorded low Fe concentrations as compared to the average shale value (47200 mg/kg d.w.) (Turekian & Wedepohl, 1961). It is more probably due to the sediments samples having higher sand content compared to global average shale values of Turekian & Wedepohl. Sand is quartz and the more quartz in the sediments, the less Fe and Al because only clays have high contents of ferroaluminosilicates. In addition, leaching of Fe compounds from the surface layer because of high salt content build-up and rain may also be the reason of low Fe content in the surface layer sediments. Furthermore, in comparison of Fe concentration detected in the surface layer sediment of Sibu river estuary in this study to Fe content reported by Omorinoye et al. (2019) in the sediment of Sibu River (4325 mg/kg d. w.), the variations in value could be ascribed to the inputs from anthropogenic activities. Salomons & Forstner (1984) have reported that iron hydroxides have the capacity of absorbing a huge some of heavy metals due to cation exchange process. Iron oxides have been reported in holding heavy metals in sediments from the aquatic environment (Horowitz & Elrick, 1987; Shaari et al., 2015). The detected average concentrations of Cd were similar in all sampling locations as well as along with sediment depth/cm (Figure 3.3). The highest concentrations of Cd were observed in the top layer sediment from the offshore of Rambungan River estuary opposite to small Satang Island recorded the highest concentrations of Cd. Beside the surface layer sediment from the offshore of Santubong resort recorded the highest concentration of Ni. The contents of Ni

detected in samples from the selected estuaries were twice lower than their corresponding coastal sites.

Mg concentrations varied from 68.8 mg/kg d.w to 499.3 mg/kg d.w. in the bottom layer sediment of the study site CZ4 to the surface layer sediment of Santubong Bay. Low contents of Ba and Co were detected in the core sediments in all sampling sites. Figure 3.3 charts revealed a decrease in Cr concentrations with an increase in sediment depth/cm with exception of study site CZ2 {0 – 0.5 cm (4.6 mg/kg d.w.) and 5.0 – 10.0 cm (4.9 mg/kg d.w.)}.

The control of river inflow on sediment transport may be the reason why low levels of Mg detected in sediments from the estuarine stations because as the water current increases, the sediment particle is lifted into water column and allows it to convey from the estuaries towards the sea coast. Thus, most of the sediment may gather in the coastal areas contributing to higher concentrations of Mg in sediments from the coastal sites than the estuary. The concentrations of Na detected in sediments from the coastal sites were almost the same as the contents of Na in sediments collected from the selected estuaries whereas, the levels of Ca detected in sediments from the coastal sites were higher compared to their corresponding estuaries. The surface layer sediment of the coastal site CZ11 recorded the highest concentration of Al and this is due to more clay content, ferroalumiosilicates. Also, this could be ascribed to the influence of anthropogenic and natural sources. Mobility of aluminum-rich sediment due to the flow of river could the prime suspect contributing to higher concentrations of Al in the coastal sites. Al metal is abundance in clays, rocks, soil, minerals (i.e., rubies, turquoise, and sapphires) (ATSDR, 2008; Shaari et al., 2015). Inverse correlations were observed between the mean contents of Na or Ca and sediment depth/cm. Shaari et al. (2015) conducted a study of heavy metals in sediment from the

estuary of the east coast of Malaysia. The average concentrations for Zn (36.13 – 125.93 μg/g d.w.), Al (0.94 – 5.59 μg/g d.w.), Co (2.00 – 11.12 μg/g d.w.), Mn (207.58 – 491.33 μg/g d.w.), Cu (14.49 – 22.33 μg/g d.w.), and Fe (6.20 – 8.95 μg/g d.w.) detected in the estuary sediment lower compared to the concentrations detected in this study. Concerning this study, the selected estuaries are associated with the South China Sea coast and near Telaga Air Township thus, discharge from the drainage system into the rivers could the major influence of higher contents of heavy metals than the study carried out by Shaari et al. (2015).

3.3.8 Trend of Heavy Metal Enrichments in Core Sediments

In order to investigate the environmental and biological hazards due to the exposure of heavy metals associated with aquatic sediment, enrichments of heavy metals were ascertained for each six sediment layers collected from each study site. Out of the 15 heavy metals of interest studied, three of them (i.e., Pb, Zn, and Cu) were enriched along the sediment depth/cm of the core sediments and also in all sampling sites (See Appendix 3.18). However, the other metals (i.e., Ba, Cr, Ni, As, Mn, Co, Al, Cd, Mg, Na, and Ca) were low enriched in all sampling sites and in all sediments depths/cm (Appendix 3.18). Generally, almost all the surface layer sediments from all study sites showed higher enrichments of studied heavy metals. It was observed that heavy metals were enriched in sediments from the coastal sites than the sediments from the selected estuaries (Appendix 3.18). Even though no significant (p-values = 0.23 was greater than the α-value of 0.05) variation of enrichment between the sediments collected from the four rivers estuary and the coastal sites and along with the sediment depths/cm were observed. The enrichment

values obtained for heavy metals in core sediments followed the order: Al < Na < Mn < Ca < Ba < Cr < Cd < Ni < Mg < Co < As < Cu <Zn < Pb (Appendix 3.18).

The enrichments of Pb were higher in all samples at all sampling sites. The estimated values for Pb in sediments collected from the Rambungan River estuary (CZ1) at depth: 5.0 – 10 cm, 10.0 – 15.0 cm, 15 – 20 cm, and 20 – 25 cm were greater than 3, indicating moderate Pb enrichment. At the depth of 0 – 5.0 cm also exhibited minor enrichment of Pb. In regards to sediment from the offshore of Rambungan River estuary opposite to small Satang Island (CZ2), the EF values obtained at a depth of 0 – 5 cm, 5 – 10 cm, 10 – 15 cm, and 15 – 20 cm were greater than 5, suggesting moderately severe Pb enrichments. At study site CZ2, the bottom layer sediments (20 – 25 cm and 25 – 30 cm) exhibited a decrease in Pb enrichment as compared to the surface and the middle layer sediments. At study site CZ4 which serve as an inlet to the location CZ5, it was observed that Pb enrichments were lower in all layers of sediments as compared to their counterpartying layers of sediment collected from study site CZ5. The obtained values of EF for Pb in the surface layer of both CZ4 and CZ5 study sites were greater than 10, suggesting severe Pb enrichments. It was observed that at a depth of 5 – 10 cm the Pb enrichment of both sites (i.e., CZ4 and CZ5) were greater than 5, indicating moderately severe Pb enrichments. In regards to Santubong River estuary (CZ7) and coastal site CZ8 sediments, there was an observation of a decrease in Pb enrichments along with the depth.

The obtained EF values in the surface layer sediment of the coastal site CZ8 is greater than 10, suggesting severe enrichment. However, the estimated EF value of Pb in the surface layer sediment from the estuary of Salak River is greater than 5, indicating moderately severe enrichment. There was an observation of moderately severe Pb enrichment at a depth of 5 – 15 cm layer sediment at the coastal site CZ8 whiles; minor Pb enrichment was recorded in the sediment from the estuary of Salak River. At the depth of 15 – 30 cm of sediment form the coastal CZ8 minor Pb enrichments were observed whereas no Pb enrichment was noticed in sediment sample collected from the estuary of Salak River. Concerning sediment from estuary of Santubong River and the coastal site CZ11, moderately severe Pb enrichment were noticed at a depth of 0 -15 cm. The bottom layer sediments from study sites CZ10 and CZ11 showed minor enrichments of Pb.

It was noticed that Zn enrichments decrease with an increase in depth at all sampling stations. Surface layer sediments from the selected estuaries have EF values ranging from 1 to 3, suggesting moderate enrichments whiles surface layer sediments from the coastal sites have EF values varying from 5 to 10, indicating moderately severe Zn enrichments. The bottom layer sediment at all sampling stations exhibited no enrichments to minor enrichments of Zn. The obtained EF values for Cu in the surface layer sediment from the coastal sites (i.e., CZ2, CZ5, CZ8, and CZ11) were lower as compared to their corresponding estuaries (i.e., CZ1, CZ4, CZ7, and CZ10). No enrichment of Ni, As, Ca, Ba, Cd, Mn, Al, Co, Na, Cr, and As were recorded in all sediment samples collected from the study sites (Appendix 3.18). Cu, Zn, and Pb enrichments in the study sites indicated that these trace elements may show hazard effects in the sediment biota by adversely influencing the primary microbial processes and cause a decline in the number of sediment microorganisms in study settings (Xu et al., 2019).

3.3.9 Possible Sources of Heavy Metals Contamination

Evaluating the sources of trace metals can help to comprehend their distribution. Thus, Pearson's correlation analysis, cluster analysis, and principal component analysis (PCA) were employed to analyze the relationship and source of the heavy metals.

3.3.9.1 Pearson's Correlation Analysis

The Spearman correlation test was employed to identify potential relationships between neurotoxic elements in each sediment separately, to discover that the availability of specific heavy metals in a sample that enables the occurrence of other metals, or if they coexist because of anthropogenic activities in the study settings. Figure 3.4 depicts significant strong negative and positive relationships between some heavy metals detected in the surface layer sediments.

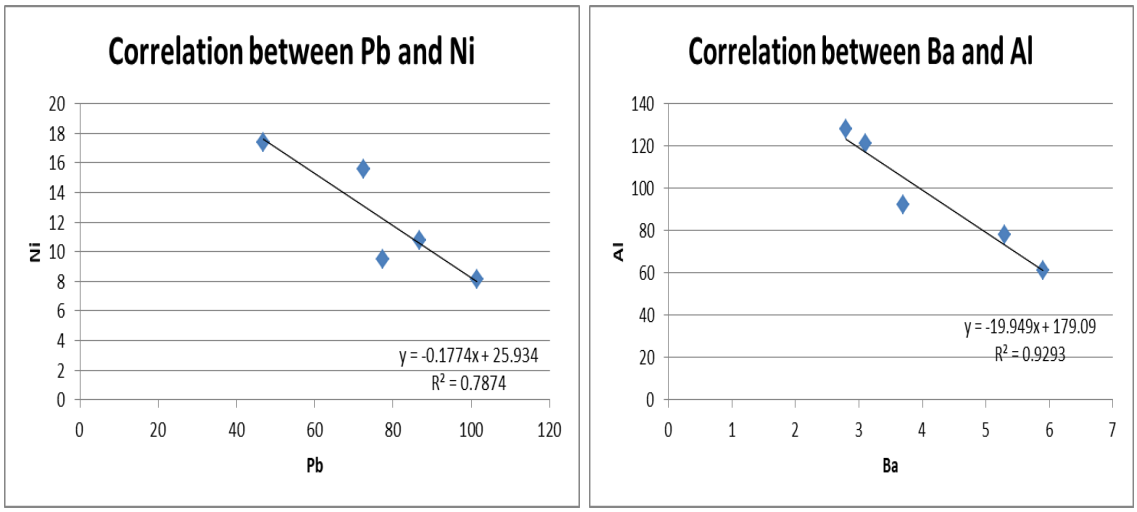

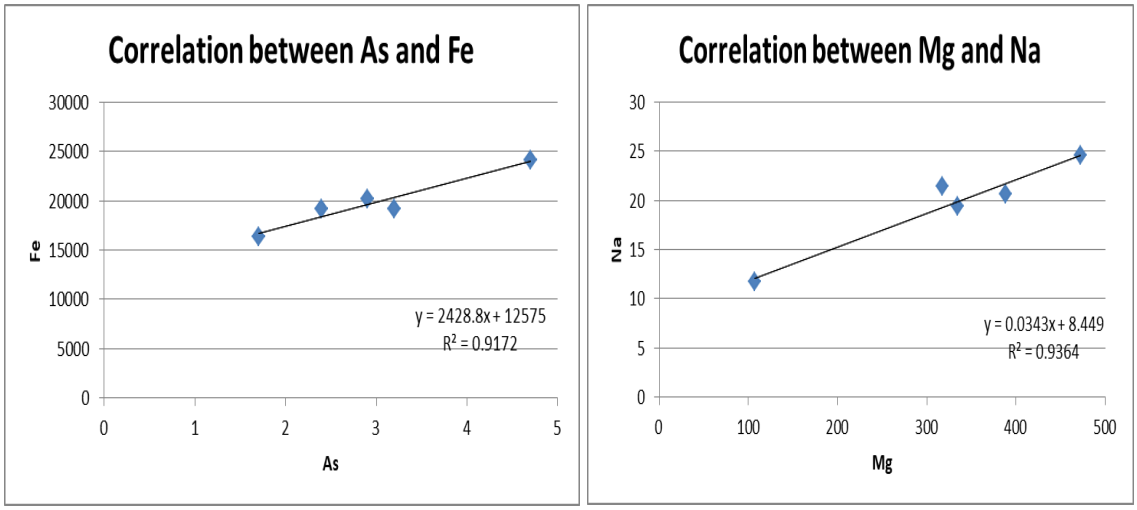

Figure 3.4: Significant strong negative and positive correlations between Pb and Ni, Ba and Al, As and Fe, and Mg and Na in the surface layer of the core sediments

Observations of strong positive correlations between Na and Zn (r = 0.62), Fe and Na (r = 0.61), Ni and Cd (r = 0.85), Mg and As (r = 0.61), Zn and Mg (r = 0.65), and Cr and Ni (r = 0.79) were noticed although the relationships were insignificance. Medium positive relationships occurred between Na and As (r = 0.57), Al and Zn (r = 0.53), and Al and Pb (r = 0.50) but the correlations were not significance. Significant strong positive correlations were documented between Mg and Na ($r = 0.97$; $p < 0.01$) and As and Fe ($r = 0.96$; $p < 0.05$) whiles; significant strong negative relationships were observed between Ba and Al ($r = -0.96$; $p < 0.01$) and Pb and Ni ($r = -0.89$; $p < 0.05$) (Figure 3.4). The coefficient values indicate that coastal and estuaries sediments collected may be receiving two or more pollutants from similar sources or the same releasing sources (Liang et al., 2017). Besides, Mn, Zn, Ca, Cd, and Cu exhibited no strong negative or positive relationship with other heavy metals (Appendix 3.19). Significant strong positive correlations between (Mg and Na) and (As and Fe) indicates similarity in geochemical features such as clay minerals (Pandey & Singh, 2015; Tian et al., 2017; Tian et al., 2020) or common pollutants sources Yang et al., 2012; Gupta et al., 2014; Yang et al., 2018).

Significant negative positive relationships between (Ba and Al) and (Pb and Ni) suggest different inputs from external sources (Zarei et al., 2014; Kanda et al., 2018; Saleem et al., 2020). Ba-Al is naturally related to Ba and Al being associated in the Earth's crust while Pb-Ni is due to anthropogenic influence. The direct correlations of Mg and Na and As and Fe within industrial, tourism, agricultural catchment suggests inputs from agronomic activities such as oil spillovers due to boat activities, application of phosphate fertilizers and pesticides and waste discharges, effluents, etc., from industries which seep into rivers to the coast via soil erosion (Wang et al., 2015; Ke et al., 2017; Fakhradini et al., 2019; Gholizadeh et al., 2019). In this study, the significant strong positive relationships between (Mg and Na) and (As and Fe) in sediment samples may be linked to oil spillovers due to boat activities and fertilizer applications from the adjacent agricultural land base source. This affirms the studies conducted by Wang et al. (2015); Ke et al. (2017); Fakhradini et al. (2019) and Gholizadeh et al. (2019).

3.3.9.2 Cluster analysis

Hierarchical agglomerative cluster analysis was conducted; the Ward Linkage method was used. The number of clusters was formed at a specific cluster cut-off value and was determined from the plot by drawing a vertical line at that value (value selected was 4.5) and the number of lines that the vertical line intersected counted. Therefore, heavy metals were classified into two clusters as display in the dendrogram (see Figure 3.5).

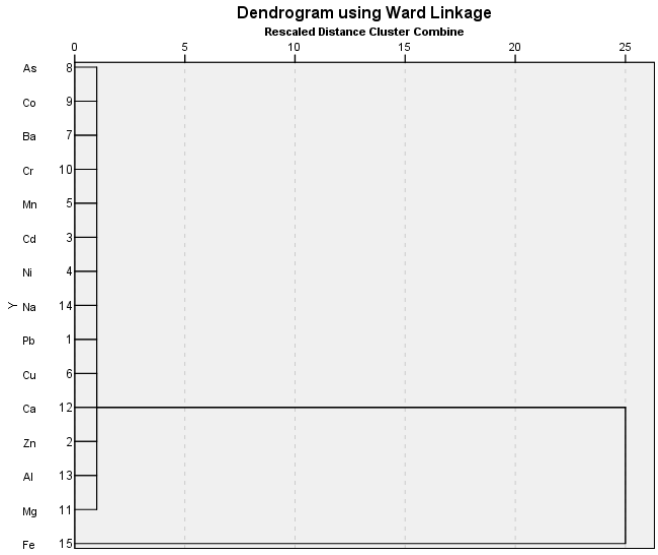

Figure 3.5: Cluster analysis of detected average concentrations of heavy metals in the core sediments of selected study sites

Cluster 1 comprises of Co, As, Ba, Cd, Cr, Na, Mn, Ni, Pb, Ca, Cu, Zn, Mg, and Al, whereas cluster 2 consist of Zn, Fe, Mg, Al, and Ca metals. The emergence of Zn, Fe, Mg, Al, and Ca metals in cluster 2 could be ascribed to their preponderance in the sediment samples at the sampling stations unlike other metals (Yang et al., 2012; Xu et al., 2019). Additionally, due to the fact that Zn, Fe, Mg, Al, and Ca metals were in the same cluster, suggest similar pollutant source. Cluster metals also show mutual relationships between and thus, could be linked with common sources (Chien et al., 2002; Dias-Ferreira et al., 2016; Bhuyan et al., 2019). Based on the dendrogram, it can be said that sub-cluster 1 contains heavy metals that reach the estuarine and coastal sediments from both natural and anthropogenic sources.

3.3.9.3 Principal Component Analysis (PCA)

Principal component analysis (PCA) was used to compare the constitutional and spatial patterns between the investigated heavy metals and the recognized undiscovered factors and to predict likely sources of these metals in the sediments. PCA

has been extensively employed to recognize the contribution of natural and anthropogenic sources (Li & Zhang, 2010). The data set was treated using Varimax rotation as the extraction method of the principal component (Appendix 3.19). The plots of loadings for studied heavy metals with percentages of cumulative variance are presented in Figure 3.6.

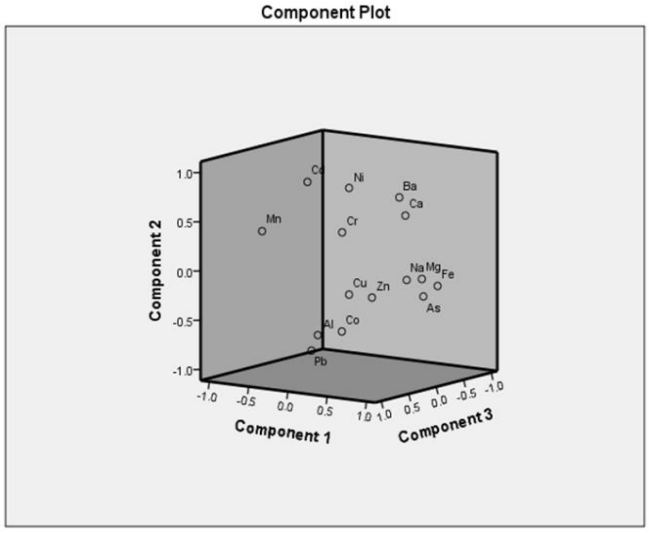

Figure 3.6: Plot of loading of three principal components in PCA results

Three principal components were extracted, which adequately covered 83.28% 58.590% of the total variance from studied metals (Figure 3.6). Component 1 accounted for 32.13%, Component 2 recorded 28.41%, and Component 3 accounted for 22.73% respectively. The Component 1 representative congeners include high positive loadings for Mg (0.99), As (0.69), Fe (0.79), and Na (0.95) and high negative loading for Mn (-0.88). Component 2 include high negative and positive loadings for Pb (-0.886), Ni (0.873) and Cd (0.874). The Component 3 representative congener is high positive loading for Al (0.808).

Lead (Pb) is used in wide industrial applications, including cable sheathing, solder ammunition, and battery recycling pigments. Furthermore, exposure to Pb in

sediment may be attributed to the corrosive and weak plumbing system. High As in sediment may come from peculiar arsenic-containing fertilizers used in the past or industrial waste. Cadmium (Cd) occurs naturally in Pb, Zn, and Cu ores, in shales and is released in the course of volcanic action or disturbance of soil-rock due to mining activities. The high negative loadings of some metals are an indication of different external sources (Attia & Ghrefat, 2013; Decena et al., 2018). The PCA results indicate that Components 1, 2, and 3 have both anthropogenic and geological contributions (Li & Zhang, 2010; Wu, 2014; Liang et al., 2017).

3.4 Chapter Summary

The concentrations of selected heavy metals in surface and core sediments collected from the coastal and four rivers estuary in Sarawak, Malaysia, were examined. In regards to surface sediments, all selected heavy metals were detected at all sampled stations, with a concentration lower than the average shale value for sedimentary rock except for Zn. Generally, pollution appeared more severe in the coastal of the studied area, probably due to their nearby point source contamination. Among the heavy metals of interest, Zn, Ni, and Cr concentrations surpassed the TEC values and should be carefully monitored and remediated because they may cause unfavorable impacts on bottom-dwelling organisms. Potential eco-toxicological risk analysis of heavy metals concentrations in surface sediments indicated that most sampling stations posed a minor or moderate ecological risk.

Controlling factors such as inflow velocity and sediment textural characteristcs influencing metals availabilty in sediment were investigated. Heavy metals enrichment in core sediment in core sediment profile in each sampling sites and depth/cm were appraised.

Bivariate and multivariate statisitcal tools were applied to help predict the possible heavy metal sources in the studied sites. The results obtained from the statistical analyses suggested that some of the metals are anthropogenic in origin such as Cd, Pb, Zn but the other metals are not as their distribution may be more related to clays or lithogenic in origin. The results will guide controlling heavy metal contamination and protecting agricultural and transportation water sources in the coastal and the four rivers estuary in the Kuching Division of Sarawak.

CHAPTER 4

DISTRIBUTION OF HYDROCARBONS IN COASTAL AND FOUR RIVERS ESTUARY SEDIMENTS IN THE KUCHING DIVISION OF SARAWAK

4.1 Introduction

Considerable amount of storm water, dredged spoils, industrial and municipal wastes, spilled oil, and sewage are released into the coastal environment via estuaries with no or little treatment, specifically under developed countries (Ramos et al., 2000; Hartmann et al., 2004; Basheer et al., 2005). These contaminants are mostly originated from the aquatic urban settings, even though they may not pose any immediate adverse effects at low concentrations, but could cause serious harm over a long period (Zakaria & Takada, 2003). One of the recalcitrant and well known organic pollutants derived from organic wastes is petroleum hydrocarbons (Damas et al., 2009). Petroleum hydrocarbons have been extensively used as indicators for identifying the petroleum sources in the aquatic ecosystem (Lucke et al., 1985; Guo et al., 2011). Oil spills originated from land-based sources such as storage facilities, river runoff, industrial and municipal wastes, etc. and transportation operations including shipping and oil tanker transportation are causing more harm in the environment (El Nemr & Abd-Allah, 2003).

The fundamental phase in determining the likely environmental and human health impacts of hydrocarbons availability in sediments is the measurement of their mass concentrations (Damas et al., 2009). The rapidness and effectiveness of analytical instrumentation for the accurate determination of hydrocarbons in environmental samples have several extraction techniques adapted to estimate the total concentration of hydrocarbons in sediment matrices (Boonyatumanond et al., 2006; 2007). Presently,

feasible and accurate analytical methods for extracting hydrocarbons for compositional analysis by gas chromatography-mass spectrometry (GC-MS) and GC- flame ionization detector (GC-FID) for assessment of petroleum hydrocarbons levels in various environment partitions creates a serious question (Ramos et al., 2000; Wang et al., 2002; Basheer et al., 2005; Damas et al., 2009). The most extensively used method for extraction of petroleum hydrocarbons in organic compounds-containing materials such as soil, sediments, etc., for analytes separation is chromatography procedures. Song et al. (2002) opined that ultrasonic extraction, mechanical shaking or stirring, and soxhlet extraction are the fundamentals techniques by which pollutants from petroleum waste are extracted environmental solid media.

Guo et al. (2011) opined that several techniques have been developed for the fractionation or pre-separation of crude oil. Such techniques are solid-phase extraction (SPE) (Theobald, 1988), classical adsorption chromatography (Campbell & Lee, 1986; Hostettler et al., 1999; Grossi et al., 2002), supercritical fluid chromatography (SFC) (Nishioka et al., 1986), florisil (El Nemr & Abd-Allah, 2003), silica and alumina combination (Grossi et al., 2002), high-performance liquid chromatography (HPLC) (Lucke et al., 1985; Guo et al., 2011), and silica gel (Zakaria et al., 2000). This study has validated GC-FID and GC-MS for qualitative and quantitative analysis of petroleum hydrocarbons in sediment samples. AHs and PAHs are the analytes considered. The technique validated was applied on sediment samples collected from the coastal and selected four river estuaries of Kuching Division, Sarawak.

One of the important areas in Kuching is the coastal areas. It is a marine biodiversity hotspot, and also recreational terminus and tourism that contribute extensively to the socio-economic development of Kuching Dvision of Sarawak (Zakaria et al., 1999;

2001; 2002; Zakaria & Mahat, 2006). Of the nine rivers that flow into the coast, the four most important in relation of anthropogenic contributions are Salak, Santubong, Sibu, and Rambungan rivers. From contamination perspective, the coastal areas especially Santubong Bay is regarded the prime sink for domestic and industrial effluents including likely agricultural contaminants emerging from adjacent land-based areas (Zakaria et al., 2000; Aly Salem et al., 2014). The contribution of pollutant, specifically oil from ship traffic, added extra environmental pressure on this area (Wang & Fingas, 1995; Yunker et al., 2002; Zakaria & Takada, 2003; Nasher et al., 2013). For these reasons, the aims of this study are thus to examine the contamination levels of the coastal and four rivers estuary by assessing the concentrations of AHs and PAHs in sediment, identify the probably sources pollutants using various diagnostic and isomeric ratios on the n-alkanes and PAHs and finally ascertaining the ecological risk of carcinogenic PAHs.

4.2 Materials and Methods

4.2.1 Spiking and Extraction of AHs and PAHs

Sediment samples were spiked following the protocol adapted by Damas et al. (2009). Uncontaminated sediments were spiked to help validate the analytical method. This coastal sediment was considered to contain the biogenic origin AHs without PAHs. Before the extraction, the concentration of 20 and 100 ng/g AHs and concentration of 10 and 50 ng/g PAHs standard solutions were spiked to individual sediment samples, respectively. Both non-spiked and spiked sediments were subjected to solvent extraction on the Soxhlet extraction apparatus.

United State Environmental Protection Agency (US EPA) 3540 modified method was adapted for the Soxhlet extraction of sediment samples (Ugwu & Ukoha, 2016). Air-dried sediment samples were grounded into powdered form before extraction.

Reasonable amount of anhydrous sodium sulphate was mixed with 15 g of the powdered sample for moisture removal in a cellulose thimble and extracted with dichloromethane (200 mL) in a Soxhlet extractor for 20 hours. The crude extract was run via a glass containing anhydrous sodium sulphate, and dried on a vacuum rotary evaporator (brand: IKA, model: RV 8V) to a relative volume of 2.0 mL. Purified nitrogen gas was used to dry the crude extract up to 1.0 mL.

4.2.2 Column Chromatography

The crude extract was clean-up on silica gel column chromatography to remove residue materials that was also extracted during extraction, such as biogenic macromolecules, lipids, and pigments to prevent other substances affect the final evaluation and analysis of the targeted hydrocarbons. The clean-up step on silica gel column chromatography was performed to separate analytes into two hydrocarbon groups, i.e., AHs and PAHs. A glass column with 55.0 cm height and 1.0 cm internal diameter-was packed with glass wool at the bottom, filled with 6.0 g of silica gel, and finally topped with 2.0 cm of potassium sulfate. 5.0 mL of *n*-hexane was used to condition the column before adding the geolipid. A dried geolipid was diluted in 2 mL *n*-hexane, and then poured to the top of the silica gel column. The column was eluted with 30 mL of n-hexane, and the eluant was collected in a 50 mL capacity pear-shaped flask AHs fraction. Subsequently, the column was eluted with a 30 mL mixture of dichloromethane and *n*-hexane (50:50, v/v) into a 50 mL capacity pear-shaped flask to collect the PAHs fraction. Purified nitrogen gas was used to dry both fractions and stored in refrigerator at 4 $^{\circ}$C until analysis.

4.2.3 Gas Chromatographic Analysis

GC-FID and GC-MS were used to analyze AHs and PAHs fractions, respectively. AHs fractions were analyzed on a Hewlett Packard Gas Chromatograph (Model 6890) equipped with a flame ionization detector (FID). The separation was performed on a DB-5 fused silica capillary column coated with a 5% diphenyl and 95% dimethyl polysiloxane stationary phase with an internal diameter of 0.25 mm, column length 30 m, and film phase thickness 0.25 µm. Before GC-FID analysis, the sample was dissolved in 500 µL *n*-hexane. Helium gas with a 1 mL/min velocity was used as a carrier gas. The initial oven temperature was programmed at 50 ^{o}C and held for 5 min. It was then increased to 300 ^{o}C at the rate of 5 ^{o}C/min and held for 15 min (Damas et al., 2009). The injector and detector temperatures were set at 250 ^{o}C and 300 ^{o}C, respectively. Exactly 1 µL of the sample was injected into the column in splitless injection mode. Identification of AHs was carried out by comparing the retention times of individual *n*-alkanes in a sample with those in a mixture of AHs standards.

PAHs fractions were analyzed on a Shimadzu Gas Chromatography-Mass Spectrometer model QP2010 Plus equipped with a quadrupole mass analyzer. The separation was carried out using a BPX-5 fused silica capillary column coated with a 5% diphenyl and 95% dimethyl polysiloxane stationary phase, with internal diameter 0.25 mm, column length 30 m, and film thickness 0.25 µm. The electron ionization energy system with ionization energy of 70 eV was used for GC-MS detection. Initially, the oven temperature was programmed at 50 ^{o}C and held isothermal for 5 minutes. The temperature was ramped to 300 ^{o}C at the rate of 6.5 ^{o}C/minute at held for 15 minutes at the final temperature. Exactly 1 µL of the sample was injected into the column in splitless injection mode (Damas et al., 2009). Fraction F2 was dissolved in 500 µL dichloromethane before

GC-MS analysis; identification of PAH components was performed by direct comparison of retention times of individual PAHs with a mixture of PAHs standards.

4.2.4 Quality Assurance and Quality Control (QA/QC)

A blank was prepared by adapting the same procedure used to prepare the samples for analysis (Ahmed et al., 2015). A blank was analyzed for indvidual sample in ten batches. Analytical blank serve as a tool to ensure no pollution by preventing targeted compounds resulting in errors in the course of analysis.

4.2.5 AHs Diagnostic Indices

4.2.5.1 Carbon Preference Index (CPI)

The carbon preference index (CPI) can be explained as the odd to even carbon-number *n*-alkanes ratio in the range of n-C_{25} to n-C_{33} (Aly Salem et al., 2014). It is used to evaluate biogenic and petrogenic input sources of AHs. CPI values equal to 1 indicate microorganisms, organic matter recycled, and/or petroleum inputs, while CPI values greater than 3 suggest natural inputs (Jeng, 2006).

$$\text{Carbon Preference Index} = \frac{1}{2}\left(\frac{nC_{25}+nC_{27}+nC_{29}+nC_{31}+nC_{33}}{nC_{24}+nC_{26}+nC_{28}+nC_{30}+nC_{32}} + \frac{nC_{25}+nC_{27}+nC_{29}+nC_{31}+nC_{33}}{nC_{24}+nC_{26}+nC_{28}+nC_{30}+nC_{32}}\right)$$

Equation 4.1

4.2.5.2 Low Molecular Weight AHs/High Molecular Weight AHs

One of the critical tools for assessing the sources of AHs in the aquatic environments is the ratio of the low molecular weight (nC_{15} to nC_{20}) to the high molecular weight (nC_{21} to nC_{34}) (Ahmed et al., 2015; Adeniji et al., 2017). The ratio ΣLMW/HMW

below 1 indicates the preponderance of *n*-alkanes originated from planktons and petroleum. The occurrence of fresh oil in the surface water is deduced when the ratio ΣLMW/HMW is > 2 (Zrafi et al., 2013).

4.2.5.3 Long Chain Hydrocarbons /Short Chain Hydrocarbons (LCH/SCH)

The *n*-alkanes ≤ nC_{26} are named as short-chain hydrocarbons (SCHs); however, those > nC_{26} are considered as the long-chain hydrocarbons (LCHs). *n*-alkanes from plankton and benthic origin are usually short-chain hydrocarbons (SCHs); the long-chain hydrocarbons (LCHs) are derived from vascular plants. Estimating the LCH/SCH ratio is generally carried to evaluate the abundance of vascular plants and/or phytoplankton in the coastal environments (Fagbote & Olanipekun, 2013). The LCH/SCH ratio is also known as the Terrigenous/Aquatic ratio(TAR).

Short Chain Hydrocarbons (LCH) = $nC_{27} + nC_{29} + nC_{31}$ Equation 4.2

Long Chain Hydrocarbons (LCH) = $nC_{15} + nC_{17} + nC_{19}$ Equation 4.3

$$\text{Terrigenous/Aquatic ratio(TAR)} = \frac{nC_{27}+nC_{29}+nC_{31}}{nC_{15}+nC_{17}+nC_{19}} \quad \text{Equation 4.4}$$

The dominance of phytoplankton is achieved when the ratio falls within the range of 0.21 – 0.9, whereas TAR values between 2.38 and 4.33 suggest a mixed origin. TAR values > 4 indicate an abundance of terrestrial plant waxes (Bianchi, 2007).

4.2.5.4 Average Carbon Length of LCH (ACL_{LCH})

The average carbon length of LCH is another essential indicator used to assess the abundance of odd carbon per molecule in the sediment samples collected with an understanding to initiating association with higher plants *n*-alkanes. It is used to identify environmental variations for a particulate ecosystem. It provides the average chain length of AHs supposed to be more persistent in an environment. Higher values of ACL suggest heavier hydrocarbons presence. The index is computed with the formula below (Sakari et al., 2008; Kiran et al., 2015).

$$\text{Average Carbon Length of LHC } (ACL_{LHC}) = \left(\frac{25(nC_{25})+27(nC_{27})+29(nC_{29})+31(nC_{31})+33(nC_{33})}{nC_{25}+nC_{27}+nC_{29}+nC_{31}+nC_{33}}\right)$$

Equation 4.5

4.2.5.5 Natural *n*-alkanes ratio (NAR)

The natural *n*-alkanes ratio (NAR) roughly measures (i.e.; a value or quantity that is nearly but not exactly correct) the proportion of natural *n*-alkanes and petroleum *n*-alkanes (Mille et al., 2007).

$$\text{Natural } n\text{-alkanes ratio (NAR)} = \frac{[\sum n-alkanes(C_{19}-C_{32})-2\sum even\ n-alkanes(C_{20}-C_{32})]}{\sum n-alkanes(C_{19}-C_{32})}$$

Equation 4.6

4.2.5.6 *n*-alkane proxy (Paq)

The *n*-alkane proxy ratio (P_{aq}) is used to estimate the different plant types (e.g., emergent vs. submerged plant types). It was put forward by Ficken et al. (2000):

n-alkane proxy (Paq): $\text{Paq} = \frac{(C_{23}+C_{25})}{(C_{23}+C_{25}+C_{29}+C_{31})}$ Equation 4.7

4.2.6 PAHs Isomeric Ratios for Sources Identification

The sources of PAHs can be evaluated using several ratios, as shown by the following equations (Yunker et al., 2002).

Ratios of anthracene/(anthracene + phenathrene) Equation 4.8

Where ratio values of 0.1 suggest a combustion source.

Ratios of fluoranthene/(fluoranthene + pyrene) Equation 4.9

Where ratio values of 0.5 suggest biomass combustion (coal, wood, or grass).

Ratios of alkyl phenanthrene/anthracene and alkyl fluoranthene/pyrene Equation 4.10

Where ratio values of 0.5 suggest a combustion source.

Ratios of 1, 7-dimethylphenanthrene (DmP)/{(2,6-DmP + 1,7-DmP) (1,7:(2,6 + 1,7-DmP)}

Equation 4.11

Where ratio values of 0.7 indicate strong wood combustion constituent.

Ratios of indeno[1,2,3-cd]pyrene/(indeno[1,2,3-cd]pyrene + benzo[ghi]perylene) {InPy/(InPy + BgP)} Equation 4.12

Where ratio values of 0.5 indicate biomass combustion.

Variations in bioavailability can occur as a function of a PAH origin. Pyrogenic (combustion-derived) PAHs have quite high octanol-water partitioning

coefficients (log K_{ow}) and low water solubility and, for that matter, are to a great extent connected with particulate matter, in doing so significantly decreasing their bioavailability (Meador et al., 1995). Contrarily, petrogenic (petroleum-derived) PAHs are generally extensively available for uptake by marine organisms due to their increased water solubility and low log K_{ow} values (Meador et al., 1995).

4.3 Results and Discussion

4.3.1 Validation of GC-FID and GC-MS Methods for AHs and PAHs Analysis, Respectively

To ensure that the techniques are feasible for their use, validation process was performed by establishing the fundamental analytical requirements of performance to be suitable for measurement of AHs and PAHs in sediment samples. To construct calibration curves for *n*-alkane and PAHs, several standard solutions were prepared in different concentrations and injected into the GC-FID and GC-MS, respectively. Figures 4.1 and 4.2 depict unresolved AHs and PAHs compounds and they were evaluated in pairs. The concentration ranges used are important compared to the concentrations often detected in environmental media. A linear correlation coefficient of > 0.9898 was recorded for all calibration curves. Regarding the measurement of this technique, all standard eluting between C_9H_{20} and $C_{33}H_{68}$ was believed to be several mixtures of branched-chain, cyclic, and normal-chain hydrocarbons. Concerning PAHs, all standards eluting between naphthalene and benzo[ghi]perylene was presumed to be alkylated and non-alkylated aromatics mixtures, consisted of two to six aromatic rings and composite patterns of cycloalkanes-aromatic. The horizontal axis of the chromatogram is the retention time and the vertical axis is the peak intensity (Figures 4.1 and 4.2).

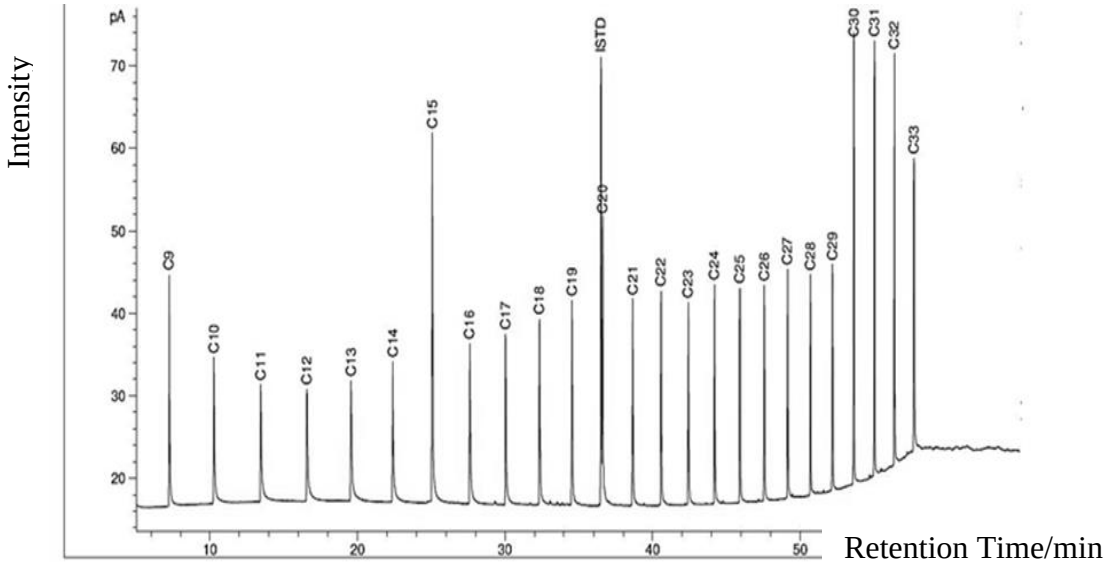

Figure 4.1: GC-FID chromatogram of AHs standard solutions

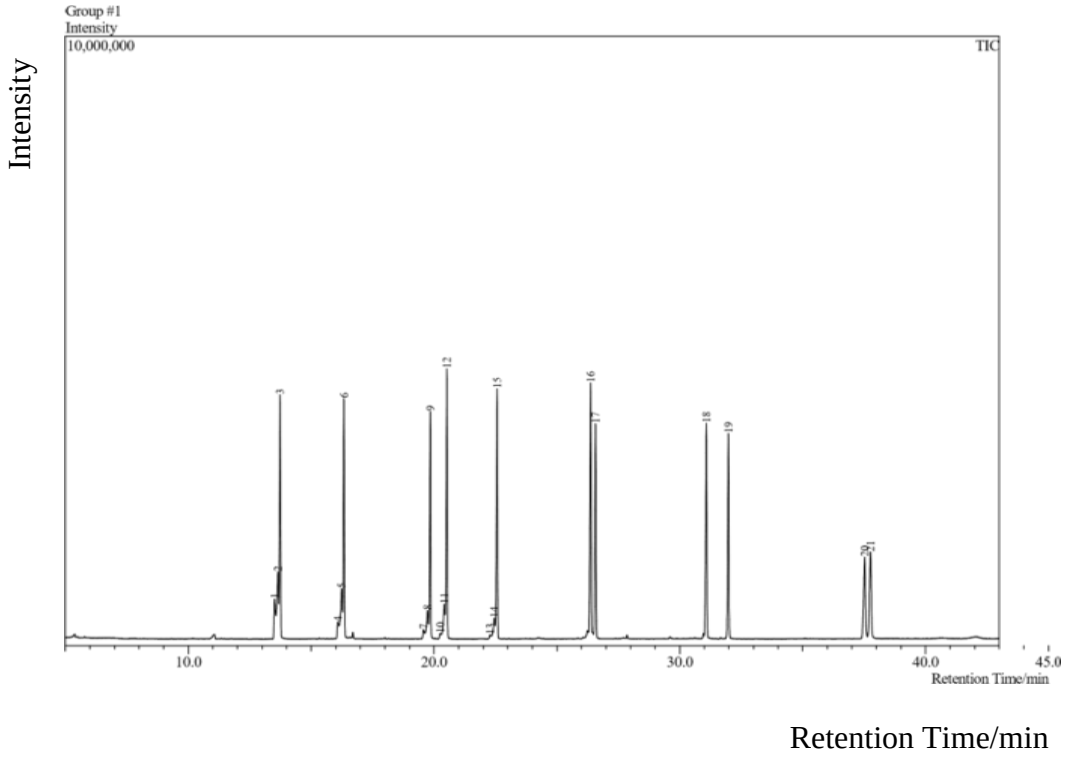

Figure 4.2: GC-MS chromatogram of PAHs standard solutions

Table 4.1: The results of GC-FID linear ranges and limits of detection from analysis of standard solutions

n-alkanes	Linear ranges (ng/mL)	LOD(ng/mL)
n-Nonane (C_9H_{20})	20 – 100	2.8
	100 – 500	
n-Decane ($C_{10}H_{22}$)	20 – 100	3.5
	100 – 500	
n-Undecane ($C_{11}H_{24}$)	20 – 100	3.1
	100 – 500	
n-Dodecane ($C_{12}H_{26}$)	20 – 100	2.3
	100 – 500	
n-Tridecane ($C_{13}H_{28}$)	20 – 100	3.6
	100 – 500	
n-Tetradecane ($C_{14}H_{30}$)	20 – 100	4.2
	100 – 500	
n-Pentadecane ($C_{15}H_{32}$)	20 – 100	2.7
	50 – 500	
n-Hexadecane ($C_{16}H_{34}$)	20 – 100	2.1
	100 – 500	
n-Heptadecane ($C_{17}H_{36}$)	20 – 100	3.3
	100 – 500	
n-Octadecane ($C_{18}H_{38}$)	20 – 100	3.7
	100 – 500	
n-Nonadecane ($C_{19}H_{40}$)	20 – 100	4.6
	100 – 500	
n-Icosane ($C_{20}H_{42}$)	20 – 100	3.1
	100 – 500	
n-Heneicosane ($C_{21}H_{44}$)	20 – 100	3.4
	100 – 500	

Table 4.1 Continued

n-Docosane ($C_{22}H_{46}$)	20 – 100	2.5
	100 – 500	
n-Tricosane ($C_{23}H_{48}$)	20 – 100	4.1
	100 – 500	
n-Tetracosane ($C_{24}H_{50}$)	20 – 100	2.9
	100 – 500	
n-Pentacosane ($C_{25}H_{52}$)	20 – 100	2.4
	100 – 500	
n-Hexacosane ($C_{26}H_{54}$)	20 – 100	2.7
	100 – 500	
n-Heptacosane ($C_{27}H_{56}$)	20 – 100	3.1
	100 – 500	
n-Octacosane ($C_{28}H_{58}$)	20 – 100	3.5
	100 – 500	
n-Nonacosane ($C_{29}H_{60}$)	20 – 100	2.7
	100 – 500	
n- Triacotane ($C_{30}H_{62}$)	20 – 100	2.2
	100 – 500	
n-Hentriacontane ($C_{31}H_{64}$)	20 – 100	3.7
	100 – 500	
n-Dotriacontane ($C_{32}H_{66}$)	20 – 100	4.1
	100 – 500	
n-Tritiacontane ($C_{33}H_{68}$)	20 – 100	2.5
	100 – 500	

Table 4.2: The results of GC-MS linear ranges and limits of detection from analysis of standard solutions

PAHs	Linear ranges (ng/mL)	LOD (ng/mL)
Naphthalene ($C_{10}H_8$)	10 – 50	3.1
	50 – 250	
Acenapthylene ($C_{12}H_8$)	10 – 50	5.3
	50 – 250	
Acenapthene ($C_{12}H_{10}$)	10 – 50	3.6
	50 – 250	
Fluorene ($C_{13}H_{10}$)	10 – 50	4.2
	50 – 250	
Phenanthrene ($C_{14}H_{10}$)	10 – 50	5.5
	50 – 250	
Anthracene ($C_{14}H_{10}$)	10 – 50	6.1
	50 – 250	
Fluoranthene ($C_{16}H_{10}$)	10 – 50	4.7
	50 – 250	
Benzo[a]anthracene ($C_{18}H_{12}$)	10 – 50	3.5
	50 – 250	
Chrysene ($C_{18}H_{12}$)	10 – 50	3.8
	50 – 250	
Benzo[b]fluoranthene ($C_{20}H_{12}$)	10 – 50	3.4
	50 – 250	
Benzo[k]fluoranthene ($C_{20}H_{12}$)	10 – 50	4.6
	50 – 250	
Benzo[a]pyrene ($C_{20}H_{12}$)	10 – 50	4.4
	50 – 250	

Table 4.2 Continued

Indeno[1,2,3-c,d]pyrene ($C_{22}H_{12}$)	10 – 50	5.7
	50 – 250	
Dibenzo[ah]anthracene ($C_{22}H_{14}$)	10 – 50	5.1
	50 – 250	
Benzo[ghi]perylene ($C_{22}H_{12}$)	10 – 50	5.9
	50 – 250	

Accuracy of an analytical technique is the closeness of measured values obtained to the certified values, and most often represented as percentage recovery by the known quantity of analyte, and it is mostly ascertained by spiking studies using reference materials (Jaouen-Madoulet et al., 2000). The accuracy was checked by spiking the sediment with known concentrations of standard solutions. Five replicate were analyzed, and the entire analytical method was tested in real samples. The recoveries of the added standard solutions at 50 ng/mL spiked level of PAHs and 100 ng/mL spiked level of *n*-alkanes are depicted in Figures 4.3 and 4.4. In regards with *n*-alkanes, the recoveries ranged from 54.2 to 104.1% whereas, the recoveries of PAHs varied from 52.4 to 94.0%

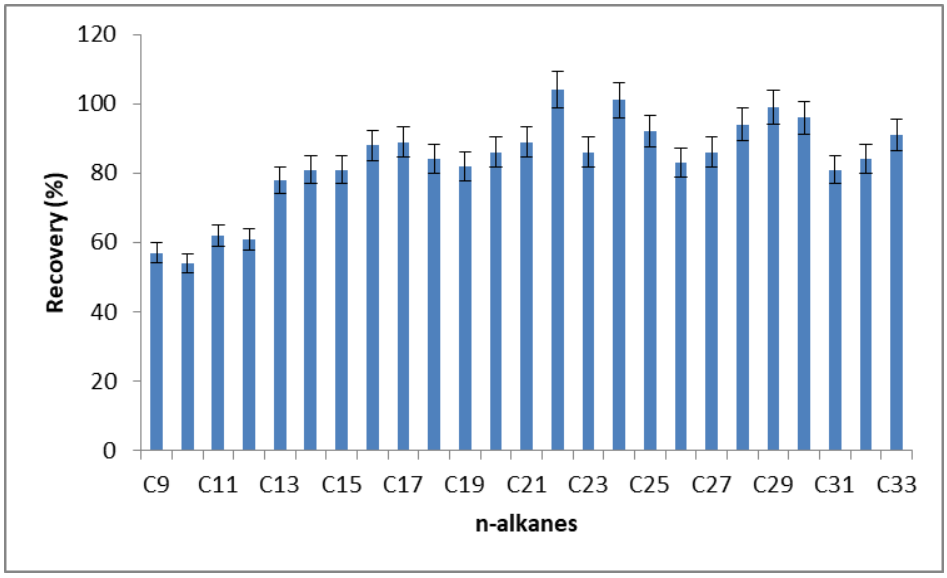

Figure 4.3: *n*-alkanes recoveries from fortified coastal sediment (spiked concentration of *n*-alkanes is 100 ng/mL)

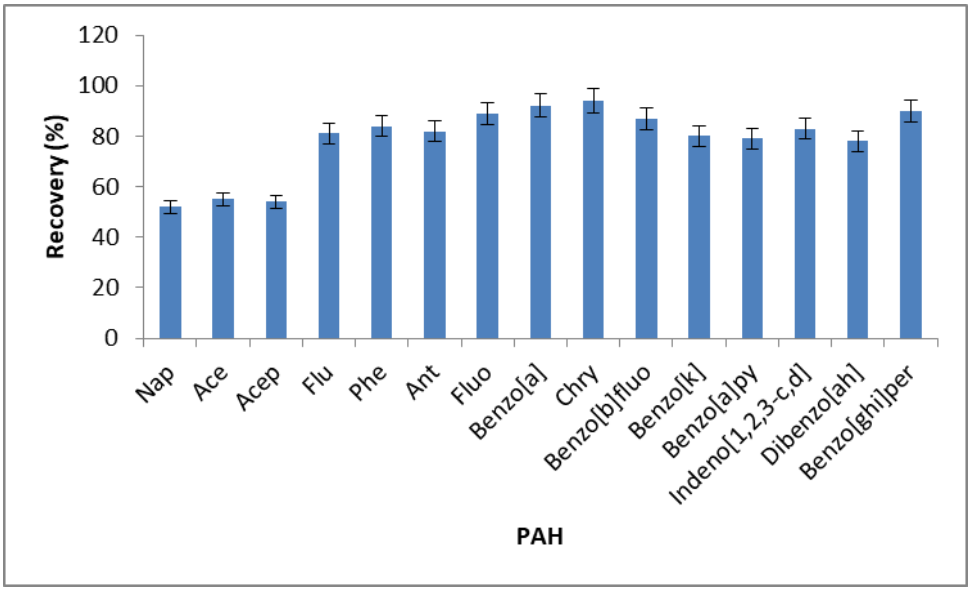

Figure 4.4: PAHs recoveries from fortified coastal sediment (spiked concentration of PAH is 50 ng/mL)

The limit of detection (LOD) of the whole method is defined as the minimum concentration of a substance that can be quantified and reported with 0.1 confidences. The LOD (ng/mL) was computed as a signal-noise ratio (S/N) of 3 while the quantification limit (LOQ) was calculated as a signal-noise ratio (S/N) of 10 (Omorinoye et al., 2019b; Omorinoye et al., 2020). For *n*-alkanes, the values of LOD ranged from 16.2 – 26.6 ng/g,

while for PAHs the LOQ varied from 17.9 – 26.4 ng/g. For LOQ, the values ranged from 22.9 – 38.2 ng/g for *n*-alkanes, while from 26.4 – 35.8 ng/g are for PAHs. The obtained LOD and LOQ values were highlighted in Tables 4.1 and 4.2.

Table 4.3: Limits of detection, limits of quantification, and relative standard deviation for *n*-alkanes analysis

n-alkanes	LOD (ng/g) S/N = 3	LOQ (ng/g) S/N = 10	RSD(n=4) % intra-day
n-Nonane (C_9H_{20})	19.7	27.4	19.1
n-Decane ($C_{10}H_{22}$)	16.2	29.3	14.9
n-Undecane ($C_{11}H_{24}$)	21.8	36.7	10.1
n-Dodecane ($C_{12}H_{26}$)	18.3	27.1	6.1
n-Tridecane ($C_{13}H_{28}$)	26.5	31.3	7.4
n-Tetradecane ($C_{14}H_{30}$)	20.8	38.2	9.1
n-Pentadecane ($C_{15}H_{32}$)	22.9	36.6	8.5
n-Hexadecane ($C_{16}H_{34}$)	17.4	24.9	6.9
n-Heptadecane ($C_{17}H_{36}$)	25.1	32.7	5.3
n-Octadecane ($C_{18}H_{38}$)	22.6	36.1	4.9
n-Nonadecane ($C_{19}H_{40}$)	19.6	29.3	7.1
n-Icosane ($C_{20}H_{42}$)	21.8	36.9	5.9
n-Heneicosane ($C_{21}H_{44}$)	17.2	22.9	7.3
n-Docosane ($C_{22}H_{46}$)	23.7	29.5	6.4
n-Tricosane ($C_{23}H_{48}$)	26.6	37.3	9.5
n-Tetracosane ($C_{24}H_{50}$)	18.2	26.1	7.8
n-Pentacosane ($C_{25}H_{52}$)	21.6	33.7	7.4
n-Hexacosane ($C_{26}H_{54}$)	21.4	35.5	6.8
n-Heptacosane ($C_{27}H_{56}$)	23.7	29.4	6.1
n-Octacosane ($C_{28}H_{58}$)	20.4	26.1	5.9
n-Nonacosane ($C_{29}H_{60}$)	16.3	26.4	6.8
n- Triacotane ($C_{30}H_{62}$)	25.7	38.1	5.7
n-Hentriacontane ($C_{31}H_{64}$)	21.2	29.3	7.1
n-Dotriacontane ($C_{32}H_{66}$)	24.7	30.6	6.4
n-Tritiacontane ($C_{33}H_{68}$)	23.3	34.1	6.8

Table 4.4: Limits of detection, limits of quantification, and relative standard deviation for PAHs analysis

PAH	LOD (ng/g) S/N = 3	LOQ (ng/g) S/N= 10	RSD (n=4) % intra-day
Naphthalene ($C_{10}H_8$)	21.4	30.6	15.4
Acenapthylene ($C_{12}H_8$)	17.9	26.4	16.6
Acenapthene ($C_{12}H_{10}$)	24.5	33.1	7.8
Fluorene ($C_{13}H_{10}$)	24.9	31.7	5.3
Phenanthrene ($C_{14}H_{10}$)	21.8	29.5	6.7
Anthracene ($C_{14}H_{10}$)	23.6	32.8	8.5
Fluoranthene ($C_{16}H_{10}$)	19.5	27.1	5.3
Benzo[a]anthracene ($C_{18}H_{12}$)	26.4	35.8	9.7
Chrysene ($C_{18}H_{12}$)	20.1	26.7	5.2
Benzo[b]fluoranthene ($C_{20}H_{12}$)	22.6	31.4	6.9
Benzo[k]fluoranthene ($C_{20}H_{12}$)	25.1	34.9	7.3
Benzo[a]pyrene ($C_{20}H_{12}$)	18.2	27.9	4.1
Indeno[1,2,3-c,d]pyrene ($C_{22}H_{12}$)	23.6	33.5	6.1
Dibenzo[ah]anthracene ($C_{22}H_{14}$)	25.2	32.8	7.5
Benzo[ghi]perylene ($C_{22}H_{12}$)	21.6	28.8	4.6

The uncertainty of measurement was calculated by adapting recommended protocol in the literature (Barwick & Ellinson, 1999; 2000). The uncertainty at which the spiked concentrations were examined is below 10% (at 95% confidence level). Although most measured concentrations were slightly smaller than the spiked concentrations but based on the U_c values and correlation coefficients for the linear regression between spiked concentration and uncertainty, indicates an almost complete balance of the recovery standard. This showed a complete extraction, minimal losses, good alignment between

spiking and calibration solution, and the analytical technique. Hence, GC-FID and GC-MS can quantify the AHs concentration and PAHs concentration, respectively in sediment samples. Figures 4.5 and 4.6 depict the link between combined U_c and spiked concentrations for selected *n*-alkanes and PAHs, respectively.

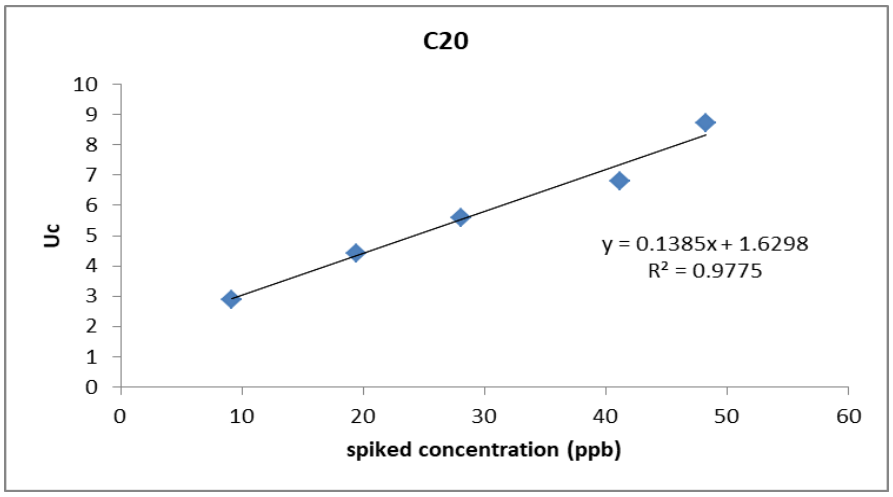

(a) Uncertainty against spiked concentrations for C_{20}

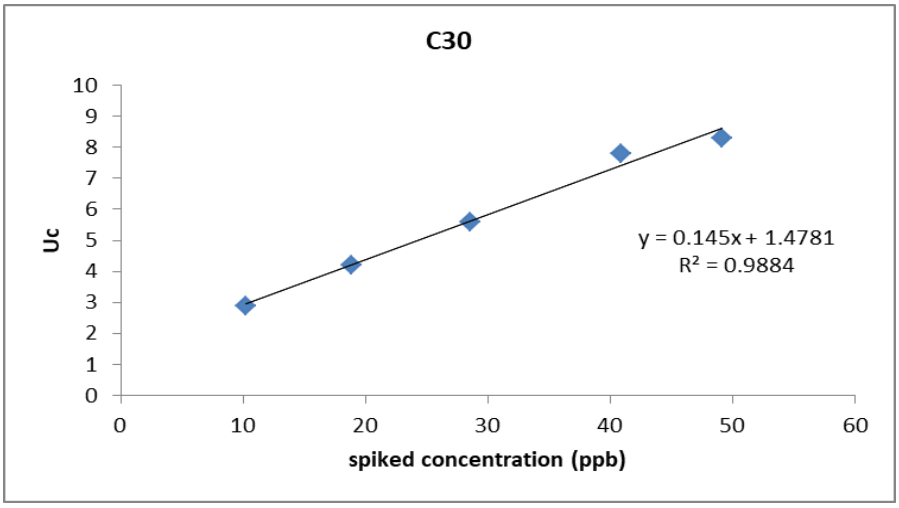

(b) Uncertainty against spiked concentrations for C_{30}

Figure 4.5: The link between combined uncertainty (U_c) and spiked concentrations for **(a)** C_{20} and **(b)** C_{30}, respectively

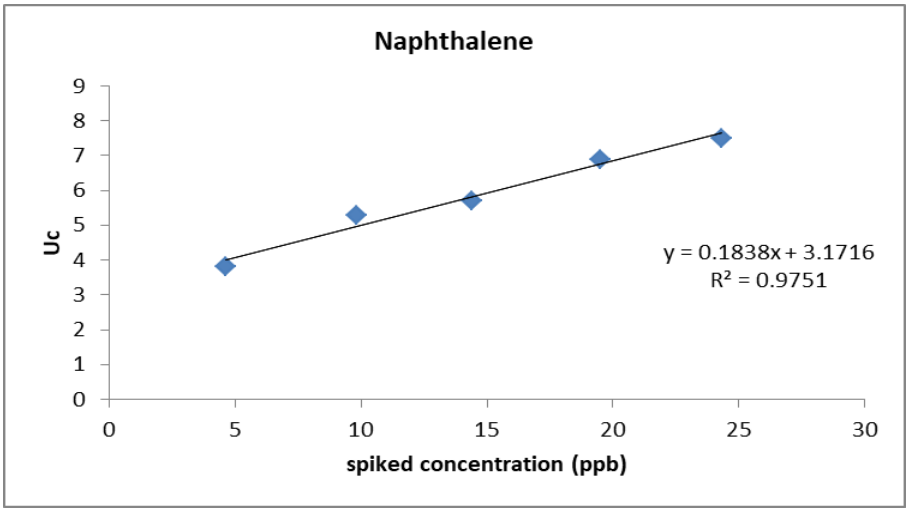

(a) Uncertainty against spiked concentrations for naphthalene

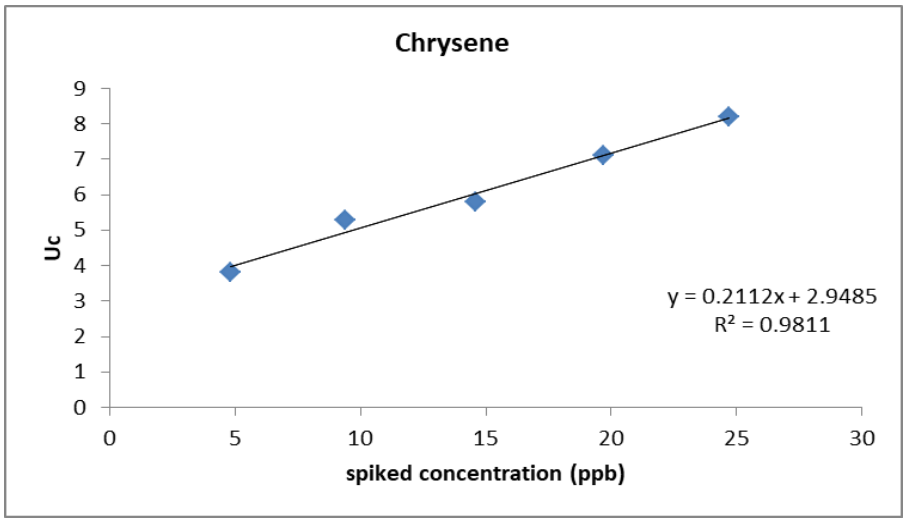

(b) Uncertainty against spiked concentrations for chrysene

Figure 4.6: The link between combined uncertainty (U_c) and spiked concentrations for **(a)** naphthalene and **(b)** chrysene, respectively

4.3.2 Evaluation of AHs in Sediment Samples

4.3.2.1 Nature of AHs Chromatogram Detected in Sediment Samples by GC-FID

After analytical method is defined and validated, sediment samples from the coastal and selected estuaries sites were analyzed. A typical AHs chromatogram analyzed

by GC-FID in sediment samples at study sites CZ5 and CZ10 are shown in Figure 4.7, respectively. For study site CZ5, the most relevant resolved compositions characterized by homologous series of *n*-alkanes is nC_{14} to nC_{33} and that of study site CZ8 is nC_{10} to nC_{33}. The abundance of the compounds present in this fraction is unresolved molecules and commonly called unresolved complex mixture (UCM). The appearance of UCM is described as a hum region between the curve characterizing the base of resolvable peaks and the solvent baseline (Figure 4.7) (Wang & Fingas, 1995; Grossi et al., 2002; Damas et al., 2009). UCM consisted of combination of alicyclic hydrocarbons and has extensively associated with remains of biodegraded petroleum (Peters et al., 2005). The LMW *n*-alkanes were not available in some of the sediment samples. The reason is that LMW organic compounds are easily volatilized to the atmosphere. In contrast, high compositions of HMW can be assumed to partition onto the phase of particulate and undergo the process of sedimentation.

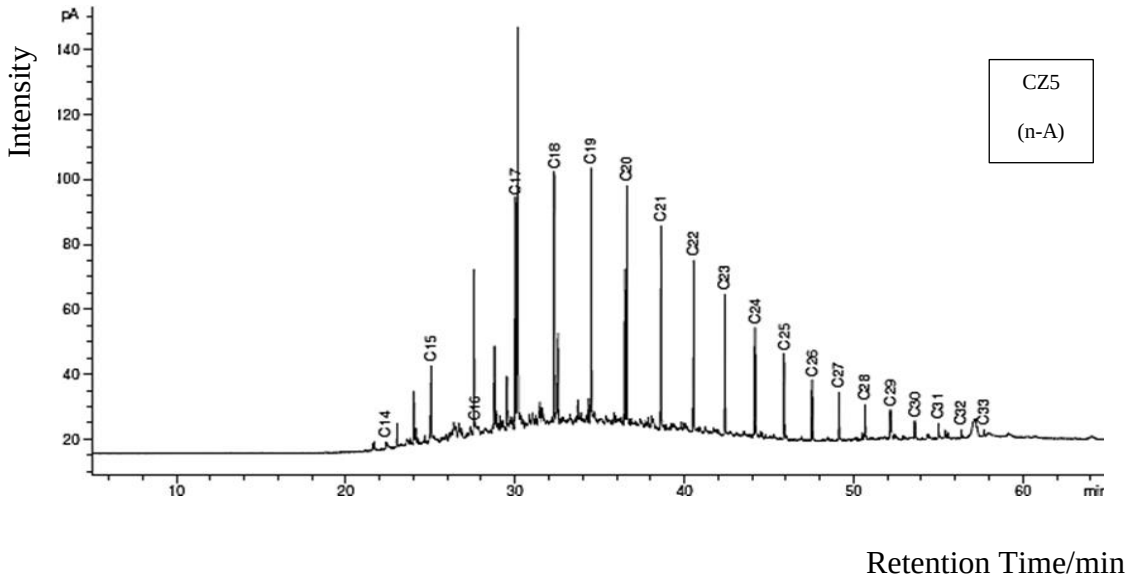

(a) Chromatogram detected in sediment sample CZ5

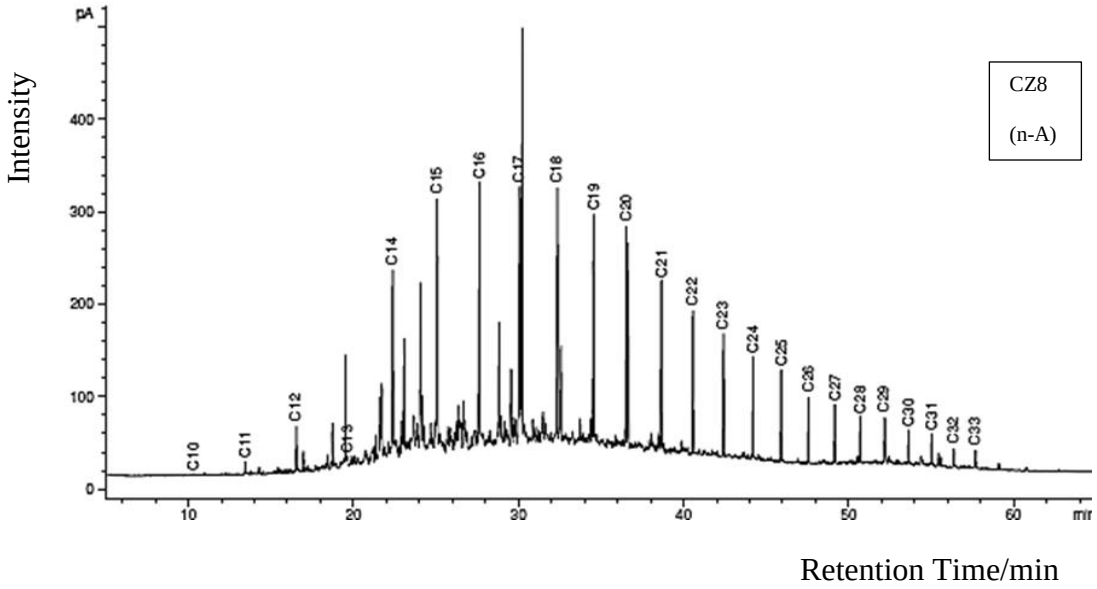

(b) Chromatogram detected in Sediment Sample CZ8

Figure 4.7: Characteristic gas chromatogram of AHs (*n*-alkanes) fractions extracted from coastal sediments in location **(a)** CZ5 and **(b)** CZ8, respectively

4.3.2.2 Assessment of AHs Contamination and Potential Sources

The *n*-alkanes contents determined in representative sediment collected from the coastal and four rivers estuary sites of Sarawak are shown in Table 4.5. The total concentrations of AHs varied from 96.63 to 367.28 ng/g dw.

Table 4.5: Content of *n*-alkanes determined in representative coastal and four rivers estuary sediment samples

n-alkane compounds	Sample									
	CZ1	CZ2	CZ3	CZ4	CZ5	CZ6	CZ7	CZ8	CZ9	CZ10
	ng/g dw									
$C_{10}H_{22}$	n.d[x]	n.d	n.d	n.d	n.d	n.d	n.d	0.15	0.47	n.d
$C_{11}H_{24}$	n.d	n.d	n.d	n.d	n.d	n.d	n.d	0.58	0.14	n.d
$C_{12}H_{26}$	n.d	n.d	n.d	n.d	n.d	n.d	n.d	1.03	0.62	n.d
$C_{13}H_{28}$	3.12	n.d	7.21	1.36	n.d	5.01	n.d	2.75	1.51	n.d
$C_{14}H_{30}$	2.49	4.22	0.87	2.33	0.15	4.90	n.d	2.05	2.08	1.52
$C_{15}H_{32}$	5.32	3.96	10.2	3.71	1.32	7.36	6.20	4.24	2.32	1.96
$C_{16}H_{34}$	12.12	9.07	6.41	8.01	1.02	2.91	7.74	6.02	3.06	3.61
$C_{17}H_{36}$	17.03	13.2	9.71	7.87	4.11	9.36	20.4	8.08	4.08	2.81
$C_{18}H_{38}$	19.88	17.7	9.98	11.3	9.05	16.5	10.2	19.2	13.1	16.2
$C_{19}H_{40}$	24.02	23.9	17.6	14.8	13.1	15.2	13.7	11.5	16.4	16.4
$C_{20}H_{42}$	3.71	3.43	5.14	4.05	1.15	14.9	5.19	2.06	2.04	9.03
$C_{21}H_{44}$	18.15	36.1	21.2	10.9	4.01	8.13	16.2	5.33	1.17	13.0
$C_{22}H_{46}$	14.62	27.9	13.1	7.11	7.81	3.06	1.04	14.9	6.76	2.34
$C_{23}H_{48}$	9.43	16.6	3.51	12.4	16.9	0.54	2.81	3.22	2.11	7.18
$C_{24}H_{50}$	7.19	23.1	8.98	9.03	7.94	1.89	5.53	6.03	9.04	1.53
$C_{25}H_{52}$	8.06	17.9	2.05	5.21	3.07	6.23	6.01	4.51	11.0	6.41
$C_{26}H_{54}$	11.23	10.1	7.36	7.83	16.9	9.04	3.63	3.48	3.06	3.03
$C_{27}H_{56}$	24.62	37.2	12.0	18.4	6.03	4.59	6.24	6.11	6.14	1.03
$C_{28}H_{58}$	12.20	13.0	16.4	6.27	2.11	10.2	10.4	4.90	5.10	0.81
$C_{29}H_{60}$	6.61	15.7	22.6	19.6	5.51	2.78	6.02	7.03	3.24	0.23
$C_{30}H_{62}$	14.01	31.0	6.31	11.7	7.32	8.31	7.21	4.51	4.08	2.71
$C_{31}H_{64}$	5.66	27.4	4.21	9.26	8.03	10.4	3.17	2.11	4.25	4.02
$C_{32}H_{66}$	n.d	25.7	7.81	13.1	5.23	9.11	5.05	6.04	5.01	1.34
$C_{33}H_{68}$	n.d	10.1	2.75	9.01	4.71	7.03	1.35	3.10	3.16	1.47

Table 4.5 Continued

[y]Sum of C_{10} to C_{33}	219.47	367.28	195.40	193.25	125.47	157.45	138.09	128.93	109.94	96.63

[x] n.d: Not-detected
[y] Sum of concentration of *n*-alkanes from $C_{10}H_{22}$ to $C_{33}H_{68}$

The AHs diagnostic indexes were evaluated (Table 4.6). Sediment sample collected from the offshore of Batang Rambungan opposite small Satang Island (CZ2) recorded the highest total concentration of *n*-alkanes. On the contrarily, sediment sample from the estuary of Santubong River (CZ10) recorded the lowest content of *n*-alkanes. Concerning detected *n*-alkanes in the sediment samples from the estuaries, Rambungan river estuary recoded the highest concentrations of *n*-alkanes as compared to the other estuaries (Santubong River estuary, Sibu River estuary, and Salak River estuary). LMW and HMW *n*-alkane were evaluated and tabulated in Table 4.6. HMW and LMW varied from 45.10 to 291.80 ng/g dw and 29.90 to 87.69 ng/g dw, respectively. Sediment from the offshore of Telaga Air opposite to small Satang Island recorded the lowest value of LMW (i.e., 29.90 ng/g dw) and sediment samples from study site CZ1 recorded the highest LMW value (i.e., 87.69 ng/g dw). However, the lowest HMW was noticed at study site CZ10 (i.e., 45.10 ng/g dw) and sample from study site CZ2 recorded the highest value of HMW (i.e., 291.80 ng/g dw). The LMW/HMW ratios were in the range of 0.26 to 1.14 in sediment at study site CZ2 to CZ10.

Table 4.6: Concentrations of *n*-alkanes (ng/g) detected and calculated distribution indices in surface sediments of coastal and in four rivers estuary of Sarawak

Sample code	LMW[a]	HMW[b]	%LMW	%HMW	LMW/HMW[c]	CPI[d]	[f]NAR	[g]TAR	Paq	CPI_{SHC}	CPI_{LHC}	LHC/SHC	[e]ACL_{LHC}	*n*-alkanes /C_{16}
CZ1	87.69	131.78	39.96	60.04	0.67	1.11	0.21	0.80	0.59	1.29	1.20	0.63	27.44	18.12
CZ2	75.48	291.80	20.55	79.45	0.26	1.21	0.13	1.96	0.45	1.16	1.36	1.05	28.53	40.49
CZ3	67.12	128.28	34.35	65.65	0.52	1.04	0.12	1.04	0.21	1.43	1.15	0.72	29.11	30.48
CZ4	53.43	139.82	27.65	72.35	0.38	1.43	0.21	1.79	0.38	1.26	1.58	1.08	28.95	24.13
CZ5	29.90	95.57	23.83	76.17	0.31	0.78	0.08	1.06	0.60	1.46	0.87	0.86	29.39	123.01
CZ6	76.14	81.31	48.36	51.64	0.94	0.83	-0.35	0.56	0.34	1.03	0.85	0.75	29.48	54.11
CZ7	63.43	74.66	45.93	54.07	0.85	0.80	0.18	0.38	0.49	2.00	0.87	0.55	27.91	17.84
CZ8	57.66	71.27	44.72	54.90	0.81	1.07	0.09	0.64	0.49	0.67	1.21	0.48	28.40	21.42
CZ9	45.82	64.12	41.68	53.32	0.72	1.34	0.12	0.60	0.56	0.77	1.61	0.69	27.74	35.93
CZ10	51.53	45.10	53.33	46.67	1.14	1.54	0.23	0.25	0.73	1.26	1.67	0.28	27.95	26.77

[a] Sum of low molecular weight AHs from C_{10} to C_{20}
[b] Sum of high molecular weight from AHs C_{21} to C_{33}
[c] Ratio of LMW alkanes to HMW alkanes
[d] Carbon Preference Index (CPI)
[e] Average Carbon Length of LHC (ACL_{LHC})

High values of LMW/HMW ratio were recorded at study sites CZ10 (1.14), and CZ1 (0.67), CZ1 (0.67), CZ9 (0.72), CZ8 (0.81), CZ7 (0.85), CZ6 (0.94), and CZ10 (1.14) which can be attributed to fresh oil inputs. On the contrarily, study sites CZ5 (0.31), CZ4 (0.38), and CZ2 (0.26) recorded low values of low LMW/HMW ratio and this could be ascribed by marine animals inputs, sedimentary bacteria, and higher plants (Wang et al., 1998; Sakari et al., 2008). The variations in LMW and HMW could be attributed to natural inputs such as microbial activity, emergent terrestrial plants etc. and anthropogenic inputs including sewage, shipping, and industrial discharges (El Nemr et al., 2013). A representative type of GC-FID chromatograms which is showed in Figure 4.7, there is a clear resolution of all *n*-alkanes and low enriched shorter chain *n*-alkanes (SHC, $C_{10}H_{22}$ – $C_{24}H_{50}$) with high enrichment of longer chain normal alkanes (LHC, $C_{25}H_{52}$ to $C_{33}H_{68}$).

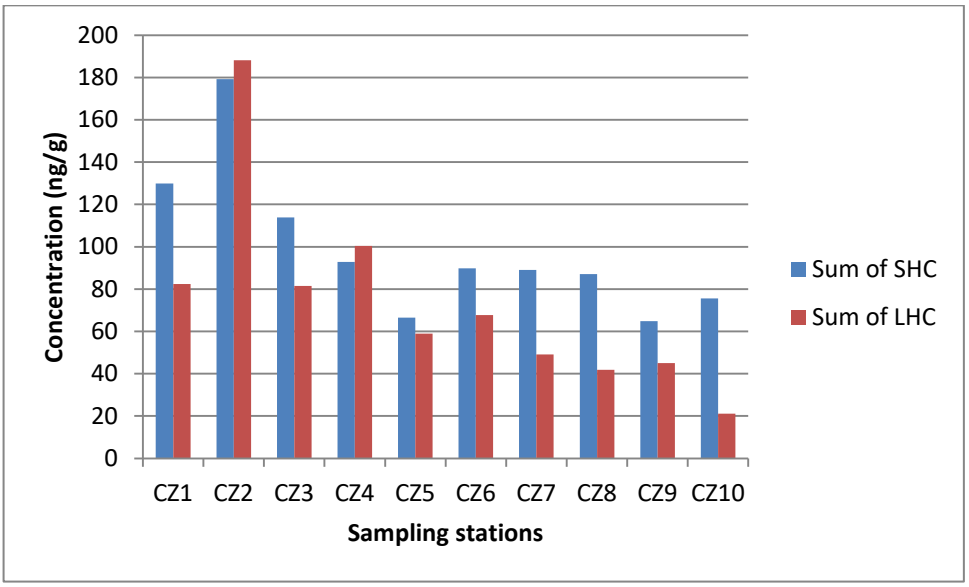

Figure 4.8: Sum of *n*-alkanes of the two ranges (∑LHC and ∑SHC) at all sampling stations

The sum of *n*-alkanes of the two ranges, ∑LHC and ∑SHC is shown in Figure 4.8. In regards to ∑LHC, study site CZ10 recorded the lowest value (21.05 ng/g), while

study site CZ2 recorded the highest value (188.1 ng/g dw). The order of decreasing ∑LHC value followed: CZ2 > CZ4 > CZ1 > CZ3 > CZ6 > CZ5 > CZ7 > CZ9 > CZ8 > CZ10. Concerning ∑SHC, study site CZ9 recorded the lowest value (64.9 ng/g dw) whereas the highest value was recorded at study site CZ2 (179.18 ng/g dw). The order of decreasing ∑SHC value followed: CZ2 > CZ1 > CZ3 > CZ4 > CZ6 > CZ7 > CZ8 > CZ10 > CZ5 > CZ9. LHC/SHC ratios were evaluated to predict whether there is phytoplankton-derived macrophyte-derived organic matter and/or dominant higher plant in the sediments of the study area (El Nemr et al., 2013). The LHC/SHC ratios values ranged from 0.28 – 1.08 (Table 4.6). The obtained ratios indicated that study sites were dominated by macrophyte waxes and/or higher plants (Commendatore et al., 2000). The anthropogenic inputs in the study area may include erosion of soil organic matter by rains and discharges from treatment plants. Biogenic inputs such as marine animals, algae, bacteria, plankton, and vascular plants could be the contributing factor (Commendatore et al., 2000).

Carbon preference index (CPI) was evaluated to predict the source of AHs contamination in the study area. According to Aly Salem et al. (2014), even carbon number is ascribed to terrestrial higher plant waxes, whereas odd number carbon is mostly linked to natural sources. CPI values from 5 to 10 are accredited to terrestrial higher plant waxes (Jeng, 2006). It has been reported that higher CPI values in sediment or soil suggest vascular plants influence (Hedges & Prahl, 1993). CPI value equal to 1 suggests microorganisms, organic matter and/or petroleum inputs (Kennicutt et al., 1987; Aly Salem et al., 2014). It was observed the values of CPI in all study sites are similar and ranges from 0.80 to 1.54, indicating that all study sites may probably contaminated with petrogenic inputs because the CPI values obtained were < 3, indicating oiled sediments (Kennicutt et al., 1987).

The hydrocarbon source is derived from crude oil and petroleum when the ratio of natural *n*-alkanes (NAR) is equal to zero and higher terrestrial plants and/or marine plants means natural *n*-alkanes ratio is equal to 1. The obtained natural *n*-alkanes ratios in this study ranged from -0.35 to 0.23, indicating both petrogenic and biogenic inputs. Terrigenous to aquatic (TAR) ratios varied from 0.25 to 1.96. Study site CZ2 recorded the highest value of TAR (1.96) and this may be due to more short-chain *n*-alkanes in the sediment which are more prone to degeneration than longer-chain *n*-alkanes (EL Nemr & Abd-Allah, 2003; Jeng & Huh, 2006). The *n*-alkane proxy (P_{aq}) is also an indicator to evaluate AHs sources in sediment. The obtained P_{aq} values ranged from 0.21 to 0.73 (See Table 4.6). Ficken et al. (2000), opined that P_{aq} values varied from 0.48 to 0.94 are due to submerged/floating species of macrophytes influence and P_{aq} values in the range of 0.21 to 0.73 are attributed to terrestrial plant. In this study, both higher plant/macrophyte waxes and phytoplankton-derived organic carbon are the contributing factors (El Nemr et al., 2013). The average carbon chain length (ACL) is another tool to recognize ecological differences. A situation of uniform ACL indicates minor environmental differences in the area (Colombo et al., 1989). When the *n*-alkanes/nC_{16} ratio value is greater than 50 then the influence is biogenic and *n*-alkanes/nC_{16} ratio less than 15 indicates petrogenic samples (Aly Salem et al., 2014). In this study, the obtained values of *n*-alkanes/nC_{16} ratio indicate combination of biogenic and petrogenic inputs.

4.3.3 Evaluation of PAHs in Sediment Samples

4.3.3.1 Characteristic PAHs Chromatogram Detected from Sediment Samples by GC-MS

Figures 4.9 is a representative chromatogram of PAHs analyzed by GC-MS in sediments collected from study sites CZ5 and CZ8, respectively. The PAH compounds BaP benzo[a], Phe, Fl, Ace, Acthy, and Naph, were detected in sediment sample at study site CZ5, while BaP, Chry, BaA, Ant, Phe, Fl, Ace, Acthy, and Naph were PAH compounds detected in sediment sample from study site CZ8. The PAHs chromatograms fractions at the two study sites that appear as an envelope with limited resolved peaks may be ascribed to weathered influence (Charrie-Duhaut et al., 2000; Damas et al., 2009). The other fraction constituents were inadequate for GC-MS to give a full scan analyses and assessment. For this reason, few PAHs compounds were evaluated.

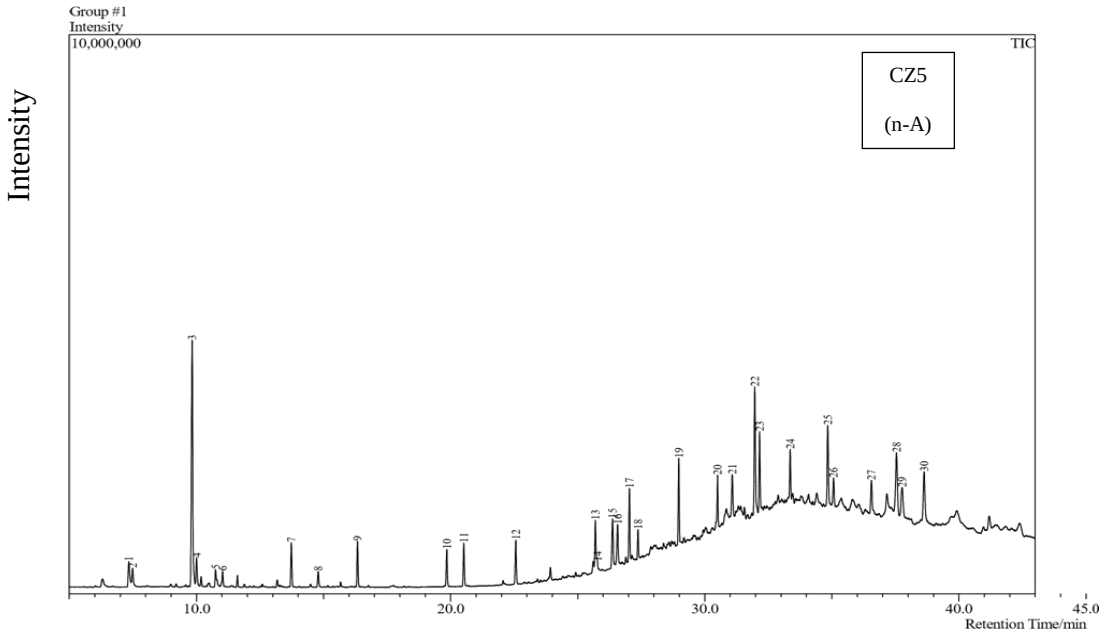

Intensity

Retention Time/min

(a) Chromatogram detected in sediment sample CZ5

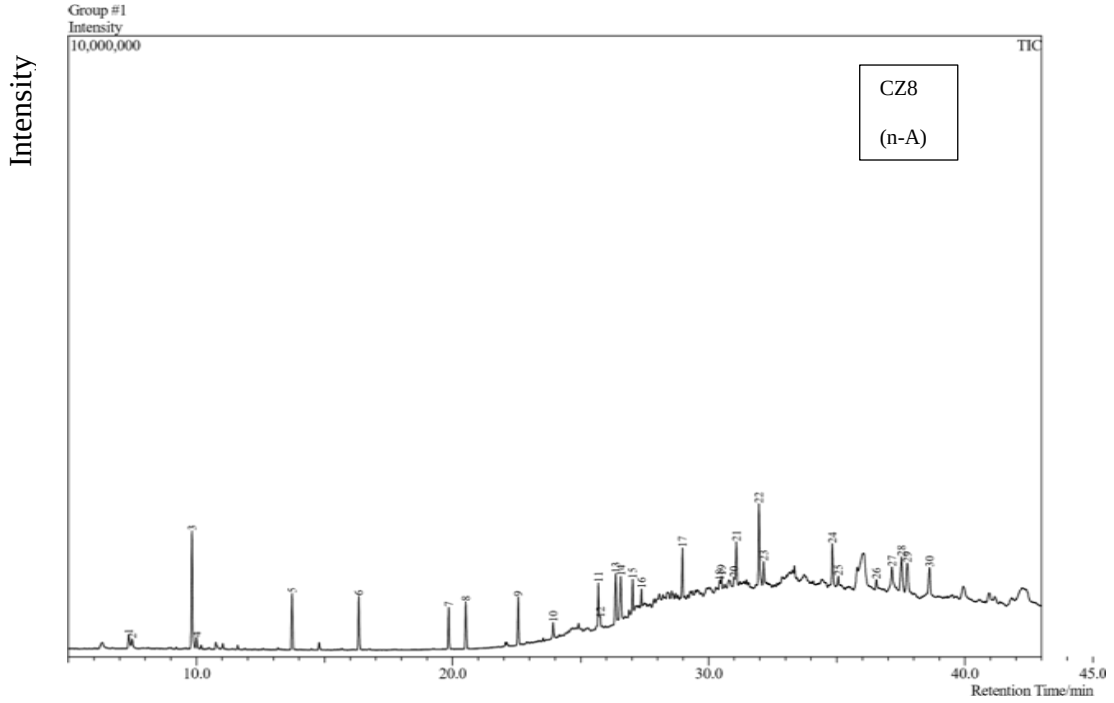

(b) Chromatogram detected in sediment sample CZ8

Figure 4.9: Characteristic gas chromatogram of PAHs fractions extracted from coastal sediments in location **(a)** CZ5 and **(b)** CZ8, respectively

4.3.3.2 Assessment of PAHs Contamination, Sources and Carcinogenic PAHs Risk

Table 4.7 shows the PAHs concentrations detected in sediment samples at various study sites including other evaluated parameters. The ∑PAHs concentrations in surface sediments were similar to each study sites. The ∑PAHs concentrations in sediment samples at the study area varied from 12.34 – 21.20 ng/g dw, with a mean value of 16.10 ± 2.06 ng/g dw. Study site CZ3 recorded the lowest ∑PAHs concentrations (12.34 ng/g dw). However, study site recorded the highest ∑PAHs concentrations (21.20 ng/g dw). At all sampling sites, the order of decreasing ∑PAHs concentrations is as follows: CZ8 > CZ5 >

CZ10 > CZ9 > CZ4 > CZ7 > CZ1 > CZ6 > CZ2 > CZ3. Different inputs sources such as fuel combustion emissions, human activities, and discharged waters may be the reasons why there was discrepancy in PAH concentrations in analyzed sediment samples.

In addition, some published works reporting PAHs concentrations in sediments from other rivers estuary and coastal sites has been depicted in Table 4.8. Comparatively, the ∑PAHs concentrations recorded in this study were lower than the ∑PAHs concentrations documented in selected studies highlighted in Table 4.8. For example, the ∑PAHs concentrations in sediments from the Red Sea, Egypt varied from 0.74 – 436.91 ng/g with an average value of 93.49 ng/g (Aly Salem et al., 2014). Furthermore, the ∑PAHs concentrations in sediments from Sadong River, Sarawak, Malaysia ranged from 18.21 – 184.25 ug/g which is higher as compared to PAHs concentrations recorded in this study (Omorinoye et al., 2019b). Baumard et al. (1998a) categorised the relative pollution levels of PAHs into 4: (i) very high, more than 5000 ng/g; (ii) high, 1000 – 5000 ng/g; (iii) moderate, 100 – 1000 ng/g; and (iv) low, 0 – 100 ng/g. The obtained PAHs concentrations in all study sites were low.

Table 4.7: Concentration of PAHs (ng/g dw) assessed in representative coastal and four rivers estuary sediment samples of Sarawak

PAHs	Sample site code									
	CZ1	CZ2	CZ3	CZ4	CZ5	CZ6	CZ7	CZ8	CZ9	CZ10
Naph	2.79	0.77	1.43	0.94	3.44	1.06	2.06	1.04	3.03	1.19
Acthy	1.43	2.91	0.73	n.d	n.d	1.93	3.49	3.91	2.16	0.84
Ace	2.21	n.d	1.21	4.01	1.06	3.41	n.d	1.28	1.48	2.04
Fl	n.d	n.d	2.17	0.11	3.21	0.64	4.33	3.96	n.d	1.31
Phe	2.05	1.57	1.04	3.42	1.26	2.82	n.d	2.71	n.d	0.51
Ant	n.d	1.04	1.22	n.d	3.37	n.d	n.d	1.06	1.04	n.d
Flu	n.d	3.21	n.d	n.d	n.d	n.d	2.51	n.d	n.d	n.d
Pyr	2.61	n.d	n.d	1.28	n.d	n.d	n.d	n.d	2.09	n.d
BaA	n.d	1.66	1.02	1.15	4.01	1.22	2.68	3.03	1.41	1.52
Chry	3.31	n.d	2.51	2.09	0.63	0.88	0.42	2.46	n.d	2.21
BbF	n.d	n.d	n.d	n.d	n.d	n.d	n.d	n.d	n.d	n.d
BkF	n.d	n.d	n.d	n.d	n.d	n.d	n.d	n.d	3.31	3.26
BaP	1.03	2.07	1.21	3.96	1.22	1.56	n.d	1.72	n.d	4.66
InP	n.d	n.d	n.d	n.d	n.d	n.d	n.d	n.d	n.d	n.d
DBA	n.d	n.d	n.d	n.d	n.d	n.d	n.d	n.d	2.35	n.d

Table 4.7 Continued

BghiP	n.d	n.d	n.d	n.d	n.d	n.d	n.d	n.d	n.d	n.d
∑PAHs	15.43	13.23	12.54	16.96	18.20	13.52	15.49	21.20	16.87	17.54
$\sum PAH_{CARC}$	4.24	3.73	4.74	7.20	5.86	3.66	3.10	7.21	4.72	11.65
% CARC	27.45	28.19	37.80	42.45	32.20	27.07	20.01	34.01	27.98	66.42
TEQ_{CARC}	1.03331	2.2360	1.3145	4.0771	1.6216	1.6829	0.2684	2.0255	2.8220	5.1402
BaPE	1.03	2.17	1.27	4.03	1.46	1.63	0.16	1.90	0.46	4.98

Table 4.8: Comparison of PAHs contents in sediments recorded from the coastal and four rivers estuary of Sarawak with those from different coastal and estuaries of the world

Location	Range	Mean	References
Coastal (CZ2, 3, 5, 6, 8, and 9), Rambungan estuary (CZ1), Sibu estuary (CZ4), Salak estuary (CZ7), Santubong estuary (CZ10), Sarawak, Malaysia	12.34 – 21.20 ng/g	16.10 ± 2.06 ng/g	This study
Africa			
Red sea, Egypt	0.74 – 436.91 ng/g	93.49 ng/g	Aly Salem et al. (2014)
Suef Gulf, Egypt	18.99 – 97.19 ng/g	45.51 ng/g	
Aqaba Gulf, Egypt	6.86 – 100.05 ng/g	40.998 ng/g	
Buffalo river estuary, South Africa	1107 – 22,310 µg/L		Adeniji et al. (2019b)
Algoa Bay, South Africa	1.17 – 10.47 mg/kg		Adeniji et al. (2019a)
Lake Victoria, Uganda	44.2 – 80.2 ng/g		Kerebba et al. (2017)
River Sasa, Nigeria	777.68 – 2431.39 ng/g		Adekunle et al. (2020)
Asia			
Sadong River, Sarawak, Malaysia	18.21 – 184.25 ug/g		Omorinoye et al. (2019b)
Langkawi Island, Malaysia	869 – 1637 ng/g	1167 ng/g	Nasher et al. (2013)

Table 4.8 Continued

Zhanjiang Bay, China	41.96 –933.90 ng/g	315.98 ng/g	Huang et al. (2012)
Zhanjiang Bay, China	22.65 –79.76 ng/g		Zhu (2007)
Deep Bay, China	184.1 – 581 ng/g	353.8 ng/g	Qiu et al. (2007)
Kyeonggi Bay, Korea	9.1 – 1400 ng/g	120 ng/g	Kim et al. (1999)
Hsin-ta Harbour, Taiwan	1156 – 3382 ng/g		Fang et al. (2003)
Europe			
Santander Bay, Spain	20 – 344,600 ng/g	49079.40 ng/g	Viguri et al. (2002)
Aquitaine Bay, France	3.5 – 853 ng/g	256 ng/g	Soclo et al. (2000)
Coast of Porto Region, Portugal	51.98 – 54.79 µg/kg dw		Rocha et al. (2011)
Douro River estuary, Portugal	58.98-156.45 µg/kg dw		Rocha et al. (2011)
America			
Narragansett Bay, USA	569 – 216,000 ng/g	21100 ng/g	Hartmann et al. (2004)
Todos Santos Bay, Mexico	7.6 – 813 ng/g	96 ng/g	Macias-Zamora et al. (2002)
Boston Harbour, USA	7266 – 358,092 ng/g		Wang et al. (2001)

The total individual PAH compounds detected in all study sites and their number of aromatic rings has been presented in Table 4.9. Also, the percentage PAHs distribution in all study sites based on the number of aromatic rings is displayed in Figure 4.10.

Table 4.9: Sum of individual PAH compounds analyzed in all stations with its abbreviation and number of aromatic rings

Compounds	Abbreviations	Number of cycles	∑	%
Naphthalene	Naph	C2	17.75	11.00
Acenaphthylene	Acthy	C2	17.40	10.80
Acenaphthene	Ace	C2	16.70	10.40
Fluorene	Fl	C2	15.73	9.77
Phenanthrene	Phe	C3	15.38	9.55
Anthracene	Ant	C3	7.73	4.80
Fluorathene	Flu	C3	5.72	3.55
Pyrene	Pyr	C4	5.98	3.70
Benzo(a)anthracene	BaA	C4	17.70	11.00
Chrysene	Chr	C4	14.51	9.01
Benzo(b)fluoranthene	BbF	C4	0	0
Benzo(k)fluoranthene	BkF	C4	6.57	4.08
Benzo(a)pyrene	BaP	C5	17.43	10.80
Indeno[1,2,3-cd]pyrene	InP	C5	0	0
Dibenzo[a,h]anthracene	DBA	C5	2.35	1.46
Benzo(ghi)perylene	BghiP	C6	0	0

Table 4.10: Percentage distribution of PAHs in various stations based on the number of carbon rings

Sites	%C2	%C3	%C4	%C5	%C6
CZ1	41.70	13.29	38.37	6.68	0
CZ2	27.80	44.00	12.55	15.65	0
CZ3	44.18	18.02	28.31	9.65	0
CZ4	29.83	20.17	26.65	23.35	0
CZ5	42.36	25.44	25.49	6.70	0
CZ6	52.07	20.86	15.53	11.54	0
CZ7	63.78	16.20	20.02	0	0
CZ8	48.07	17.78	25.90	8.11	0
CZ9	39.54	6.17	40.37	13.93	0
CZ10	30.67	2.91	39.85	26.57	0

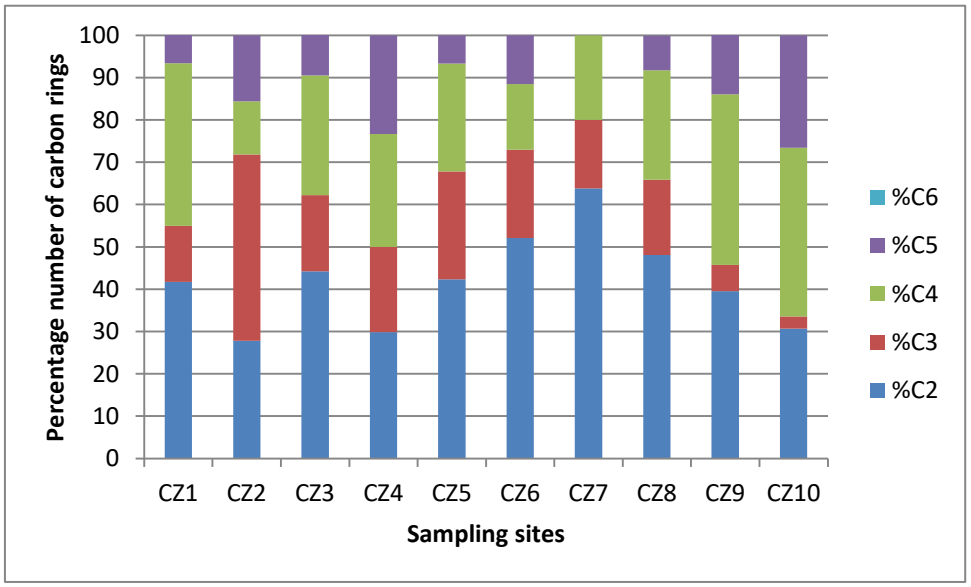

Figure 4.10: PAHs source characterization in sediment

The fundamental sources of PAHs in the aquatic ecosystem originate mainly from petrogenic or pyrolytic (Stout et al., 2004). It has been reported that pyrolytic PAHs derived from combustion mainly contained four or more rings (Baumard et al., 1998a; Aly Salem et al., 2014). Also, petrogenic PAHs derived from petroleum sources contained less than four aromatic rings (Baumard et al., 1998a). To distinguish between petrogenic or pyrolytic PAHs sources, ratio of 2 – 3 rings to 4 – 6 rings was used to predict in this study (De Luca et al., 2005). Study sites CZ10, CZ2, and CZ9 had ∑LPAH/∑HPAH ratios < 1, indicating pyrogenic inputs, whereas study sites CZ7, CZ6, CZ5, CZ4, CZ3, and CZ2 had ∑LPAH/∑HPAH ratios > 1, suggesting petrogenic sources (Tables 4.10, 4.11, and Figure 4.10).

Table 4.11: PAHs isomeric ratio in sediment from the coastal and four rivers estuary of Sarawak

Sites	TH	∑COMB[a]	∑COMB/ ∑PAH	∑LPAH[b]	∑HPAH[c]	∑LPAH/ ∑HPAH	Phe/ Ant	Ant/ (Phe+Ant)	Flu/ Pyr	Flu/ (Flu+Pyr)	BaA/ +Phe)	(BaA	Flu/ (Flu+Phe)
CZ1	234.90	6.95	0.45	8.48	6.95	1.22	-	-	-	-	-		-
CZ2	380.51	6.94	0.53	6.29	6.94	0.90	1.51	0.40	-	-	0.51		0.67
CZ3	207.94	4.74	0.38	7.80	4.74	1.65	0.85	0.54	-	-	0.50		-
CZ4	210.21	8.48	0.50	8.48	8.48	1.00	-	-	-	-	0.25		-
CZ5	143.67	5.88	0.32	12.32	5.88	2.10	0.37	0.73	-	-	0.76		-
CZ6	170.97	3.66	0.27	9.86	3.66	2.69	-	-	-	-	0.30		-
CZ7	153.58	5.61	0.36	9.88	5.61	1.76	-	-	-	-	-		-
CZ8	150.13	7.21	0.34	13.99	7.21	1.94	2.56	0.28	-	-	0.53		-
CZ9	126.81	6.81	0.40	7.71	9.16	0.84	-	-	-	-	-		-
CZ10	114.17	11.65	0.66	5.89	11.65	0.51	-	-	-	-	0.75		-

[a] ∑COMB = Flu + Chry + Pyr + BaA + BbF + BaP + BkF + InP + BghiP
[b] ∑LPAH[b] = Naph + Acthy + Ace + Fl + Phe + Ant
[c] ∑HPAH = Flu + Pyr + BaA + Chry + BbF + BkF + BaP + InP + DBA + BghiP

Several isomeric ratios have been used to examine whether PAHs in sediments are influenced by petrogenic or pyrogenic sources. Some of them are (i) Phe/Ant ratio (Baumard et al., 1998a, b; Soclo et al., 2000); (ii) Ant/ (Phe + Ant) ratios (Magi et al., 2002; Qiao et al., 2006; Aly Salem et al., 2014). Ant/ (Phe + Ant) ratios show whether the main contaminant of sediment is pyrogenic or petrogenic inputs. The thermodynamically more stable character of Phe and its abundance over Ant indicate that PAHs in sediments were mainly ascribed to petrogenesis. When the Phe/Ant ratio is high then contamination source is petroleum products. It has been reported that Ant/(Phe + Ant) greater than 0.1 or Phe/Ant ratio greater than 10 indicates that the source of PAHs pollution is from pyrolytic inputs (Baumard et al., 1998a; Qiao et al., 2006). The estimated Ant/(Phe + Ant) and Phe/Ant ratios in all sampling sites were greater than 0.1 and less than 10, respectively, indicating that PAHs contamination in sediments is mainly from petrogenic inputs and combustion (Chen & Chen, 2011).

Other isomeric ratios for evaluating the PAH contamination source in sediment are: (iii) Flu/Pyr ratio (Guinan et al., 2001); (iv) Flu/(Flu + Pyr) ratio (Guinan et al., 2001; Li et al., 2006). The assessment of Flu/Pyr and Flu/(Flu + Pyr) ratios were not successful because all the study sites sediment exhibited no detection of Flu or Pyr or both. However, (v) BaA/(BaA +Phe) ratio was estimated and all the values in all study sites were < 1, suggesting petroleum inputs. It has been reported that extensive combustion affects the PAHs levels in environment (El Nemr et al., 2013). The sum of major combustion-specific compounds (∑COMB) varied from 3.66 – 11.65 ng/g dw, and ratios of ∑COMB to the sum of PAHs varied from 0.27 – 0.66. In this study, the sum of major combustion-specific compounds (∑COMB) ranged from 3.66 to 11.65 ng/g dw, suggesting extensive combustion activities has taken place in the study area.

The average PAHs concentrations were compared to the effect range-low (ERL) and effect range-medium (ERM) to ascertain the biological effects of PAHs on sediments in the study area (Li et al., 2012). The two effect range values explain the PAH concentration ranges for a given PAH compound. The biological adverse impact are rare when PAHs concentration < ERL. Unfavourable biological effects would occur sometime when PAH concentration ≥ ERL but < ERM. Adverse biological impact would happen often when PAH concentration ≥ ERM. In this study, adverse biological effects were assumed rarely because the PAHs concentrations in sediments from all study sites were lower than the effect range-low values.

Table 4.12: Guidelines values (i.e., ERL and ERM) of PAHs in surface sediments (ng/g dw)

	Effect range-low	Effect range-medium	Present study				
			Mean	Minimum	Maximum	>ERL	<ERM
Naph	160.00	2100.00	1.78	0.77	3.03	-	-
Acthy	16.00	500.00	2.18	0	3.91	-	-
Ace	44.00	640.00	2.09	0	4.01	-	-
Fl	19.00	540.00	2.25	0	3.96	-	-
Phe	240.00	1500.00	1.71	0	3.42	-	-
Ant	853.00	1100.00	1.55	0	3.37	-	-
Flu	600.00	5100.00	2.86	0	3.21	-	-
Pyr	665.00	2600.00	1.99	0	2.61	-	-
BaA	261.00	1600.00	1.97	0	3.03	-	-
Chry	384.00	2800.00	1.81	0	3.31	-	-
BbF	320.00	1880.00	-	0	-	-	-
BkF	280.00	1620.00	3.29	0	-	-	-
BaP	430.00	1600.00	2.18	0	4.66	-	-
InP	-	-	-	0	-	-	-
DBA	63.40	260.00	2.35	0	2.35	-	-
BghiP	230.00	1600.00	-	0	0	-	-

It has been documented that some PAHs compounds have carcinogenicity behaviour and thus, their presence in the ecosystem is highly concern (Qiao et al., 2006; Liu et al., 2009a; Wang et al., 2009). The likely health risk of PAH can be evaluated by using BaP equivalent (BaPE). In this study, the BaPE values were obtained using Equation 4.13 (Gesine and Erika, 1999; Wang et al., 2009).

$$BaPE=0.08(InP)+0.06(DBA)+BaP+0.07(BkF)+0.06(BaA) \quad \text{(Equation 4.13)}$$

In this study, the obtained BaPE values for all samples varied from 0.16 to 4.98 ng/g dw. Study site CZ10 reported the highest BaPE value, indicating that carcinogenic PAHs in this study site (Santubong estuary) may show high toxicity than other study sites (Zhang et al., 2012). Thirty-six point eight percent out of the ∑PAH (i.e., 160.98 nd/g dw) denotes $\sum PAH_{CARC}$ and study site CZ10 recorded the highest percentage (66.42%).

The potential toxicological effects of carcinogenic PAHs on human health were evaluated by multiplying each toxic equivalency factor by it corresponding carcinogenic PAHs compound (Table 4.11). The toxic equivalent factors of seven carcinogenic PAHs were fetched from the United Nations Environment Programme (UNEP) (1992) database. These are BkF (0.1), BaA(0.1), BaP(1.0), BbF(0.1), DBA(1.0), Chry(0.001), and InP(0.1). The total toxicity or toxic equivalents (TEQs) were computed by Equation 4.14 (Guo et al., 2011):

$$TEQs = TEF_i \times \sum Conc._i \quad \text{(Equation 4.14)}$$

Toxic equivalent factor of each PAH compound is represented by TEF_i and the concentration of individual PAH compound is denoted by $Conc._i$. The obtained total TEQ_{CARC} values varied from 0.2684 to 5.1402 ngTEQ/g. The highest total TEQ_{CARC} value was reported in sediment from study site CZ10 (Table 4.11).

4.4 Chapter Summary

This chapter describes the distribution, source and risk assessment of hydrocarbons in sediments collected from coastal sites and four rivers estuary of Kuching. The recommended methods can quantify the available *n*-alkanes and PAHs in sediments. AHs diagnostic indicators were used to evaluate the sources of AHs in sediments. PAHs

isomeric ratios were used to determine the sources of PAHs. The effect range-medium (ERM) and effect range-low (ERL) was applied to evaluate the biological effects of PAHs of the studied area. Seven carcinogenic PAHs ($PAHs_{CARC}$) toxic equivalency factors were used to ascertain the likely adverse effects of PAHs on human health. This chapter highlights the necessary need to monitor and control these contaminants caused by anthropogenic in the coastal and estuarine areas.

CHAPTER 5

CONCLUSION AND RECOMMENDATIONS

5.1 Conclusion

Contamination of heavy metals, AHs, and PAHs in the coastal and estuaries sediment could harm water quality and aquatic organisms, leading to potential long-term health risks for humans and the environment. The purpose of this study was to conduct an assessment of heavy metals, AHs, and PAHs contamination in sediments of the coastal and four rivers estuary (i.e., Rambungan, Sibu, Santubong, and Salak) in Kuching. The average concentrations of heavy metals in the coastal and four rivers estuary were generally low and below upper continental shale values. The order of detected heavy metals in sediments in all study sites followed: Fe > Mg > Al > Cu > Zn > Pb > Ca > Na > Ni > Mn > Cr > Ba > As > Co > Cd. Potential eco-toxicological risk analysis of heavy metals concentrations in surface sediments indicated that most sampling sites posed minor to moderate ecological risks. Anthropogenic influence from agricultural land-based sources near the study area is the main contributing factor of heavy metals deposition in core sediments. Correlation analysis, cluster analysis, and principal component analysis revealed that some of the detected heavy metals were more likely to be derived from lithogenic sources while others such as Cd, Pb,and Zn were derived from anthropogenic sources such as industrial wastewater, domestic sewage, metal processing, and pesticides application.

Hydrocarbons were evaluated in surface sediments. The sum of *n*-alkanes concentrations ($C_{10}H_{22}$ – $C_{33}H_{68}$) varied from 96.63 – 367.28 ng/g dw. Study site CZ10 recorded the lowest contents of *n*-alkanes, while study site CZ2 recorded the highest

concentrations of *n*-alkanes. Therefore, the variations in concentration of *n*-alkanes may be accredited to the anthropogenic inputs and natural processes. The ∑PAHs concentrations ranged from 12.54 – 21.20 ng/g dw. Study site CZ3 recorded the lowest content of ∑PAHs (12.54 ng/g dw), whereas samples from the Santubong Bay recorded the highest concentration of ∑PAHs (21.20 ng/g dw).

The obtained values for isomeric ratios of most sites were > 1, indicating inputs from petrogenic sources with exception for study sites CZ10, CZ2, and CZ9 which isomeric ratios were < 1, suggesting pyrogenic inputs. The average concentrations of PAHs were compared to ERL and ERM values. It was noticed that the obtained results for all study sites were below ERL, suggesting no adverse biological effect. PAHs' risk assessment was evaluated based on BaP equivalent technique, and the results indicated no risks in all studied sites.

This study can help to understand heavy metals and hydrocabons distribution, their sources, and potential risk in the studied environment. In addition, the outcomes of this study contribute to the assessment of urbanization's influence on the river and coastal sites and could help in establishing quality limits of heavy metals, AHs and PAHs and planning alleviation programs.

5.2 Recommendations

Although this study established the background concentrations of heavy metals and hydrocarbons in sediments of the study area, their eco-toxic risks, and source of distribution, a more thorough examination is needed to make a comprehensive

environmental assessment of contamination. Based on the above statement, the following recommendations are suggested:

1). Future confirmation analysis of heavy metals and hydrocarbons of the coastal and four rivers estuary sediment within the catchment areas;

2). Description of baseline concentrations of AHs and PAHs in sediments at the studied area is necessary and

3). A study on the levels and ecological risk assessment of so-called unregulated contaminants such as pharmaceuticals, herbicides, pesticides in sediments and water and their impacts on non-target organisms (i.e., algae, daphid and fish) is very important to consider for future research.

REFERENCES

Abbas, M. H. H., & Abdelhafez, A. A. (2013). Role of ETDA in arsenic mobilization and its uptake by maize grown on an As-polluted soil. Chemosphere, 90(2), 588–594.

Abdollahi, S., Raoufi, Z., Faghiri, I., Savari, A., Nikpour, Y., & Mansouri, A. (2013). Contamination levels and spatial distributions of heavy metals and PAHs in surface sediment of Imam Khomeini Port, Persian Gulf, Iran. Marine Pollution Bulletin, 71(1–2), 336–345.

Abdullah, M. P. (1995). Oil-related pollution status of coastal waters of Peninsular Malaysia. In: D. Watson, K.S. Ong, and G. Vigers (Eds.). *ASEAN Criteria and Monitoring: Advances in Marine Environmental Management and Human Health Protection. Proceedings of the ASEAN-Canada Midterm Technical Review Conference on Marine Science (24-28 October 1994), Singapore. EVS Environment Consultants, Vancouver, and National Science and Technology Board*, Singapore, pp. 215–224.

Abdullah, A. R., & Samah, A. A. (1996). Oil and grease in coastal waters. In: A.R. Abdullah and C.W. Wang (Eds.). *Chapter 3: Oil and Grease Pollution in the Malaysian Marine Environment*, Department of Environment, Malaysia, pp. 31–83.

Abdullah, A. R., Tahir, N. M., & Wei, L. K. (1994). Hydrocarbons in seawater and sediment from the west coast of Peninsular Malaysia. Bulletin Environmental Contamination and Toxicology, 53, 618–626.

Adam, I. K. U., Miltner, A., & Kastner, M. (2015). Degradation of 13C-labeled pyrene in soil-compost mixtures and fertilized soil. Applied Microbiology and Biotechnology, 99, 9813–9824.

Adekola, F. A., & Eletta, O. A. A. (2007). A study of heavy metal pollution of Asa River, Ilorin, Nigeria; trace metal monitoring and geochemistry. Environmental Monitoring and Assessment, 125, 157–163.

Adekunle, A. S., Oyekunle, J. A. O., Oladele, A. S., Ojo, O. S., & Maxakato, N. W. (2020). Evaluation of polycyclic aromatic hydrocarbons (PAHs) and health risk assessment of surface water and sediments of River Sasa, Ife North Local Government Area, Nigeria. Chemistry Africa, 3, 1109–1122.

Adeniji, A. O., Okoh, O. O., & Okoh, A. I. (2019a). Distribution pattern and health risk assessment of polycyclic aromatic hydrocarbons in the water and sediment of Algoa Bay, South Africa. Environmental Geochemistry and Health, 41, 1303–1320.

Adeniji, A. O., Okoh, O. O., & Okoh, A. I. (2019b). Levels of polycyclic aromatic hydrocarbons in the water and sediment of Buffalo River Estuary, South Africa and their health risk assessment. Archives of Environmental Contamination and Toxicology, 76, 657–669.

Adeniji, A. O., Okoh, O. O., & Okoh, A. I. (2017). Petroleum hydrocarbon profiles of water and sediment of Algoa Bay, Eastern Cape, South Africa. International Journal of Environmental Research and Public Health, 14(10), 1263.

Adomako, D., Nyarko, B. J. B., Dampare, S. B. & Serfor-Armah, Y. (2008). Determination of toxic elements in waters and sediments from River Subin in the Ashanti Region of Ghana. Environmental Monitoring and Assessment, 141, 165–175.

Adriano, D. C., Wenzel, W., Vangronsveld, J., & Bolan, N. (2004). Role of assisted natural remediation in environmental cleanup. Geoderma, 122(2), 121–142.

Adriano, D. C. (2001*). Trace Elements in the Terrestrial Environment: Biogeochemistry, Bioavailability, and Risks of Metals*, 2nd edition, New York: Springer -Verlag, pp. 867.

Agnello, A. C., Bagard, M., van Hullebusch, E. D., Esposito, G., & Huguenot, D. (2016). Comparative bioremediation of heavy metals and petroleum hydrocarbons co-contaminated soil by natural attenuation, phytoremediation, bioaugmentation, and bioaugmentation-assisted phytoremediation, Science of The Total Environment, 563–564, 693–703.

Ahmed, N., Siddiqui, N. A., Rahman, A. H. B. A, Jamil, M., Sajid, M. Z., & Zaidi, F. K. (2021). Evaluation of hydrocarbon source rock potential: Deep marine shales of Belaga Formation of Late Cretaceous-Late Eocene, Sarawak, Malaysia. Journal of King Saud University-Science, 33, 101268.

Ahmed, O. E., Mahmoud, S. A., & Mousa, A. E. M. (2015). Aliphatic and polyaromatic hydrocarbons pollution at the drainage basin of Suez Oil Refinery Company. Current Science International, 4(1), 27–44.

Alexakis, D., & Gamvroula, D. (2014). Arsenic, chromium, and other potentially toxic elements in the rocks and sediments of Oropos-Kalamos Basin, Attica, Greece. Applied and Environmental Soil Science, *2014*. Article ID: 718534, pp. 1–8.

Ali, H., Khan, E. & Ilahi, I. (2019). Environmental chemistry and ecotoxicology of hazardous heavy metals: environmental persistence, toxicity and bioaccumulation. Journal of Chemistry, 2019, 1–14. Article ID 6730305.

Ali, H., & Khan, E. (2017). Environmental chemistry in the twenty first century. Environmental Chemistry Letters, 15(2), 329–346.

Alsaleh, K.A.M., Meuser, H., Usman, A.R.A., Al-Wabel, M.I., & Al-Farraj, A.S. (2018). A comparison of two digestion methods for assessing heavy metals level in urban soils influenced by mining and industrial activities. Journal of Environmental Management, 206, 731–739.

Anderson, R. V., Vinikour, W. S., & Brower, J. E. (1978). The distribution of Cd, Cu, Pb, and Zn in the biota of two freshwater sites with different trace metal inputs. Ecography, 1(4), 377–384.

Australian and New Zealand Enviornment and Conservation Council, ANZECC & Agriculture and Resource Management Council of Australia and New Zealand, ARMCANZ (2000). Australian and New Zealand Guidelines for Fresh and Marine Water Quality.

Aly Salem, D. M. S., Morsy, F. A. M., El Nemr, A., El-Sikaily, A., & Khaled, A. (2014). The monitoring and risk assessment of aliphatic and aromatic hydrocarbons in sediments of the Red Sea, Egypt. Egypt Journal of Aquatic Research, 40(4), 333–348.

Asare, E. A., Assim, Z. B., Wahi, R. B., Bakeh, T., & Dapaah, S. S. (2021a). Trend analysis of anthropogenic activities affecting trace metals deposition in core sediments from the coastal and four rivers estuary of Sarawak, Malaysia. Environmental Science and Pollution Research, 29(11), 16294–16310.

Asare, E. A., Assim, Z. B., & Wahi, R. (2021b). Validation of an analytical technique, distribution, and risk assessment of aliphatic and polycyclic aromatic hydrocarbons

in surface sediments of the coastal and selected estuaries of Sarawak. Arabian Journal of Geosciences, 14, 1943.

Aslam, M.W., Meng, B., Abdelhafiz, M.A., Liu, J., & Feng, X. (2021). Unravelling the interactive effect of soil and atmospheric mercury influencing mercury distribution and accumulation in the soil-rice system. Science of The Total Environment, 803, 149967.

Attia, O. E. A., & Ghrefat, H. (2013). Assessing heavy metal pollution in the recent bottom sediments of Mabahiss Bay, North Hurdhada, Red Sea, Egypt. Environmental Monitoring and Assessment, 185(12), 9925.

Bacosa, H. P., & Inoue, C. (2015). Polycyclic aromatic hydrocarbons (PAHs) biodegradation potential and diversity of microbial consortia enriched from tsunami sediments in Miyagi, Japan. Journal of Hazardous Materials, 283, 689–697.

Bahadar, H., Mostafalou, S., & Abdollahi, M. (2014). Growing burden of diabetes in Pakistan and the possible role of arsenic and pesticides. Journal of Diabetes and Metabolic Disorders, 13, 117.

Baker, J. E., Capel, P. D., & Eisenreich, S. J. (1986). Influence of colloids on sediment-water partition coefficients of polychlorobiphenyl congeners in natural waters. Environmental Science and Technology, 20(11), 1136–1143.

Bale, A. J., & Kenny, A. J. (2008). Sediment analysis and seabed characterisation. In : A. Eleftherio & A. McIntyre (Eds.). *Methods for the Study of Marine Benthos*, Oxford: Blackwell Science Ltd, pp. 43–46.

Barak, N. A. E., & Mason, C. F. (1989). Heavy metal in water, sediment and invertebrates from rivers in eastern England. Chemosphere, 19(10–11), 1709–1714.

Barwick, V. J., & Ellinson, S. L. R. (1999). Measurement uncertainty: approaches to the evaluation of uncertainties associated with recovery. Analyst, 124, 981–990.

Barwick, V. J., & Ellinson, S. R. L. (2000). Protocol for uncertainty evaluation from validation data; VAM Project 3.2.1, Development and harmonisation of measurement uncertainty principles. Part D. Report No: LGC/VAM/1998/088.

Basheer, C., Obbard, J. P., & Lee, H. K. (2005). Analysis of persistent organic pollutants in marine sediments using a novel microwave assisted solvent extraction and liquid-phase microextraction technique. Journal of Chromatography A, 1068(2), 221–228.

Baumard, P., Budzinski, H., & Garrigues, P. (1998a). Polycyclic aromatic hydrocarbons in sediments and mussels of the western Mediterranean Sea. Environmental Toxicology and Chemistry, 17, 765–776.

Baumard, P., Budzinski, H., Michon, Q., Garrigues, P., Burgeot, T., & Bellocq, J. (1998b). Origin and bioavailability of PAHs in the Mediterranean Sea from mussel and sediment records. Estuarine Coastal and Shelf Science, 47(1), 77–90.

Berti, W. R. & Jacobs, L. W. (1996). Chemistry and phytotoxicity of soil trace elements from repeated sewage sludge applications. Journal of Environmental Quality, 25(5), 1025–1032.

Bhuyan, M. S., Bakar, M. A., Rashed-Un-Nab, M., Senapathi, V., Chung, S. Y., & Islam, M. S. (2019). Monitoring and assessment of heavy metal contamination in surface water sediment of the Old Brahmaputra River, Bangladesh. Applied Water Science, 9, 125.

Bianchi, T. S. (2007). *Biogeochemistry of Estuaries*, 6th edition, Oxford University Press: Northants, UK; pp. 20–720.

Blaylock, J. M., & Huang, J. W. (2000). Phytoextraction of metals. In: I. Raskin & B. D., Ensley (Eds). *Phytoremediation of Toxic Metals: Using Plants to Clean Up the Environment*. New York: John Wiley and Sons Inc., pp 53-69.

Blumer, M. (1976). Polycyclic aromatic compounds in nature. Scientific American, 234(3), 34–45.

Boonyatumanond, R., Wattayakorn, G., Amano, A., Inouchi, Y., & Takada, H. (2007). Reconstruction of pollution history of organic contaminants in the upper Gulf of Thailand by using sediment cores: First report from Tropical Asia Core (TACO) project. Marine Pollution Bulletin, 54(5), 554–565.

Boonyatumanond, R., Wattayakom, G., Togo, A., & Takada, H. (2006). Distribution and origins of polycyclic aromatic hydrocarbons in estuarine, rivers and marine sediments in Thailand. Marine Pollution Bulletin, 52(8), 942–956.

Bridge, G. (2004). Contested terrain: mining and the environment. Annual Review of Environment Resources, 29, 205–259.

Breitfeld, H. T., Hall, R., Galin, T., & BouDagher-Fadel, M. K. (2018). Unravelling the stratigraphy and sedimentation history of the uppermost Cretaceous to Eocene sediments of the Kuching in West Sarawak (Malaysia). Borneo Journal of Asian Earth Sciences, 160, 200–223.

Breitfeld, H. T. (2015). *Provenance, stratigraphy and tectonic history of Mesozoic to Cenozoic sedimentary rocks of West and Central Sarawak, Malaysia*. PhD Thesis, Royal Holloway University, London, UK, 808pp.

Breitfeld, H. T., Galin, T., & Hall, R. (2014). U-Pb detrital Zircon ages from Sarawak: Changes in provenance reflecting the tectonic evolution of Southeast Asia. *AGU Fall Meeting 2014 Abstracts*, San Francisco, V43D-4921.

Bryan, G. W., & Langston, W. J. (1992). Bioavailability, accumulation and effects of heavy metals in sediments with special reference to United Kingdom estuaries: a review. Environmental Pollution, 76(2), 89–131.

Campbell, R. M., & Lee, M. L. (1986). Supercritical fluid fractionation of petroleum- and coal-derived mixtures. Analytical Chemistry, 58(11), 2247–2251.

Cardwell, R. D., Brancato, M. S., Toll, J., DeForest, D., & Tear, L. (1999). Aquatic ecological risks posed by tributyltin in United States surface waters: pre-1989 to 1996 data, IEEE Cat. No. 99CH37008.

Caruso, J. A., Zhang, K., Schroeck, N. J., McCoy, B., & McElmurry, S. P. (2015). Petroleum coke in the urban environment: A review of potential health effects, International Journal of Environmental Research and Public Health, 12, 6218–6231.

Cheloni, G., & Slaveykova, V. (2018). Combined effects of trace metals and light on photosynthetic microorganisms in aquatic environment. Environments, 5(7), 81.

Cheng, X., Drozdova, J., Danek, T., Huang, Q., Qi, W., Yang, S., Zou, Y., Xiang, Y., & Zhao, X. (2018). Pollution assessment of trace elements in agricultural soils around copper mining area. Sustainability, 10, 4533.

Chen, R., Chen, H., Song, L., Yao, Z., Meng, F., & Teng, Y. (2019). Characterization and source apportionment of heavy metals in the sediments of Lake Tai (China) and its surrounding soils. Science of The Total Environment, 694, 133819.

Chen, H., Teng, Y., Lu, S., Wang, Y., & Wang, J. (2015). Contamination features and health risk of soil heavy metals in China. Science of The Total Environment, 512–513, 143–153.

Chen, C. W., & Chen, C. F. (2011). Distribution, origin, and potential toxicological significance of polycyclic aromatic hydrocarbons (PAHs) in sediments of Kaohsiung Harbor, Taiwan. Marine Pollution Bulletin, 63(5–12), 417–423.

Chien, L. C., Hung, T. C., Choang, K. Y., Yeh, C. Y., Meng, P. J., Shieh, M. J., & Han, B. C. (2002). Daily intake of TBT, Cu, Zn, Cd and As for fishermen in Taiwan. Science of the Total Environment, 285(1–3), 177–185.

Charrie-Duhaut, A., Lemoine, S., Adam, P., Connan, J., & Albrecht, P. (2000). Abiotic oxidation of petroleum bitumens under natural conditions. Organic Geochemistry, 31(10), 977–1003.

Chiu, T. R., Khan, M. F., Latif, M. T., Nadzir, M. S. M., Hamid, H. H. A., Yusoff, H., & Ali, M. M. (2018). Distribution of polycyclic aromatic hydrocarbons (PAHs) in surface sediments of Langkawi Island, Malaysia. Sains Malaysiana, 47(5), 871–882.

Christensen, E. R. & Arora, S. (2007). Source apportionment of PAHs in sediments using factor analysis by time records: application to Lake Michigan, USA. Water Resources, 41(1), 168–176.

Chong, M. & Idrus, F. (2016). Study of sediment characteristics, TOM and trace metals in the sediment of the Sarawak EEZ, In: M. Samur, M.L. Shabdin, L. Nyanti, A.R. Khairul Adha, R. Hadil, and J.M. Mobilik. *Proceedings of Aquatic Science Colloquium 2016: Experience Sharing in Aquatic Science Research IV: Malaysia*

Exclusive Economic Zone (EEZ) Cruise and other Aquatic Science Research, Faculty of Resource Science and Technology, Universiti Malaysia Sarawak.

Chung, M. K., Hu, R., Cheung, K. C., & Wong, M. H. (2007). Pollutants in Hong Kong soils: polycyclic aromatic hydrocarbons. Chemosphere, 67(3), 464–473.

Colombo, J. C., Pelletier, E., Brochu, C., Khalil, M., & Catoggio, J. A. (1989). Determination of hydrocarbon sources using n-alkane and polyaromatic hydrocarbon distribution indexes. Case study: Rio de La Plata Estuary, Argentina. Environmental Science Technology, 23(7), 888–894.

Commendatore, M. G., Esteves, J. L., & Colombo, J. C. (2000). Hydrocarbons in coastal sediments of Patagonia, Argentina: levels and probable sources. Marine Pollution Bulletin, 40(11), 989–998.

Cui, C., Ma, L., Shi, J., Lin, K., Luo, Q., & Liu, Y. (2014). Metabolic pathway for degradation of anthracene by halophilic Martelella sp. AD-3. International Biodeterioration and Biodegradation, 89, 67–73.

Culbard, E. B., Thornton, I., Watt, J., Moorcroft, S., & Brooks, K. (1983). Sources and distribution of lead and cadmium in United Kingdom dusts and soils. *Proceeding of 4th International Conference on Heavy Metals in the Environment*. CEP, Edinburgh, pp 426–429.

Curtosi, A. E. P., Vodopivez, C. L., & MacCormack, W. P. (2007). Polycyclic aromatic hydrocarbons in soil and surface marine sediment near Jubany Station Antarctica. Role of permafrost as a low-permeability barrier. Science of the Total Environment, 383(1–3), 193–204.

Damas, E. Y. C., Medina, M. O. C., Clemente, C. A. N., & Diaz, M. A. D. (2009). Validation of an analytical methodology for the quantitative analysis of petroleum hydrocarbons in marine sediment samples. Quimica Nova, 32(4), 855–860.

Davies, B. E., & Ginnever, R. C. (1979). Trace metal contamination of soils and vegetables in shipham, Somerset. The Journal Agricultural Science, 93(3), 753–756.

Department of statistics Malaysia official portal, https://www.dosm.gov.my

Decena, S. C. P., Arguelles, M. S., & Robel, L. L. (2018). Assessing heavy metal contamination in surface sediments in an urban river in the Philippines. Polish Journal of Environmental Studies, 27(5), 1983–1995.

De Luca, G., Furesi, A., Micera, G., Panzanelli, A., Piu, P.C., Pilo, M.I., Spano, N., & Sanna, G. (2005). Nature distribution and origin of polycyclic aromatic hydrocarbons (PAHs) in the sediments of Olbia Harbor (Northern Sardinia, Italy). Marine Pollution Bulletin, 50(11), 1223–1232.

Dias-Ferreira, C., Pato, R. L., Varejao, J. B., Tavares, A. O., & Ferreira, A. J. D. (2016). Heavy metal and PCB spatial distribution pattern in sediments within an urban catchment – contribution of historical pollution sources. Journal of Soils and Sediments, 16, 25942605.

Di Baccio, D., Tognetti, R., Sebastiani, L., & Vitagliano, C. (2003). Responses of *Populus deltoids* × *Populus nigra* (*Populus* × *euramericana*) clone I-214 to high zinc concentrations. New Phytologist, 159(2), 443–452.

Dong, C., Bai, X., Sheng, H., Jiao, L., Zhou, H., & Shao, Z. (2015). Distribution of PAHs and the PAH-degrading bacteria in the deep-sea sediments of the high-latitude Arctic Ocean. Biogeosciences, 12, 2163–2177.

Dong, C-D., Chen, C-F, & Chen, C-W (2012). Determination of polycyclic aromatic hydrocarbons in industrial harbour sediments by GC-MS. Environmental Research and Public Health, 9(6), 2175–2188.

Doutch, H. F. (1992). Aspects of the structural histories of the Tertiary sedimentary basins of East, Central and West Kalimantan and their margins. BMR Journal of Australian Geology and Geophysics, 13(3), 237–250.

Duedahl-Olesen, L., Navaratnam, M. A., Jewula, J., & Jensen, A. H. (2015). PAH in some brands of tea and coffee. Polycyclic Aromatic Compounds, 35(1), 74–90.

Ergonul, M.B. & Altindag, A. (2014). Heavy metal concentrations in the muscle tissues of seven commercial fish species from Sinop Coasts of the Black Sea. Rocznik Ochrona Srodowiska 16(1), 34–51.

El Nemr, A., El-Sadaawy, M. M., Khaled, A., & Draz, S. O. (2013). Aliphatic and polycyclic aromatic hydrocarbons in the surface sediments of the Mediterranean: assessment and source recognition of petroleum hydrocarbons. Environmental Monitoring and Assessment, 185, 4571–4589.

El Nemr, A., & El-Said, G. F. (2012). Assessment of n-alkane and polycyclic aromatic hydrocarbons contaminated in the surface sediments of Egyptian Mediterranean coast. Blue Biotechnology Journal, 1(4), 557–580.

El Nemr, A., & Abd-Allah, A. M. A. (2003). Contamination of polycyclic aromatic hydrocarbons (PAHs) in microlayer and subsurface waters along Alexandria coast, Egypt. Chemosphere, 52(10), 1711–1716.

Eurachem, Middlesex (1998). The fitness for Purpose of Analytical Methods: a Laboratory Guide to Method Validation and Related.

Fagbote, O. E., & Olanipekun, E. O. (2013). Characterization and sources of aliphatic hydrocarbons of the sediments of River Oluwa at Agbabu Bitumen deposit area, Western Nigeria. Journal of Scientific Research and Report, 2(1), 228–248.

Fakhradini, S. S., Moore, F., Keshavarzi, B., & Lahijanzadeh, A. (2019). Polycyclic aromatic hydrocarbons (PAHs) in water and sediment of Hoor Al-Azim wetland, Iran: a focus on source apportionment, environmental risk assessment, and sediment-water partitioning. Environmental Monitoring and Assessment, 191, 233.

Fang, M. D., Lee, C. L., & Yu, C. S. (2003). Distribution and source recognition of polycyclic aromatic hydrocarbons in the sediments of Hsinta Harbour and adjacent coastal areas, Taiwan. Marine Pollution Bulletin, 46(8), 941–953.

Farkas, A., Erratico, C., & Vigano, L. (2007). Assessment of the environmental significance of heavy metal pollution in surficial sediments of the River Po. Chemosphere, 68(4), 761–768.

Ficken, K. J., Li, B., Swain, D. L., & Eglinton, G. (2000). An n-alkane proxy for the sedimentary input of submerged/floating freshwater aquatic macrophytes. Organic Geochemistry, 31(7–8), 745–749.

Florida Department of Environmental Protection (2008). Derivation of Numerical Sediment Quality Guidelines for Florida Coastal Waters Using the Weight of Evidence Approach. Florida Sediment Quality Assessment (SQAGs), Volume 1, Chapter 5.

Fu, J., Zhao, C., Luo, Y., Liu, C., Kyzas, G.Z., Luo Y., Zhao, D., An, S., & Zhu, H. (2014). Heavy metals in surface sediments of the Jialu River, China: Their relations to environmental factors. Journal of Hazardous Materials, 270, 102–109.

Funk, W., Dammann, V., & Donnevert, G. (2007). Quality Assurance in Analytical Chemistry: applications in environmental, food and material analysis, biotechnology, and medical engineering, Wiley-VCH, Weinheim, Germany.

Gao, S. (2019). Geomorphology and Sedimentology of Tidal Flats. In: G. M. E., Perillo, E., Wolanski, D. R., Cahoon, & C. S. Hopkinson, *An Integrated Ecosystem Approach*, Coastal Wetlands, 2nd ed., Elsevier, pp. 259–381.

Garcia-Miragaya, J., Castro, S., & Paolini, J. (1981). Lead and zinc levels and chemical fractionation in road-side soils of Caracas, Venezuela. Water Air and Soil Pollution, 15(3), 285–297.

Gee, G.W., & Bauder, J.W. (2002). Particle-size analysis. In: Dane, J.H., Topp, G.C. (Eds.), Methods of Soil Analysis. Part 4, First ed., Physical and Mineralogical Methods. SSSA and ASA, Madison, WI, pp. 255 -294.

Gesine, W., & Erika, T. (1999). Polycyclic aromatic hydrocarbons (PAHs) in sediments of the Baltic Sea and of the German coastal waters. Chemosphere, 38(7), 1603–1614.

Gholizadeh, A., Taghavi, M., Moslem, A., Neshat, A. A., Lari Najafi, M., Alahabadi, A., Ahmadi, E., Ebrahimi Aval, H., Asour, A. A., Rezaei, H., Gholami, S., & Miri, M. (2019). Ecological and health risk assessment of exposure to atmospheric heavy metals. Ecotoxicology and Environmental Safety, 184, 109622.

Giesy, J. P., Solomon, K. R., Coates, J. R., Dixon, K. R., Giddings, J. M., & Kenaga, E. E. (1999). Chlorpyrifos: ecological risk assessment in North American aquatic environments. Reviews of Environmental Contamination and Toxicology, 160, 1–129.

Gonullu, H., Karadas, S., Oncu, M. R., Dulger, A. C., & Keskin, S. (2013). The analysis of the cases of aspired fuel oil and gasoline through siphonage method. Journal of Pakistan Medical Association, 63(3), 383–384.

Gray, J. (1981). The ecology of marine sediments: an introduction to the structure and function of marine sediments. *Cambridge Studies in Modern Biology*, 2.

Grossi, V., Massias, D., Stora, G., & Bertrand, J. C. (2002). Burial, exportation and degradation of acyclic petroleum hydrocarbons following asimulated oil spill in bioturbated Mediterranean coastal sediments. Chemosphere, 48(9), 947–954.

Guan, Q., Wang, F., Xu, C., Pan, N., Lin, J., Zhao, R., Yang, Y., & Luo, H. (2017). Source appointment of heavy metals in agricultural soil based on PMF: A case study in Hexi corridor, Northwest China. Chemosphere, 193, 189–197.

Guinan, J., Charlesworth, M., Service, M., & Oliver, T. (2001). Sources and geochemical constraints of polycyclic aromatic hydrocarbons (PAHs) in sediments and mussels of two Northern Irish SeaLoughs. Marine Pollution Bulletin, 42(11), 1073–1081.

Gupta, S.K., Chabukdhara, M., Kumar, P., Singh, J., & Bux, F. (2014). Evaluation of ecological risk of metal contamination in river Gomti, India: A biomonitoring approach. Ecotoxicology and Environmental Safety, 110, 49–55.

Gupta, P.K. (2007). Soil, Plant, Water and Fertilizer Analysis. Agrobios India, 344.

Guo, W., Wang, Y., Shi, J., Zhao, X., & Xie, Y. (2019). Sediment information on natural and anthropogenic-induced change of connected water systems in Chagan Lake, North China. Environmental Geochemistry and Health, 42, 795–808.

Guo, L., Tan, S., Li, X., & Lee, H. K. (2016). Fast automated dual-syringe based dispersive liquid-liquid microextraction coupled with gas chromatography-mass spectrometry

for the determination of polycyclic aromatic hydrocarbons in environmental water samples. Journal of Chromatography A, 1438, 1–9.

Guo, J. Y., Wu, F. C., Zhang, L., Liao, H. Q., Zhang, R. Y., Li, W., Zhao, X., Chen, J., & Mai, B. (2011). Screening level of PAHs in sediment core from Lake Hongfeng, Southwest China. Archives of Environmental Contamination and Toxicology, 60(4), 90–596.

Haile, N. S. (1974). Borneo. In: A.M. Spencer (Ed.), Mesozoic-Cenozoic Orogenic Belts: Data for Orogenic Studies. Geological Society of London, Special Publication, 4, 333–347.

Hakanson, L. (1980). An ecological risk index for aquatic pollution control of sediment ecological approach. Water Research, 14(8), 975–1001.

Hamid, M. Y. A., & Sidhu, H. S. (1993). Metal finishing wastewater: Characteristics and minimization. In: B. G. Yeoh, K. S. Chee, S. M. Phang, Z. Isa, A. Idris, M. Mohamed (eds.), *Waste Management in Malaysia: Current Status and Prospects for Bioremediation*, Ministry of Science, Technology and the Environment, Malaysia, pp. 41–49.

Harris K. A. (2010). *Hydrocarbons in Sea Otters (Enhydra lutris) and their Habitat in Coastal British Columbia, Canada.* MS Thesis, The School of Earth and Ocean Sciences, University of Victoria, Canada.

Haritash, A. K., & Kaushik, C. P. (2009). Biodegradation aspects of polycyclic aromatic hydrocarbons (PAHs): A review. Journal of Hazardous Materials, 169(1–3), 1–15.

Hartmann, P. C., Quinn, J. G., Cairns, R. W., & King, J. W. (2004). The distribution and sources of polycyclic aromatic hydrocarbons in Narragansett Bay surface sediments. Marine Pollution Bulletin, 48(3–4), 351–358.

Hedges, J. I., & Prahl, F. G. (1993). Early diagenesis: consequences for applications of molecular biomarkers. In: M.H. Engel, M.H. & S.A. Macko (Eds.), *Organic Geochemistry: Principles and Applications.* Plenum Press, New York, pp. 237–253.

Hennig, J., Breitfeld, H. T., Hall, R., & Nugraha, A. M. S. (2017). The Mesozoic tectono-magmatic evolution at the Paleo-Pacific subduction zone in West Borneo. Gondwana Research, 48, 292–310.

Hilton, J., Davison, W., & Ochsenbein, U. (1985). A mathematical model for analysis of sediment coke data: Implications for enrichment factor calculations and trace metal transport mechanisms. Chemical Geology, 48(1–4), 281–291.

Holme, N. A., & McIntyre, A. D. (1984). *Methods for the Study of Marine Benthos*. Oxford: Blackwell Scientific Publications.

Hossner, L. R. (1996). *Dissolution for Total Elemental Analysis*. In: Sparks, J. M., Bigham (edition), Methods of Soil Analysis: Part 3- Chemical Methods. SSSA and ASA, Madison, WI, pp. 49–64.

Hostettler, F. D., Pereira, W. E., Kvenvolden, K. A., van Genn, A., Luoma, S. N., Fuller, C. C., & Anima, R. (1999). A record of hydrocarbon input to San Francisco Bay traced by biomarker proles in surface sediment and sediment cores. Marine Chemistry, 64, 115–127.

Horowitz, A. J., & Elrick, K. A. (1987). The relation of stream sediment surface area, grain size and composition to trace element chemistry. Applied Geochemistry, 2(4), 437–451.

Hu, J., Liu, C., Zhang, G., Zhang, Y., Li, S., Zhao, Z., Liu, B., & Guo, Q. (2016). Distribution characteristics and source apportionment of polycyclic aromatic hydrocarbons (PAHs) in the Liao River drainage basin, northeast China. Environmental Monitoring and Assessment, 188(4), 227.

Huang, Z., Zhao, W., Xu, T., Zheng, B., & Yin, D. (2019). Occurrence and distribution of antibiotic resistance genes in the water and sediments of Qingcaosha Reservoir, Shanghai. China. Environmental Sciences Europe, 31, 1–9.

Huang, W., Wanga, Z., & Yan, W. (2012). Distribution and sources of polycyclic aromatic hydrocarbons (PAHs) in sediments from Zhanjiang Bay and Leizhou Bay, South China. Marine Pollution Bulletin, 64(9), 1962–1969.

Husain, M., Harith, M., Rosnan, Y., & Kky, K. (1998). Sedimentological characteristics of sediments of the South China Sea, Area II: Sarawak, Sabah and Brunei Darussalam waters. In Proceedings of *2nd Technical Seminar on Marine Fishery Resources Survey in the South China Sea Area II: Sarawak*. 14-15 December 1998, Kuala Lumpur, Malaysia (pp. 95-110). Samut Prakan, Thailand: Training Department, Southeast Asian Fisheries Development Center, SEAFDEC Publications.

Ismail, A., & Rosniza, R. (1997). Trace metals in sediments and molluscs from an estuary receiving pig farms effluent. Environmental Technology, 18(5), 509–515.

Islam, M. S., Ahmed, M. K., Raknuzzaman, M., Habibullah -Al- Mamun, M., & Islam, M. K. (2015). Heavy metal pollution in surface water and sediment: A preliminary

assessment of an urban river in a developing country. Ecological Indicators, 48, 282–291.

ISO/TS 21748: 2004 - ISO 3534 – 1 Statistics. Vocabulary and Symbols. Part 1: Probability and general statistical terms, 1st ed., Geneva, 1993.

Jaouen-Madoulet, A., Abarnou, A., Le Guellec, A. M., Loizeau, V., & Leboulenger, F. (2000). Validation of an analytical procedure for polychlorinated biphenyls, coplanar polychlorinated biphenyls and polycyclic aromatic hydrocarbons in environmental samples. Journal chromatography A, 886(1-2), 153–173.

Jeng, W. L. (2006). Higher plant n-alkane average chain length as an indicator of petrogenic hydrocarbon contamination in marine sediments. Marine Chemistry, 102(3–4), 242–251.

Jeng, W. L., & Huh, C. A. (2006). A comparison of sedimentary aliphatic hydrocarbon distribution between the southern Okinawa Trough and a nearby river with high sediment discharge. Estuarine Coastal and Shelf Science, 66(1), 217–224.

Jernelov, A., Landner, L., & Larsson, T. (1975). Swedish perspectives on mercury pollution. Journal of Water Pollution Control Federation, 47(4), 810–822. PMID: 1142547.

Ji, H., Li, H., Zhang, Y., Ding, H., Gao, Y., & Xing, Y. (2018). Distribution and risk assessment of heavy metals in overlying water, porewater, and sediments of Yongding River in a coal mine brownfield. Journal of Soils and Sediments, 18, 624–639.

Jia, L., Liu, H., Kong, Q., Li, M., Wu, S., & Wu, H. (2019). Interactions of high-rate nitrate reduction and heavy metal mitigation in iron-carbon-based constructed wetlands for purifying contaminated groundwater. Water Research, 169, 115285.

Kao, S-J., Shiah,F-K., Wang, C-H., & Liu, K-K. (2007). Efficient trapping of organic carbon in sediments on the continental margin with high fluvial sediment input off southwestern Taiwan. Continental Shelf Research, 26(20), 2520–2537.

Kachenko, N. G., & Singh, B. (2006). Heavy metals contamination in vegetables grown in urban and metal smelter contaminated sites in Australia. Water, Air, and Soil Pollution, 169, 101–123.

Kadhum, S. A., Ishak, M. Y., & Zulkifli, S. Z. (2016). Evaluation and assessment of baseline contamination in surface sediments from the Bernam River, Malaysia. Environmental Science and Pollution Research, 23, 6312–6321.

Kadhum, S. A., Ishak, M. Y., Zulkifli, S. Z., & Hashim, R. B. (2015). Evaluation of the status and distributions of heavy metal pollution in surface sediments of the Langat River Basin in Selangor Malaysia. Marine Pollution Bulletin, 101(1), 391–396.

Kanda, A., Ncube, F., Hwende, T., & Makumbe, P. (2018). Assessment of trace element contamination of urban surface soil at informal industrial sites in a low-income country. Environmental Geochemistry and Health, 40, 2617–2633.

Kao, S-J., Shiah,F-K., Wang, C-H., & Liu, K-K. (2007). Efficient trapping of organic carbon in sediments on the continental margin with high fluvial sediment input off southwestern Taiwan. Continental Shelf Research, 26(20), 2520–2537.

Karbassi, A. R., Monavari, S. M., Nabi Bidhendi, G. R., Nouri, J., & Nematpour, K. (2008). Metal pollution assessment of sediment and water in the Shur River. Environmental Monitoring and Assessment, 147, 107.

Kara, M., Dumanoglu, Y., Altiok, H., Elbir, T., Odabasi, M., & Bayram, A. (2015). Spatial variation of trace elements in seawater and sediment samples in a heavily industrialized region. Environmental Earth Sciences, 73, 405–421.

Keshavarzifard, M., Moore, F., Keshavarzi, & Reza, S. (2017). Polycyclic aromatic hydrocarbons (PAHs) in sediment and sea urchin (*Echinometra mathaei*) from the intertidal ecosystem of the northern Persian Gulf: Distribution, sources, and bioavailability. Marine Pollution Bulletin, 123(1–2), 373–380.

Keshavarzifard, M., Zakaria, M. P., & Keshavarzifard, S. (2019). Evaluation of polycyclic aromatic hydrocarbons contamination in the sediments of the Johor Strait, Peninsular Malaysia. Polycyclic Aromatic Compounds, 39(1), 44–59.

Ke, X., Gui, S., Huang, H., Zhang, H., Wang, C., & Guo, W. (2017). Ecological risk assessment and source identification of heavy metals in surface sediments from the Liaohe River protected area, China. Chemosphere, 175, 473–481.

Kennish, L. (1992). Toxicity of heavy metals: effects of Cr and Se on human's health. Journal of Indian Public Health Education, 2, 36–64.

Kennicutt, M. C., Barker, C., Brooks, J. M., DeFreitas, D. A., & Zhu, G. H. (1987). Selected organic matter source indicators in the Orinoco, Nile and Changjiang deltas. Organic Geochemistry, 11(1), 41–51.

Kerebba, N., Ssebugere, P., Kwetegyeka, J., Arinaitwe, K., & Wasswa, J. (2017). Concentrations and sources apportionment of polycyclic aromatic hydrocarbons in

sediments from the Uganda side of Lake Victoria. Environmental Science: Processes Impacts, 19(4), 570–577.

Khodami, A., Surif, M., Wan Maznah, W. O., & Daryanabard, R. (2017). Assessment of heavy metal pollution in surface sediments of the Bayan Lepas area, Penang, Malaysia. Marine Pollution Bulletin, 114(1), 615–622.

Kim, G. B., Maruya, K. A., Lee, R. F., Lee, J. H., Kon, C. H., & Tanabe, S. (1999). Distribution and sources of polycyclic aromatic hydrocarbons in sediments from Kyeonggi Bay, Korea. Marine Pollution Bulletin, 38(1), 7–15.

Kiran, R., Krishna, V. V. J. G., Naik, B. G., Mahalakshmi, G., Rengarajan, R., Mazumdar, A., & Sarma, N. S. (2015). Can hydrocarbons in coastal sediments be related to terrestrial flux? A case study of Godavari river discharge (Bay of Bengal). Current Science, 108(1), 96–100.

Kwon, Y. T., Lee, C. W., & Ahn, B. Y. (2001). Sedimentation pattern and sediments bioavailability in a wastewater discharging area by sequential metal analysis. Microchemical Journal, 68(2–3), 135–141.

Lai Budi, N. B., Assim, Z. B., Abdul Fatah, A. A., Jafa, J. B., Fasihuddin, B. A., & Wan Morni, W. Z. (2016). Spatial distribution and source of hydrocarbons in sediments from Sarawak Economic Exclusive Zone, Malaysia, In: M. Samur, M. L. Shabdin, L. Nyanti, A. R. Khairul Adha, R. Hadil, & J. M. Mobilik. *Aquatic Science Colloqium 2016: Experiences Sharing in Aquatic Science Research IV: Malaysia Exclusive Economic Zone (EEZ) Cruise and other Aquatic Science Research, Monograph, Universiti Malaysia Sarawak, Kota Samarahan.* Volume 4.

Laflamme, R. E., & Hites, R. A. (1978). The global distribution of polycyclic aromatic hydrocarbons in recent sediments. Geochimica et Cosmochimica Acta, 42(3), 289–303.

Law, A. T., & Veelu, R. (1989). Petroleum hydrocarbons along the coastal area of Port Dickson. Pertanika, 12(3), 345–348.

Law, A. T. (1990). Petroleum hydrocarbon distribution in the coastal waters of Sabah, South China Sea. In: A. K. M. Mohsin, M. I. Mohamed & M. A. Ambak (Eds). *Matahari Expedition 1985. A Study on the Offshore Waters of the Malaysian Exclusive Economic Zone.* Faculty of Fisheries and Marine Science, Universiti Sains Malaysia, Occasional Publication No. 9, pp. 57–64.

Law, A. T. & Yusof, R. (1986). Hydrocarbon distribution in the South China Sea. In: A. K. M. Mohsin, M. I. Mohamed & M. A. Ambak (Eds). Matahari Expedition 1985. *A Study on the Offshore Waters of the Malaysian Exclusive Economic Zone.* Faculty of Fisheries and Marine Science, Universiti Pertanian Malaysia. Occasional Publication No. 3, pp. 93–100.

Law, A. T., & Zulkifli, M. (1987). Distribution of petroleum hydrocarbon in the south-western portion of the South China Sea. In: A. K. M. Mohsin, A. R. Ridzwan & M. A. Ambak (Eds). *Matahari Expedition 1986. A Study on the Offshore Waters of the Malaysian Exclusive Economic Zone.* Faculty of Fisheries and Marine Science, Universiti Pertanian Malaysia. Occasional Publication No. 4, pp. 53–60.

Law, A. T. & Libi, S. (1988). Petroleum hydrocarbon distribution in the coastal waters off Sarawak. In: A. K. M. Mohsin, M. I. Mohamed & M. A. Ambak (Eds). *Matahari Expedition 1987. A Study on the Offshore Waters of the Malaysian Exclusive*

Economic Zone. Faculty of Fisheries and Marine Science, Universiti Pertanian Malaysia. Occasional Publication No. 6, pp. 61–67.

Law, A. T., Shazili, N. A., Yaacob, R., Chark, L. H., Saadon, M. N., & Shamsuddin, L. (1991). Coastal oceanographic studies in the Straits of Malacca and South China Sea: In the Port Dickson coastal waters. *Conference on the Intensification of Research in Priority Areas*. *December 1991*. Penang, Malaysia. pp. 12.

Law, A. T., Wong, Y. H., Chung, D., & Abol-Munafi, A. B. (1999). Effects of water soluble fraction of a Malaysian crude oil and some selected aromatic hydrocarbons on Macrobrachium rosenbergii (de Man) egg hatchability in brackish water. p. 71-76. In: I. Watson, , G. Vigers, K. S. Ong, C. McPherson, N. Millson, A. Tang & D. Gass (Eds.). *ASEAN Marine Environmental Management: Towards Sustainable Development and Integrated Management of the Marine Environment in ASEAN. Proceedings of the Fourth ASEAN-Canada Technical Conference on Marine Science (26-30 October 1998)*, Langkawi, Malaysia. Environment Consultants, Vancouver, and Department of Fisheries, Malaysia. pp. 609.

Lehnik-Habrink, P., Hein, S., T, Win, T., Bremser, W., & Nehls, I. (2010). Multi-residue analysis of PAH, PCB, and OCP optimized for organic matter of forest soil. Journal of Soils and Sediments, 10(8), 1487–1498.

Li, Y., & Duan, X. (2015). Polycyclic aromatic hydrocarbons in sediments of China Sea. Environmental Science and Pollution Research, 22, 15432–15442.

Liang, J., Feng, C., Zeng, G., Gao, X., Zhong, M., Li, X., He, X., & Fang, Y. (2017). Spatial distribution and source identification of heavy metals in surface soils in a typical coal mine city, Lianyuan, China. Environmental Pollution, 225, 681–690.

Liu, J., Xiang, R., Chen, Z., Chen, M, Yan, W., Zhang, L., & Chen, H. (2013). Sources, transport and deposition of surface sediments from the South China Sea. Deep-Sea Research Part I: Oceanographic Research Papers, 71, 92–102.

Likuku, A. S., Mmolawa, K., & Gaboutloeloe, G. K. (2013). Assessment of heavy metal enrichment and degree of contamination around the copper–nickel mine in the Selebi Phikwe Region, Eastern Botswana. Environment and Ecology Research, 1, 32–40.

Li, Z., Liu, J., Chen, H., Li, Q., Yu, C., Huang, X., & Guo, H. (2019). Water environment in the Tibetan Plateau: heavy metal distribution analysis of surface sediments in the Yarlung Tsangpo River Basin. Environmental Geochemistry and Health, 17, 1–9.

Liu, Y., Guo, H. C., Yu, Y. J., Huang, K., & Wang, Z. (2007). Sediment chemistry and the variation of three altiplano lakes to recent anthropogenic impacts in southwestern China. Water SA, 33(2), 305–310.

Li, G., Xia, X., Yang, Z., Wang, R., & Voulvoulis, N. (2006). Distribution and sources of polycyclic aromatic hydrocarbons in the middle and lower reaches of the Yellow River, China. Environmental Pollution, 144(3), 985–993.

Li, W. H., Tian, Y. Z., Shi, G. L., Guo, C. S., Li, X., & Feng, Y. C. (2012). Concentrations and sources of PAHs in surface sediments of the Fenhe reservoir and watershed, China. Ecotoxicology and Environmental Safety, 75(1), 198–206.

Liu, A. X., Lang, Y. H., Xue, L. D., & Liu, J., (2009a). Ecological risk analysis of polycyclic aromatic hydrocarbons (PAHs) in surface sediments from Laizhou Bay. Environmental Monitoring and Assessment, 159(1–4), 429– 436.

Liu, G., Zhang, G., Jin, Z., & Li, J. (2009b). Sedimentary record of hydrophobic organic compounds in relation to regional economic development: a study of Taihu Lake, East China. Environmental Pollution, 157(11), 2994–3000.

Liu, W. X., Dou, H., Wei, Z. C., Chang, B., Qiu, W. X., Liu, Y., & Tao, S. (2009c). Emission characteristics of polycyclic aromatic hydrocarbons from combustion of different residential coals in North China. Science of The Total Environment, 407(4), 1436–1446.

Loeppert, R.H., & Suarez, D. (1996). Carbonate and gypsum. In: Sparks, Bigham, J.M. (Eds.), Methods of Soil Analysis. Part 3. Chemical Methods. SSSA and ASA, Madison, WI, pp. 437–474.

Long, E. R., MacDonald, D. D., Smith, S. L., & Calder, F. D. (1995). Incidence of adverse biological effects within ranges of chemical concentrations in marine and estuarine sediments. Environmental Management, 19, 81–97.

Loska, K. & Wiechuła, D. (2003). Application of principal component analysis for the estimation of source of heavy metal contamination in surface sediments from the Rybnik Reservoir. Chemosphere, 51(8), 723–733.

Lucke, R., Later, D. W., Wright, C. W., Chess, E. K., & Weimar, W. C. (1985). Integrated, multi-stage chromatographic method for the separation and identification of polycyclic aromatic hydrocarbons in complex coal liquids. Analytical Chemistry, 57(3), 633–639.

Macias-Zamora, J. V., Mendoza-Vega, E., & Villaescusa-Celaya, J. A. (2002). PAHs composition of surface marine sediments: a comparison to potential local sources in Todos Santos Bay, BC, Mexico. Chemosphere, 46(3), 459–468.

Magi, E., Bianco R., Ianni C., & Carro M. D. (2002) Distribution of polycyclic aromatic hydrocarbons in the sediments of the Adriatic Sea. Environmental Pollution, 119(1), 91–98.

Maanan, M., Saddik, M., Maanan, M., Chaibi, M., Assobhei, O., & Zourarah, B. (2015). Environmental and ecological risk assessment of heavy metals in sediments of Nador lagoon, Morocco. Ecological Indicators, 48, 616–626.

Massachusetts Department of Environmental Protection (MADEP) (2004). *Method for the determination of volatile petroleum hydrocarbons (VPH),* Revision 1.1, Massachusetts Department of Environmental Protection, Executive Office of Environmental Affairs, Commonwealth of Massachusetts, Boston.

Medeiros, P. M., Bicego, M. C., Castelo, R. M., Rosso, C. D., Fillamann, G., & Zamboni, A. J. (2005). Natural and anthropogenic hydrocarbon inputs to sediments of Patos Lagoon estuary, Brazil. Environmental International, 31(1), 77–87.

Meyer, W., Seiler, T. B., Christ, A., Redelstein, R., Puettmann, W., Hollert, H., & Achten, C. (2014). Mutagenicity, dioxin-like activity and bioaccumulation of alkylated picene and chrysene derivatives in a German lignite. Science of the Total Environment, 497–498, 634–641.

Meador, J. P., Stein, J. E., Reichert, W. L., & Varanasi, U. (1995). Bioaccumulation of polycyclic aromatic hydrocarbons by marine organisms. Reviews of Environmental Contamination and Toxicology, 143, 79–165.

Mille, G., Asia, L., Guiliano, M., Malleret, L., & Doumenq, P. (2007). Hydrocarbons in coastal sediments from the Mediterranean Sea (Gulf of Fos area, France). Marine Pollution Bulletin, 54(5), 566–575.

Mito, S., Sohrin, Y., Norisuye, K., Matsui, M., Hasegawa, H., Maruo, M., Tsuchiya, M., & Kawashima M. (2004). The budget of dissolved trace metals in Lake Biwa, Japan. Limnology, 5, 7–16.

Monaci, F., & Bargagli, R. (1997). Barium and other trace metals as indicators of vehicle emissions. Water, Air, and Soil Pollution, 100, 89–98.

Morillo, J., Usero, J., & Gracia, I. (2004). Heavy metal distribution in marine sediments from the southwest coast of Spain. Chemosphere, 55(3), 431–442.

Morley, R. J. (1998). Palynological evidence for Tertiary plant dispersals in the SE Asian region in relation to plate tectonics and climate. In: R. Hall & J.D. Holloway (Eds.), *Biogeography and Geological Evolution of SE Asia.* Backhuys Publishers, Leiden, The Netherlands, pp. 211–234.

Morni, W. Z. W., Ab Rahim, S. A. K., Rumpet, R., Musel, J., & Hassan, R. (2017). Checklist of gastropods from the exclusive economic zone (EEZ), Sarawak, Malaysia. Tropical Life Sciences Research, 28(1), 117–129.

Moorthy, B., Chu, C., & Carlin, D. J. (2015). Polycyclic aromatic hydrocarbons: From metabolism to lung cancer. Toxicological Sciences, 145, 5–15.

Mouton, J., Mercier, G., Drogui, P., & Blais, J. F. (2009). Experimental assessment of an innovative process for simultaneous PAHs and Pb removal from polluted soil. Science of The Total Environment, 407(20), 5402–5410.

Muller, G. (1969). Index of geoaccumulation in sediments of the Rhine River, Journal of Geology, 2, 108–118.

Muller, G. (1979). Schwermetalle in den sediments des Rheins—Veranderungen Seitte. Umschan 78, 778–783.

Muthukumar, A., Idayachandiran, G., Kumaresan, S., Kumar, T. A., & Balasubramanian, T. (2013). Petroleum hydrocarbons (PHC) in sediments of three different ecosystems from Southeast Coast of India. International Journal of Pharmaceutical and Biological Archives, 4(3), 543–549.

Mulder, M. D., Heil, A., Kukucka, P., Kuta, J., Pribylova, P., Prokes, R., & Lammel, G. (2015). Long-range atmospheric transport of PAHs, PCBs and PBDEs to the central and eastern Mediterranean and changes of PCB and PBDE congener patterns in summer 2010. Atmospheric Environment, 111, 51–59.

Nasher, E., Heng, L. Y., Zakaria, Z., & Surif, S. (2013). Assessing the Ecological Risk of Polycyclic Aromatic Hydrocarbons in Sediments at Langkawi Island, Malaysia. The Scientific World Journal, *2013*, Article ID 858309:1–13.

Nawrot, N., Wojciechowska, E., Matej-Łukowicz, K., Walkusz-Miotk, J., & Pazdro, K. (2020). Spatial and vertical distribution analysis of heavy metals in urban retention tanks sediments: a case study of Strzyza Stream, Environmental Geochemistry and Health, 42, 1469–1485.

Nawrot, N., Matej-Łukowicz, K., & Wojciechowska, E. (2018). Change in heavy metals concentrations in sediments deposited in retention tanks in a stream after a flood. Polish Journal of Environmental Studies, 28(1), 9–14.

Nawrot, N., & Wojciechowska, E. (2018). Assessment of trace metals leaching during rainfall events from building rooftops with different types of coverage – Case study. Journal of Ecological Engineering, 19(3), 45–51.

Nayak, G. N. (2015). Bioavailability of metals in estuarine sediments and their possible impacts on the environment. Environmental Social Science, 2(1), 1–4.

National Research Council (US) (NRC) (2003). *Oil in the Sea III: Input, Fates and Effects*. Washington: National Academies Press, pp. 277.

Neff, J. M. (1979). *Polycyclic Aromatic Hydrocarbon in the Aquatic Environment: Sources, Fates and Biological Effects.* London Applied Science Publishers, pp. 262.

Nguyen, C. C., Hugie, C. N., Kile, M. L., & Navab-Daneshmand, T. (2019). Association between heavy metals and antibiotic-resistant human pathogens in environmental reservoirs: a review. Frontiers of Environmental Science and Engineering, 13, 46.

Nishioka, M., Whiting, D. G., Campbell, R. M., & Lee, M. L. (1986). Supercritical fluid fractionation and detailed characterization of the sulfur heterocycles in a catalytically cracked petroleum vacuum residue. Analytical Chemistry, 58(11), 2251–2255.

Nriagu, J. O. (1992). Toxic metal pollution in Africa. Science of the Total Environment, 121, 1–37.

Nwaichi, E. O., & Dhankher, O. P. (2016). Heavy metals contaminated environments and the road map with phytoremediation. Journal of Environmental Protection, 7, 41–51.

Omorinoye, A. O., Assim, Z. B., Jusoh, I. B., Durumin Iya, N. I., Bamigboye, O. S., & Asare, E. A. (2020). Distribution and sources of aliphatic hydrocarbons in sediments from Sadong River, Sarawak, Malaysia, Research Journal of Chemistry and Environment, 24(6), 70–77.

Omorinoye, A. O., Assim, Z. B., Jusoh, I. B., Durumin Iya. N. I., & Asare, E. A. (2019a). Vertical profile of heavy metal contamination in sediments from Sadong River, Sarawak, Malaysia. Indian Journal of Environmental Protection, 39(11), 971–978.

Omorinoye, A. O., Assim, Z. B., Jusoh, I. B., Bamigboye, O. S., & Alebiosu, M. T. (2019b). Distribution of polycyclic aromatic hydrocarbons (PAHs) in sediments from

Sadong River, Sarawak, Malaysia. Asian Journal Applied Science and Technology, 3(4), 57–66.

Osullivan, A., Wicke, D., & Cochrane T. (2012). Heavy metal contamination in an urban stream fed by contaminated air-conditioning and stormwater discharges. Environmental Science and Pollution Research, 19(3), 903–911.

Ou, S. M., Zheng, J. H., Zheng, J. S., Richardson, B. J., & Lam, P. K. S. (2004). Petroleum hydrocarbons and polycyclic aromatic hydrocarbons in the surficial sediments of Xiamen Harbour and Yuan Dan Lake, China. Chemosphere, 56(2), 107–112.

Pan, K., & Wang, W.-X. (2012). Trace metal contamination in estuarine and coastal environments in China. Science of the Total Environment, 421, 3–16.

Pandey, J. & Singh, R. (2015). Heavy metals in sediments of Ganga River: up- and downstream urban influences. Applied Water Science, 7, 1669–1678.

Parry, G. D. R, Johnson, M. S., & Bell, R. M. (1981). Trace metal survey of soil as a component of strategic and local planning policy development. Environmental Pollution Series B, Chemical and Physical, 2(2), 97–107.

Peters, K. E., Walters, C. C., & Moldowan, J. M. (2005). The Biomarker Guide. Volume 1: Biomarkers and Isotopes in the Environment and Human History. Volume 2: *Biomarkers and Isotopes in Petroleum Exploration and Earth History.* Second Edition. (First edition published 1993 by Chevron Texaco.), Cambridge, New York, Melborne: Cambridge University Press, pp. 1132.

Peters, K. E., & Moldowan, J. M. (1993). *The Biomarker Guide: Interpreting Molecular Fossils in Petroleum and Ancient Sediments*, New Jersey: Prentice-Hall Inc.

Pejman, A., Bidhendi, G. N., Ardestani, M., Saeedi, M., & Baghvand, A. (2015). A new index for assessing heavy metals contamination in sediments: a case study. Ecological Indicators, 58, 365–373.

Pekey, H., Karakas, D., Ayberk, S., Tolun, L., & Bakoglu, M. (2004). Ecological risk assessment using trace elements from surface sediments of Izmit Bay (Northeastern Marmara Sea) Turkey. Marine Pollution Bulletin, 48(9–10), 946–953.

Pieters, P. E., Trail, D. S., & Supriatna, S. (1987). Correlation of Early Tertiary rocks across Kalimantan. *Indonesian Petroleum Association, Proceedings 16th annual convention Jakarta, I,* 291–306.

Pongpiachan, S., Tipmanee, D., Deelaman, W., Muprasit, J., Feldens, P., & Schwarzer, K. (2013). Risk assessment of the presence of polycyclic aromatic hydrocarbons (PAHs) in coastal areas of Thailand affected by the 2004 tsunami. Marine Pollution Bulletin, 76, 370–378.

Porstner, U. (1989). *Lecture Notes in Earth Sciences (Contaminated Sediments).* Springer Verlag, Berlin, pp. 107-109.

Pourkhabbaz, A., Zarei, I., & Khuzestani, R. B. (2014). An assessment of metal contamination risk in sediments of Hara Biosphere Reserve, southern Iran with a focus on application of pollution indicators. Environmental Monitoring and Assessment, 186, 6047–6060.

Pradit, S., Wattayakorn, G., Angsupanich, S., Baeyens, W., & Leermakers M. (2010). Distribution of trace elements in sediments and biota of Songkhla Lake, Southern Thailand. Water, Air, and Soil Pollution, 206(1), 155.

Protano, C., Zinna, L., Giampaoli, S., Spica, V.R., Chiavarini, S., & Vitali M. (2014). Heavy metal pollution and potential ecological risks in rivers: a case study from Southern Italy. Bulletin of Environmental Contamination and Toxicology, 92, 75–80.

Pulford, I., & Watson, C. (2003). Phytoremediation of heavy metal – contaminated land by trees – a Review. Environment international, 29(4), 529–540.

Qiao, M., Huang, S., & Wang, Z. (2008). Partitioning characteristics of PAHs between sediment and water in a shallow Lake. Journal of Soils and Sediments, 8(2), 69–73.

Qiu, Y. W., Zhang, G., Guo, L. L., Li, J., Liu, G. Q., Liu, X., & Li, X. D. (2007). Characteristics of PAHs in the ecosystem of Deep Bay and their ecological risk. Environmental Science, 28(5), 1056–1061.

Qiao, M., Wang, C., Huang, S., Wang, D., & Wang, Z. (2006). Composition, sources, and potential toxicological significance of PAHs in the surface sediments of the Meiliang Bay, Taihu Lake, China. Environmental International, 32(1), 28–33.

Quevenco, R. (2011). Sustainable management of coastal waters: A profile of the history and levels of coastal pollution in the Caribbean emerges. IAEA Bulletin, 53(1), 32–37.

Rasheed, M. A., Rao, P. L. S., Boruah, A., Hassan, S. Z., Patel, A., Velani, V., & Patel, P. (2015). Geological characterization of coals using proximate and ultimate analysis of Tadkeshwar Coals, Gujarat. Geosciences, 5(4), 113–119.

Rahman, R. A., & Surif, S. (1993). Metal finishing wastewater: characteristics and minimization. In: B. G. Yeoh , K. S. Chee, S. M. Phang, Z. Isa, A. & Idris, M. Mohamed (Eds.), *Waste Management in Malaysia: Current Status and Prospects for*

Bioremediation. Ministry of Science, Technology and the Environment, Malaysia. pp. 3–7.

Ramos, L., Vreuls, J. J., & Brinkman, U. A. (2000). Miniaturised pressurized liquid extraction of polycyclic aromatic hydrocarbons from soil and sediment with subsequent large-volume injection-gas chromatography. Journal of Chromatography A, 891(2), 275–286.

Raza, M., Zakaria, M. P., Hashim, N. R., Yim, U. H., Kannan, N., & Ha, S. Y. (2013). Composition and source identification of polycyclic aromatic hydrocarbons in mangrove sediments of Peninsular Malaysia: indication of anthropogenic input. Environmental Earth Sciences, 70(6), 2425–2436.

Razak, E. S. A., Khan, M. F., & Ali, M. M. (2016). Distribution of polycyclic aromatic hydrocarbons in surface sediments of the straits of Malacca. Journal of Sustainability and Management, Special Issue Number 1, 118–128.

Redwan, M., & Elhaddad, E. (2017). Heavy metals seasonal variability and distribution in Lake Qaroun sediments, El-Fayoum, Egypt. Journal of African Earth Science, 134, 48–55.

Rodriguez, J. H., Wannaz, E. D., Salazar, M. J., Pignata, M. L., Fangmeier, A., & Franzaring, J. (2012). Accumulation of polycyclic aromatic hydrocarbons and heavy metals in the treefoliage of *Eucalyptus rostrata*, *Pinus radiate*, and *Populus hybridusin* the vicinity of a large aluminium smelter in Argentina. Atmospheric Environment, 55, 35–42.

Rocha, M. J., Ferreira, P. C., Reis, P. A., Cruzeiro, C., & Rocha, E. (2011). Determination of polycyclic aromatic hydrocarbons in coastal sediments from the Porto Region

(Portugal) by microwave-assisted extraction, followed by SPME and GC-MS. Journal of Chromatographic Science, 49(9), 695–701.

Rushdi, A. I., Al-Mutlaq, K., El-Mubarak, A. H., & El-Otaibi (2013). Occurrence and sources of aliphatic hydrocarbons in surface soils from Riyadh city, Saudi Arabia. Journal of the Saudi Society of Agricultural Sciences, 12(1), 9–18.

Rushton, L., Schnatter, A. R., Tang, G., & Glass, D. C. (2014). Acute myeloid and chronic lymphoid leukemias and exposure to low-level benzene among petroleum workers. British Journal of Cancer, 110, 783–787.

Rust, A. J., Burgess, R. M., McElroy, A. E., Cantwell, M. G., & Brownawell, B. J. (2004). Influence of soot carbon on the bioaccumulation of sediment-bound polycyclic aromatic hydrocarbons by marine benthic invertebrates: an interspecies comparison. Environmental Toxicology and Chemistry, 23(11), 2594–2603.

Sabiha-Javied Mehmood, T., Chaudhry, M. M., Tufail, M., & Irfan, N. (2009). Heavy metal pollution from phosphate rock used for the production of fertilizer in Pakistan. Microchemical Journal, 91(1), 94–99.

Sahnquillo, A., Rigo, I. A., & Rauret, G. (2003). Overview of the use of leaching/extraction tests for risk assessment of trace metals in contaminated soils and sediments. Trends in Analytical Chemistry, 22(3), 152–159.

Sakari, M., Zakaria, M. P., Junos, M. B. M., Annuar, N. A., Yun, H. Y., Heng, Y. S., Zainuddin, S. M. H. S., & Chai, K. L. (2008). Spatial distribution of petroleum hydrocarbon in sediments of major rivers from east coast of Peninsular Malaysia. Coastal Marine Science, 32(1), 9–18.

Sakari, M., Zakaria, M. P., Mohamed, C. A. R, Lajis, N. H., Abdullah, M. H., & Shabazi, A. (2011). Polycyclic aromatic hydrocarbons and hopane in Malacca Coastal water: 130 Years of evidence for their land-based sources. Environmental Forensics, 12, 63–78.

Sakan, S. M., Djordjevic, D. S., Manojlovic, D. D., & Polic, P. S. (2009). Assessment of heavy metal pollutants accumulation in the Tisza river sediments. Journal of Environmental Management, 90(11), 3382–3390.

Saleem, M., Aftab, J., Hasaney, S. I., Kahkishan, S., Haider, S. W., & Muzzaffar, M. (2016). Toxicity level, Ecological risk assessment of Heavy metals and distribution in the surface sediment of Hub River, Hub River estuary and Gadani coast, Baluchistan, Pakistan. International Network for Natural Sciences, 8(5), 219–232.

Salomons, W., & Forstner, U. (1984). *Metals in the Hydrocycle*. Springer, Berlin, Germany.

Sammarco, P. W., Kolian, S. R., Warby, R. A. F., Bouldin, J. L., Subra, W. A., & Porter, S. A. (2016). Concentrations in human blood of petroleum hydrocarbons associated with the BP/Deepwater horizon oil spill, Gulf of Mexico. Archives of Toxicology, 90, 829–837.

Sanip, M. M. M., Fadzil, M. F., Suratman, S., Rozmi, S., & Tahir, N. M. (2019). Distribution and sources of polycyclic aromatic hydrocarbons in coastal surface sediments off Terengganu. Malaysian Journal of Analytical Sciences, 23(6), 1120–1132.

Saraee, K. R. E., Abdi, M. R., Naghavi, K., Saion, E., Shafaei, A., & Soltani, N. (2011). Distribution of heavy metals in surface sediments from the South China Sea

ecosystem, Malaysia. Environmental Monitoring and Assessment, 183(1–4), 545–554.

Sarma, H. (2011). Metal hyperaccumulation in plants: A review focusing on phytoremediation technology. Journal of Environmental Science and Technology. 4(2), 118–138.

Scott, R. M. (1989). *Chemical Hazards in the Workplace*, CRC Press, Boca Raton, Orlando, ISBN 978 – 0 – 87371 – 134 – 0, pp. 107–108.

Sekabira, K., Oryem Origa, H., Basamba, T. A., Mutumba, G., & Kakudidi E. (2010). Assessment of heavy metal pollution in the urban stream sediments and its tributaries. International Journal of Environmental Science and Technology, 7, 435–446.

Shaari, H., Mohamad Azmi, S. N. H., Sultan, K., Bidai, J., & Mohamad, Y. (2015). Spatial distribution of selected heavy metals in surface sediments of the EEZ of the East Coast of Peninsular Malaysia. International Journal of Oceanography, *2015*, Article ID: 618074, 10 pages.

Shazili, N., Rashid, M., Husain, M., & Yaakob, R. (1998). Trace metals in surface sediment of the South China Sea, Area II: Sarawak, Sabah and Brunei. *In Proceedings of 2nd Technical Seminar on Marine Fishery Resources Survey in the South China Sea Area II: Sarawak*. 14-15 December 1998, Kuala Lumpur, Malaysia (pp. 95-110). Samut Prakan, Thailand: Training Department, Southeast Asian Fisheries Development Center, SEAFDEC Publications.

Shen, Z. G., Li, X. D., Wang, C. C., Chen, H. M., & Chua, H. (2002). Lead phytoextraction from contaminated soil with high-biomass plant species. Journal of Environmental Quality, 31(6), 1893–1900.

Shih, Y. J., Binh, N. T., Chen, C. W., Chen, C. F., & Dong, C. D. (2016). Treatability assessment of polycyclic aromatic hydrocarbons contaminated marine sediments using permanganate, persulfate and Fenton oxidation processes. Chemosphere, 150, 294–303.

Shyleshchandran, M. N., Mohan, M., & Ramasamy, E. V. (2018). Risk assessment of heavy metals in Vembanad Lake sediments (south-west coast of India), based on acid-volatile sulfide (AVS)-simultaneously extracted metal (SEM) approach. Environmental Science and Pollution Research, 25, 7333–7345.

Silveira, A., Jr., Pereira, J. A., Poleto, C., de Lima, J. L. M. P., Goncalves, F. A., Alvarenga, L. A., & Isidoro, J. M. P. G. (2016). Assessment of loose and adhered urban street sediments and trace metals: A study in the city of Pocos de Caldas, Brazil. Journal of Soils and Sediments, 16, 2640–2650.

Sim, S. F., Ling, T. Y., Nyanti, L., Gerunsin, N., Wong, Y. E., & Kho, L. P. (2016). Assessment of heavy metals in water, sediment, and fishes of a large tropical hydroelectric dam in Sarawak, Malaysia. Journal of Chemistry, *2016*. Article ID 8923183, 1–10.

Sim, H. C. (2003). The impact of urbanization on family structure: the experience of Sarawak, Malaysia. Journal of Social Issues in Southeast Asia, 18(1), 89–109.

Smargiassi, A., Goldberg, M. S., Wheeler, C. P., Valois, M-F., Mallach, G., Kauri, R. S., Bartlett, S., Raphoz, M., & Liu, L. (2014). Associations between personal exposure

to air pollutants and lung function tests and cardiovascular indices among children with asthma living near an industrial complex and petroleum refineries. Environmental Research, 132, 38–45.

Sparks, D. L. (2005). Toxic metals in the environment: The role of surfaces. *Elements,* 1(4), 193–197.

Soclo, H. H., Garrigues, P., & Ewald, M. (2000). Origin of polycyclic aromatic hydrocarbons (PAHs) in coastal marine sediments: case studies in Cotonou (Benin) and Aquitaine (France) areas. Marine Pollution Bulletin, 40(5), 387–396.

Song, Y. F., Jing, X., Fleischmann, S., & Wilke, B. M. (2002). Comparative study of extraction methods for the determination of PAHs from contaminated soils and sediments. Chemosphere, 48(9), 993–1001.

Suman, S., Sinha, A., & Tarafdar, A. (2016). Polycyclic aromatic hydrocarbons (PAHs) concentration levels, pattern, source identification and soil toxicity assessment in urban traffic soil of Dhanbad, India. Science of The Total Environment, 545–546, 353–360.

StatSoft (1999). STATISTICA for windows, Computer Programme Manual: Tulsa, OK.

Stout, S. A., Uhler, A. D., & Emsbo-Mattingly, S. D. (2004). Comparative evaluation of background anthropogenic hydrocarbons in surficial sediments from nine urban waterway. Environmental Science and Technology, 38(11), 2987–2994.

Szefer, P., Kusak, A., Szefer, K., Jankowska, H., Wolowicz, M., & Ali, A. A. (1995). Distribution of selected metals in sediment cores of puck bay, Baltic Sea. Marine Pollution Bulletin, 30(9), 615–618.

Tan, W. H., Tair, R., Ali, S. A. M., Talibe, A., Sualin, F., & Payus, C. (2016). Distribution of heavy metals in seawater and surface sediment in coastal area of Tuaran, Sabah. Transactions on Science and Technology, 3(1–2), 114–122.

Tan, D. N. K. (1981). Nomenclature of the Upper Cretaceous – Tertiary molasse deposits in West Sarawak. *Malaysian Geological Survey Annual Report for 1981*, 348–355.

Tang, N., Hakamata, M., Sato, K., Okada, Y., Yang, X., Tatematsu, M., & Hayakawa, K. (2015). Atmospheric behaviors of polycyclic aromatic hydrocarbons at a Japanese remote background site, Noto peninsula, from 2004 to 2014. Atmospheric Environment, 120, 144–151.

Tariq, S. R., Shafiq, M., & Chotana, G. A. (2016). Distribution of heavy metals in the soils associated with the commonly used pesticides in cotton fields. Scientifica, *2016.* Article ID 7575239.

Tavakoly Sany, S. B., Hashim, R., Salleh, A., Rezayi, M., Mehdinia, A., & Safari, O. (2014). Polycyclic aromatic hydrocarbons in coastal sediments of Klang Strait, Malaysia: Distribution pattern, risk assessment, and sources, *PloS ONE*, *9*(4):e94907.

Tehrani, G. M., Sany, S. B. T., Hashim, R., & Salleh, A. (2016). Predictive environmental impact assessment of total petroleum hydrocarbons in petrochemical wastewater effluent and surface sediment. Environmental Earth Sciences, 75, 177.

Tiana, K., Wua, Q., Liua, P., Hua, W., Huanga, B., Shid, B., Zhou, Y., Kwon, B., Choi, K., Ryu, J., Khim, J. S., & Wang, T. (2020). Ecological risk assessment of heavy metals in sediments and water from the coastal areas of the Bohai Sea and the Yellow Sea. Environment International, 136, 105512.

Tian, K., Huang, B., Xing, Z., & Hu, W. (2017). Geochemical baseline establishment and ecological risk evaluation of heavy metals in greenhouse soils from Dongtai, China. Ecological Indicators, 72, 510–520.

The Agency for Toxic Substances and Disease Registry, ATSDR (2008). *Toxicological Profile for Aluminum*, US Department of Health and Human Services, Public Health Service, Atlanta, Ga, USA.

The American Society for Testing and Materials, ASTM D3976-92 (2015). Standard Practice for Preparation of Sediment Samples for Chemical Analysis, ASTM International, West Conshohocken, PA, www.astm.org.

The Agency for Toxic Substances and Disease Registry, ATSDR (1996). *Hazardous Substance Emergency Events Surveillance (HSEES)*, U.S. Department of Health and Human Services: Public Service, Atlanta, Georgia, pp. 1–57.

Theobald, N. (1988). Rapid preliminary separation of petroleum hydrocarbons by solid-phase extraction cartridges. Analytica Chimica Acta, 204, 135–144.

Tolosa, I., de Mora, S., Sheikholeslami, M. R., Villeneuve, J. P., Bartocci, J., & Cattini, C. (2004). Aliphatic and aromatic hydrocarbons in coastal Caspian Sea sediments. Marine Pollution Bulletin, 48(1–2), 44–60.

Tomlinson, D. C., Wilson, D. J., Harris, C. R., & Jeffrey, D. W. (1980). Problem in assessment of heavy metals in estuaries and the formation of pollution index. Helgol. Wiss. Meeresunlter, 33, 566–575.

Turekian, K. K., & Wedepohl, K. H. (1961). Distribution of the elements in some major units of the earth's crust. Geological Society of America Bulletin, 72(2), 175–192.

Tsang, H. L., Wu, S. C., Leung, C. K., Tao, S., & Wong, M. H. (2011). Body burden of POPs of Hong Kong residents, based on human milk, maternal and cord serum. Environmental International, 37(1), 142–151.

Ugwu, K. E., & Ukoha, P. (2016). Impacts of extraction methods and solvent systems in the assessment of toxic organic compounds in solid matrix. *Asian Journal* Chemistry and Pharmaceutical Sciences, 1(1), 23–28.

United State Environmental Protection Agency, USEPA, (2009). Risk-based Concentration Table. Philadelphia PA: United States Environmental Protection Agency, Washington, DC.

United State Environmental Protection Agency, USEPA (2007). Procedure for Determination of Sediment Particle Size (Grain Size), 73505.

United State Environmental Protection Agency, USEPA, (1989). Risk Assessment Guidance for Superfund. In: Human Health Evaluation Manual Part A, Interim Final, vol. I. United States Environmental Protection Agency, Washington (DC). 1989 EPA/540/1-89/002.

United Nations Environment Programme, UNEP (1992). Determination of Petroleum Hydrocarbons in Sediments Reference Methods for Marine Pollution Studies No. 72.

Vaezzadeh, V., Zakaria, M. P., Shaui-Hwai, A. T., Ibrahim, Z. Z., Mustafa, S., Abootalebi-Jahromi, F., Masood, N., Magam, S.M., & Alkhadher, S. A. A. (2015). Forensic investigation of aliphatic hydrocarbons in the sediments from selected mangrove ecosystems in the west coast of Peninsular Malaysia. Marine Pollution Bulletin, 100(1), 311–320.

Vaezzadeh, V., Zakaria, M. P., Mustafa, S., Ibrahim, Z. Z., Shaui-Hwai, A. T., Keshavarzifard, M., Magam, S. M., & Masood, N. (2013). *Distribution of polycyclic aromatic hydrocarbons (PAHs) in sediment from Muar and Pulau Merambong, Peninsular Malaysia. Proceedings of the International Conference on Environmental Forensics, Springer Singapore*.

van Hattum, M. W. A., Hall, R., Pickard, A. L., & Nichols, G. J. (2013). Provenance and geochronology of Cenozoic sandstones of northern Borneo. Journal of Asian Earth Sciences, 76, 266–282.

Vignet, C., Joassard, L., Lyphout, L., Guionnet, T., Goubeau, M., Le Menach, K., Brion, F., Kah, O., Chung, B-C., Budzinski, H., Begout, M-L., & Cousin, X. (2015). Exposures of zebrafish through diet to three environmentally relevant mixtures of PAHs produce behavioral disruptions in unexposed F1 and F2 descendant, Environmental Science and Pollution Research, 22, 16371–16383.

Viguri, J., Verde, J., & Irabien, A. (2002). Environmental assessment of polycyclic aromatic hydrocarbons (PAHs) in surface sediments of the Santander Bay, Northern Spain. Chemosphere, 48(2), 157–165.

Villanueva, F., Tapia, A., Cabanas, B., Martinez, E., & Albaladejo, J. (2015). Characterization of particulate polycyclic aromatic hydrocarbons in an urban atmosphere of central-southern Spain. Environmental Science and Pollution Research, 22, 18814–18823.

Volkman, J. K., Revill, A. T., & Murray, A. P. (1997). Applications of biomarkers for identifying sources of natural and pollutant hydrocarbons in aquatic environments.

In: R. P. Eganhouse (Ed), *Molecular Markers in Environmental Geochemistry*. Washington DC: American Chemical Society Press, pp.279–313.

Wang, L., Li, H., Dang, J., Zhao, Y., Zhu, Y., & Qiao, P. (2020). Effects of urbanization on water quality and the macrobenthos community structure in the Fenhe River, Shanxi Province, China. Journal of Chemistry, *2020*. Article ID 8653486.

Wang, J., Liu, G., Lu, L., & Liu, H. (2016). Metal distribution and bioavailability in surface sediments from the Huaihe River, Anhui, China. Environmental Monitoring and Assessment, 188(1), 3.

Wang, M., Wang, C., Hu, X., Zhang, H., He, S., & Lv, S. (2015). Distributions and sources of petroleum, aliphatic hydrocarbons and polycyclic aromatic hydrocarbons (PAHs) in surface sediments from Bohai Bay and its adjacent river, China. Marine Pollution Bulletin, 90(1–2), 88–94.

Wang, C., Dao, X., Zhang, L. L., Lv, Y. B., & Teng, E. J. (2015). Characteristics and toxicity assessment of airborne particulate polycyclic aromatic hydrocarbons of four background sites in China. Zhongguo Huanjing Kexue/China. Environmental Science, 35, 3543–3549.

Wang, J.-Z., Chen, T.-H., Zhu, C.-Z., & Peng, S.-C. (2014). Trace organic pollutants in sediments from Huaihe River, China: Evaluation of sources and ecological risk. Journal of Hydrology, 512, 463–469.

Wang, L. L., Yang, Z. F., Niu, J. F., & Wang, J. Y. (2009). Characterization, ecological risk assessment and source diagnostics of polycyclic aromatic hydrocarbons in water column of the Yellow River Delta, one of the most plenty biodiversity zones in the world. Journal of Hazardous Material, 169(1–3), 460–465.

Wang, X. Sato, T. Xing, B., & Tao, S. (2005). Health risks of heavy metals to the general public in Tianjin, China via consumption of vegetables and fish. Science of The Total Environment, 350(1–3), 28–37.

Wang, X. C., Zhang, Y. X., & Robert, F. C. (2001). Distribution and partitioning of polycyclic aromatic hydrocarbons (PAHs) in different size fractions in sediments from Boston Harbor, United States. Marine Pollution Bulletin, 42(11), 1139–1149.

Wang, Z., Li, K., Fingas, M., Sigouin, L., & Menard, L. (2002). Characterization and source identification of hydrocarbons in water samples using multiple analytical techniques. Journal of Chromatography A, 971(1–2), 173–184.

Wang, Z., Fingas, M., Blenkinsopp, S., Sergy, G., Landriault, M., Sigouin, L., Foght, J., Semple, K., & Westlake, D. W. S. (1998). Comparison of oil changes due to biodegradation and physical weathering in different oils. Journal of Chromatography A, 809(1–2), 89–107.

Wang, Z., & Fingas, M. (1995). Differentiation of the source of spilled oil and monitoring of the oil weath-ering process using gas chromatography - mass spectrometry. Journal of Chromatography A, 712(2), 312–343.

Watkinson, R. J., & Morgan, P. (1990). Physiology of aliphatic hydrocarbon-degrading microorganisms. Biodegradation, 1, 79–92.

Wei, M., Yanwen, Q., Binghui, Z., & Lei, Z. (2008). Heavy metal pollution in Tianjin Bohai Bay, China. Journal of Environmental Sciences, 20(7), 814–819.

Weissmannova, H. D., & Pavlovsky, J. (2017). Indices of soil contamination by heavy metals – Methodology of calculation for pollution assessment (minireview). Environmental Monitoring and Assessment, 189, 616.

Weissmannova, H. D., Pavlovsky, J., & Chovanec, P. (2015). Heavy metal contaminations of urban soils in Ostrava, Czech Republic: Assessment of metal pollution and using principal component analysis. International Journal of Environmental Research, 9(2), 683–696.

Wen, J., Yi, Y., & Zeng, G. (2016). Effects of modified zeolite on the removal and stabilization of heavy metals in contaminated lake sediment using BCR sequential extraction. Journal of Environmental Management, 178, 63–69.

Wilcke, W., Amelung, W., Krauss, M., Mrtius, C., Bandeira, A., & Garcia, M. V. B. (2003). Polycyclic aromatic hydrocarbon (PAH) patterns in climatically different ecological zones of Brazil. Organic Geochemistry, 34, 1405–1417.

Wilford, G. E., & Kho, C. H. (1965). Penrissen area, West Sarawak, Malaysia. *Malaysian Geological Survey, Borneo Region, Report* 2, 195pp.

Wong, C. S., Sanders, G., Engstrom, D. R., Long, D. T., Swackhamer, D. L., & Eisenreich, S. J. (1995). Accumulation, inventory and diagenesis of chlorinated hydrocarbons in Lake Ontario sediments. Environmental Science and Technology, 29(10), 2661–2672.

Wu, B. (2014). Potential ecological risk of heavy metals and metalloid in the sediments of Wuyuer River basin, Heilongjiang province, China. Ecotoxicology, 23, 589–600.

Wu, Y., Zhang, J., & Zhu, Z. (2003). Polycyclic aromatic hydrocarbons in the sediments of the Yalujiang estuary, North China. Marine Pollution Bulletin, 46(5), 619–625.

Wuana, R. A., & Okieimen, F. E. (2011). Heavy metals in contaminated soils: A review of sources, chemistry, risks and best available strategies for remediation. International Scholarly Research Network ISRN Ecology, *2011*. Article ID 402647, pp. 20.

Xu, J., Xu, L., Zheng, L., Liu, B., Liu, J., & Wang, X. (2019). Distribution, risk assessment, and source analysis of heavy metals in sediment of rivers located in the hilly area of southern China. Journal of Soils and Sediment, 19, 3608–3619.

Xu, J., Guo, J. Y., Liu, G. R., Shi, G. L., Guo, C. S., Zhang, Y., & Feng, Y. C. (2014). Historical trends of concentrations, source contributions and toxicities for PAHs in dated sediment cores from five lakes in western China. Science of The Total Environment, 470–471, 519–526.

Yan, G., Mao, L., Liu, S., Mao, Y., Ye, H., Huang, T., Li, F., & Chen, L. (2018). Enrichment and sources of trace metals in roadside soils in Shanghai, China: A case study of two urban/rural roads. Science of The Total Environment, 631–632, 942–950.

Yang, Y., Chen, F., Zhang, L., Liu, J., Wu, S., & Kang, M. (2012). Comprehensive assessment of heavy metal contamination in sediment of the Pearl River Estuary and adjacent shelf. Marine Pollution Bulletin, 64(9), 1947–1947.

Yi, Y., Yang, Z., & Zhang, S. (2011). Ecological risk assessment of heavy metals in sediment and human health risk assessment of heavy metals in fishes in the middle and lower reaches of the Yangtze River basin. Environmental Pollution, 159(10), 2575–2585.

Yoon, J., Cao, X., Zhou, Q., & Lena Q. M. (2006). Accumulation of Pb, Cu, and Zn in native plants growing on acontaminated Florida site. Science of the Total Environment, 368(2–3), 456–464.

Yunker, M. B., Macdonald, R. W., Vingarzan, R., Mitchell, R. H., Goyette, D., & Sylvestre, S. (2002). PAHs in the Fraser River basin: a critical appraisal of PAH

ratios as indicators of PAH source and composition. Organic Geochemistry, 33(4), 489–515.

Yunker, M. B., & Macdonald, R. W. (1995). Composition and origins of polycyclic aromatic hydrocarbons in the Mackenzie River and on the Beaufort Sea shelf. Arctic, 48, 118–129.

Yusoff, A. H., Zulkifli, S. Z., Ismail, A., & Mohamed, C. A. R. (2015). Vertical trend of trace metals deposition in sediment core off Tanjung Pelepas harbour, Malaysia. Procedia Environmental Sciences, 30, 211–216.

Yusoff, H. B., Assim, Z. B., & Mohamad, S. B. (2012). Aliphatic hydrocarbons in surface sediments from South China Sea off Kuching Division, Sarawak. The Malaysian Journal of Analytical Sciences, 16(1), 1–11.

Zakaria, M. P., Takada, H., & Tsutsumi, S. (1999). American Chemical Society (ACS) national meeting. *Division of Environmental Chemistry (J).* 39(2), 6.

Zakaria, M. P., Horinouchi, A., Tsutsumi, S., Takada, H., Tanabe, S., & Ismail, A. (2000). Oil pollution in the Strait of Malacca, Malaysia: Application of molecular markers for source identification. Environmental Science and Technology, 34(7), 1189–1196.

Zakaria, M. P., Okuda, T., & Takada, H. (2001). Polycyclic aromatic hydrocarbons (PAHs) and hopanes in stranded tar-balls on the coasts of Peninsular Malaysia: applications of biomarkers for identifying sources of oil pollution. Marine Pollution Bulletin, 42(12), 1357–1366.

Zakaria, M. P., Takada, H., Kumata, H., Nakada, N., Ohno, K., & Mihoko, Y. (2002). Distribution of polycyclic aromatic hydrocarbons (PAHs) in rivers and estuaries in

Malaysia: widespread input of petrogenic hydrocarbons. Environmental Science and Technology, 36(9), 1907–1918.

Zakaria, M. P., & Takada, H. (2003). Petroleum hydrocarbon pollution: A closer look at the Malaysian legislations on marine environment. Paper presented at First joint seminar on oceanography, NRCT-JSPS. Chieng Mai, Thailand. December 2003.

Zakaria, M. P., & Mahat, A. A. (2006). Distribution of polycyclic aromatic hydrocarbon (PAHs) in sediments in the Langat Estuary. Coastal Marine Science, 30(1), 387–395.

Zarcinas, B., Ishak, C., McLaughlin, M., & Cozens, G. (2004). Heavy metals in soils and crops in Southeast Asia. Environmental Geochemistry and Health. 26, 343–357.

Zarei, I., Pourkhabbaz, A., & Khuzestani, R. B. (2014). An assessment of metal contamination risk in sediments of Hara Biosphere Reserve, southern Iran with a focus on application of pollution indicators. Environmental Monitoring and Assessment, 186, 6047–6060.

Zhang, Z. H., & Balasubramanian, R. (2016). Investigation of particulate emission characteristics of a diesel engine fueled with higher alcohols/biodiesel blends. Applied Energy, 163, 71–80.

Zhang, C., Yu, Z-G., Zeng, G-M., Jiang, M., Yang, Z-Z., Cui, F., Zhu, M-Y., Shen, L-Q., & Hu, L. (2014). Effects of sediment geochemical properties on heavy metal bioavailability. Environmental International, 73, 270–281.

Zhang, Y., Guo, C. S., Xu, J., Tian, Y. Z., Shi, G. L., & Feng, Y. C. (2012). Potential source contributions and risk assessment of PAHs in sediments from Taihu Lake, China: Comparison of three receptor models. Water Research, 46(9), 3065–3073.

Zheng, X., Han, B., Thavamani, P., Duan, L., & Naidu, R. (2015). Composition, source identification and ecological risk assessment of polycyclic aromatic hydrocarbons in surface sediments of the Subei Grand Canal, China. Environmental Earth Sciences, 74, 2669–2677.

Zhu, Q. (2014). *Coal Sampling and Analysis Standards*. IEA Clean Coal Centre, IEACCC Ref: CCC/235.

Zhu, W. F. (2007). *Occurrence of polycyclic aromatic hydrocarbons in coastal sediments off Guangdong Province*. Guangzhou Institute of Geochemistry, Chinese Academy of Sciences, pp. 1–57.

Zrafi, I., Hizem, L., Chalghmi, H., Ghrabi, A., Rouabhia, M., & Saidane-Mosbahi, D. (2013). Aliphatic and aromatic biomarkers for petroleum hydrocarbon investigation in marine sediment. Journal of Petroleum Science Research, 2(4), 145–15

APPENDICES

Appendix A: Journal Publications

1. **Asare, E. A**., Assim, Z. B., Wahi, R. B., Bakeh, T., & Dapaah, S. S. (2021). Trend analysis of anthropogenic activities affecting trace metals deposition in core sediments from the coastal and four rivers estuary of Sarawak, Malaysia. *Environmental Science and Pollution Research*. DOI:10.1007/s11356-021-17008-1. (**Scopus and Web of Science**)
2. **Asare, E. A.**, Assim, Z. B., & Wahi, R. (2021). Validation of an analytical technique, distribution, and risk assessment of aliphatic and polycyclic aromatic hydrocarbons in surface sediments of the coastal and selected estuaries of Sarawak. *Arabian Journal of Geosciences*, 14:1943. DOI:10.1007/s12517-021-08337-z. (**Scopus and Web of Science**)
3. **Asare, E. A**., Assim, Z. B., Wahi, R. B., Tahir, R. B., & Droepenu, E. K. (2021). Application of fuzzy evaluation technique and grey clustering method for water quality assessment of the coastal and estuaries of selected rivers in Sarawak. *Bulletin of National Research Centre*, 45(1):1–11.
4. **Asare, E. A.**, Assim, Z. B., Wahi, R. & Fianko, J. R. (2022). Eco-toxic risk assessment and source distribution of trace metals in surface sediments of the coastal and in four rivers estuary of Sarawak. *Beni-Suef University Journal of Basic and Applied Sciences*, 11(1):1–18. (**Scopus and Web of Science**)

Appendix B: ICP-OES calibration curves of selected heavy metals with the equation of the lines and R-values.

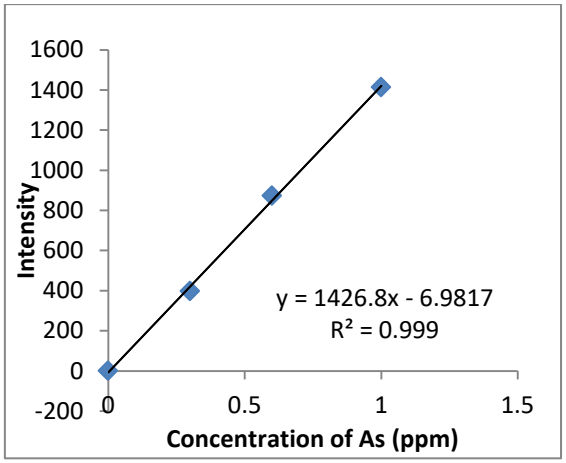

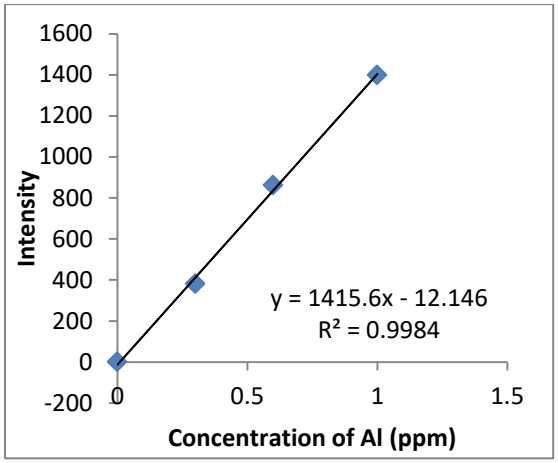

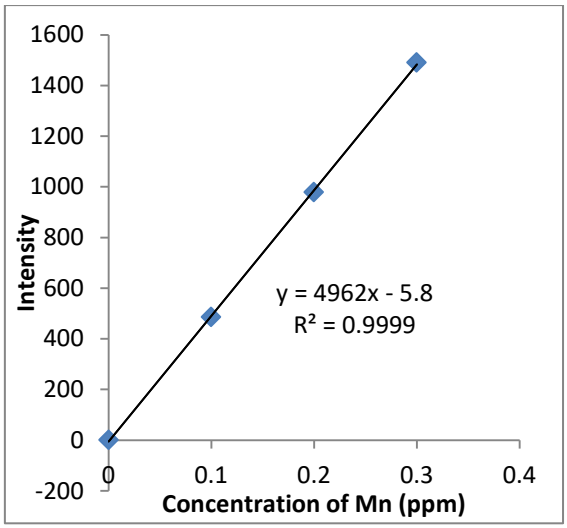

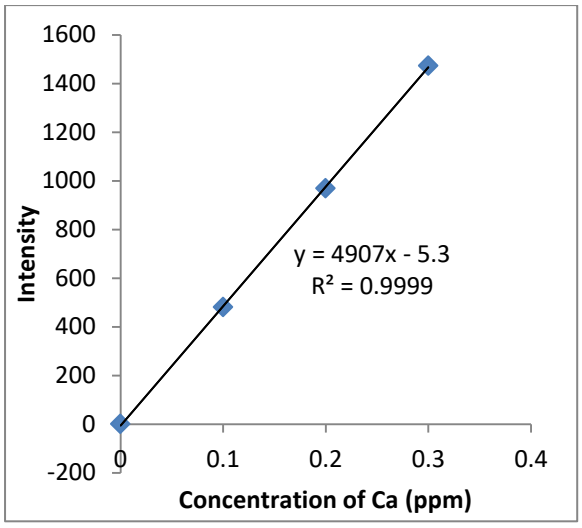

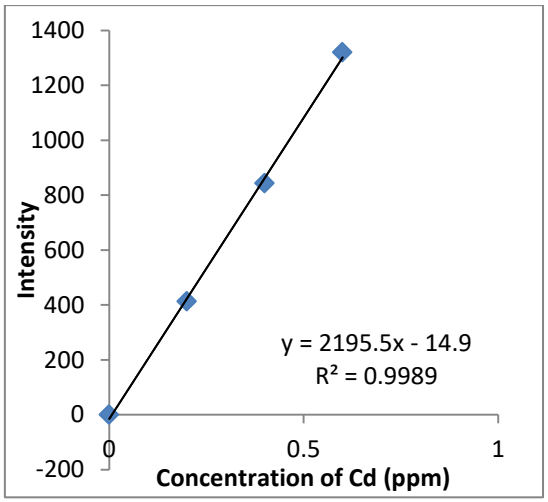

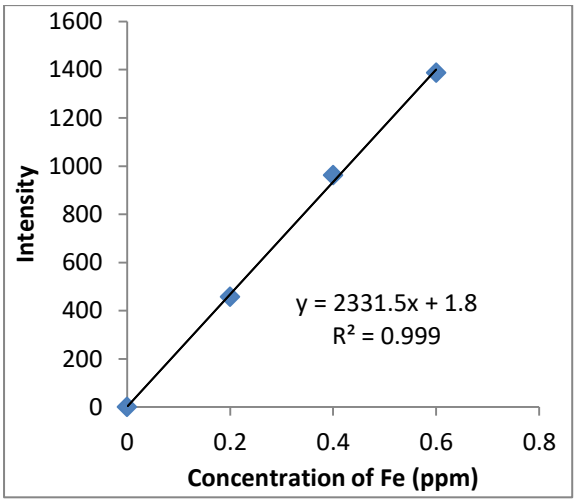

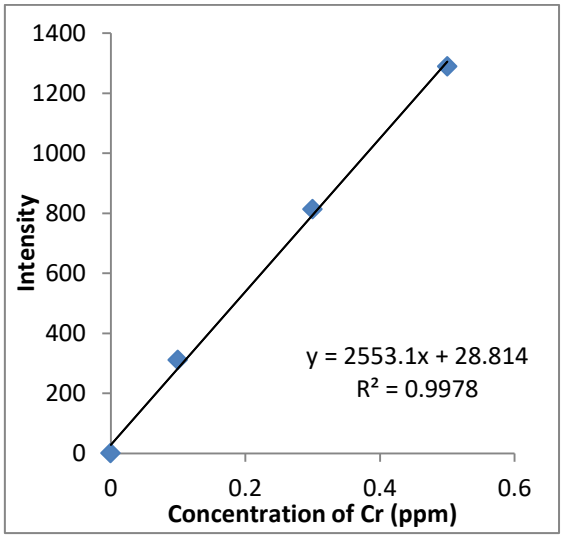
Intensity
Concentration of Cr (ppm)
y = 2553.1x + 28.814
R² = 0.9978

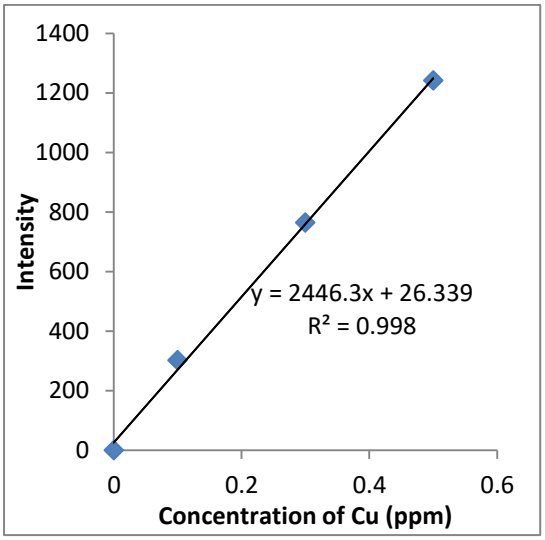
Intensity
Concentration of Cu (ppm)
y = 2446.3x + 26.339
R² = 0.998

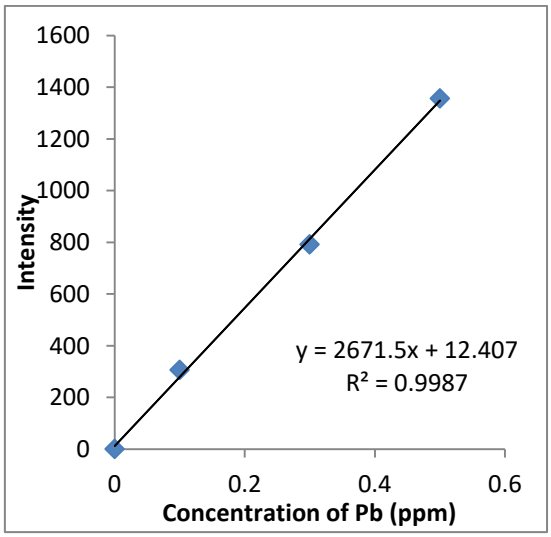
Intensity
Concentration of Pb (ppm)
y = 2671.5x + 12.407
R² = 0.9987

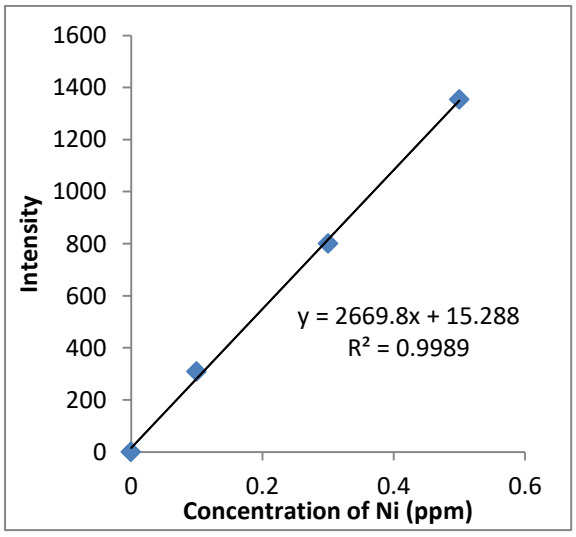
Intensity
Concentration of Ni (ppm)
y = 2669.8x + 15.288
R² = 0.9989

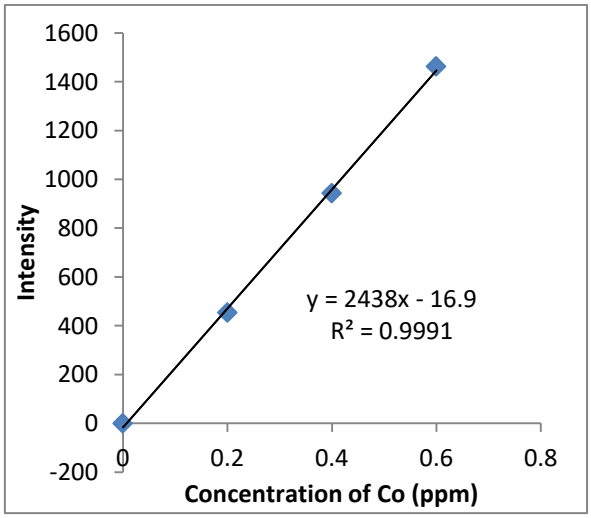
Intensity
Concentration of Co (ppm)
y = 2438x - 16.9
R² = 0.9991

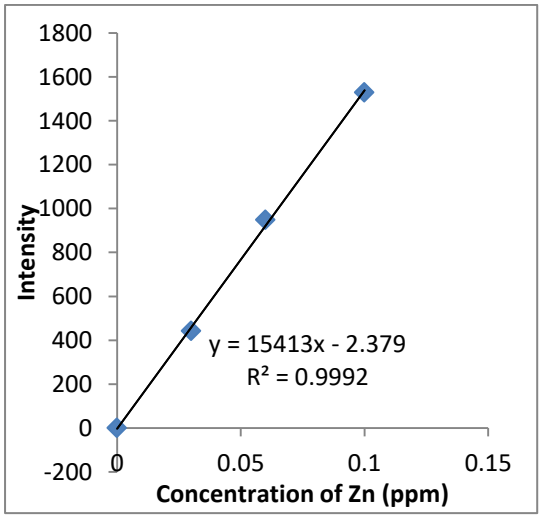
Intensity
Concentration of Zn (ppm)
y = 15413x - 2.379
R² = 0.9992

Appendix C: Textural classification of core sediment in selected sample sites.

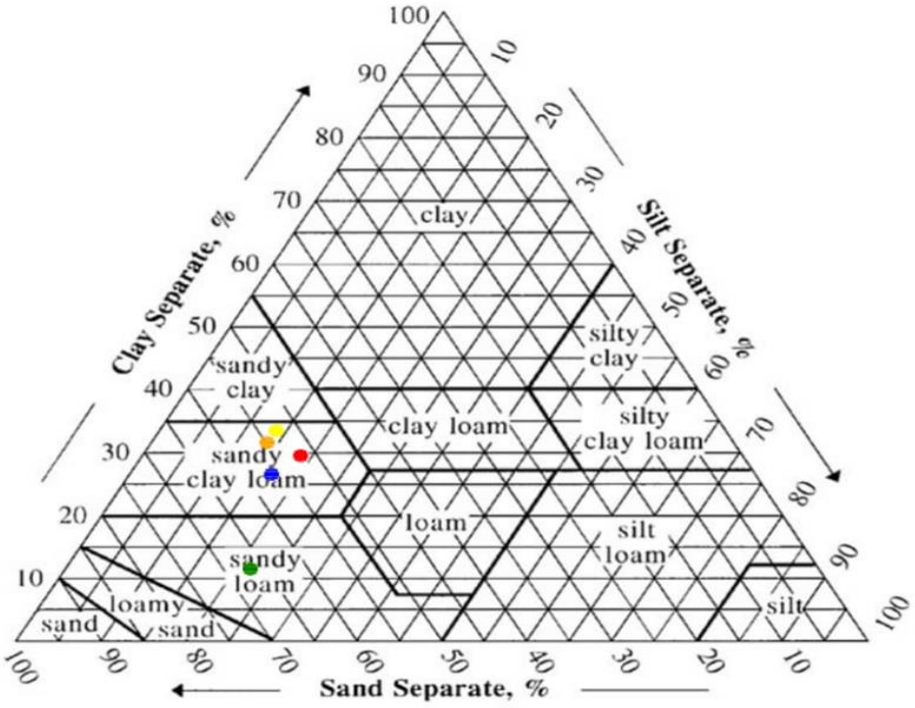

Appendix D1: Detected average concentration of Pb (mg/kg d.w) in core sediment samples of selected study sites

Depth (cm)	CZ1	CZ2	CZ4	CZ5	CZ7	CZ8	CZ10	CZ11
0 – 5	72.4 ± 0.3	86.7 ± 0.6	101.4 ± 0.4	162.7 ± 0.3	46.9 ± 0.2	188.9 ± 0.7	77.4 ± 0.3	94.3 ± 0.5
5 –10	60.7 ± 0.7	73.2 ± 0.4	56.6 ± 0.3	80.4 ± 0.7	30.2 ± 0.4	107.2 ± 0.8	61.2 ± 0.6	76.7 ± 0.8
10 – 15	27.1 ± 0.2	59.5 ± 0.3	41.9 ± 0.8	66.8 ± 0.9	21.7 ± 0.5	60.6 ± 0.5	55.0 ± 0.6	54.1 ± 0.8
15 – 20	21.6 ± 0.4	41.2 ± 0.5	30.2 ± 0.6	50.2 ± 0.6	18.5 ± 0.5	27.4 ± 0.3	22.7 ± 0.8	48.9 ± 0.6
20 – 25	19.4 ± 0.7	20.1 ± 0.8	22.4 ± 0.6	54.1 ± 0.7	16.8 ± 0.4	31.5 ± 0.5	19.1 ± 0.8	33.7 ± 0.9
25 – 30	11.3 ± 0.5	9.8 ± 0.2	15.8 ± 0.7	36.3 ± 0.5	8.9 ± 0.3	32.4 ± 0.8	13.4 ± 0.7	29.4 ± 0.3

Appendix D2: Detected average concentration of Zn (mg/kg d.w) in core sediment samples of selected sample sites

Depth (cm)	CZ1	CZ2	CZ4	CZ5	CZ7	CZ8	CZ10	CZ11
0 – 5	90.4 ± 1.6	204.1 ± 2.9	86.7 ± 1.3	362.1 ± 3.4	109.2 ± 2.1	431.8 ± 4.6	88.4 ± 0.9	381.9 ± 1.4
5 –10	73.6 ± 0.4	172.4 ± 1.8	50.9 ± 1.1	309.7 ± 3.4	80.9 ± 1.1	404.4 ± 2.8	67.2 ± 2.2	322.4 ± 5.2
10 – 15	48.8 ± 1.0	81.9 ± 0.8	44.4 ± 1.6	212.2 ± 4.1	63.4 ± 0.9	351.5 ± 1.3	42.9 ± 2.2	207.9 ± 3.1
15 – 20	46.2 ± 1.1	60.2 ± 0.9	40.1 ± 1.1	91.6 ± 1.3	51.9 ± 0.8	271.7 ± 3.1	33.2 ± 0.9	161.2 ± 1.1
20 – 25	34.9 ± 0.4	29.7 ± 0.4	30.7 ± 0.7	77.9 ± 1.4	40.3 ± 0.6	206.1 ± 4.2	26.8 ± 0.5	124.6 ± 1.3
25 – 30	21.4 ± 0.5	26.4 ± 1.1	27.4 ± 0.3	40.1 ± 0.6	23.6 ± 0.2	101.2 ± 4.3	19.4 ± 0.3	102.7 ± 4.4

Appendix D3: Detected average concentration of Cd (mg/kg d.w) in core sediment samples of slected study sites

Depth (cm)	CZ1	CZ2	CZ4	CZ5	CZ7	CZ8	CZ10	CZ11
0 – 5	0.03 ± 0.001	0.061 ± 0.002	0.024 ± 0.001	0.055 ± 0.001	0.033 ± 0.001	0.039 ± 0.001	0.018 ± 0.001	0.057 ± 0.002
5 –10	0.024 ± 0.001	0.017 ± 0.001	0.018 ± 0.001	0.041 ± 0.003	0.027 ± 0.001	0.034 ± 0.001	0.014 ± 0.001	0.037 ± 0.001
10 – 15	0.034 ± 0.001	0.019 ± 0.001	0.014 ± 0.001	0.036 ± 0.002	0.034 ± 0.001	0.027 ± 0.001	0.025 ± 0.001	0.034 ± 0.002
15 – 20	0.051 ± 0.002	0.023 ± 0.001	0.056 ± 0.003	0.031 ± 0.001	0.029 ± 0.001	0.021 ± 0.001	0.022 ± 0.001	0.029 ± 0.001
20 – 25	0.041 ± 0.001	0.021 ± 0.001	0.041 ± 0.002	0.033 ± 0.001	0.047 ± 0.001	0.024 ± 0.001	0.017 ± 0.001	0.022 ± 0.003
25 – 30	0.034 ± 0.001	0.012 ± 0.001	0.047 ± 0.002	0.029 ± 0.001	0.039 ± 0.003	0.026 ± 0.001	0.024 ± 0.002	0.021 ± 0.001

Appendix D4: Detected average concentration of Ni (mg/kg d.w) in core sediment samples of selected study sites

Depth (cm)	CZ1	CZ2	CZ4	CZ5	CZ7	CZ8	CZ10	CZ11
0 – 5	15.6 ± 0.6	10.8 ± 0.4	8.1 ± 0.2	29.4 ± 1.1	17.4 ± 0.6	24.5 ± 1.0	9.5 ± 0.3	33.4 ± 1.4
5 –10	12.2 ± 0.3	13.8 ± 0.2	7.3 ± 0.1	23.1 ± 0.7	12.2 ± 0.4	18.1 ± 0.8	7.1 ± 0.3	20.5 ± 0.9
10 – 15	9.9 ± 0.3	7.7 ± 0.2	11.3 ± 0.8	19.4 ± 0.8	13.6 ± 0.4	14.3 ± 0.4	8.4 ± 0.3	16.8 ± 0.7
15 – 20	11.4 ± 0.4	7.1 ± 0.2	7.9 ± 0.1	12.8 ± 0.1	10.2 ± 0.1	10.9 ± 0.1	10.2 ± 0.2	14.3 ± 0.3
20 – 25	10.9 ± 0.2	8.3 ± 0.1	8.2 ± 0.1	10.1 ± 0.1	9.8 ± 0.1	11.2 ± 0.2	11.6 ± 0.3	11.4 ± 0.5
25 – 30	8.3 ± 0.1	6.6 ± 0.1	10.4 ± 0.2	9.5 ± 0.3	6.7 ± 0.3	10.7 ± 0.2	9.4 ± 0.3	10.9 ± 0.3

Appendix D5: Detected average concentration of Mn (mg/kg d.w) in core sediment samples of selected study sites

Depth (cm)	CZ1	CZ2	CZ4	CZ5	CZ7	CZ8	CZ10	CZ11
0 – 5	8.2 ± 0.2	4.4 ± 0.2	9.4 ± 0.3	14.7 ± 0.2	7.3 ± 0.2	12.4 ± 0.2	4.1 ± 0.1	16.8 ± 0.5
5 –10	5.4 ± 0.1	5.4 ± 0.1	8.8 ± 0.2	11.4 ± 0.3	5.5 ± 0.1	9.8 ± 0.2	6.3 ± 0.1	13.1 ± 0.3
10 – 15	3.1 ± 0.1	5.1 ± 0.1	6.7 ± 0.1	9.6 ± 0.2	4.3 ± 0.1	7.1 ± 0.2	7.5 ± 0.1	10.6 ± 0.2
15 – 20	3.4 ± 0.1	5.6 ± 0.1	4.2 ± 0.1	6.2 ± 0.2	3.9 ± 0.1	5.4 ± 0.1	5.9 ± 0.2	9.4 ± 0.3
20 – 25	2.6 ± 0.1	3.4 ± 0.1	5.6 ± 0.1	5.6 ± 0.1	4.6 ± 0.1	3.6 ± 0.1	5.4 ± 0.1	6.7 ± 0.2
25 – 30	3.3 ± 0.2	2.7 ± 0.1	2.4 ± 0.1	4.1 ± 0.1	3.9 ± 0.1	2.7 ± 0.2	4.7 ± 0.2	5.7 ± 0.1

Appendix D6: Detected average concentration of Cu (mg/kg d.w) in core sediment samples of selected study sites

Depth (cm)	CZ1	CZ2	CZ4	CZ5	CZ7	CZ8	CZ10	CZ11
0 – 5	46.4	28.7	98.2	124.3	40.5	86.4	101.1	133.3
	± 1.3	± 1.1	± 2.5	± 3.8	± 1.2	± 1.7	± 3.3	± 2.9
5 –10	38.7	26.1	70.4	101.1	32.8	70.8	64.3	109.7
	± 0.9	± 1.3	± 1.8	± 2.3	± 0.7	± 1.4	± 1.6	± 2.8
10 – 15	32.6	18.4	36.8	90.8	32.9	61.1	47.4	94.3
	± 0.8	± 0.4	± 1.1	± 1.8	± 1.1	± 1.7	± 1.1	± 1.9
15 – 20	20.4	19.2	31.1	77.4	22.4	53.3	36.3	39.6
	± 0.9	± 1.1	± 1.4	± 1.8	± 1.3	± 1.9	± 1.1	± 1.5
20 – 25	16.6	14.7	24.3	39.7	20.1	41.9	28.3	30.1
	± 0.6	± 0.4	± 1.1	± 1.1	± 0.7	± 2.1	± 1.0	± 1.5
25 – 30	13.9	9.4	21.7	20.1	14.3	36.4	21.8	26.4
	± 0.5	± 0.2	± 0.4	± 0.8	± 0.6	± 1.4	± 1.1	± 0.9

Appendix D7: Detected average concentration of Ba (mg/kg d.w) in core sediment samples of selected study sites

Depth (cm)	CZ1	CZ2	CZ4	CZ5	CZ7	CZ8	CZ10	CZ11
0 – 5	3.1 ± 0.1	2.8 ± 0.1	3.7 ± 0.2	6.1 ± 0.3	5.9 ± 0.2	4.3 ± 0.1	5.3 ± 0.2	4.8 ± 0.1
5 –10	2.7 ± 0.1	2.1 ± 0.1	4.1 ± 0.1	4.8 ± 0.1	4.3 ± 0.2	3.6 ± 0.1	3.7 ± 0.1	4.1 ± 0.2
10 – 15	2.3 ± 0.1	1.6 ± 0.1	3.8 ± 0.1	3.1 ± 0.2	5.4 ± 0.2	3.1 ± 0.2	3.1 ± 0.1	3.3 ± 0.1
15 – 20	3.2 ± 0.2	2.0 ± 0.1	3.9 ± 0.1	2.4 ± 0.1	3.6 ± 0.2	2.3 ± 0.1	4.3 ± 0.3	2.5 ± 0.1
20 – 25	1.9 ± 0.1	1.3 ± 0.1	3.2 ± 0.1	1.6 ± 0.1	3.1 ± 0.2	1.2 ± 0.1	2.9 ± 0.1	2.3 ± 0.1
25 – 30	1.4 ± 0.2	1.4 ± 0.1	2.9 ± 0.1	1.1 ± 0.1	3.5 ± 0.2	0.9 ± 0.1	2.2 ± 0.2	1.3 ± 0.1

Appendix D8: Detected average concentration of As (mg/kg d.w) in core sediment samples of slected study sites.

Depth (cm)	CZ1	CZ2	CZ4	CZ5	CZ7	CZ8	CZ10	CZ11
0 – 5	3.2 ± 0.2	2.9 ± 0.1	1.7 ± 0.1	5.8 ± 0.3	2.4 ± 0.2	3.8 ± 0.2	4.7 ± 0.3	7.9 ± 0.5
5 –10	2.4 ± 0.1	3.2 ± 0.1	2.3 ± 0.1	3.9 ± 0.2	2.7 ± 0.2	3.9 ± 0.3	3.3 ± 0.2	7.5 ± 0.6
10 – 15	3.0 ± 0.1	2.4 ± 0.1	1.4 ± 0.1	3.4 ± 0.2	2.6 ± 0.1	3.1 ± 0.1	4.1 ± 0.2	5.8 ± 0.3
15 – 20	1.7 ± 0.1	1.8 ± 0.1	1.1 ± 0.2	2.9 ± 0.1	3.1 ± 0.3	2.6 ± 0.1	3.8 ± 0.1	4.4 ± 0.2
20 – 25	0.9 ± 0.1	0.6 ± 0.1	0.8 ± 0.1	2.1 ± 0.1	3.7 ± 0.3	2.4 ± 0.1	2.3 ± 0.2	3.9 ± 0.3
25 – 30	1.3 ± 0.3=1	0.9 ± 0.1	0.4 ± 0.01	1.4 ± 0.1	2.9 ± 0.2	1.8 ± 0.1	1.7 ± 0.1	3.4 ± 0.3

Appendix D9: Detected average concentration of Co (mg/kg d.w) in core sediment samples of selected study sites

Depth (cm)	CZ1	CZ2	CZ4	CZ5	CZ7	CZ8	CZ10	CZ11
0 – 5	4.3 ± 0.2	3.2 ± 0.3	3.6 ± 0.5	3.9 ± 0.2	2.4 ± 0.2	5.1 ± 0.3	4.2 ± 0.2	3.6 ± 0.4
5 –10	4.1 ± 0.3	2.6 ± 0.1	3.9 ± 0.2	2.4 ± 0.1	1.6 ± 0.1	4.8 ± 0.2	3.8 ± 0.2	3.1 ± 0.2
10 – 15	3.0 ± 0.2	2.9 ± 0.2	2.4 ± 0.2	2.6 ± 0.3	1.7 ± 0.3	4.1 ± 0.3	2.1 ± 0.2	2.7 ± 0.2
15 – 20	3.4 ± 0.3	3.1 ± 0.2	2.6 ± 0.1	2.0 ± 0.1	1.9 ± 0.1	3.7 ± 0.3	2.6 ± 0.2	2.3 ± 0.2
20 – 25	2.5 ± 0.2	2.1 ± 0.1	2.1 ± 0.1	1.3 ± 0.1	0.9 ± 0.1	2.3 ± 0.1	2.3 ± 0.2	1.7 ± 0.1
25 – 30	2.1 ± 0.2	0.9 ± 0.1	1.0 ± 0.1	0.8 ± 0.1	1.1 ± 0.1	1.8 ± 0.1	2.5 ± 0.2	1.1 ± 0.1

Appendix D10: Detected average concentration of Cr (mg/kg d.w) in core sediment samples of selected study sites

Depth (cm)	CZ1	CZ2	CZ4	CZ5	CZ7	CZ8	CZ10	CZ11
0 – 5	6.4 ± 0.3	4.6 ± 0.2	4.1 ± 0.2	5.4 ± 0.3	5.3 ± 0.2	7.8 ± 0.4	4.8 ± 0.2	4.3 ± 0.3
5 –10	4.9 ± 0.3	4.9 ± 0.2	2.9 ± 0.2	5.1 ± 0.4	4.5 ± 0.3	6.1 ± 0.2	3.6 ± 0.3	3.8 ± 0.2
10 – 15	4.4 ± 0.2	3.3 ± 0.3	2.1 ± 0.1	3.1 ± 0.2	4.8 ± 0.2	5.8 ± 0.4	3.8 ± 0.2	3.3 ± 0.2
15 – 20	4.6 ± 0.3	2.9 ± 0.1	1.9 ± 0.1	2.7 ± 0.2	3.6 ± 0.3	4.3 ± 0.4	1.4 ± 0.2	2.4 ± 0.2
20 – 25	3.2 ± 0.3	3.4 ± 0.2	2.6 ± 0.2	2.1 ± 0.2	3.1 ± 0.3	3.7 ± 0.3	2.8 ± 0.2	2.1 ± 0.1
25 – 30	2.7 ± 0.3	2.5 ± 0.3	3.4 ± 0.3	1.3 ± 0.2	2.7 ± 0.2	2.4 ± 0.2	1.6 ± 0.2	1.9 ± 0.2

Appendix D11: Detected average concentration of Mg (mg/kg d.w) in core sediment samples of selected study sites

Depth (cm)	CZ1	CZ2	CZ4	CZ5	CZ7	CZ8	CZ10	CZ11
0 – 5	317.4 ± 4.3	472.1 ± 3.8	107.4 ± 2.1	481.9 ± 4.7	334.3 ± 3.3	499.3 ± 5.9	388.1 ± 2.8	326.4 ± 6.1
5 –10	299.9 ± 3.1	421.5 ± 4.2	111.9 ± 2.6	409.6 ± 4.4	346.8 ± 2.9	492.9 ± 4.6	380.6 ± 3.7	318.1 ± 2.8
10 – 15	301.7 ± 5.1	382.8 ± 3.5	79.3 ± 2.6	401.3 ± 6.1	208.7 ± 3.1	384.1 ± 2.5	274.4 ± 2.3	304.9 ± 3.4
15 – 20	248.1 ± 2.6	327.4 ± 3.1	88.7 ± 2.5	348.4 ± 3.5	214.4 ± 2.6	366.5 ± 2.9	208.8 ± 2.9	278.1 ± 3.1
20 – 25	206.4 ± 3.7	309.6 ± 3.4	68.8 ± 1.6	321.1 ± 4.8	198.9 ± 2.4	309.3 ± 2.9	198.7 ± 1.4	256.7 ± 2.3
25 – 30	210.1 ± 2.4	227.9 ± 3.2	70.4 ± 2.1	296.4 ± 3.1	204.9 ± 2.7	281.1 ± 3.3	169.7 ± 2.4	203.4 ± 2.6

Appendix D12: Detected average concentration of Ca (mg/kg d.w) in core sediment samples of selected study sites

Depth (cm)	CZ1	CZ2	CZ4	CZ5	CZ7	CZ8	CZ10	CZ11
0 – 5	14.7	36.2	30.4	43.7	51.3	64.9	39.2	61.4
	± 0.3	± 1.1	± 1.1	± 1.4	± 1.1	± 2.1	± 0.9	± 1.6
5 –10	17.3	40.5	36.7	40.2	27.9	48.3	30.6	56.1
	± 0.6	± 0.5	± 0.8	± 0.6	± 0.9	± 0.8	± 1.1	± 1.5
10 – 15	11.3	29.8	19.3	38.9	38.4	45.4	30.8	50.4
	± 0.4	± 0.6	± 0.3	± 1.0	± 0.9	± 1.3	± 0.7	± 1.1
15 – 20	10.9	19.4	25.2	34.1	40.7	35.6	25.1	46.7
	± 0.2	± 0.4	± 0.5	± 0.4	± 0.6	± 0.6	± 0.9	± 0.8
20 – 25	13.4	21.3	30.7	31.4	29.8	33.8	19.7	41.1
	± 0.6	± 0.8	± 0.9	± 1.5	± 1.1	± 1.1	± 0.6	± 1.4
25 – 30	30.9	20.9	26.9	28.1	20.1	40.4	22.1	38.4
	± 0.5	± 0.8	± 1.1	± 1.1	± 0.6	± 1.2	± 1.1	± 1.3

Appendix D13: Detected average concentration of Al (mg/kg d.w) in core sediment samples of selected study sites

Depth (cm)	CZ1	CZ2	CZ4	CZ5	CZ7	CZ8	CZ10	CZ11
0 – 5	121.3 ± 2.4	127.9 ± 2.1	92.3 ± 1.9	134.8 ± 2.2	61.1 ± 1.4	91.8 ± 2.7	77.9 ± 2.1	139.6 ± 1.9
5 –10	141.7 ± 2.5	89.1 ± 2.1	64.7 ± 1.5	98.3 ± 2.4	52.4 ± 1.8	93.4 ± 1.6	64.2 ± 1.2	117.8 ± 2.6
10 – 15	96.8 ± 1.6	94.5 ± 1.5	60.9 ± 1.7	93.7 ± 1.3	30.9 ± 1.1	71.6 ± 1.7	51.8 ± 1.5	89.2 ± 1.8
15 – 20	89.2 ± 1.8	106.2 ± 2.6	44.1 ± 1.1	89.2 ± 1.6	41.2 ± 1.0	68.1 ± 1.2	40.2 ± 0.9	80.4 ± 1.6
20 – 25	101.1 ± 3.3	78.9 ± 1.1	50.6 ± 1.4	73.6 ± 1.1	29.4 ± 0.8	60.9 ± 2.1	52.3 ± 1.8	71.8 ± 1.4
25 – 30	67.4 ± 1.5	79.3 ± 1.2	36.7 ± 0.8	44.9 ± 1.1	24.7 ± 0.9	39.7 ± 0.8	30.8 ± 1.1	45.4 ± 1.4

Appendix D14: Detected average concentration of Na (mg/kg d.w) in core sediment samples of selected study sites

Depth (cm)	CZ1	CZ2	CZ4	CZ5	CZ7	CZ8	CZ10	CZ11
0 – 5	21.4 ± 0.8	24.6 ± 1.1	11.7 ± 0.4	28.1 ± 0.7	19.4 ± 0.4	22.4 ± 1.1	20.7 ± 1.1	29.4 ± 1.3
5 –10	14.4 ± 0.5	18.6 ± 0.8	15.2 ± 0.6	25.6 ± 0.5	15.7 ± 0.7	19.7 ± 0.5	17.3 ± 0.3	27.6 ± 1.1
10 – 15	16.8 ± 0.3	20.1 ± 1.1	13.7 ± 0.6	21.4 ± 0.7	13.9 ± 0.6	18.1 ± 0.7	18.1 ± 0.5	25.1 ± 0.9
15 – 20	15.1 ± 0.3	14.3 ± 0.4	9.9 ± 0.4	19.8 ± 1.1	11.3 ± 0.4	14.8 ± 0.3	14.0 ± 0.2	21.6 ± 0.9
20 – 25	10.6 ± 0.5	10.9 ± 0.6	9.4 ± 0.6	16.2 ± 0.7	8.6 ± 0.8	10.9 ± 0.8	10.9 ± 0.6	19.8 ± 0.6
25 – 30	11.4 ± 0.3	9.3 ± 0.2	8.8 ± 0.2	14.9 ± 1.0	8.9 ± 1.3	11.4 ± 0.5	11.8 ± 0.7	17.3 ± 0.5

Appendix D15: Detected average concentration of Fe (mg/kg d.w) in core sediment samples of selected study sites

Depth (cm)	CZ1	CZ2	CZ4	CZ5	CZ7	CZ8	CZ10	CZ11
0 – 5	19142.0 ± 6.7	20186.2 ± 6.4	16322.2 ± 5.4	33381.4 ± 6.3	19244.1 ± 5.2	29131.4 ± 6.2	24170.3 ± 5.5	35124.6 ± 8.9
5 –10	16033.2 ± 4.2	18463.7 ± 4.1	14275.9 ± 3.7	31684.9 ± 5.9	17168.7 ± 4.4	27426.6 ± 3.8	23672.7 ± 6.1	33644.3 ± 3.6
10 – 15	15188.7 ± 5.8	16335.5 ± 10.3	14381.4 ± 9.8	30926.1 ± 9.7	16301.4 ± 5.1	25871.6 ± 5.1	23088.1 ± 8.9	30911.1 ± 7.9
15 – 20	13946.1 ± 4.6	14898.3 ± 9.5	13913.7 ± 5.6	29118.4 ± 9.6	15397.8 ± 2.9	24812.0 ± 3.7	22814. ± 6.8	29349.6 ± 4.3
20 – 25	13529.4 ± 7.7	14146.2 ± 8.8	12636.4 ± 3.9	26763.1 ± 9.1	15004.4 ± 6.4	23089.6 ± 8.9	22077.3 ± 6.1	27081.2 ± 5.1
25 – 30	12086.1 ± 8.5	13861.6 ± 7.9	12011.5 ± 2.9	20431.3 ± 5.8	14117.5 ± 6.6	19338.8 ± 4.1	21462.5 ± 7.4	24653.8 ± 6.8

Appendix E: Graph of average concentrations of selected heavy metals (mg/kg d.w.) against sediment depth/cm

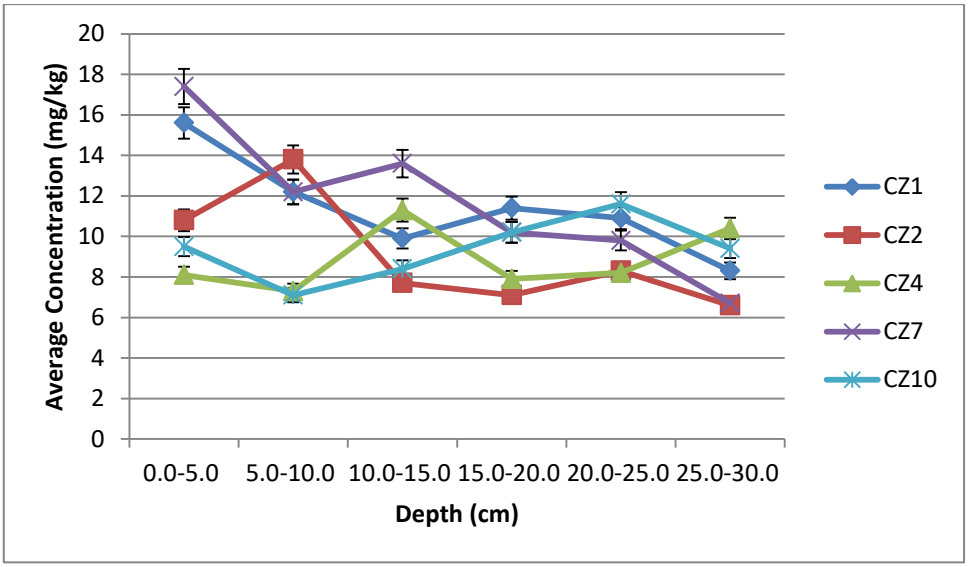

(d) Mean concentrations of Ni (mg/kg d.w)

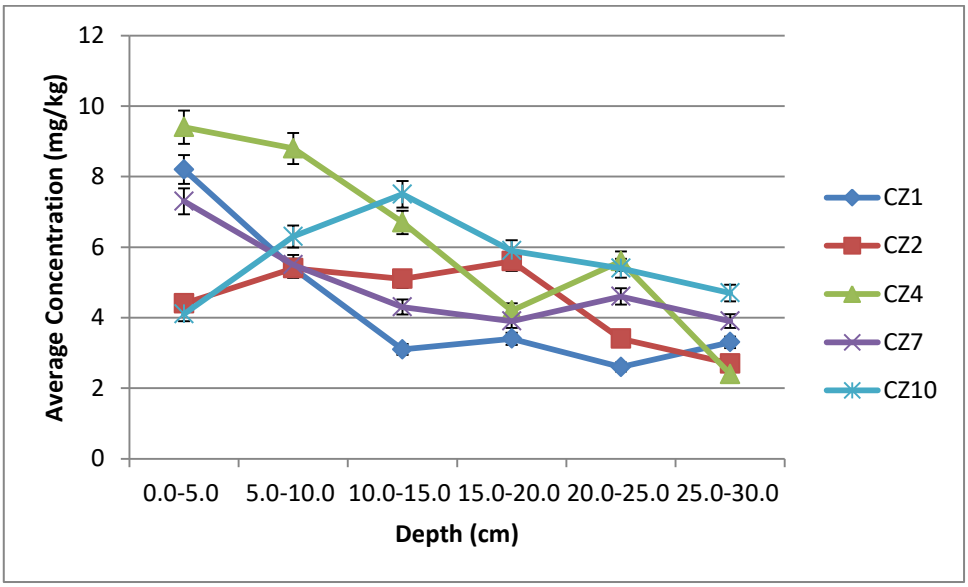

(e) Mean concentrations of Mn (mg/kg d.w)

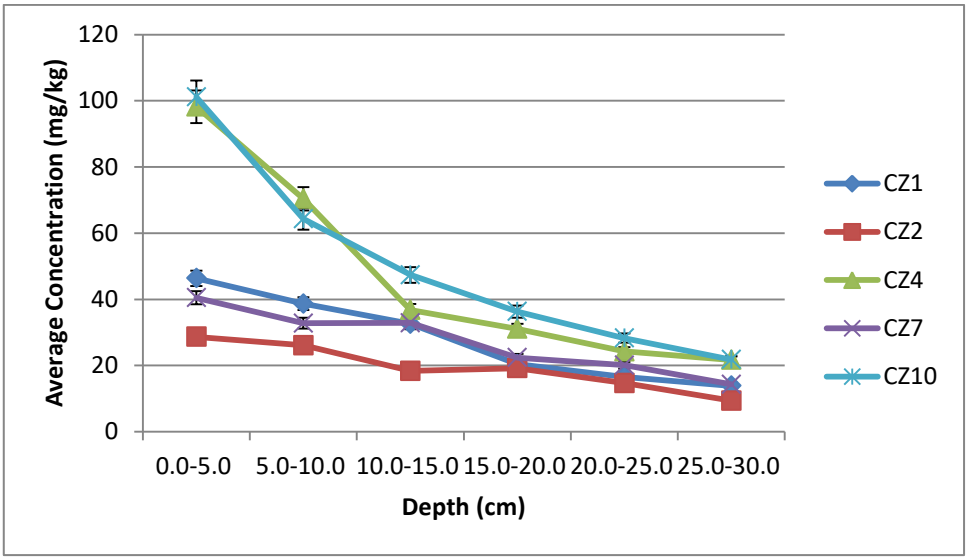

(f) Mean concentrations of Cu (mg/kg d.w)

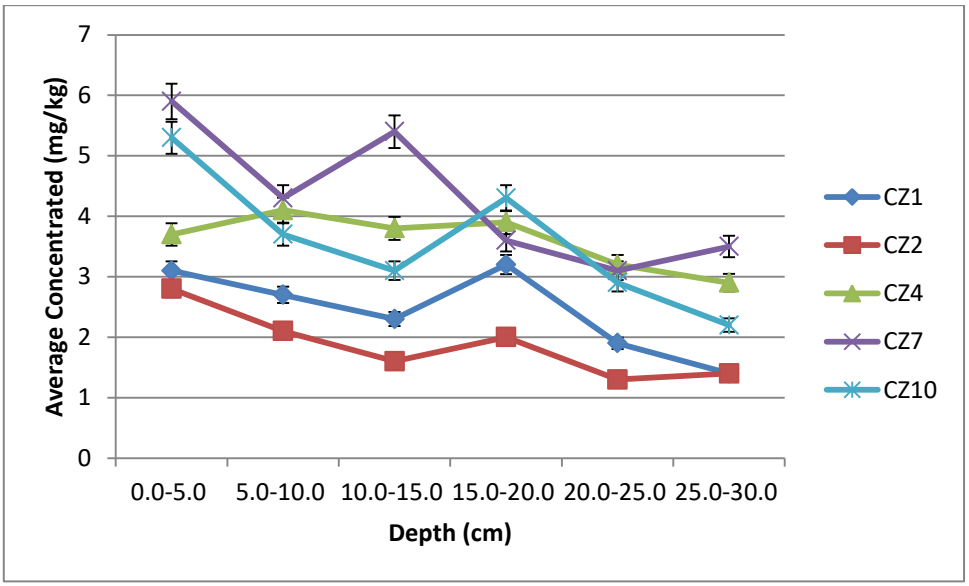

(g) Mean concentrations of Ba (mg/kg d.w)

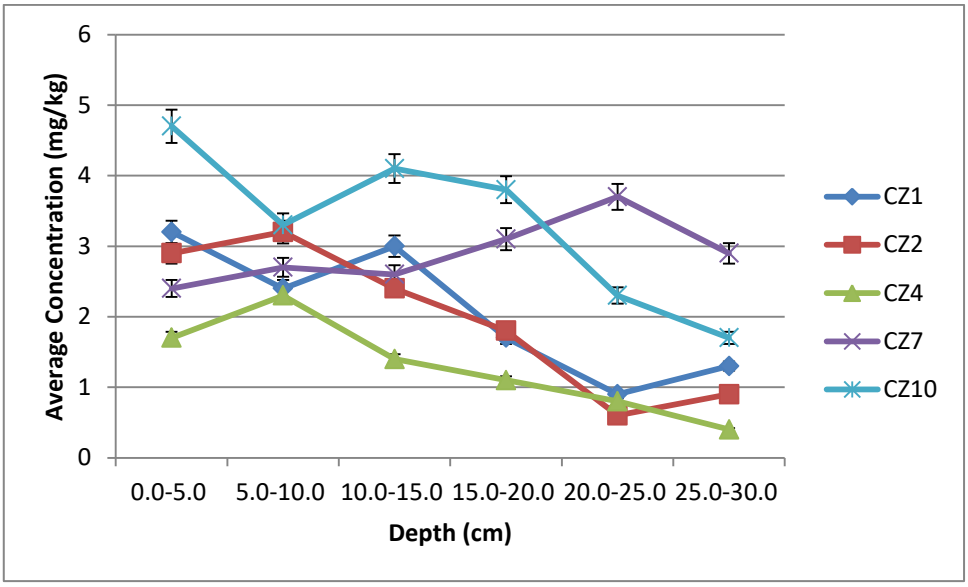

(h) Mean concentrations of As (mg/kg d.w)

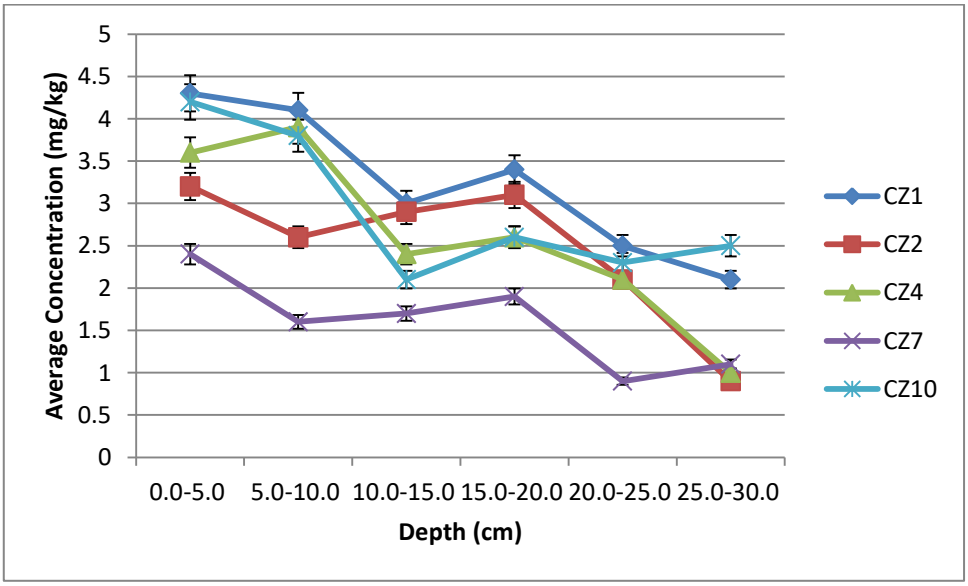

(i) Mean concentrations of Co (mg/kg d.w)

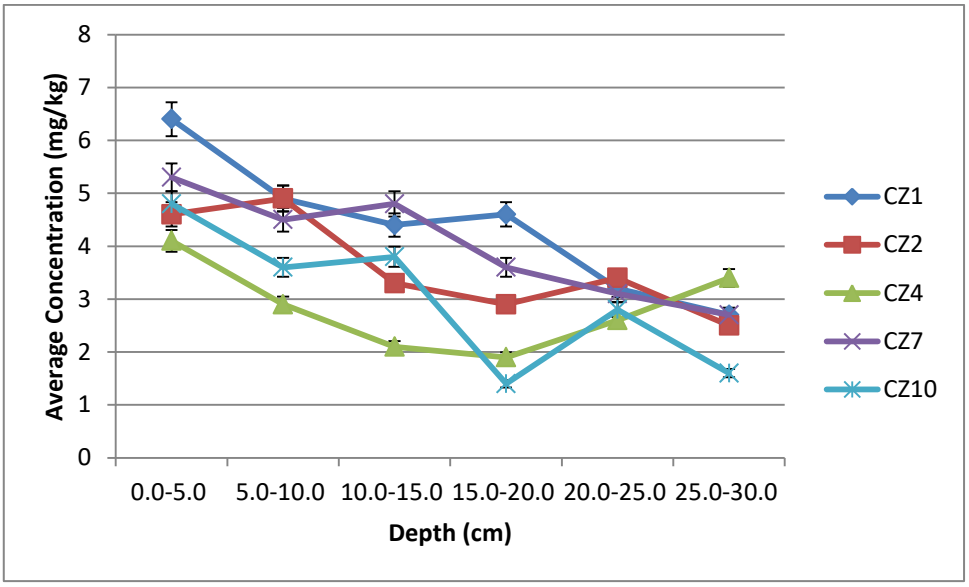

(j) Mean concentrations of Cr (mg/kg d.w)

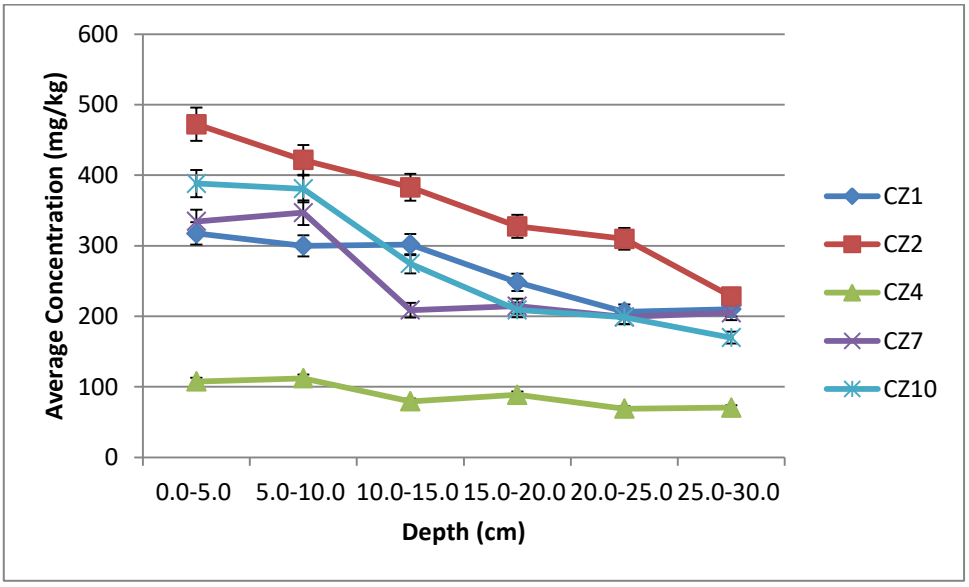

(k) Mean concentrations of Mg (mg/kg d.w)

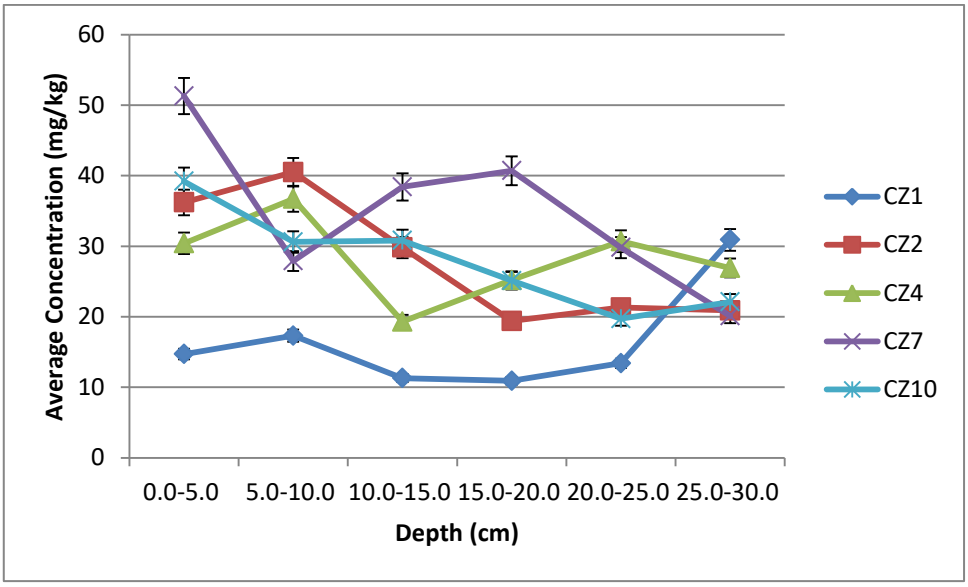

(l) Mean concentrations of Ca (mg/kg d.w)

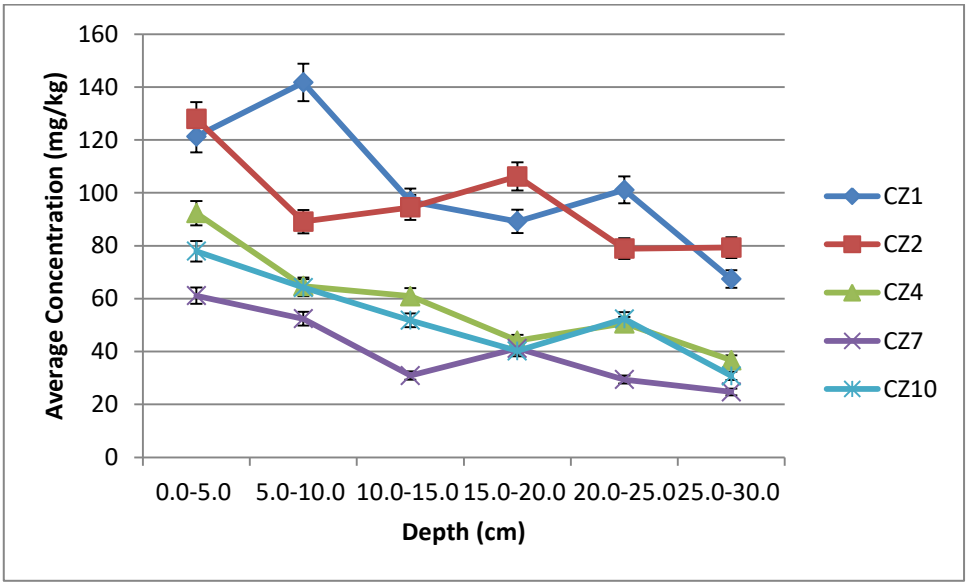

(m) Mean concentrations of Al (mg/kg d.w)

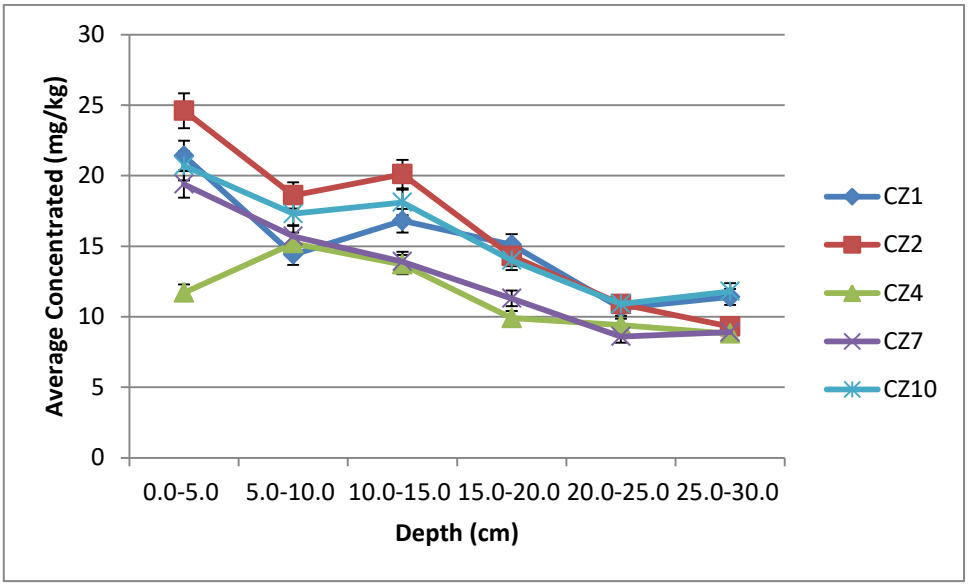

(n) Mean concentrations of Na (mg/kg d.w)

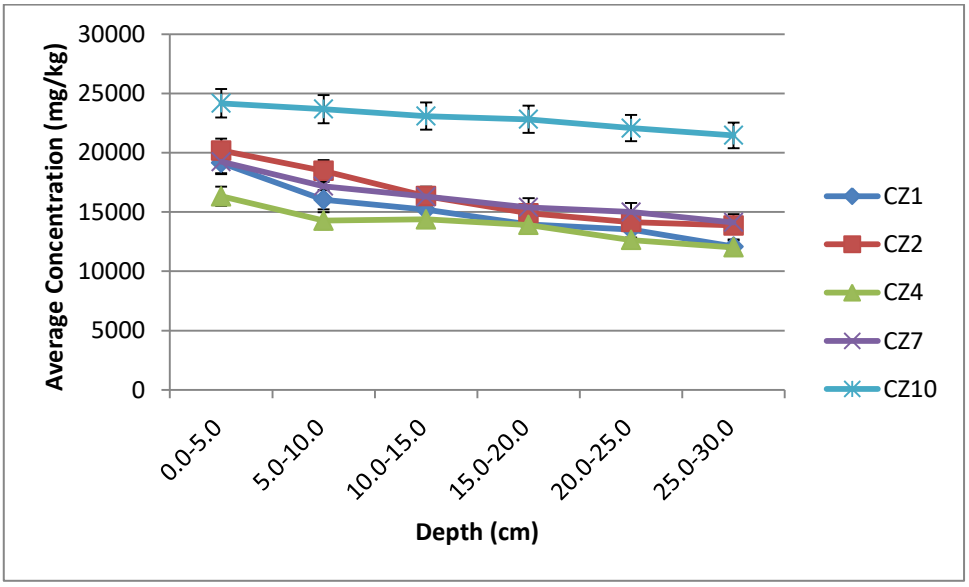

(o) Mean concentrations of Fe (mg/kg d.w)

Appendix F: No enriched heavy metals in the vertical profiles of core sediments collected of selected study site

Site/Depth (cm)	CZ1	CZ2	CZ4	CZ5	CZ7	CZ8	CZ10	CZ11
				Cd				
0 – 5.0	0.25	0.14	0.23	0.21	0.27	0.18	0.12	0.21
5.0 – 10.0	0.24	0.15	0.20	0.20	0.25	0.20	0.09	0.17
10.0 – 15.0	0.35	0.59	0.15	0.18	0.33	0.16	0.17	0.17
15.0 – 20.0	0.58	0.24	0.63	0.17	0.30	0.13	0.15	0.16
20.0 – 25.0	0.48	0.23	0.51	0.19	0.49	0.16	0.12	0.13
25.0 – 30.0	0.44	0.14	0.62	0.22	0.44	0.21	0.17	0.13
				Ni				
0 – 5.0	0.57	0.37	0.35	0.61	0.63	0.58	0.27	0.22
5.0 – 10.0	0.53	0.52	0.36	0.51	0.49	0.46	0.21	0.42
10.0 – 15.0	0.45	0.33	0.52	0.44	0.58	0.38	0.26	0.38
15.0 – 20.0	0.57	0.33	0.39	0.31	0.46	0.31	0.31	0.34
20.0 – 25.0	0.56	0.41	0.45	0.26	0.45	0.34	0.37	0.29
25.0 – 30.0	0.48	0.33	0.60	0.32	0.33	0.38	0.30	0.31

Mn								
0 – 5.0	0.03	0.01	0.03	0.30	0.02	0.24	0.01	0.27
5.0 – 10.0	0.02	0.02	0.03	0.12	0.02	0.20	0.02	0.22
10.0 – 15.0	0.01	0.02	0.03	0.18	0.02	0.15	0.02	0.19
15.0 – 20.0	0.01	0.02	0.02	0.12	0.01	0.12	0.01	0.18
20.0 – 25.0	0.01	0.01	0.03	0.12	0.02	0.09	0.01	0.14
25.0 – 30.0	0.02	0.01	0.01	0.11	0.02	0.08	0.01	0.13
Ba								
0 – 5.0	0.013	0.011	0.018	0.015	0.025	0.012	0.018	0.011
5.0 – 10.0	0.014	0.009	0.023	0.012	0.020	0.011	0.013	0.010
10.0 – 15.0	0.012	0.008	0.022	0.008	0.027	0.010	0.011	0.009
15.0 – 20.0	0.019	0.011	0.023	0.007	0.019	0.008	0.015	0.007
20.0 – 25.0	0.011	0.008	0.021	0.005	0.017	0.006	0.011	0.007
25.0 – 30.0	0.009	0.008	0.020	0.004	0.020	0.038	0.008	0.004
As								
0 – 5.0	0.61	0.52	0.38	0.63	0.45	0.47	0.71	0.82
5.0 – 10.0	0.54	0.63	0.59	0.45	0.57	0.52	0.51	0.83

10.0 – 15.0	0.72	0.53	0.35	0.40	0.58	0.44	0.65	0.68
15.0 – 20.0	0.04	0.44	0.29	0.36	0.73	0.38	0.61	0.54
20.0 – 25.0	0.24	0.15	0.23	0.29	0.90	0.38	0.38	0.52
25.0 – 30.0	0.04	0.24	0.12	0.25	0.75	0.38	0.29	0.50
				Co				
0 – 5.0	0.56	0.39	0.55	0.29	0.31	0.44	0.43	0.26
5.0 – 10.0	0.64	0.35	0.68	0.19	0.23	0.44	0.40	0.23
10.0 – 15.0	0.49	0.44	0.42	0.21	0.26	0.39	0.23	0.22
15.0 – 20.0	0.53	0.52	0.46	0.17	0.31	0.37	0.28	0.20
20.0 – 25.0	0.46	0.37	0.41	0.12	0.15	0.25	0.35	0.16
25.0 – 30.0	0.43	0.16	0.17	0.10	0.19	0.19	0.29	0.11
				Cr				
0 – 5.0	0.18	0.12	0.13	0.09	0.14	0.14	0.10	0.06
5.0 – 10.0	0.16	0.14	0.11	0.08	0.14	0.12	0.08	0.06
10.0 – 15.0	0.15	0.11	0.08	0.05	0.15	0.13	0.09	0.06
15.0 – 20.0	0.17	0.10	0.07	0.05	0.13	0.09	0.03	0.04
20.0 – 25.0	0.12	0.13	0.11	0.04	0.11	0.08	0.07	0.04

25.0 – 30.0	0.12	0.10	0.15	0.03	0.10	0.07	0.04	0.04
				Mg				
0 – 5.0	0.054	0.074	0.021	0.045	0.055	0.054	0.051	0.029
5.0 – 10.0	0.061	0.072	0.025	0.041	0.064	0.062	0.051	0.030
10.0 – 15.0	0.063	0.074	0.017	0.039	0.040	0.047	0.037	0.031
15.0 – 20.0	0.063	0.069	0.020	0.038	0.044	0.047	0.029	0.030
20.0 – 25.0	0.048	0.069	0.017	0.038	0.042	0.042	0.028	0.030
25.0 – 30.0	0.055	0.052	0.018	0.046	0.046	0.046	0.025	0.026
				Ca				
0 – 5.0	0.003	0.006	0.006	0.004	0.010	0.008	0.005	0.006
5.0 – 10.0	0.004	0.007	0.009	0.004	0.006	0.006	0.004	0.006
10.0 – 15.0	0.003	0.006	0.005	0.004	0.008	0.006	0.005	0.006
15.0 – 20.0	0.003	0.004	0.006	0.004	0.009	0.005	0.004	0.006
20.0 – 25.0	0.004	0.005	0.008	0.004	0.007	0.005	0.003	0.005
25.0 – 30.0	0.009	0.005	0.008	0.005	0.005	0.0007	0.004	0.005
				Al				
0 – 5.0	0.004	0.004	0.002	0.004	0.002	0.002	0.002	0.002

5.0 – 10.0	0.005	0.004	0.002	0.002	0.002	0.002	0.002	0.002
10.0 – 15.0	0.004	0.003	0.001	0.002	0.001	0.002	0.001	0.002
15.0 – 20.0	0.004	0.004	0.002	0.002	0.002	0.002	0.001	0.002
20.0 – 25.0	0.004	0.003	0.001	0.002	0.001	0.002	0.001	0.002
25.0 – 30.0	0.003	0.003	0.001	0.001	0.001	0.002	0.001	0.001
Na								
0 – 5.0	0.006	0.006	0.004	0.004	0.005	0.003	0.004	0.003
5.0 – 10.0	0.016	0.005	0.005	0.004	0.005	0.003	0.004	0.003
10.0 – 15.0	0.005	0.006	0.005	0.004	0.004	0.003	0.004	0.004
15.0 – 20.0	0.005	0.005	0.005	0.003	0.004	0.002	0.003	0.003
20.0 – 25.0	0.004	0.004	0.004	0.003	0.003	0.002	0.002	0.003
25.0 – 30.0	0.005	0.003	0.004	0.004	0.003	0.003	0.003	0.003

Appendix G: Pearson correlation analyses between analyzed detected average concentrations of heavy metals in surface sediment samples of selected study sites

	Pb	Zn	Cd	Ni	Mn	Cu	Ba	As	Co	Cr	Mg	Ca	Al	Na	Fe
Pb	1.00														
Zn	0.112	1.00													
Cd	-0.657	-0.368	1.00												
Ni	-0.887*	-0.063	0.848	1.00											
Mn	0.093	-0.537	0.671	0.196	1.00										
Cu	0.472	-0.661	-0.398	-0.680	0.114	1.00									
Ba	-0.648	-0.445	0.256	0.279	-0.126	0.280	1.00								
As	-0.166	-0.083	-0.468	-0.086	-0.742	0.214	0.231	1.00							
Co	0.466	-0.394	-0.386	-0.391	-0.043	0.489	-0.375	0.550	1.00						
Cr	-0.589	-0.235	0.612	0.790	0.158	-0.466	-0.048	0.250	0.247	1.00					
Mg	-0.377	0.653	-0.300	0.248	-0.865	-0.563	-0.005	0.610	-0.090	0.247	1.00				
Ca	-0.461	0.198	-0.011	0.102	-0.374	-0.040	0.752	-0.015	-0.765	-0.440	0.241	1.00			
Al	0.503	0.528	-0.285	-0.167	-0.073	-0.400	-0.964**	-0.025	0.407	0.193	0.250	-0.727	1.00		

Na	-0.379	0.620	-0.177	0.357	-0.737	-0.663	-0.159	0.566	0.010	0.439	0.968**	0.027	0.407	1.00	
Fe	-0.262	0.063	-0.496	-0.071	-0.865	0.141	0.373	0.958*	0.303	0.102	0.711	0.258	-0.159	0.610	1.00

*Correlation is significant at the 0.5 level (2 – tailed)

**Correlation is significant at the 0.1 level (2 – tailed)

Appendix H1: Characteristic gas chromatogram of *n*-alkanes fractions extracted from the estuary sediment in locations CZ1

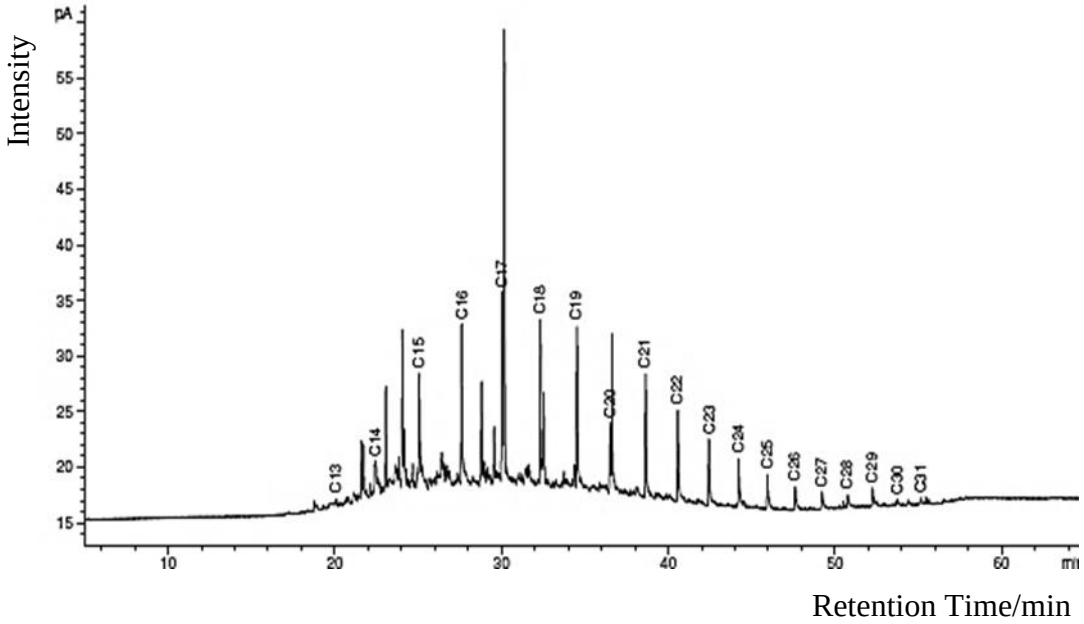

Appendix H2: Characteristic gas chromatogram of *n*-alkanes fractions extracted from the coastal sediment in location CZ2

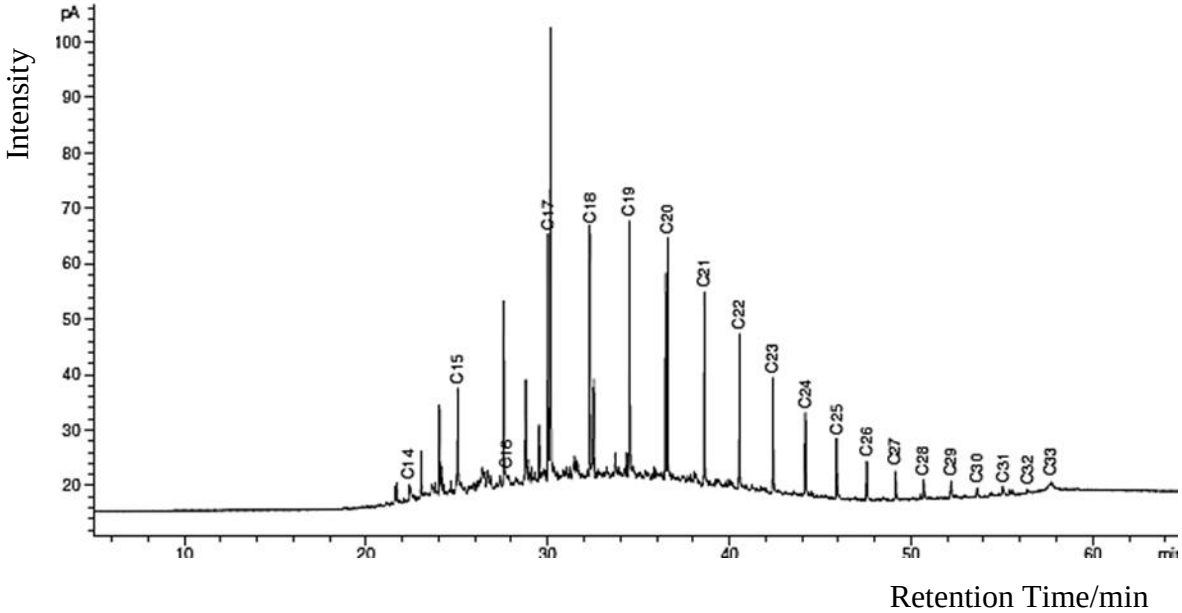

Appendix H3: Characteristic gas chromatogram of *n*-alkanes fractions extracted from the coastal sediment in location CZ3

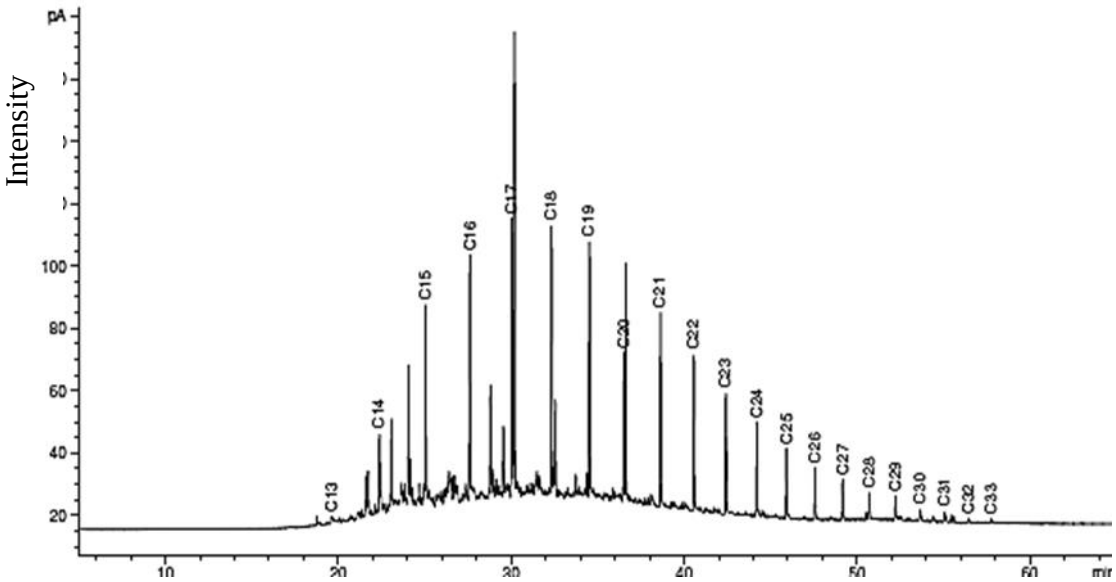

Appendix H4: Characteristic gas chromatogram of *n*-alkanes fractions extracted from the estuary sediment in location CZ4

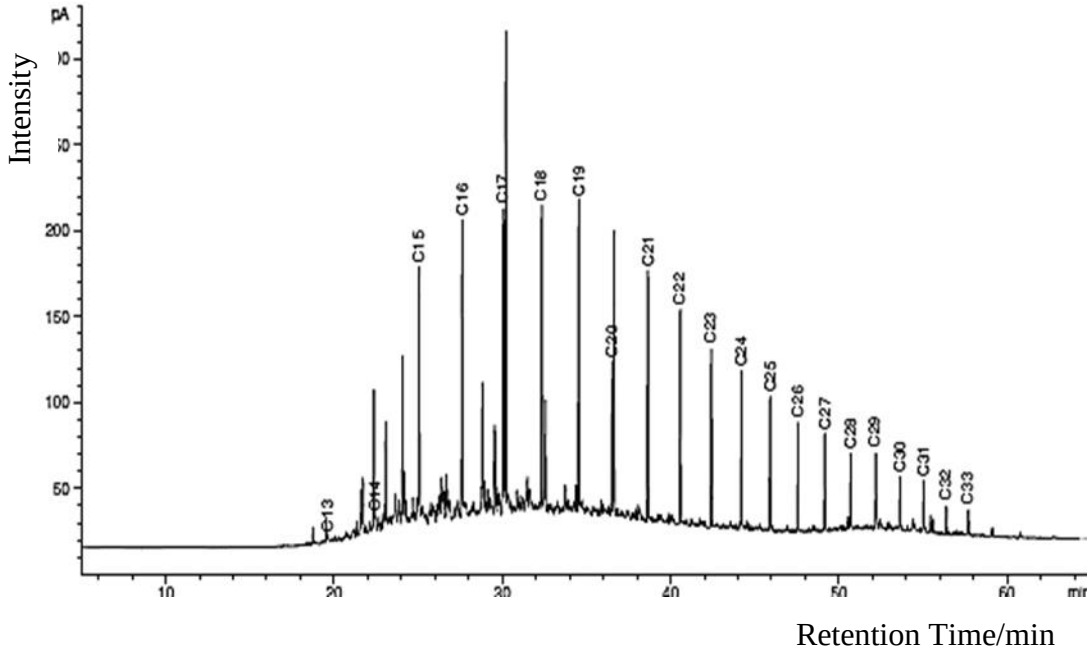

Appendix H5: Characteristic gas chromatogram of *n*-alkanes fractions extracted from the coastal sediment in location CZ6

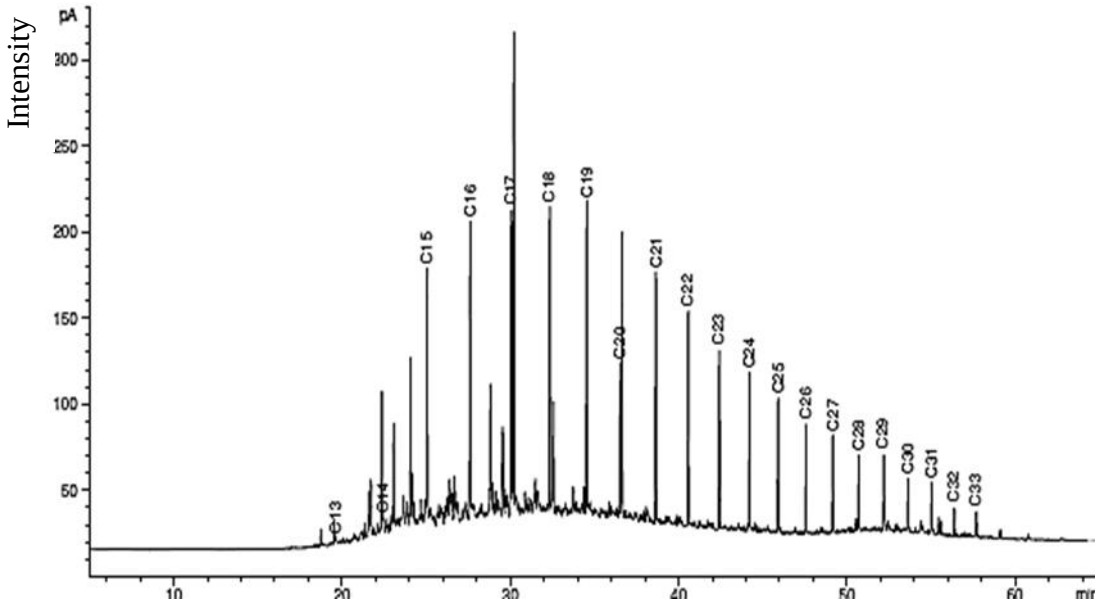

Appendix H6: Characteristic gas chromatogram of *n*-alkanes fractions extracted from the coastal sediment in location CZ7

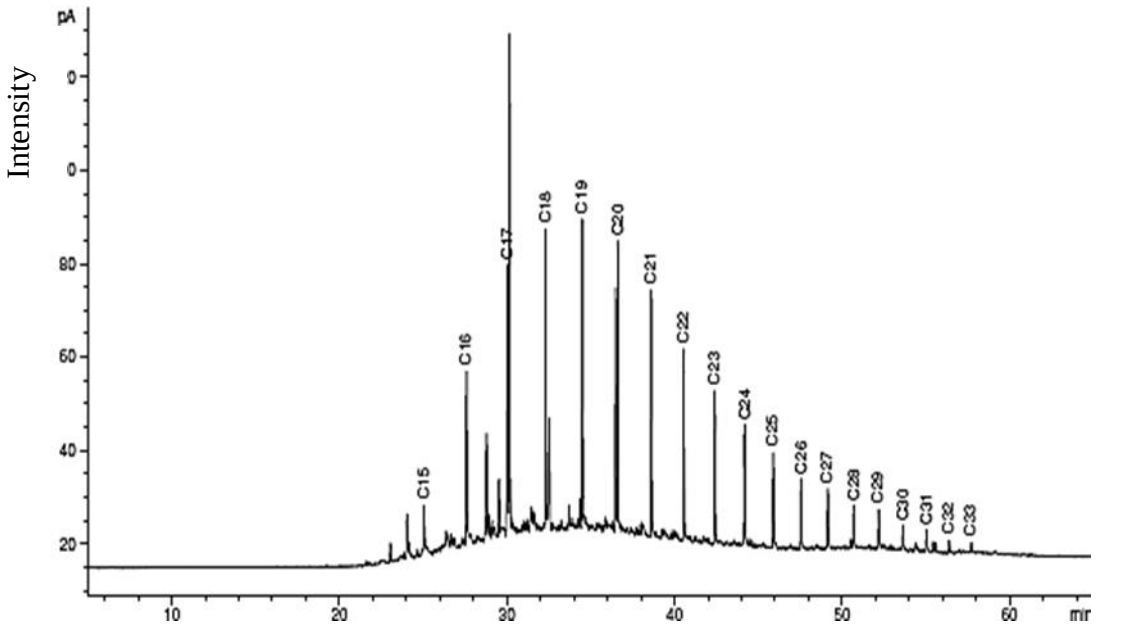

Appendix H7: Characteristic gas chromatogram of *n*-alkanes fractions extracted from the estuary sediment in location CZ9.

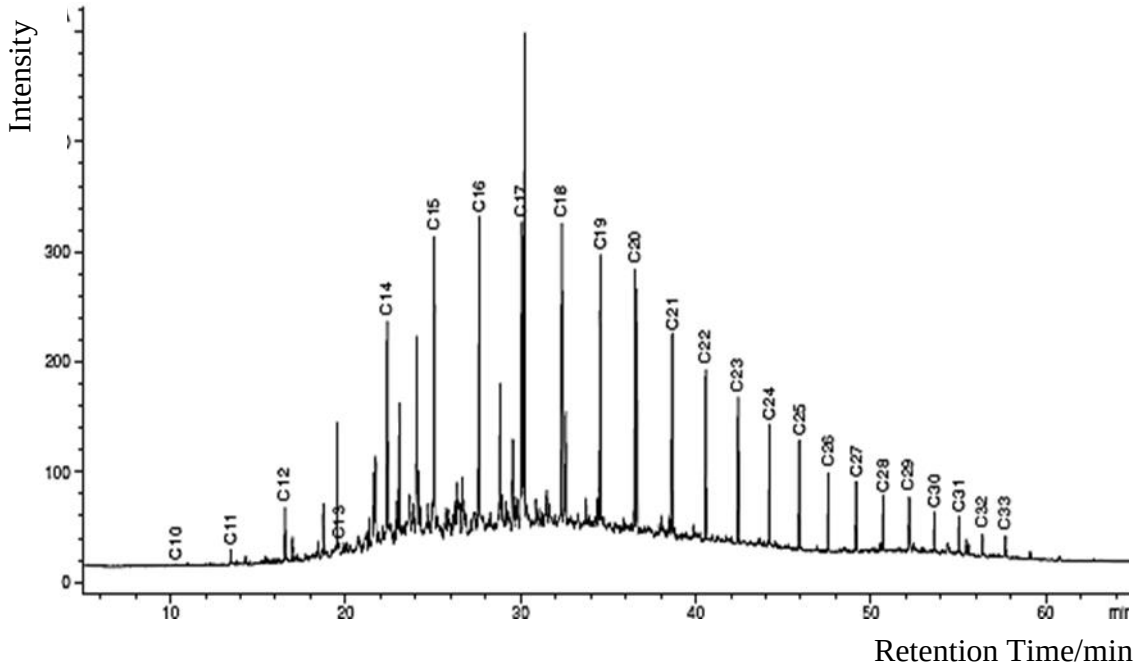

Appendix H8: Characteristic gas chromatogram of *n*-alkanes fractions extracted from the estuary sediment in location CZ10.

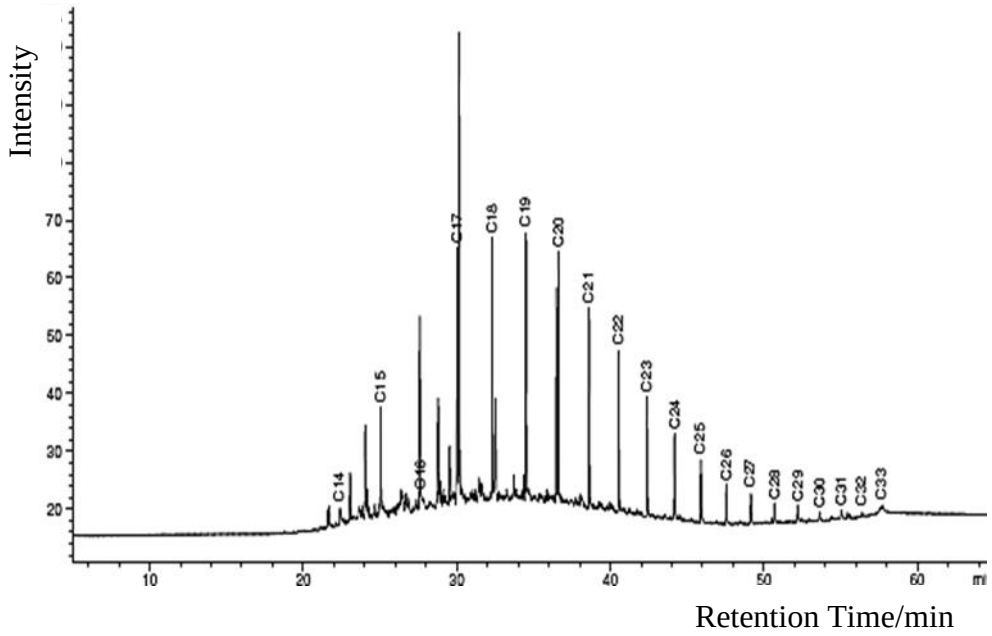

Appendix I1: Characteristic gas chromatogram PAH fractions extracted from the estuary sediment in location CZ1

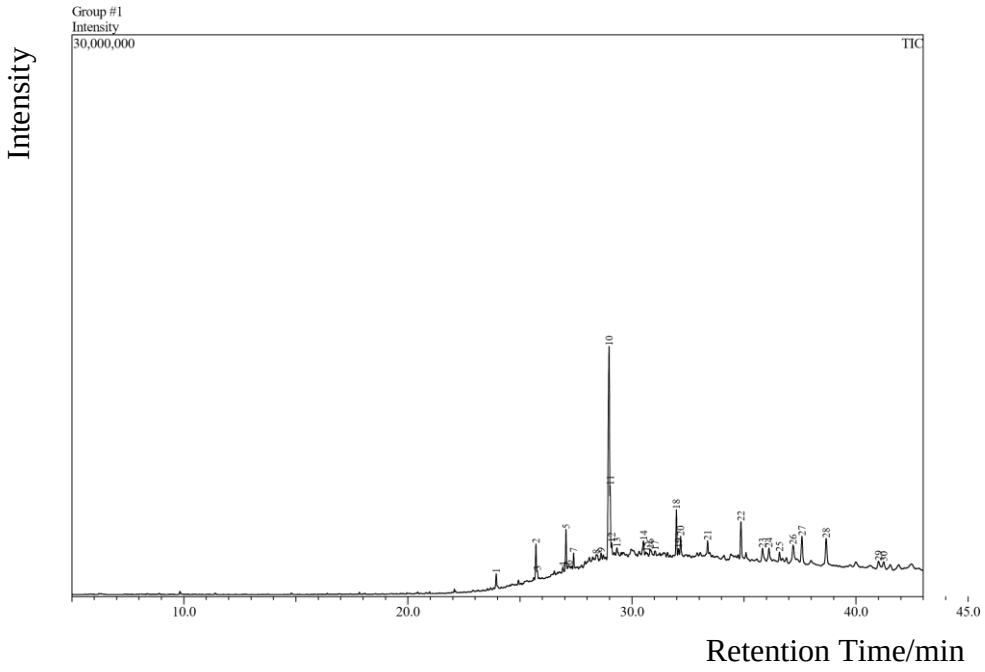

Appendix 12: Characteristic gas chromatogram PAH fractions extracted from the coastal sediment in location CZ2

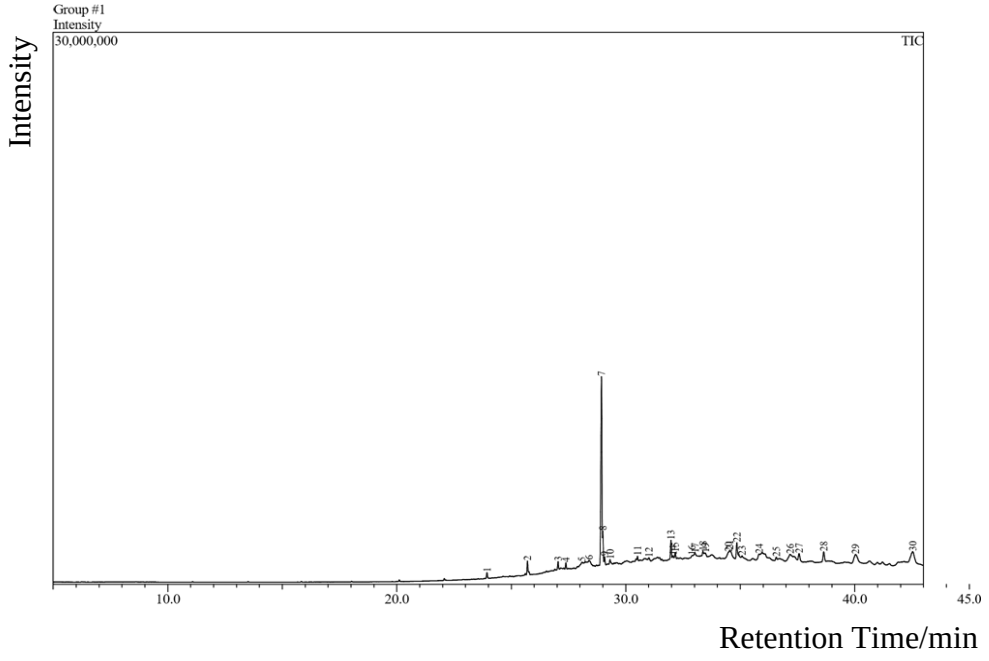

Appendix I3: Characteristic gas chromatogram PAH fractions extracted from the coastal sediment in location CZ3

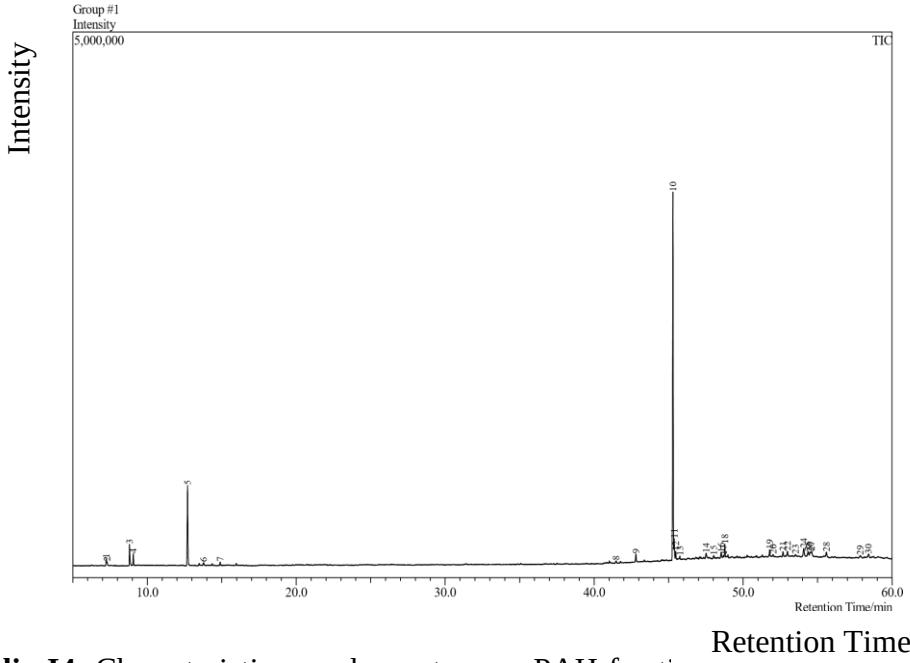

Intensity

Retention Time/min

Appendix I4: Characteristic gas chromatogram PAH fractions extracted from the estuary sediment in location CZ4

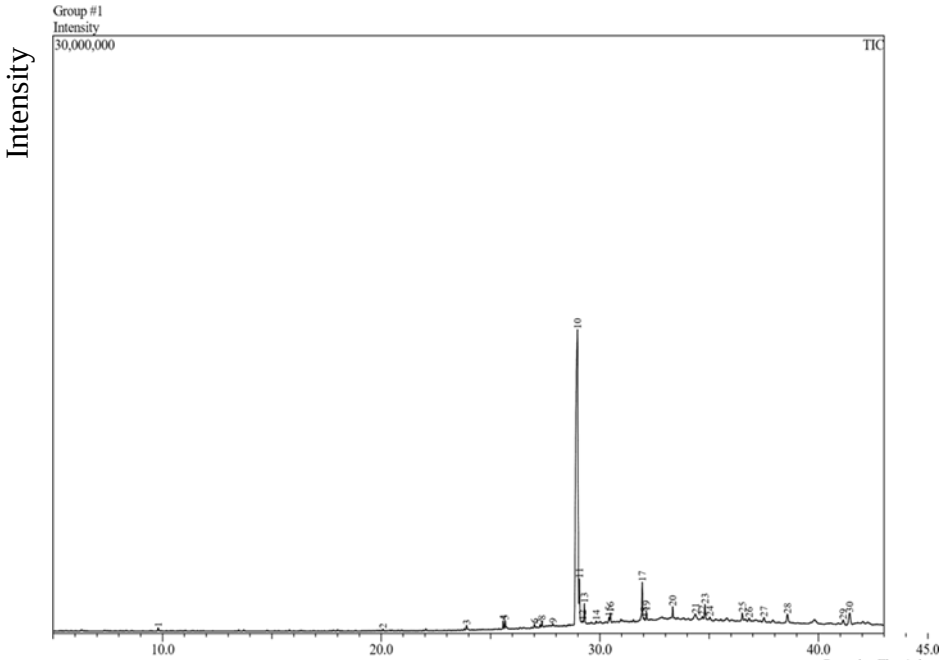

Intensity

Retention Time/min

Appendix I5: Characteristic gas chromatogram PAH fractions extracted from the coastal sediment in location CZ6

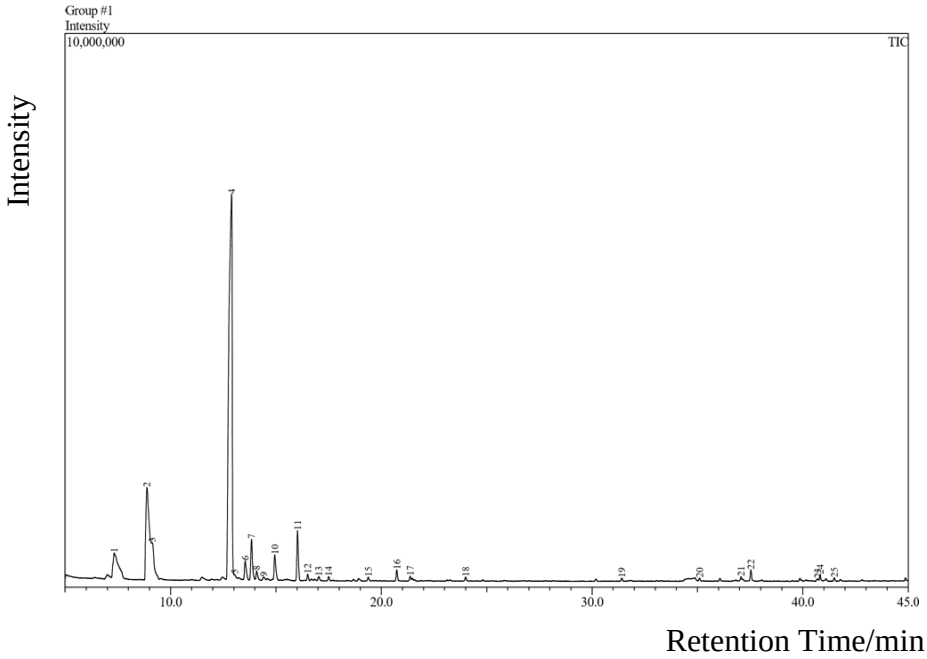

Appendix I6: Characteristic gas chromatogram PAH fractions extracted from the estuary sediment in location CZ7

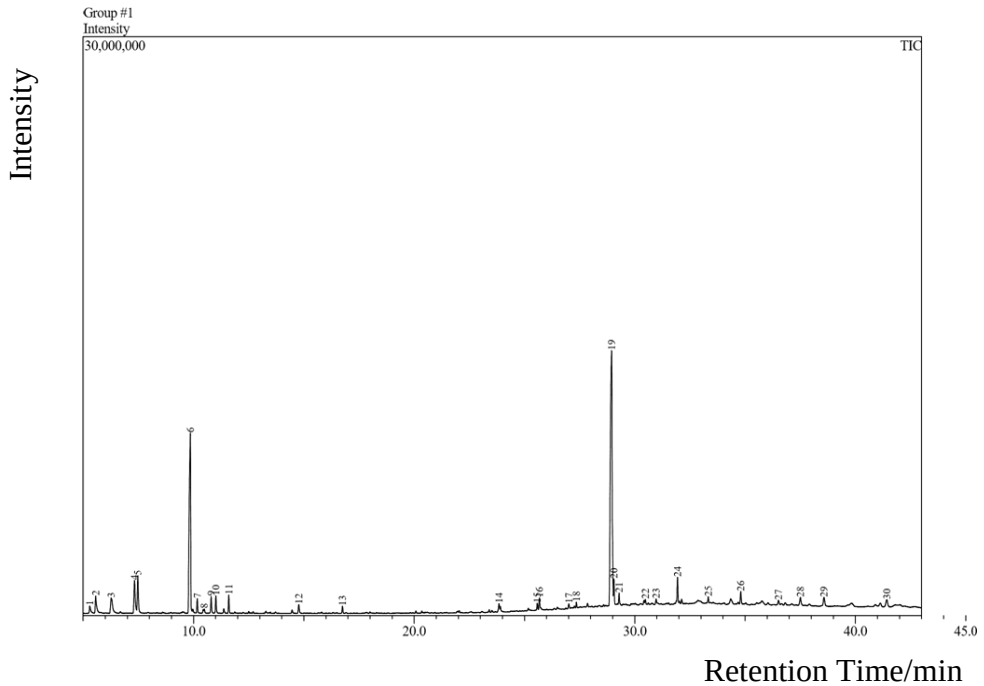

Appendix I7: Characteristic gas chromatogram PAH fractions extracted from the coastal sediment in location CZ9

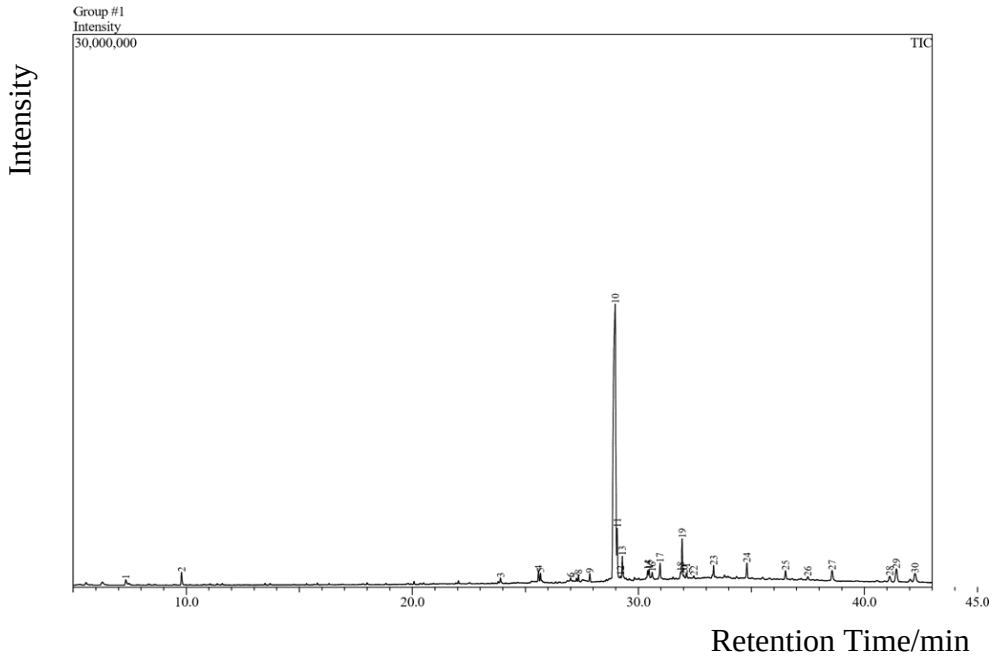

Appendix I8: Characteristic gas chromatogram PAH fractions extracted from the estuary sediment in location CZ10